Cyclic, cationic complexes of Pt^{II} and Pd^{II} with heterocyclic ligands, including nucleobases:

synthesis, structure, host-guest chemistry with anions and non-covalent interactions with DNA

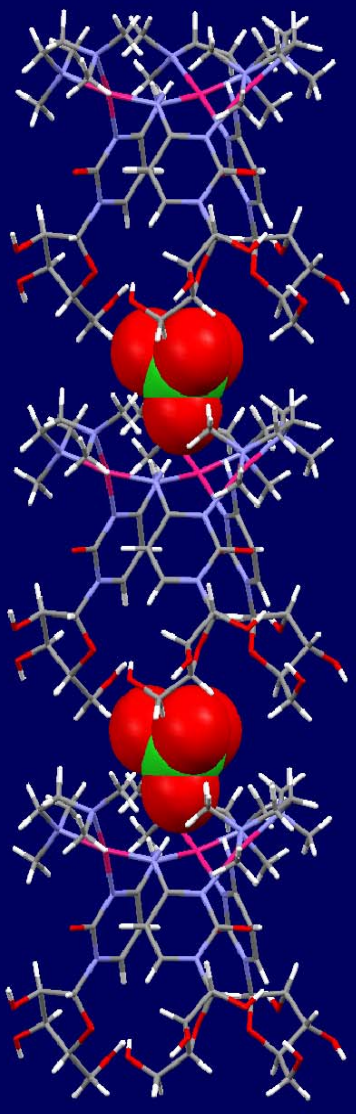

Wei-Zheng Shen

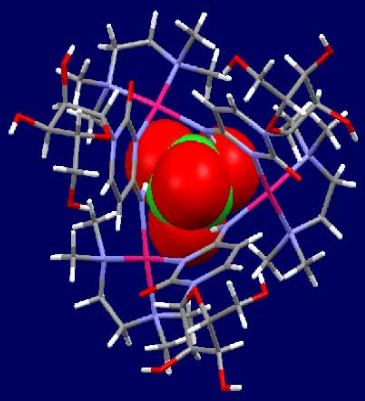

Cyclic, cationic complexes of Pt^{II} and Pd^{II} with heterocyclic ligands, including nucleobases:

synthesis, structure, host-guest chemistry with anions and non-covalent interactions with DNA

Wei-Zheng Shen

Universität Dortmund

Fachbereich Chemie der Universität Dortmund

Cyclic, cationic complexes of Pt^{II} and Pd^{II} with heterocyclic ligands, including nucleobases:

synthesis, structure, host-guest chemistry with anions and non-covalent interactions with DNA

Wei-Zheng Shen

Ph.D. Thesis submitted to the
Fachbereich Chemie, Universität Dortmund, Germany
for obtaining the degree of a
Doktor der Naturwissenschaften

Ph.D. Advisor: Prof. Dr. Bernhard Lippert

Referee: P. D. Dr. Iris M. Oppel

This work was carried out between January 2004 and March 2007 at the Lehrstuhl für Bioanorganische Chemie, Fachbereich Chemie, Universität Dortmund, Deutschland.

My special thanks go to my Ph. D. Supervisor

Prof. Dr. Bernhard Lippert

for the opportunity to study in his group, the interesting science, his enthusiasm, patience and continuous support. His influence on me is much more than a scientific supervisor and will get along with me in my whole life.

I would also like to thank P. D. Dr. Iris M. Oppel for kindly acting as referee; P. D. Dr. Andrea Erxleben and Dr. Jens Müller for numerous scientific discussions and suggestions during these three years; Dr. Gabriele Trötscher-Kaus for talking with me whenever I have stress. Specially, Dr. Jens Müller gave me a lot of encouragement during my thesis writing and later carefully read and corrected my thesis.

I would like to express my gratitude to Prof. Dr. Martin Engelhard, Prof. Dr. Dr. h. c. Rolf Kinne, Dr. Jutta Roetter, Niklas Büdenbender and International Max Planck Research School for assistance and financial support. I am indebted to Ms. Michaela Markert and Ms. Birgit Thormann for their secretarial assistance and support, especially concerning the difficulties about filling various complicated German forms.

I would like to thank Dr. Patrick Lax for translating the summary into German; Dr. Pablo Sanz Miguel, Dr. Myriam Gil, Barbara Müller and Tushar van der Wijst for carefully reading parts of my thesis.

I thank Prof. Dr. Burkhard Costisella, Ms. Danzmann, Ms. Nettelbeck, Dr. Jens Müller, and Ms. Marta Morell Cerdà for recording the NMR spectra; Mr. Markus Hüffner for measuring the elemental analyses; Ms. Wilga Buß for recording the Raman spectra; Dr. Hans Preut for teaching me the X-ray crystallography; Ms. Marta Morell Cerdà and Dr. Michael Roitzsch for showing me the program of the X-ray crystallographic machine; Dr. Andrea Erxleben, Dr. Pablo Sanz Miguel, Dr. Thorsten Oldag for generously sharing their experiences and knowledge on X-ray crystallography; Mr. Thorsten Grund for his technical support.

I would like to thank Dr. Bo Zou and Jessica Irrgang in Prof. Christof M. Niemeyer's group for teaching me Atomic Force Microscopic technique from the very beginning.

I would like to thank the group of Dr. Félix Zamora in Madrid for the collaboration work on Atomic Force Microscopy; Dr. Félix for numerous

interesting scientific discussions; Dr. Pablo Sanz Miguel for spending a lot of time in taking care of my life in Madrid; Lorena Welte for the help in the AFM experiments; Antonio Romero for teaching me run the gel electrophoresis; Alejandro Guijarro for kindly inviting me to see the “fighting bull”; Vicente López for the wonderful time in Chinese Noodle restaurant. I should say that it was really wonderful time in Madrid although the weather made me allergic all the time.

My past three years in Dortmund has been a worthwhile and memorable experience because of the easy-going, accommodating and nice colleagues, Dr. Deepali Gupta, Dr. Pablo Sanz Miguel, Dr. Michael Roitzsch, Dr. Patrick Lax, Lars Holland, Barbara Müller, Thea Welzel, Dr. Fabian Polonius, Dominik Böhme, Nicole Düpre and Dominik Megger in the laboratory; Dr. Marta Garijo Aňorbe, Dr. Myriam (Elisa) Gil Bardají and Marta Morell Cerdà in the office. A lot of Spanish words I have learned from these three lovely Spanish girls. Dr. Myriam (Elisa) Gil Bardají, I will forever remember the memorable time we spent together in Rimini and later in Florence. Dr. Deepali Gupta shared the same laboratory with me at the beginning one and half years, thanks for those wonderful “lectures” you have ever given to me and I can never forget you are always there when I need you.

I would also like to thank my Chinese friends, Lei Wang, Lin Li, Shuang Zhao, Haixia Zhou, Huachang Lu, Zhong Guo and Yaowen Wu for the invaluable help for the work and also for the life during the past three years. I am very happy to see all of them will obtain Doctor degree in the nearly future here in Germany. I am proud of all of us.

Last, but certainly not least, my special thanks to my parents for bring me to this wonderful world, supporting me to get the good educations, encouraging me to realize my own value, leaving me free to go abroad to do what I want although I am the only child of them, and also to my husband for his patience, understanding and accompanying. I dedicate this thesis to them.

谨以此文献给我的父亲和母亲

以及我的爱人

A GENERAL INTRODUCTION

Metal-DNA Interactions

DNA is a linear polyanion with each nucleotide carrying a negative charge at the bridging phosphate group (Figure 1). For charge neutralization, there are natural counter ions within cells, predominantly K^+, Na^+ and Mg^+. Therefore, DNA may likewise be targeted by other non-physiological cationic metal entities.[1]

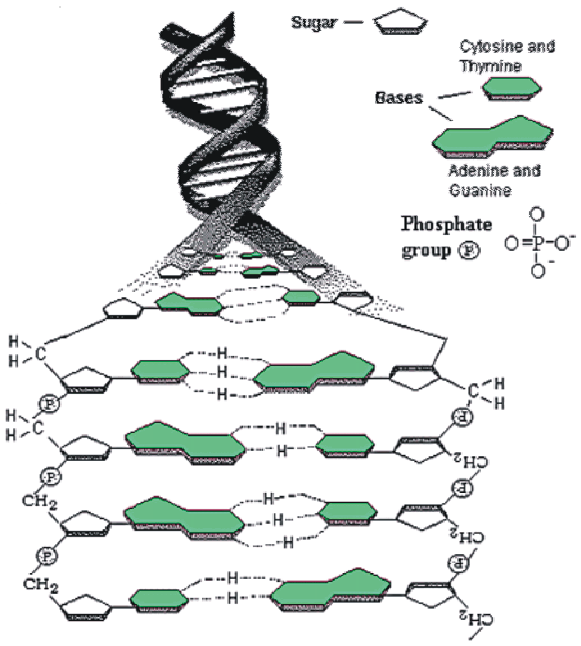

Figure 1. Two views of DNA molecule (Taken from the National Health Museum, US)

Where and how does the metal bind? Depending on the type of metal ion, its binding preference and its co-ligands, binding may occur directly between the metal and the nucleobase (ring, sugar, phosphate) or in an indirect manner (H-bonding, stacking) between co-ligands and the nucleobase.

In order to study the metal-DNA interaction at the atomic level, model

nucleobases (with N(1) alkylated pyrimidines and N(9) alkylated purines) are frequently applied in this research. It simplifies the large size of the nucleic acids and provides the best chance of synthesizing and extensively characterizing the products and derivatives. Some selected examples of metal-binding sites are shown in Figure 2. Metal binding can take place at endocyclic N atoms, deprotonated exocyclic N atoms, exocyclic O atoms and aromatic C atoms. Chelate formation through an endocyclic N atom and an exocyclic group, such as O or NH^- groups, is likewise possible. Multiple metal-binding modes and combinations are feasible. Coligands of the metal can influence the binding site at the nucleobase, e.g. by exercising steric constraints.[2,3]

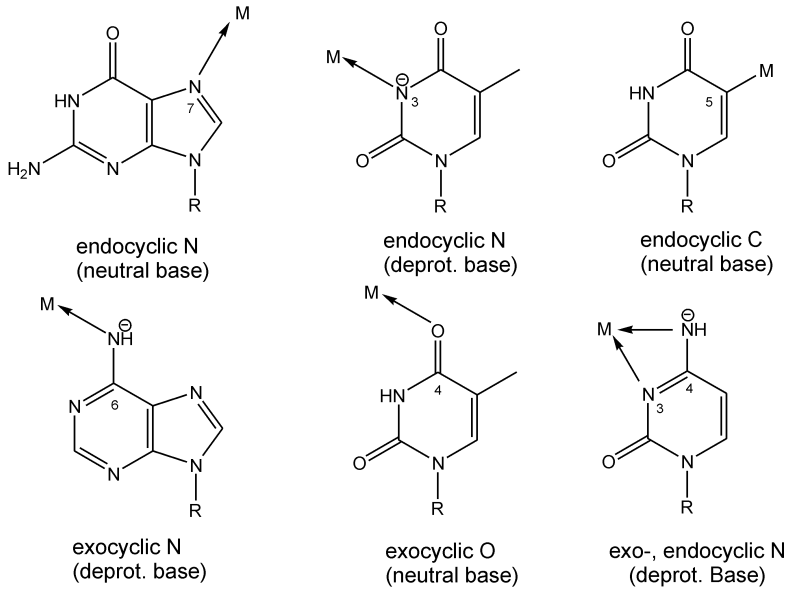

Figure 2. Selected metal (M) binding patterns to heterocyclic parts of nucleobases. Multiple M binding modes and combinations are possible. (Adopted from ref. 3.)

Related to these investigations on metal-DNA interactions, Cisplatin, one of the most used anticancer drugs, has been extensively studied.[4] Much has been learned till now concerning the mode of Cisplatin action on DNA. After Cisplatin enters the cell, it is usually converted to the active form by aquation. Then it forms with DNA mono- and diadducts at the heterocyclic regions of the

nucleobases. This is possible both inside the nucleus and in the mitochondria. The kinetically preferred binding sites are the guanine-N(7) and adenine-N(7) sites, which are located in the major groove of DNA. The most abundant adducts are *cis*-$Pt^{II}(NH_3)_2$ cross links with the N(7) sites of the two adjacent guanine bases, so-called G,G-intrastrand adducts. They account for ca. 50-60% of all identified DNA adducts, and are widely believed to be responsible for the biological effect. The formation of Cisplatin adducts on DNA triggers a cascade of events carried out by different proteins. This may lead to either repair of the lesion or apoptosis, hence cell death. Details of these processes are presently not well understood.[5]

Supramolecular Chemistry

Supramolecular chemistry has been defined by one of its leading proponents, Jean-Marie Lehn, as the 'chemistry of molecular assemblies and of the intermolecular bond'.[6,7] Beyond the molecule, supramolecular chemistry aims at developing highly complex chemical systems from components interacting by noncovalent intermolecular forces. Some important aspects of the supramolecular chemistry are listed further on:

— Self-assembly

Molecular self-assembly is a process in which molecules spontaneously form ordered aggregates; the interactions involved are generally weak and noncovalent, and include hydrogen bonding, electrostatic interactions (ion-ion, ion-dipole, dipole-dipole), as well as hydrophobic, π-π stacking, and van der Waals forces. However, relatively weak covalent bonds, such as coordination bonds between metal ions and ligands are increasingly recognized as being appropriate for self-assembly.[8]

The preparation of specific synthetic molecular assemblies represents a challenging problem, but supramolecular chemistry has now advanced to the point where the task may be addressed. The “molecular library” strategy, first applied by Verkade in 1980’s,[9] was later elaborated by Fujita[10] and systematized by Stang.[11] According to this design approach, construction of almost any type of macrocyclic system that contains transition metals can be achieved by assessing the appropriate angles between the binding sites of the donor and accepter subunit.

— Template

Specificity is an important goal in the application of self-assembly to the formation of defined supramolecular chemistry structures that can also be favored over non-specific oligomers, if “secondary effects” stabilize one defined species over all others.[12] Templates[13] represent a particular type of such secondary effects in that the geometry of the assembly receives structural information from its environment (the template) rather than its own properties. However, the control of mixture compositions by templating is a tempting challenge and the design of suitable templates is by no means trivial.

More recently, different kinds of templating strategies were used by Fujita for coordination architectures. For example, in the same system, large templates such as dibenzoyl induce the formation of an open square-pyramidal cone via parallel linkage, while small tetrahedral templates such as CBr_4 induce the templation of a closed tetrahedron structure via antiparallel linkages.[14] An aromatic sandwich compound is obtained in the presence of a triphenylbenzene template.[15] Some templates can be removed and be refilled by various organic molecules.[16] A nontubular structure is just formed with the assistance of a rodlike template.[17,18]

— Molecular Recognition

Since Pedersen's discovery of synthetic crown ethers in the later 1960s,[19,20] there has been a growing interest in the phenomenon of molecular recognition. The study of crown ethers and related compounds has, in fact, given rise to a new branch of chemistry known as 'host-guest' (or supramolecular) chemistry. In host-guest systems, a host species is developed in an attempt to recognize selectively a desired guest and to coordinate in some manner to that guest, thus to form a complex. Most of these complexes can also be referred to as supramolecular systems because the host-guest pairs have different characteristics than would have a simple non-interacting mixture of the host and guest. While many kinds of molecular species can form complexes, their utility as hosts is quite limited unless there is a mechanism in place to allow the species to distinguish between different guest species. A number of different factors can be used to affect changes in a potential host species to allow for differentiation of various guests. Among the changes in the host cavity are the size of the cavity, its shape, the number of coordination sites, and the type of the coordinating species.[21]

The concept of crown ether has lately been extended by Pecoraro et al. to metallacrown analogs.[22] According to this concept, the methylene carbons of standard crown ether are substituted by transition metal ions and nitrogen atoms. Because of the nature of the metallacrown analogy, it is possible that they could function not only as cation or anion recognition agents, but they may also be able to selectively bind ionic compounds, recognizing the cation and the anion simultaneously.

Many supramolecular hosts have been synthesized to investigate the role of the interactions through the molecular recognition of guests. Depending on the properties of the hosts, guest molecules could be simple aions, such as

spherical halides, trigonal planar nitrates, and tetrahedral sulphates etc.,[23] and simple cations, such as K^+, Na^+, and Li^+ etc.[24,25] The scope of the guest molecules is likewise involved in biological systems, such as nucleosides, nucleotides, amino acids, peptides, and small organic molecules.[26] For example, the macrocyclic organopalladium hosts, synthesized by Loeb et al., can recognize nucleobases,[27] and chiral metalloporphyrin receptors show preferential binding to amino acids.[28] Stang et al. synthesized a series of platinum and palladium macrocyclic squares for host-guest complexation using a dihydroxynaphthalene compound as an example. Fish et al., on the other hand, reported the molecular recognition of aromatic and aliphatic amino acid guests by cyclic Cp*Rh-nucleobase, nucleoside, nucleotide trimers in aqueous solution at physiological pH. This could be considered as the simplest model for the interactions between DNA/RNA bases and their binding proteins.[29,30,31]

— Dynamic combinational chemistry

Dynamic combinational chemistry (DCC) has actively developed in recent years.[32,33,34] It relies on the dynamic generation of molecular and supramolecular diversity through the reversible combination of covalently and noncovalently linked building blocks. The virtual combinational libraries (VCLs), comprised of all possible combinations that may potentially be generated in dynamic equilibrium, supply the DCC requirements for extensive libraries of molecules. This DCC/VCLs approach is actually expressed among all those accessibles, which are expected to be presenting the strongest interaction with a given target.[35] DCC is thus rooted in supramolecular chemistry,[4] being based on two of its main themes, self-assembly in the generation of the library constituents and molecular recognition in their interaction with the target entity.

Aim of the Project

According to the “Molecular library” approach proposed by Stang,[10] the molecular architecture is determined by the geometry of metal entities and by the geometrical disposition of donor atoms at the ligand(s). Appling *cis*- metal binding sites and N-heterocyclic ligands, such as model nucleosides (1-methylcytosine and cytidine), 2-aminopyridine, pyrazine and 2,2’-bipyrazine, three-dimensional metal complexes can be designed and synthesized. Particular attention is paid to steric effects of the co-ligand and their influence on the size and structure of the complex formed.

The resulting complexes are used for host-guest interaction studies. Depending on the charge, dimensionality and topology, they function as anion receptors and for molecular encapsulation. The affinity of a guest for a host is reflected by the association constant for the binding process.

Small biological molecules, such as amino acids, nucleobases and oligonucleotides, are likewise applied to investigate their interactions with the synthesized metal complexes. Moreover, DNA condensation and aggregation with metal complexes shall be studied by applying Atomic Force Microscopy.

References

[1] (a) Katz, S. *J. Am. Chem. Soc.* **1952**, *74*, 2238. (b) Shack, J.; Jenkins, R. J.; Thompsett, J. M. *J. Biol. Chem.* **1953**, *203*, 373.

[2] Lippert, B. Coord. Chem. Rev. **2000**, *200-202*, 487-516.

[3] Lippert, B.; Müller, J. *Concepts and Models in Bioinorganic Chemistry*, Wiley-VCH, Weinheim, eds. Kraatz, H. B.; Metzler-Nolte, N. **2006**, 137-159.

[4] Rosenberg, B.; VanCamp, L.; Trosko, J. E.; Mansour, V. H. *Nature,* **1969**, *222*, 385.

[5] Wang, D.; Lippard, S. J. *Nat. Drug Discovery*, **2005**, *4*, 307.

[6] Lehn, J.-M. *Supramolecular Chemistry: Concepts and Perspectives* (VCH, New York), **1995**.

[7] Atwood, J. L.; Davies, J. E. D.; MacNicol, D. D.; Vögtle, F.; Lehn, J.-M.; eds. *Comprehensive Supramolecular Chemistry* (Pergamon, Oxford), **1996**.

[8] (a) Olenyuk, B.; Whiteford, J. A.; Fechtenkotter, A.; Stang, P. J. *Nature,* **1999**, *398*, 796. (b) Lehn, J.-M. *NATO ASI Ser., Ser. E* **1996**, *320*, 511.

[9] Stricklen, P. M.; Volcko, E. J.; Verkade, J. G. *J. Am. Chem. Soc.* **1983**, *105*, 2494.

[10] (a) Fujita, M.; Ogura, K. *Coord. Chem. Rev.* **1996**, *148*, 249. (b) Fujita, M. *Chem. Soc. Rev.* **1998**, *27*, 417.

[11] (a) Olenyuk, B.; Fechtenkötter, A.; Stang, P. J. *J. Chem. Soc. Dalton Trans.* **1998**, 1707. (b) Stang. P. J. *Chem. Eur. J.* **1998**, *4*, 19. (c) Leininger, S.; Olenyuk, B.; Stang, P. J. *Chem. Rev.* **2000**, *100*, 853.

[12] Schalley, C. A.; Lützen, A.; Albrecht, M. *Chem. Eur. J.* **2004**, *10*, 1072.

[13] (a) Gerbeleu, N. V.; Arion, V. B.; Burgess, J. *Template Synthesis of Macrocyclic Compounds*, Wiley-VCH, Weinheim, **1999**. (b) Diederich, F.; Stang, P. J. *Templated Organic Synthesis*, Wiley-VCH, Weinheim, **2000**.

[14] Umemoto, K.; Yamaguchi, K.; Fujita, M. *J. Am. Chem. Soc.* **2000**, *122*, 7150.

[15] Kumazawa, K.; Yamanoi, Y.; Yoshizawa, M.; Kusukawa, T.; Fujita, M. *Angew. Chem., Int. Ed.* **2004**, *43*, 5936.

[16] Kumazawa, K.; Biradha, K.; Kusukawa, T.; Okano, T.; Fujita, M. *Angew. Chem., Int. Ed.* **2003**, *42*, 3909.

[17] (a) Aoyagi, M.; Biradha, K.; Fujita, M. *J. Am. Chem. Soc.* **1999**, *121*, 7150. (b) Tominage, M.; Tashiro, S.; Aoyagi, M.; Fujita, M. *Chem. Comm*. **2002**, 2038. (c) Aoyagi, M.; Tashiro, S.; Tominage, M.; Biradha, K.; Fujita, M. *Chem. Comm.* **2002**, 2036. (d) Tashiro, S.; Tominage, M.; Kusukawa, T.; Sakamoto, S.; Yamaguchi, K.; Fujita, M. *Angew. Chem., Int. Ed.* **2003**, *42*, 3267.

[18] Fujita, M.; Tominage, M.; Hori, A.; Therrien, B. *Acc. Chem. Res.* **2005**, *38*, 371.

[19] Pedersen, C. J. *J. Am. Chem. Soc.* **1967**, *89*, 2495.

[20] Pedersen, C. J. in *Synthetic Multidentate Macrocyclic Compounds*, eds. Izatt, R. M.; Christensen, J. J.; (Academic Press, New York, **1978**), Vol. 1.

[21] Pecoraro, V. L.; Stemmler, A. J.; Gibney, B. R.; Bodwin, J. J.; Wang, H.; Kampf, J. W.; Barwinski, A. *Prog. Inorg. Chem.* **1997**, *45*, 83.

[22] (a) Lah, M. S.; Pecoraro, V. L. *Comments Inorg. Chem.* **1990**, *11*, 59. (b) Pecoraro, V. L.; Stemmler, A. J.; Gibney, B. R.; Bodwin, J. J.; Wang, H.; Kampf, J. W.; Barwinski, A. *Prog. Inorg. Chem.* **1997**, *45*, 83. (c) Bodwin, J. J.; Cutland, A. D.; Malkani, R. G.; Pecoraro, V. L. *Coord. Chem. Rev.* **2001**, *216-217*, 489.

[23] Bowman-James, K. *Acc. Chem. Res.* **2005**, *38*, 671.

[24] Gibney, B. R.; Wang, H.; Kampf, J. W.; Pecoraro, V. L. *Inorg. Chem*. **1996**, *35*, 6187.

[25] Lah, M. S.; Pecoraro, V. L. *J. Am. Chem. Soc.* **1989**, *111*, 7258.

[26] (a) Fish, R. H.; Jaouen, G. *Organometallics,* **2003**, *22*, 2166. (b) Badjic, J. D.; Nelson, A.; Cantrill, S. J.; Turnbull, W. B.; Stoddart, J. F. *Acc. Chem. Res.* **2005**, *38*, 723.

[27] Kickham, J. E.; Loeb, S. J.; Murphy, S. L. *J. Am. Chem. Soc.* **1993**, *115*, 7031 and references therein.

[28] Mizutani, T.; Ema, T.; Tomita, T.; Kuroda, Y.; Ogoshi, H. *J. Am. Chem. Soc.* **1994**, *116*, 4240 and references therein.

[29] Chen, H.; Maestre, M. F.; Fish, R. H. *J. Am. Chem. Soc.* **1995**, *117*, 3631.

[30] Smith, D. P.; Baralt, E.; Morales, B.; Olmstead, M. M.; Maestre, M. F.; Fish, R. H. *J. Am. Chem. Soc.* **1992**, *114*, 10647.

[31] Smith, D. P.; Kohen, E.; Maestre, M. F.; Fish, R. H. *Inorg. Chem.* **1993**, *32*, 4119.

[32] Lehn, J.-M. *Chem. Eur. J.* **1999**, *5*, 2455.

[33] Cousin, G. R.; Poulsen, S. A.; Sanders, J. K. M. *Curr. Opin. Chem. Biol.* **2000**, *4*, 270.

[34] Lehn, J.-M.; Eliseev, A. *Science,* **2001**, *291*, 2331.

[35] Davis, A. V.; Robert, M. Y.; Kenneth, N. R. *Proc. Natl. Acad. Sci.* USA **2002**, *99*, 4793.

B LIGANDS

1-Methylcytosine

1-Methylcytosine is used as a model for the nucleoside cytidine of DNA and RNA in research work.[1] The methyl group at the N(1) position substitutes the sugar entity of the nucleoside or the sugar phosphate entity of the nucleotide, because this part is virtually never involved in Pt and Pd binding. In aqueous medium, 1-methylcytosine exists predominantly as a keto-amino-tautomer (Scheme 1). The endocyclic N(3) site is the preferred binding site of the soft Pt and Pd electrophiles[2] under neutral conditions (pK_{a1} = 4.9),[3] while the exocyclic N(4) site, due to the delocalization of the lone eletron pair into the π-system of the pyrimidine ring, is a poor nucleophile and only coordinates to metals following prior deprotonation (pK_{a2} = 16.7).[4] Metal coordination to N(3) leads to a decrease of pK_{a2} value,[5] therefore permitting Pt^{II} coordination at N(4) to take place in neutral and even moderately acidic solution.[6] Details of these process (metal migration from N(3) to N(4); formation of dinuclear *N3,N4*-bridged species) have been studied,[7] but are not clarified in every detail. There is even the possibility that redox processes may be involved.[8] The other potential metal binding site is O(2). Metal coordination to N(3) effectively reduces the available negative electrostatic potential at O(2); therefore with *N3,O2*-bridged complexes the metal-O(2) interactions usually are weaker than those between the metal and N(3).[5] The possible metal coordination modes of cytosine are presented with selected examples in Table 1.

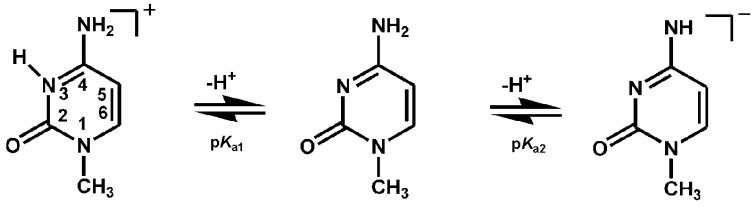

Scheme 1. Acid-base equilibria of 1-methylcytosine.

Table 1. Different coordination modes of cytosine with metal entities.

Coordination modes	Complexes	Lit.
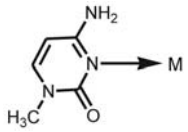	*cis*-$[Pt(NH_3)_2(1\text{-}MeC)_2]^{2+}$	9
	trans-$[Pt(NH_3)_2(1\text{-}MeC)_2]^{2+}$	10
	$[Pt(NH_3)(1\text{-}MeC)_3]^{2+}$	11
	cis-$[Pt(PMe_3)_2(1\text{-}MeC)_2]^{2+}$	12
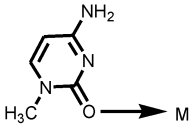	$[Ni(en)_2(1\text{-}MeC\text{-}O_2)]^{2+}$	13
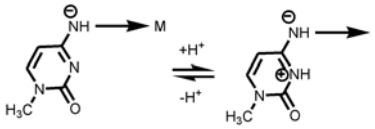	*trans, trans, trans*-$[Pt(OH)_2(1\text{-}MeC\text{-}N4)_2(NH_3)_2]^{2+}$	8
	trans-$[Pt(1\text{-}MeC\text{-}N4)_2(NH_3)_2]^{2+}$	14
	trans-$[Pt(1\text{-}MeC\text{-}N4)Cl_2(1\text{-}MeC\text{-}N3)]^{2+}$	15
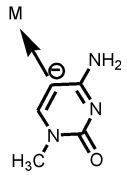	$[Hg(cytidine\text{-}C5)X]^{+}$	16
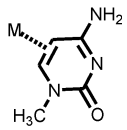	$[Ru^{II}(hedta)(cytosine\text{-}C5\text{-}C6)]^{-}$	17
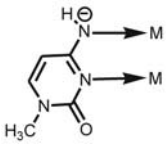	*cis*-$[Pt(1\text{-}MeC\text{-}N3,N4)(NH_3)_2]_2^{2+}$	18
	trans-$[(NH_3)_2Pt(1\text{-}MeC^{-}\text{-}N3,N4)MY]^{n+}$; M = Pd^{2+}	6
	trans-$[(NH_3)_2Pt(1\text{-}MeC^{-}\text{-}N3,N4)Hg]^{2+}$	19
	trans-$[(NH_3)_2Pt(1\text{-}MeC^{-}\text{-}N3,N4)Cu]^{2+}$	20
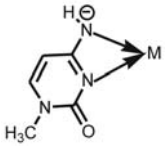	*trans*-$[Pt^{IV}(1\text{-}MeC^{-}\text{-}N3,N4)(OH)(1\text{-}MeC)(NH_3)_2]^{2+}$	21
	trans,trans-$[Pt^{IV}(1\text{-}MeC^{-}\text{-}N3,N4)_2(NH_3)_2]^{2+}$	
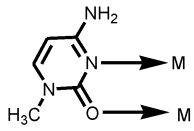	$[Ag(NO_3)(1\text{-}MeC\text{-}N3,O2)]_2$	22
	$[(NH_3)_2Pt(1\text{-}MeU\text{-}N3,O4)(1\text{-}MeC\text{-}N3,O2)Cu(1\text{-}MeC\text{-}N3,O2)(1\text{-}MeC\text{-}N3,O4)Pt(NH_3)_2]^{4+}$	5
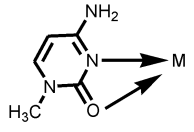	$[Tl(1\text{-}MeC\text{-}O2,N3)]^{+}$	23
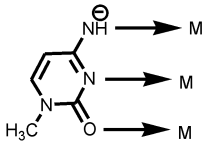	*trans*-$[(NH_3)_2Pt(1,5\text{-}DiMeC^{-}\text{-}O2,N3,N4)_2Ag_2]^{2+}$	24
	cis-$[(NH_3)_2Pt(1\text{-}MeC^{-}\text{-}O2,N3,N4)_2\{Pd(en)\}_2]^{4+}$	25

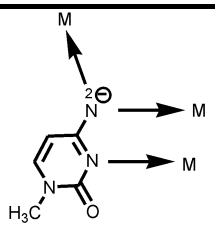	$[(CH_3Hg)_3(1\text{-}MeC^{2-}\text{-}N3,N4)]^+$	26
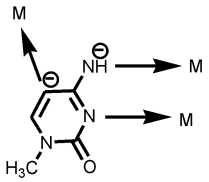	$[\{(NH_3)_2Pt(1\text{-}MeC^{2-}\text{-}N3,N4,C5)_2Hg_3(OH)(NO_3)\}_2]^{4+}$	27

Pt^{II} or Pd^{II} coordinate to 1-methylcytosine in different modes, which can frequently be deduced from ^1H NMR spectroscopy. For example, Pt^{II} coordination to the N(3) position causes the electron density of the pyrimidine ring to become reduced, so that the resonances of protons on the aromatic ring (H(5)/H(6)) shift downfield. In contrast, Pt^{II} coordination to the N(4) position of the anionic nucleobase, leads to an upfield shift of aromatic protons. Two examples are listed in Table 2.

Table 2. Chemical shift (ppm) of free, N(3) platinum coordinated[10] and N(3), N(4) platinum coordinated[6] 1-methylcytosine in D_2O.

Compound	H6(d)	H5(d)	N1-CH_3(s)	pD
1-MeC	7.55	5.95	3.35	7.0
trans-$[Pt(NH_3)_2(1\text{-}MeC\text{-}N3)_2]^{2+}$	7.65	6.07	3.45	7.4
trans-$[(NH_3)_2Pt(1\text{-}MeC^{-}\text{-}N3,N4)_2PdCl]^+$	7.01	5.57	3.30	5.0

Recently, It was also found that, at high pH, the metal migration process from N(3) to N(4) competes with hydrolytic deamination of the exocyclic amino group of the cytosine nucleobase to give uracil.[28]

Cytidine

Cytidine (Cytd) is one of the pyrimidine nucleosides in RNA, composed of cytosine and ribose (Scheme 2). It is involved in important functions in the cellular metabolism and is modified in numerous ways to give enzyme

inhibitors, antiviral agents, and anticancer agents. The pK_{a1} value of cytidine (4.2) is slightly lower than that of the parent cytosine nucleobase. There are relatively few crystal structures of Pt^{II} or Pd^{II} complexes containing cytidine or cytidine phosphate. To the best of our knowledge from the Cambridge Structural Database, only four examples have been reported so far; namely $[Pt(5'\text{-cytidine monophosphate})(en)]_2(H_2O)_2$ with 5'-cytidine monophosphate acting as a bridge ligand through N(3) and one oxygen atom of the phosphate anion;[29] [*cis*-$Pt(\text{cytidine-3'-phosphate})_2(NH_3)_2$], in which *cis*-$Pt^{II}(NH_3)_2$ binds to N(3) of two cytidine-3'-phosphate units;[30] two monomers of Pt and Pd coordinated with N(3) of cytidine.[31,32]

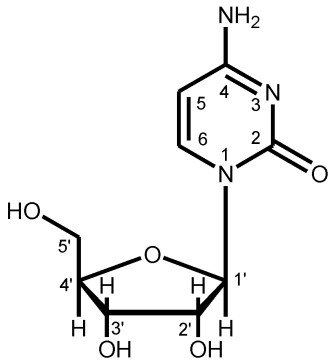

Scheme 2. Composition of cytidine.

2-Aminopyridine

2-Aminopyridine (Hampy) is a versatile ligand widely applied in coordination chemistry.[33] Established metal binding positions include the endocyclic nitrogen atom[34] or the exocyclic amino group,[35] occasionally in equilibrium,[36] and simultaneously both positions, either in a chelating[37] or bridging fashion[38] (Scheme 3).

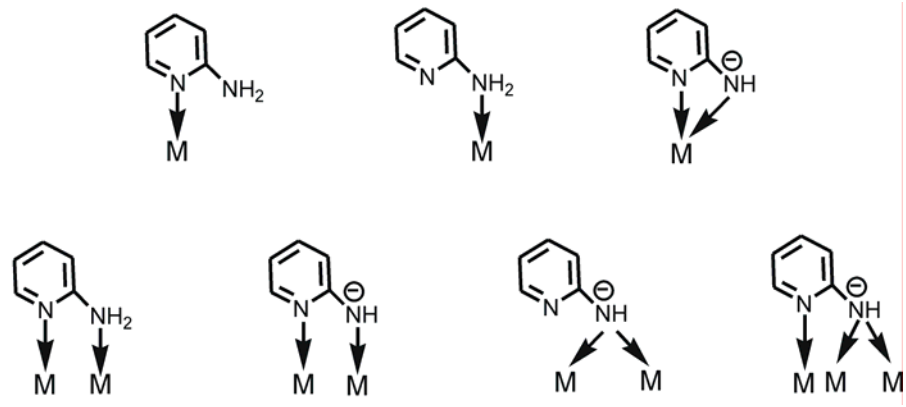

Scheme 3. Known coordination modes of 2-aminopyridine.

The ring nitrogen atom N(1) can be protonated under acidic conditions (pK_{a1} between 6.71[39] and 6.89[40]). A +2 cation is formed in strongly acidic medium (pK_a = -7.55[40]) and is not further considered here. The exocyclic amino group N(2) can be deprotonated in strongly basic medium (pK_{a2} between 23.5[39] and 27.7[41]). Relevant acid-base equilibria are presented in Scheme 4. Although the pK_{a2} value is high, metal coordination can take place at the exocyclic amino group without previous deprotonation. In contrast to 1-methylcytosine, the exocyclic amino group of 2-aminopyridine has its lone electron pair located at the exocyclic N atom rather than delocalized into the pyridine ring. Metal binding to the electron pair causes a dramatic increase in acidity of the amino protons. Consequently, amide formation is facile and enables a second metal to bind to this site.

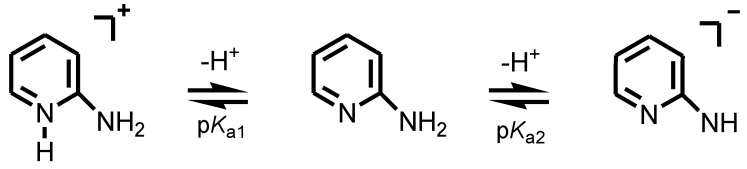

Scheme 4. Acid-base equilibria of 2-aminopyridine (twofold protonated form is not shown and potential minor tautomers of neutral and cationic species are ignored).

Formation of multinuclear (n = 2, 3) complexes with ampy ligands following deprotonation of the exocyclic amino group appears to be quite common and is of interest to the chemistry of small clusters,[42] to metal-metal bond

formation,[38, 43] as well as the generation of receptor molecules,[44] among others. Yet another interesting aspect of 2-aminopyridine and its derivatives relates to their use as surrogates of the nucleobase cytosine in artificial nucleobase triplets.[45]

Pyrazine

Pyrazine (1,4-diazine, pz) is the smallest, and hence most rigid, linear aromatic linker available for self-assembly processes.[46] It is less basic than pyridine, pyridazine and pyrimidine. The acid-base equilibria of pyrazine are shown in Scheme 5. The pK_{a1} value is between 0.6[47] and 1.1[48], while pK_{a2} is –6.25.[49] The two nitrogen atoms contribute one electron each to the aromatic π-system and have lone pairs in sp^2 orbitals in the plane of the ring.

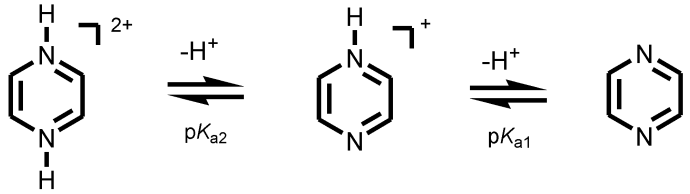

Scheme 5. Acid-base equilibria of pyrazine.

Pyrazine can be considered as a classical ligand in transition metal chemistry due to the multifaceted roles it has played in fundamental areas of chemistry. For example, pz-bridged mixed valence dinuclear Ru^{II}/Ru^{III} complexes were instrumental in understanding intramolecular electron transfer (ET),[50] related compounds were involved in studies of magnetic exchange interactions,[51] and solvent dynamic properties were evaluated in the process of ET between pyrazine-bridged Ru_3 clusters in combination with vibrational spectroscopy.[52, 53] Modifications of the basicity of the pyrazine ring as a consequence of coordination of transition metal fragments has been another area of topical research,[54] as has been the fluxional behavior of this ligand.[55] Finally, pyrazine-bridged dinuclear complexes of Ru^{II} and Pt^{II} have been prepared and studied with regard to their antitumor activity.[56] More recently, pyrazine is commonly used as a ditopic donor ligand in the generation of self-

assembling coordination networks and metal-based supramolecular architectures.[57,58]

2,2'-Bipyrazine

2,2'-bipyrazine (2,2'-bpz) is composed of two pyrazine rings connected via the C(2)-C(2') positions. It undergoes rotation about the central C(2)-C(2') bond (5.4 kcal mol^{-1}),[59] giving rise to *cis*- and *trans*- conformers (Scheme 6).

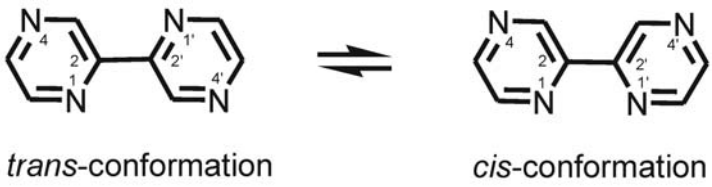

Scheme 6. 2,2'-bipyrazine in different conformations.

The acid-base equilibria of 2,2'-bipyrazine are shown in Scheme 7 . The pK_{a1} and pK_{a2} values are 0.45 and –1.35, respectively.[60] Since the ring nitrogen atoms are unprotonated over a wide pH range, 2,2'-bpz is considered to be a rather versatile ligand.

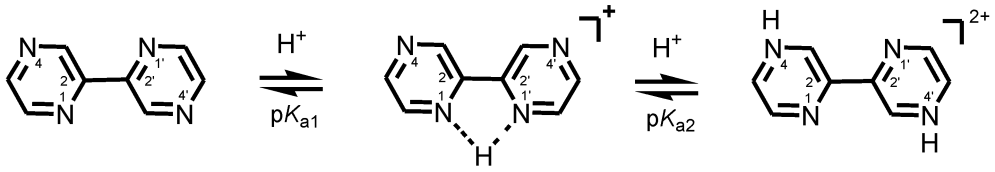

Scheme 7. Acid-base equilibria of 2,2'-bipyrazine.

Four coordination modes of 2,2'-bipyrazine have been found up to now, which are depicted in Scheme 8. The chelation mode (i) via N(1) and N(1') positions was confirmed in [Pd(en)(2,2'-bpz-*N1,N1'*)]$(ClO_4)_2$.[61] Mode (ii) and mode (iv) via N(4) and N(4') positions in *trans*- and *cis*- conformations, respectively, are realized in $[\{Pt(en)(2,2'\text{-bpz-}N4,N4')\}_3]^{6+}$ with different anions.[62] All of them can be applied as building blocks for larger aggregates by combining them

with suitable metal fragments according to mode (iii). Depending on the geometry of the metal fragments, either hexanuclear, cup-shaped species form with *cis* geometry metal fragments,[63] or a flat triangle with *trans* geometry metal fragments.[64] (Details see chapter IV.)

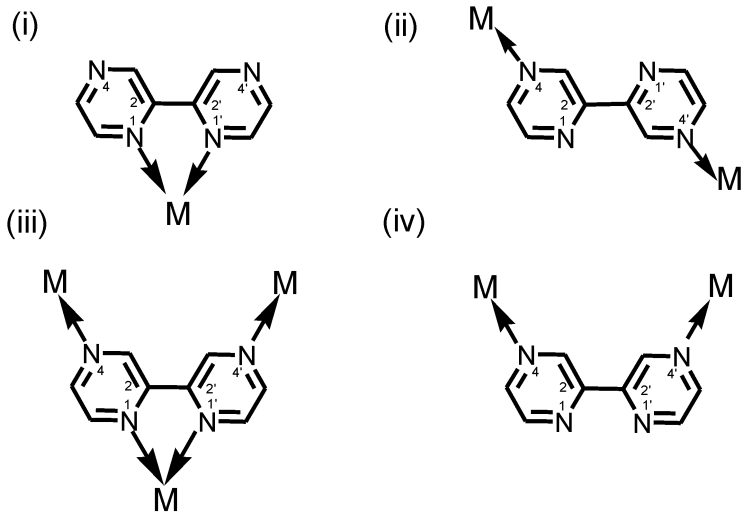

Scheme 8. Known coordination modes of 2,2'-bipyrazine (Adapted from ref. 63).

References

[1] Frederick, W.; Bernhauer, K. *Z. Physiol. Chem.* **1959***, 317*, 116,

[2] (a) Mansy, S.; Rosenberg, B.; Thomson, A. J. *J. Am. Chem. Soc.* **1973**, *95*, 1633. (b) Lippert, B. *Prog. Inorg. Chem.* **1989**, *37*, 1.

[3] Krumm, M. *Diplomarbeit*, University Dortmund, **1989**.

[4] Harris, M. G.; Stewart, R. *Can. J. Chem.* **1977**, *55*, 3807.

[5] Lippert, B.; Thewalt, U.; Schöllhorn, H.; Goodgame, D. M. L.; Rollins, R. W. *Inorg. Chem.* **1984**, *23*, 2807.

[6] (a) Krumm, M.; Lippert, B.; Randaccio, L.; Zangrando, E. *J. Am. Chem. Soc.* **1991**, *113*, 5129. (b) Krumm, M.; Zangrando, E.; Randaccio, L.; Menzer, S.; Lippert, B. *Inorg. Chem.* **1993**, *32*, 700.

[7] Sanz Miguel, P. J.; Lax, P.; Lippert, B. *J. Inorg. Biochem.* **2006**, *100*, 980.

[8] Lippert, B.; Schöllhorn, H.; Thewalt, U. *J. Am. Chem. Soc.* **1986**, *108*, 6616.

[9] Schöllhorn, H.; Thewalt, U.; Raudaschl-Sieber, G.; Lippert, B. *Inorg. Chim. Acta* **1986**, *124*, 207.

[10] Lippert, B.; Lock, C. J. L.; Speranzini, R. A. *Inorg. Chem.* **1981**, *20*, 808.

[11] Faggiani, R.; Lock, C. J. L.; Lippert, B. *Inorg. Chim. Acta* **1985**, *106*, 75

[12] Trovó, G.; Valle, G.; Longato, B.; *J. Chem. Soc., Dalton Trans.* **1993**, 669.

[13] Cervantes, G.; Fiol, J. J.; Terrón, A.; Moreno, V.; Alabart, J. R.; Aguiló, M.; Gómez, M; Solans, X. *Inorg. Chem.* **1990**, *29*, 5168.

[14] Müller, J.; Zangrando, E.; Pahlke, N.; Freisinger, E.; Randaccio, L.; Lippert, B. *Chem. Eur. J.* **1998**, *4*, 397.

[15] Sanz Miguel, P. J.; Lax, P.; Willermann, M.; Lippert, B. *Inorg. Chim. Acta* **2004**, *357*, 4552.

[16] Dale, R. M. K.; Livingston, D. C.; Ward, D. C. *Proc. Natl. Acad. Sci.* USA **1973,** *70*, 2238.

[17] Zhang, S.; Holl, L. A.; Shepherd, R. E. *Inorg. Chem.* **1990**, *29*, 1012.

[18] Britten, J. F.; Lippert, B.; Lock, C. J. L.; Pilon, P. *Inorg. Chem.* **1982**, *21*, 1936.

[19] Krumm, M.; Zangrando, E.; Randaccio, L.; Menzer, S.; Danzmann, A.; Holthenrich, D.; Lippert, B. *Inorg. Chem.* **1993**, *32*, 2183.

[20] Fusch, G. *Dissertation,* University of Dortmund, **1994**.

[21] Schöllhorn, H.; Beyerle-Pfnür, R.; Thewalt, U.; Lippert, B. *J. Am. Chem. Soc.* **1986**, *108*, 3680.

[22] Kistenmacher, T. J.; Rossi, M.; Marzilli, L. G. *Inorg. Chem.* **1979,** *18*, 240.

[23] Renn, O.; Preut, H.; Lippert, B. *Inorg. Chim. Acta.* **1991**, *188*, 133.

[24] Holthenrich, D.; Krumm, K.; Zangrando, E.; Pichierri, F.; Randaccio, L.; Lippert, B. *J. Chem. Soc., Dalton Trans.* **1995**, 3275.

[25] Holthenrich, D.; Zangrando, E.; Chiarparin, E.; Lippert, B. *J. Chem. Soc., Dalton Trans.* **1997**, 4407.

[26] Charland, J. P.; Simard, M.; Beauchamp, A. L. *Inorg. Chim. Acta* **1983**, *80*, L57.

[27] Rauter, H.; Mutikainen, I.; Blomberg, M.; Lock, C. J. L.; Amo-Ochoa, P.; Freisinger, E.; Randaccio, L.; Zangrando, E.; Chiarparin, E.; Lippert, B. *Angew. Chem. Int. Ed.* **1997**, *36*, 1296.

[28] Sanz Miguel, P. J. *Dissertation,* University of Dortmund, **2006**.

[29] Louie, S.; Bau, R. *J. Am. Chem. Soc.* **1977**, *99*, 3874.

[30] Wu, S.-M.; Bau, R. *Biochem. Biophys. Res. Comm.* **1979**, *88*, 1435.

[31] Melanson, R.; Rochon, F. D. *Inorg. Chem*. **1978**, *17*, 679.

[32] Khan, B. T.; Mohan, K. M.; Khan, S. R. A.; Venkatasubramanian, K.; Satyanarayana, T. *Polyhedron* **1996**, *15*, 63.

[33] See, e.g.: (a) Mizota, M.; Sakai, K. *Acta Crystallogr., Sect. E* **2004**, *60*, m473. (b) Sakai, K.; Akiyama, N.; Mizota, M. *Acta Crystallogr., Sect. E* **2003**, *59*, m459. (c) Xu, X.; James, S. L.; Mingos, D. M. P.; White, A. J. P.; Williams, D. J. *J. Chem. Soc., Dalton Trans*. **2000**, 3783. (d) Yip, J. H. K.; Suwarno; Vittal, J. J. *Inorg. Chem*. **2000**, *39*, 3537.

[34] See, e.g.: (a) Krizanovic, O.; Sabat, M.; Beyerle-Pfnür, R.; Lippert, B. *J. Am. Chem. Soc.* **1993**, *115*, 5538. (b) Navarro Ranninger, M. C.; Martinez-Carrera, S.; Garcia-Blanco, S. *Acta Crystallogr., Sect. C* **1985**, *41*, 21. (c) Uhlig, E.; Mädler, M. *Z. Anorg. Allg. Chem.* **1965**, *338*, 199. (d) Haghighi, S.; McAuliffe, C. A.; Hill, W. E.; Kohl, H. H.; Friedman, M. E. *Inorg. Chim. Acta.* **1980**, *43*, 113.

[35] Al Obaidi, N.; Hamor, T. A.; Jones, C. J.; Mc Cleverty, J. A.; Paxton, K. *J. Chem. Soc., Dalton Trans.* **1987**, 1063

[36] Marzilli, L. G.; Summers, M. F.; Zangrando, E.; Bresciani-Pahor, N.; Randaccio, L. *J. Am. Chem. Soc.* **1986**, *108*, 4830.

[37] (a) Spannenberg, A.; Arndt, P.; Kempe, R. *Angew. Chem. Int. Ed.* **1998**, *37*, 832. (b) Kempe, R.; Arndt, P. *Inorg. Chem.* **1996**, *35*, 2644. (c) Calhorda, M. J.; Carrondo, M. A. A. F. De C. T.; Gomes da Costa, R.; Dias, A. R.; Duarte, M. T. L. S.; Hursthouse, M. B. *J. Organomet. Chem.* **1987**, *320*, 53.

[38] (a) Cotton, F. A.; Yokochi, A. *Inorg. Chem.* **1998**, *37*, 2723. (b) Li, Y.; Han, B.; Kadish, K. M.; Bear, J. L. *Inorg. Chem.* **1993**, *32*, 4175. (c) Chakravarty, A. R.; Cotton, F. A.; Tocher, D. A. *Inorg. Chem.* **1984**, *23*, 4693.

[39] Stewart, R.; Harris, M. G. *J. Org. Chem.* **1978**, *43*, 3123.

[40] Brignell, P. J.; Johnson, C. D.; Katritzky, A. R.; Shakir, N.; Tarhan, H. O.; Walter, G. *J. Chem. Soc.* **1967**, *Sec. B*, 1233.

[41] Bordwell, F. G.; Singer, D. L.; Satish, A. V. *J. Am. Chem. Soc.* **1993**, *115*, 3543.

[42] See, e.g.: (a) Deeming, A. J.; Peters, R.; Hursthouse, M. B.; Backer-Dirks, J. D. J. *J. Chem. Soc.*, *Dalton Trans*. **1982**, 1205. (b) Cabeza, J. A.; Del Rio, I.; Llammazares, A.; Riera, V. *Inorg. Chem*. **1995**, *34*, 1620. (c) Andreu, P. L.; Cabeza, J. A.; Llamazares, A.; Riera, V.; García-Granda, S.; Van der Maelen, J. F. *J. Organomet, Chem*. **1992**, *434*, 123.

[43] See, e.g.: (a) Charland, J.-P.; Beauchamp, A. L. *J. Crystallogr. Spectrosc. Res.* **1985**, *15*, 581. (b) Yip, J. H. K.; Feng, R.; Vittal, J. J. *Inorg. Chem*., **1999**, *38*, 3586. (c) Schneider, A.; Freisinger, E.; Beck, B.; Lippert, B. *J. Chem. Soc., Dalton Trans*. **2000**, 837.

[44] (a) Beck, B.; Schneider, A.; Freisinger, E.; Holthenrich, D.; Erxleben, A.; Albinati, A.; Zangrando, E.; Randaccio, L.; Lippert, B. *Dalton Trans*. **2003**, 2533. (b) Rauter, H.; Mutikainen, I.; Blomberg, M.; Lock, C. J. L.; Amo-Ochoa, P.; Freisinger, E.; Randaccio, L.; Zangrando, E.; Chiarparin, E.; Lippert, B. *Angew. Chem. Int. Ed*. **1997**, *36*, 1296.

[45] (a) Strazewski, P.; Tamm, C. *Angew. Chem.* **1990**, *102*, 37. (b) Hildbrand, S.; Leumann, C. J. *Angew. Chem.* **1996**, *108*, 2100. (c) Hildbrand, S.; Blaser, A.; Parel, S. P.; Leumann, C. J. *J. Am. Chem. Soc.* **1997**, *119*, 5499. (d) Cassidy, S. A.; Slickers, S. P.; Trent, J. O.; Capalidi, D. L.; Roselt, P. D.; Reese, C. B.; Neidle, S.; Fox, K. R. *Nucleic Acids Res.* **1997**, *25*, 4891.

[46] Carlucci, L.; Ciani, G.; Proserpio, D. M.; Rizzato, S. *J. Chem. Soc., Dalton Trans.* **2000**, 3821.

[47] Albert, A.; Phillips, J. N. *J. Chem. Soc.* **1956**, 1294.

[48] Keyworth, D. A. *J. Org. Chem.* **1959**, *24*, 1355.

[49] Brignell, P. J.; Johnson, C. D.; Katritzky, A. R.; Shakir, N.; Tarhan, H. O.; Walker, G. *J. Chem. Soc. B* **1967**, 1233.

[50] (a) Creutz, C. *Prog. Inorg. Chem.* **1983**, *30*, 1. (b) Taube, H. *Angew. Chem. Int. Ed.* **1984**, *23*, 329.

[51] See, e.g.: Cotton, F. A.; Kim, Y.; Ren, T. *Inorg. Chem.* **1992**, *31*, 2608.

[52] (a) Ito, T.; Hamaguchi, T.; Nagino, H.; Yamaguchi, T.; Washington, J.; Kubiak, C. P. *Science* **1997**, *277*, 660. (b) Ito, T.; Hamaguchi, T.; Nagino, H.; Yamaguchi, T.; Kido, H.; Zavarine, I. S.; Richmond, T.; Washington, J.; Kubiak, C. P. *J. Am. Chem. Soc.* **1999**, *121*, 4625.

[53] (a) Londergan, C. H.; Salsman, J. C.; Ronco, S.; Dolkas, L. M.; Kubiak, C. P. *J. Am. Chem. Soc.* **2002**, *124*, 6236. (b) Londergan, C. H.; Kubiak, C. P. *Chem. Eur. J.* **2003**, *9*, 5962.

[54] See, e.g.: (a) Ford, P.; Rudd, D. P.; Gaunder, R.; Taube, H. *J. Am. Chem. Soc.* **1968**, *90*, 1187. (b) Taube, H. *Pure Appl. Chem.* **1979**, *51*, 901. (c) Slep, L. D.; Pollak, S.; Olabe, J. A. *Inorg. Chem.* **1999**, *38*, 4369.

[55] (a) Chen, Y.; Shepherd, R. E. *Inorg. Chem.* **1998**, *37*, 1249. (b) Krumm, M.; Zangrando, E.; Randaccio, L.; Menzer, S.; Lippert, B. *Inorg. Chem.* **1993**, *32*, 700.

[56] (a) Iengo, E.; Mestroni, G.; Geremia, S.; Calligaris, M.; Alessio, E. *J. Chem. Soc., Dalton Trans.* **1999**, 3361. (b) Komeda, S.; Kalayda, G. V.; Lutz, M.; Spek, A. L.; Yamanaka, Y.; Sato, T.; Chikuma, M.; Reedijk, J. *J. Med. Chem.* **2003**, *46*, 1210.

[57] See, e.g.: (a) Carlucci, L.; Ciani, G.; Proserpio, D. M.; Sironi, A. *Angew. Chem. Int. Ed.* **1995**, *34*, 1895. (b) Carlucci, L.; Ciani, G.; Proserpio, D. M.; Sironi, A. *J. Am. Chem. Soc.* **1995**, *117*, 4562. (c) Lu, J.; Paliwala, T.; Lim, S. C.; Yu, C. ; Niu, T. ; Jacobsen, A. B. *Inorg. Chem.* **1997**, *36*, 923. (d) Tong, M.-L.; Chen, X.-M.; Yu, X.-L.; Mak, T. C. W. *J. Chem. Soc.,*

Dalton Trans. **1998**, 5. (e) Kondo, M.; Okubo, T.; Asami, A.; Noro, S.-i.; Yoshitoni, T.; Kitagawa, S.; Ishii, T.; Matsuzaka, H.; Seki, K. *Angew. Chem. Int. Ed.* **1999**, *38*, 140. (f) Carlucci, L.; Ciani, G.; Porta, F.; Proserpio, D. M.; Santagostini, L. *Angew. Chem. Int. Ed.* **2002**, *41*, 1907. (g) Kumagai, H.; Kawata, S.; Kitagawa, S. *Inorg. Chim. Acta* **2002**, *337*, 387. (h) Manson, J. L.; Arif, A. M.; Miller, J. S. *Chem. Commun.* **1999**, 1479. (i) Kraft, S.; Hanuschek, E.; Beckhaus, R.; Haase, D.; Saak, W. *Chem. Eur. J.* **2005**, *11*, 969.

[58] For coordination polymers involving substituted pyrazine ligand see, e.g.: Näther, C.; Wriedt, M.; Jess, I. *Inorg. Chem.* **2003**, *42*, 2391 and refs. cited.

[59] (a) Neto, N.; Muniz-Miranda, M. *Spectrochem. Acta* **1994**, *50A*, 357. (b) Barone, V.; Minichino, L.; Fliszar, S.; Russo, N. *Can. J. Chem.* **1988**, *66*, 1313.

[60] Crutchley, R. J.; Kress, N.; Lever, A. B. P. *J. Am. Chem. Soc.* **1983**, *105*, 1170.

[61] Schnebeck, R.-D.; Randaccio, L.; Zangrando, E.; Lippert, B. *Angew. Chem. Int. Ed.* **1998**, *37*, 119.

[62] Schnebeck, R.-D.; Freisinger, E.; Lippert, B. *Angew. Chem. Int. Ed.* **1999**, *38*, 168.

[63] Schnebeck, R.-D.; Freisinger, E.; Glahé, F.; Lippert, B. *J. Am. Chem. Soc.* **2000**, *122*, 1381.

[64] Schnebeck, R.-D.; Freisinger, E.; Lippert, B. *J. Chem. Soc., Chem. Commun.* **1999**, 675.

C RESULTS AND DISCUSSIONS

Chapter I

Cyclic Trimers vs. *Head-Tail* Dimers in Metal-Nucleobase Complexes

1 Aim of the project

The aim of this project was to design and synthesize cyclic oligomeric complexes by using 1-methylcytosine as a bridging ligand. The metal binding behavior is probed by attaching Pd^{II} to the N(3) and the deprotonated N(4) positions of this nucleobase. The resultant cyclic oligomer can be subjected to host-guest interaction studies. The challenge is to prevent formation of the dinuclear *head-tail* complex and instead try to obtain a larger cyclic one. In an extension of this work, 1-methylcytosine is substituted by cytidine in order to enlarge the cavity of the host model complexes.

2 Oligomerization of pyrimidine nucleobase complexes of *cis*-$M^{II}L_2$ (M = Pt, Pd)

1:1 complexes of type *cis*-$M^{II}L_2(Nb)(H_2O)$ (M = Pt or Pd, Nb = nucleobase; L = neutral ligand; charge of complex omitted) have a tendency to undergo condensation reactions with formation of oligomeric species. Similarly, reaction of dinuclear *cis*-$[L_2M(OH)_2ML_2]^{2+}$ with 2 equiv of nucleobase can lead to formation of oligomeric nucleobase complexes. These processes can be accompanied by nucleobase deprotonation. With N(1) blocked pyrimidine bases, cyclic dimers[1,2,3,4] and in one case a cyclic trimer[5] have been structurally characterized. There is a good chance that larger oligomers with

cyclic or open structures exist.[6] In general, the two bases in a cyclic dimer adopt a *head-tail* arrangement, in agreement with expectations from its way of formation from monomeric *cis*-$M^{II}L_2(Nb)(H_2O)$. Occasionally this arrangement is also reached via isomerization of a corresponding *head-head* dimer.[7] Without exception and irrespective of the mutual orientation of the two bases (*head-tail* or *head-head*), in all dinuclear X-ray structurally characterized complexes derived from *cis*-$M^{II}L_2$, the two metals are mutually *syn* and both metal ions are essentially coplanar with the two nucleobases. This is depicted for the *head-tail* dimer HT1 in Figure 1. As a consequence, the metal coordination planes are more or less parallel or slightly tilted, with the d_z^2 orbitals pointing toward each other. M···M contacts are relatively short (*ca.* 3.0 ± 0.2 Å), depending on the bulk of the L ligands, the tilt angle of the metal coordination planes, and the torsion angle about the M···M vectors. Although interrelated in a number of cases,[8] a universal relationship between these parameters appears not to exist.[9] In the case of M^{II} = Pt and with small L ligands such as NH_3, the short approach of the Pt centers facilitates metal oxidation and metal-metal bond formation.

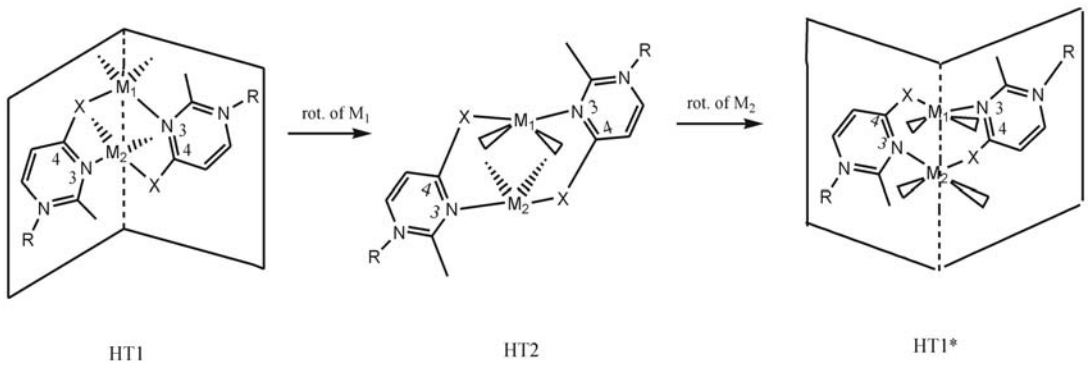

Figure 1. Interelationship between two enatiomers (HT1, HT1*) of *head-tail* dimers and hypothetical second *head-tail* dimer HT2. Rotation of M planes by 180° leads to the different forms. Note that HT1 and HT1* are V-shaped, with the two metals *syn,* and have relatively short M···M distances (3.0 ± 0.2 Å with pyrimidine bases). In contrast, in HT2 the two nucleobases are essentially parallel, the mutual orientation of the metals is halfway between *syn* and *anti*, and the M···M distance is long (≥ 5 Å with pyrimidine bases).

It is obvious that increasing steric bulk of the L ligands leads to a lengthening of the intramolecular metal-metal distance, but it is presently unknown to which extent the M···M distance can be stretched with the *head-tail* structure HT1 still retained. From model building it becomes evident that an elongation of the metal-metal distance causes the metal ions bonded to the exocyclic X group (N(4)H in case of cytosine; O(4) or O(2) in case of uracil and thymine) to move out of the nucleobase plane. After a rotation of one of the two metal planes by 180°, the bond between the metal and the exocyclic group of the base is almost at right angle to the base plane. Structural features of this second, hypothetical *head-tail* dimer (HT2) can be described as follows: The cation has no longer the characteristic V-shape of HT1, but rather the two bases are oriented approximately parallel like steps of a stair with no overlap (Figure 1). Unlike in HT1, the L_2 ligands of both metal entities point in different directions in HT2, thus avoiding any steric interference. Finally, the M···M distance is long (estimated ≥ 5 Å). It is unclear, if HT2 can exist with pyrimidine nucleobases as a bridging ligand. The sp^2 hybridization of the exocyclic X groups and the spatial orientation of the lone electron pair(s) seem to make such an arrangement not very favorable. However, from model building it becomes evident that for two tetrahedral metal ions, a HT2 orientation is possible. In fact, the known dinuclear complex $[\{Ag(1\text{-MeC-}N3,O2)\}_2]^{2+}$ [10]proves that such a structure is possible, even though in the mentioned silver complex the bridging modes involve exocyclic O(2) groups rather than $N(4)H^-$ groups. Irrespective of the question of existence of HT2 as a stable entity with square-planar metals, it is worth to note that successive rotation of both metal planes leads again to a *head-tail* dimer HT1*, although its chirality is opposite to that of HT1. This discussion on metal plane rotation has anticipated that no bond breakage takes place during this process. It is obvious that opening of a single M-nucleobase bond would facilitate this rearrangement process greatly and likewise would speed up the interconversion of the two *head-tail* enantiomers.

Our attempt to obtain a HT2 form of $[\{cis\text{-}Pd(1\text{-}MeC^-)a_2\}_2]^{2+}$ by applying bpy, bipzp and tmeda as a_2 entity, which have increasing steric hindrance that might favor HT2 over HT1, was clearly not successful. Rather, the cyclic trimer $[\{Pd(1\text{-}MeC^-)(tmeda)\}_3]^{3+}$ and later the corresponding cytidine species were detected in solution and eventually isolated, and two HT1/HT1* dimer structures with bpy and bipzp as ancillary ligands were obtained as well. In this trimer, like in HT1 and in contrast to HT2, the metal ions are again close to coplanar with the nucleobase planes, albeit the metals adopt mutual *anti* orientations. The relationship between HT1/HT1*, the hypothetical HT2, and the cyclic trimer Pd_3 thus can be reduced to their differences in relative orientations of the two metals at N(3) and the exocyclic groups X: The metals are *syn* in the case of HT1/HT1*, *anti* in the case of Pd_3, and intermediate in the hypothetical HT2.

3 *Head-tail* dimer structures

3.1 Chirality of *head-tail* dimers

The fact that square-planar metal complexes frequently display the phenomenon of chirality, appears to be widely overlooked.[11] Only in the case of bis(nucleobase) complexes derived from Cisplatin has there been an awareness that different enantiomers are possible and may in fact have different biological effects.[12, 13, 14] *Head-tail* dimers derived from two square-planar *cis*-$M^{II}L_2$ (M = Pt, Pd) entities and two identical bridging ligands are likewise chiral, but this feature is rarely discussed in the literature.[15] The *head-head* dimer, on the other hand, is achiral (if ligand canting is ignored), as it has a plane of symmetry.

There appears to be no convention presently in use to describe the chirality of *head-tail* dimers and to differentiate the enantiomers. Adopting the convention to designate molecular configurations of bis(guanine) complexes of *cis*-$Pt^{II}a_2$

(use of two skew lines[12]) and modifying it for dinuclear complexes, the following convention is proposed for pyrimidine model nucleobases (e.g. 1-MeC, 1-MeU, 1-MeT): The nucleobase orientation is designated by an arrow pointing from N(1) to the para-position (N(4) in 1-MeC, O(4) in 1-MeU and 1-MeT). By connecting the two exocyclic 4-positions in the *head-tail* dimer with a line, and determining its rise, one comes up with either a negative rise (Λ-form) or a positive rise (Δ-form) (Scheme 1). In terms of the convention proposed by Cramer and Dahlstrom[12] the Λ-form can be related to a left-handed helix, while the Δ-form can be related to a right handed one.

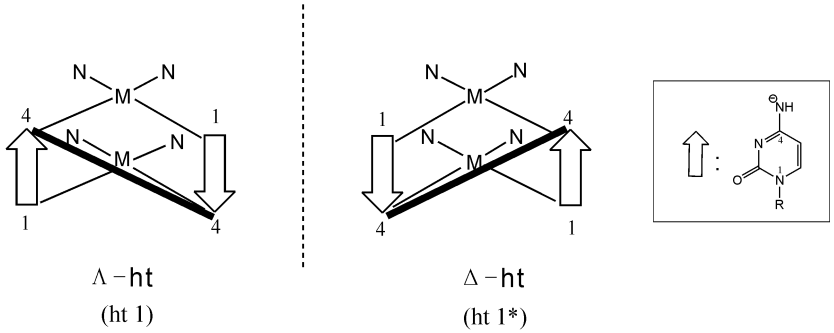

Scheme 1.

For the solid state a canting (tilting) of the heterocyclic ligands in either direction is feasible (Scheme 2).

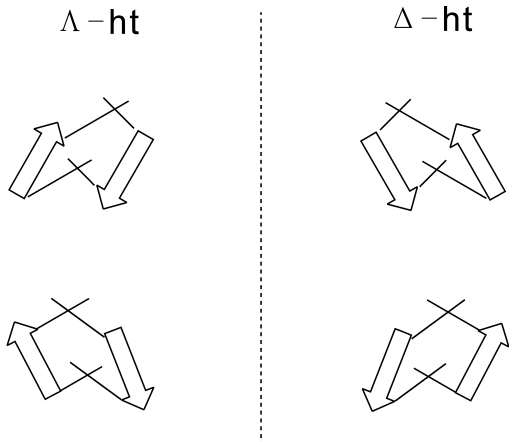

Scheme 2.

If viewed along the M···M vector (from the top or the bottom) the canting can either be right- or left-handed, depending on whether the top metal plane is rotated clockwise or counter-clockwise with respect to an eclipsed orientation of the two metal planes (Scheme 3).

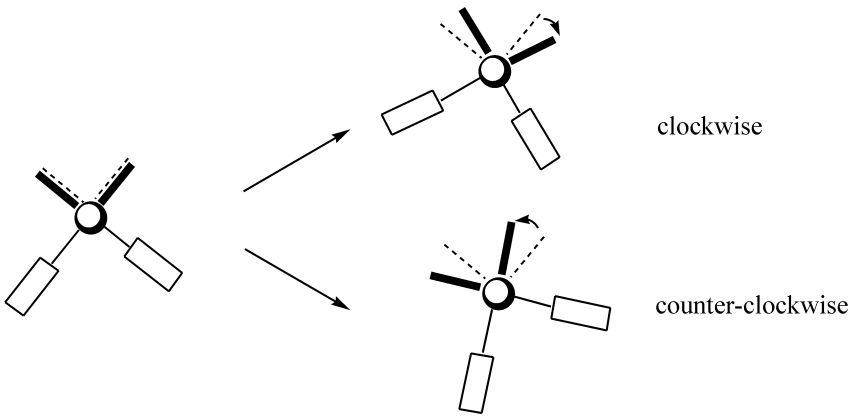

Scheme 3.

The torsion (twist) angle ω of the two metal planes in 1-MeU and 1-MeT *head-tail* dimers derived from *cis*-$Pt^{II}a_2$ is usually in the range of 14-30°.[9]

With regard to *head-head* dinuclear complexes, it is obvious that it has a plane of symmetry, hence is achiral (provided that the planes of the heterocyclic ligands are truely perpendicular to the metal planes) (Scheme 4).

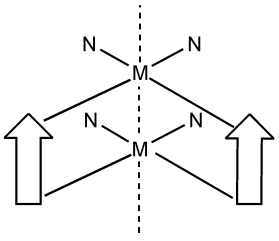

Scheme 4.

In reality, the ligands may also be tilted to the right or the left, resulting in a torsion about the M···M vector (Scheme 5).

Scheme 5.

3.2 Characterization of [{Pd(1-MeC$^-$-*N3,N4*)(bpy)}$_2$](ClO$_4$)$_2$ ·4H$_2$O (I-1)

The reaction was performed at a ratio of 1:1 between [Pd(bpy)(H$_2$O)$_2$]$^{2+}$ and 1-MeC in alkaline solution. Yellow crystals suitable for X-ray crystallography were successfully isolated. In compound **I-1**, two Pd^{II}(bpy) units are bridged by two 1-MeC$^-$ ligands via N(3) and N(4) sites in a *head-tail* fashion with a short Pd···Pd distance (2.8511(9) Å) because of the pronounced π-stacking of the bpy rings. A view of the cation is given in Figure 2. Selected bond lengths and angles are listed in Table 1.

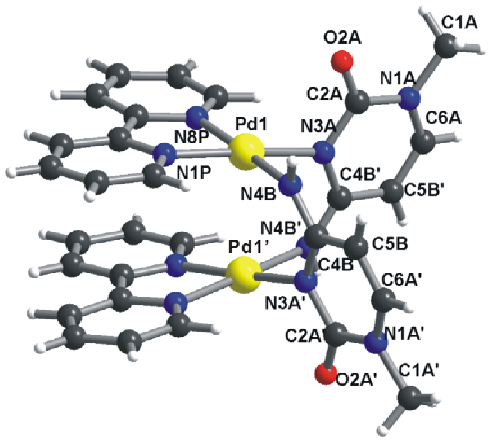

Figure 2. View of [{Pd(1-MeC$^-$-*N3,N4*)(bpy)}$_2$]$^{2+}$ (**I-1**) cation with atom numbering scheme.

Pd(1) and Pd(1') are interrelated by a two-fold-axis in symmetry code (-x, y, 0.5-z). The Pd(1)···Pd(1') distance (2.8511(9) Å) is quite similar to those observed for several analogs in *head-tail* isomers; 2.899(2) Å for

ht-[Pt_2(bpy)$_2$(μ-α-pyrrolidinonato)$_2$](ClO_4)$_2$, [16] and 2.89 Å for *ht*-[Pt_2(bpy)$_2$(μ-pivalamidato)$_2$]$^{2+}$.[17] The dihedral angle between 1-MeC$^-$ and the metal coordination plane is 85.6(5)º, similar as in Pt^{II} and Pd^{II} analogs.[18] The mean-plane calculations performed for the Pd coordination planes indicate that the average four-atom deviation is 0.045 Å for the N(3A)/N(4B)/N(1P)/N(8P) plane. The dihedral angle between the two Pd coordination planes within the dimeric unit is 19.6(2)^o and the average torsional twist angle about the Pd···Pd axis is ω =13.43(1)^o, where ω = 0^o denotes that the two Pd coordination planes stack in an eclipsed fashion. The two bpy ligands are also found to be planar, where the 12-atom mean deviations are 0.025 Å. Within the dimer unit, the tilt angle between the two bpy planes is 6.9(1)^o, which is 12.7(1)^o smaller than that between the two Pd coordination planes, indicating that a relatively strong π-stacking interaction is achieved within the unit (Figure 4). The intraplanar spacing between these bpy planes is 3.64(1) Å, while the interplanar spacing between these bpy planes is 3.67(2) Å.

Table 1. Selected distances (Å) and angles (º) for compound **I-1**[a].

[{Pd(1-MeC$^-$-*N3,N4*)(bpy)}$_2$](ClO_4)$_2$·4H_2O (I-1)			
Pd1-N1P	2.029(5)	Pd1-N8P	2.014(5)
Pd1-N3A	2.023(5)	Pd1-N4B[a]	2.000(6)
Pd1···Pd1[a]	2.8511(9)		
N1P-Pd1-N3A	173.9(2)	Pd1[a]···Pd1-N1P	92.8(1)
N1P-Pd1-N8P	80.2(2)	Pd1[a]···Pd1-N3A	83.9(2)
N1P-Pd1-N4B[a]	95.9(2)	Pd1[a]···Pd1-N8P	101.6(1)
N3A-Pd1-N8P	95.3(2)	Pd1[a]···Pd1-N4B[a]	79.5(2)
N4B[a]-Pd1-N8P	175.9(2)	N3A-Pd1-N4B[a]	88.7(2)
N8P-Pd1-Pd1[a]-N1P	-13.98(1)	N3A-Pd1-Pd1[a]-N4B	-12.88(1)

[a] Symmetry transformations used to generate equivalent atoms: -x, y, 1/2-z.

As *head-tail* dimers are inherently chiral (see Figure 3), both enantiomers are present in a 1:1-ratio.

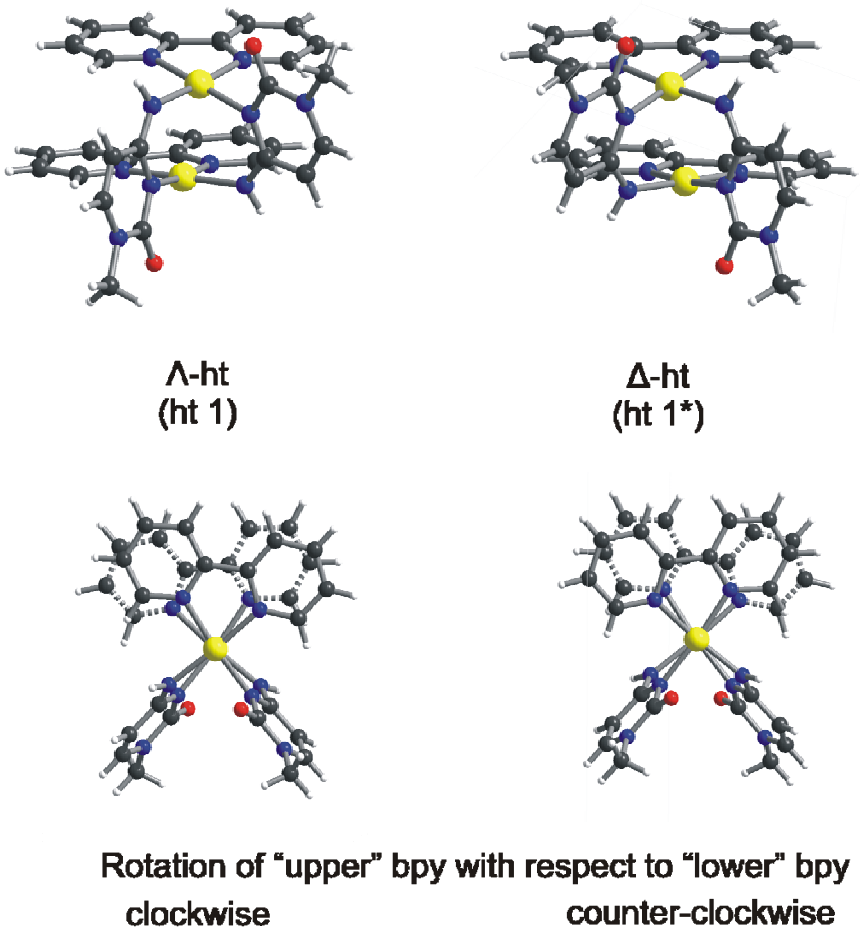

Figure 3. View of the two enantiomers of **I-1** present in the crystal lattice.

As shown in Figure 4, the two different enantiomers are stacked on top of each other, forming a one-dimensional array of bpy units. The interdimer Pd···Pd distances (6.39(2) Å), e.g. Pd(1A)···Pd(1E) and Pd(1F)···Pd(1D), are much too long for any metal-metal interaction. Clearly, stacking interactions dictate the packing pattern.

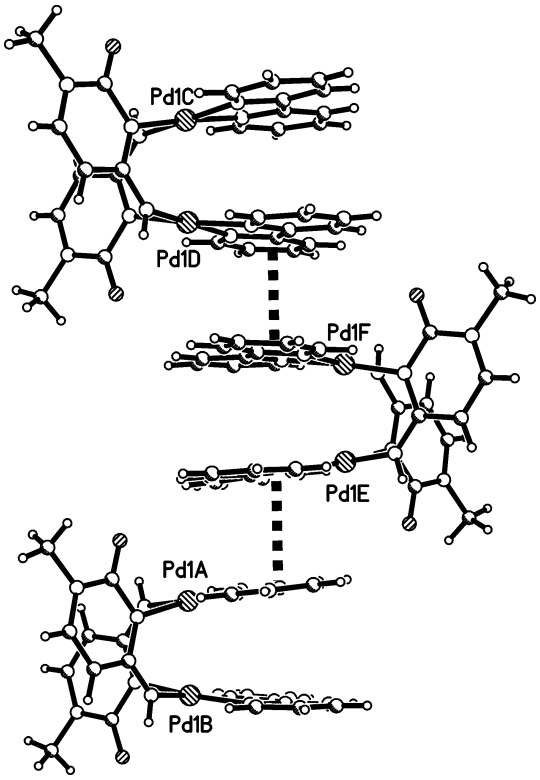

Figure 4. A view showing the packing of the different enantiomers of the *head-tail* dimers **1**. [Symmetry codes: (A&B) -x, y, 0.5-z; (A&E) 0.5-x, 0.5-y, 1-z; (A&F) -0.5+x, 0.5-y, -0.5+z; (F&D) 0.5-x, 0.5-y, 1-z.]

3.3 Reactions of Pd^{II}(bipzp) with 1-MeC

NMR scale reactions were performed with Pd^{II}(bipzp) and 1-MeC in a 1:1-ratio. The time course of the reaction was followed by ^{1}H NMR spectroscopy. The stackplot of the downfield region in the ^{1}H NMR spectra is shown in Figure 5.

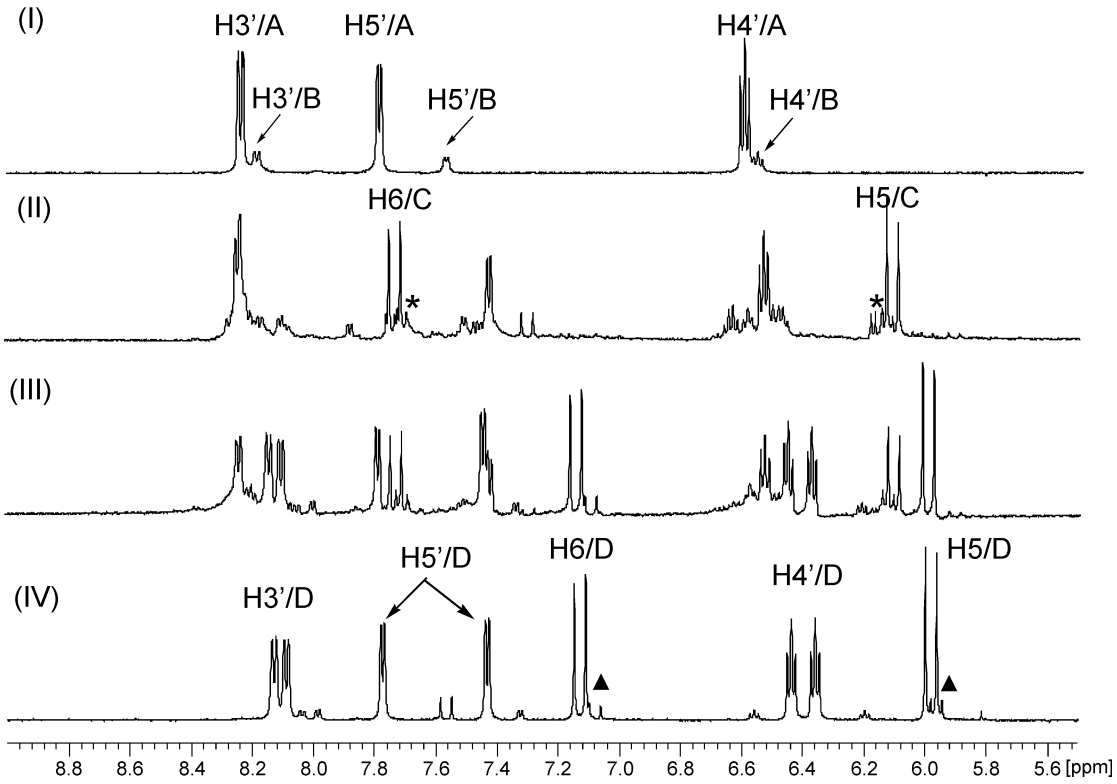

Figure 5. Low field section of ^{1}H NMR spectra (D_2O) obtained upon mixing $[Pd(bipzp)(D_2O)_2]^{2+}$ and 1-MeC (1:1) and addition of NaOD: (I) The starting compound $[Pd(bipzp)(D_2O)_2]^{2+}$ (A) and small amount of $PdCl_2(bipzp)$ (B) (II) Three hours after addition of 1-MeC. (III) After adjustment of the pD value to 9, and heating the sample at 60 °C for one day. (IV) After additional heating at 60 °C for 12 h; pD 7.5. For assignment of A-D see text.

The resonances for bis(pyrazol-1-yl)propane include the three protons H(3'), H(4') and H(5') of the two symmetry-related pyrazole rings and two methyl groups of the aliphatic chain (Scheme 6).

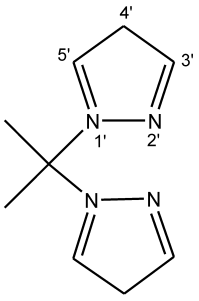

Scheme 6. 2,2'-bis(pyrazol-1-yl)propane.

They are observed at 8.24 ppm (H3', d, ^{3}J = 3.0 Hz), 7.79 ppm (H5', d, ^{3}J = 3.0 Hz), 6.60 ppm (H4', t, ^{3}J = 3.0 Hz) and 2.85 ppm (CH_3, s) in

$[Pd(bipzp)(D_2O)_2](NO_3)_2$ (A) solution at pD 2.2 (spectrum (I)). Resonance (B) are assigned to small amount of $Pd(bipzp)Cl_2$ compound. After addition of 1-MeC (C) to the $[Pd(bipzp)(D_2O)_2](NO_3)_2$ (A) solution, a small amount of $[Pd(bipzp)(1\text{-MeC-}N3)(D_2O)](NO_3)$ (*) was formed immediately. When the pD was adjusted to 9, the resonances of compound (D) were found in spectrum (III). Its 1-MeC$^-$ resonances (D_2O, pD 7.5) are observed at 7.13 ppm (H6, d, ^3J = 7.6 Hz), 5.98 ppm (H5, d, ^3J = 7.6 Hz) and 3.35 ppm ($N(1)CH_3$, s). Compared with free 1-MeC, the H(6) and H(5) resonances of compound (D) are both upfield shifted, which is consistent with a μ(1-MeC$^-$-*N3,N4*) mode. The resonances of the pyrazole protons are split into two sets of signals of identical intensities, 8.13 ppm (H3', d, ^3J = 3.0 Hz) and 8.09 ppm (H3', d, ^3J = 3.0 Hz), 7.78 ppm (H5', d, ^3J = 3.0 Hz) and 7.44 ppm (H5', d, ^3J = 3.0 Hz), 6.44 ppm (H4', t, ^3J = 3.0 Hz) and 6.37 ppm (H4', t, ^3J = 3.0 Hz), and 2.66 ppm and 1.68 ppm ($C(1)CH_3$, s), which suggests the two non-equivalent pyrazole "halves" of bipzp as a consequence of different *trans*-positioned Pd donor atoms N(3) and N(4). Compound (D) was successfully isolated and identified by X-ray crystallography as a *head-tail* (HT1) dimer structure. Because of their similar shifts, the signals ▲ in spectrum (IV) are tentatively assigned to a second dinuclear species, the *head-head* rotamer of compound D.

3.4 Characterization of $PdCl_2$(bipzp) (I-2)

Bis(pyrazol-1-yl)propane easily reacts with $PdCl_2$ to form $PdCl_2$(bipzp) in good yield. Crystallization during the synthesis work obtained a sample suitable for X-ray analysis. A view of the molecule, which has been reported before,[19] is shown in Figure 6.

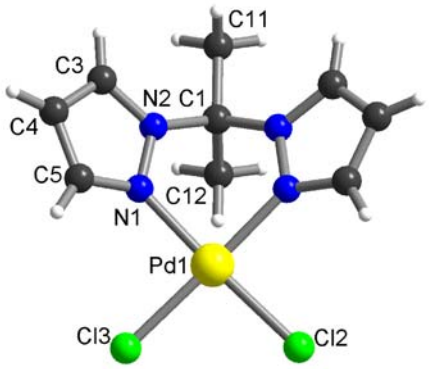

Figure 6. View of the molecule $PdCl_2$(bipzp) (**I-2**) with atom numbering scheme.

Table 2 provides a few selected structural details. Bond distances and bond angles within the bis(pyrazol-1-yl)propane are normal and agree with the previously reported values.[20] The Pd-N distances are 2.018(3) and 2.022(3) Å and are likewise normal. The angles about the Pd deviate slightly from an ideal square-planar coordination sphere (*e.g.* N(1)-Pd(1)-N(1A), 87.7(1)°, Cl(2)-Pd(1)-Cl(3), 91.82(4)°). The dihedral angle of two pyrazole rings is 118.7(1)°.

Table 2. Selected distances (Å) and angles (º) for compound **I-2**.

$PdCl_2$(bipzp) (I-2)			
Pd1-N1	2.018(3)	Pd1-Cl2	2.280(1)
Pd1-N1A	2.022(3)	Pd1-Cl3	2.287(1)
C1-C11	1.514(6)	N2-C1	1.473(5)
Pd1···C1	3.250(4)		
Cl2-Pd1-Cl3	91.82(4)	Cl3-Pd1-N1A	176.97(9)
Cl2-Pd1-N1	177.2(1)	N1-Pd1-N1A	87.7(1)
Cl2-Pd1-N1A	89.64(8)	N2-C1-N2A	106.7(3)
Cl3-Pd1-N1	90.8(1)	C11-C1-C12	110.2(3)
N-Pd-N/N-N-N-N	17.3(2)	pz/pz	61.3(1)

3.5 Characterization of [{Pd(1-MeC$^-$-*N3,N4*)(bipzp)}$_2$](NO$_3$)$_2$·7H$_2$O (I-3)

1:1 mixtures of 1-MeC and $[Pd(bipzp)(D_2O)_2]^{2+}$ were heated at 60° for one day at pH 9. $[Pd(bipzp)(D_2O)_2]^{2+}$ was applied as a sterically bulky entity with the intention to prevent *syn* structures from being formed. However, the yellow crystals, which were obtained in good yield, and characterized by X-ray crystallography, proved the compound to have a *head-tail* dimer structure. A view of the cation of compound **I-3** is given in Figure 7. Selected bond lengths and angles are listed in Table 3.

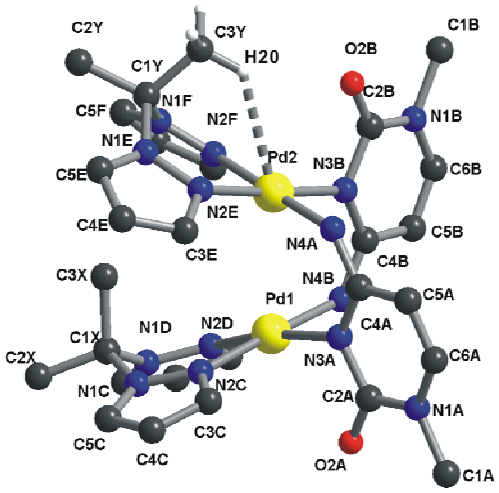

Figure 7. View of the cation [{Pd(1-MeC$^-$-*N3,N4*)(bipzp)}$_2$]$^{2+}$ (**I-3**) with atom numbering scheme. Most of the hydrogen atoms are omitted for better view. The CH_3 protons shown are in calculated positions. The hydrogen bond of Pd(2)···H(20) is 2.63(3) Å.

The six-membered chelate rings (N(2D)-N(1D)-C(1X)-N(1C)-N(2C)-Pd(1), N(2E)-N(1E)-C(1Y)-N(1F)-N(2F)-Pd(2)) in the compound are in a "boat-type" conformation, with significant differences between the chelate rings at Pd(1) and Pd(2) owing to the steric hindrance of the sp^3-carbon atom of the aliphatic chain. The bipzp ligand with pyrazole rings E and F is arching its back and leaves a space for the methyl groups of the other bipzp with rings C and D. The dihedral angles between the two pyrazole rings are 128.5(4)° (E vs. F) and 140.0(3)° (C vs. D). The distance between Pd(1) and Pd(2) is 3.01(5) Å,

slightly longer than the average distance in structurally related compounds.[21] The Pd(1)-N(3A) bond is 2.047(7) Å, 0.052 Å longer than the bond Pd(2)-N(3B) (1.995(9) Å). The distance Pd(1)···C(1X) is also 0.13 Å longer than the distance Pd(2)···C(1Y). The significant difference could be owing to the presence an intramolecular interaction between the methylic hydrogen H(20) and Pd(2) and the lack of such interaction between the methylic hydrogen and Pd(1). The value of the Pd(2)···H(20) distance (2.63(3)Å) is smaller than the sum of the van der Waals radii (r_H 1.2, r_{Pd} 1.9[22] or 1.63 Å[23]).

Table 3. Selected distances (Å) and angles (°) for compound **I-3**

[{Pd(1-MeC$^-$-*N3,N4*)(bipzp)}$_2$](NO$_3$)$_2$·7H$_2$O (I-3)			
Pd1-N2C	2.026(7)	Pd2-N2E	2.010(8)
Pd1-N2D	2.025(7)	Pd2-N2F	2.010(7)
Pd1-N3A	2.047(7)	Pd2-N3B	1.995(9)
Pd1-N4B	1.980(7)	Pd2-N4A	1.973(7)
Pd1···Pd2	3.01(5)	Pd1···C1X	3.40(3)
		Pd2···C1Y	3.27(3)
N2C-Pd1-N2D	88.5(3)	N2F-Pd2-N4A	179.3(3)
N2C-Pd1-N3A	92.7(3)	N3B-Pd2-N4A	91.8(3)
N2C-Pd1-N4B	178.3(3)	N1F-C1Y-N1E	107.7(7)
N2D-Pd1-N3A	169.8(3)	N1D-C1X-N1C	108.8(6)
N2D-Pd1-N4B	91.0(3)	C2Y-C1Y-C3Y	111.1(7)
N3A-Pd1-N4B	87.5(3)	C2X-C1X-C3X	110.1(6)
N2E-Pd2-N2F	89.8(3)	Pyrazole(E) vs. (F)	51.5(4)
N2E-Pd2-N3B	176.8(3)	Pyrazole(C) vs. (D)	40.0(3)
N2E-Pd2-N4A	90.3(3)	C1Y-N2F-N1F	119.5(8)
N2F-Pd2-N3B	88.0(3)	C1X-N2D-N1D	122.3(7)

The X-ray crystal structure reveals the presence of a water cluster in the lattice. Five water molecules of crystallization adopt a cyclic pentamer structure (Figure 8). Vertices of the pentamer are the atoms O(1w), O(3w). O(4w), O(5w) and O(7w). The distances of Ow···Ow are in the range of 2.605 to 2.771 Å and angles are from 101.7^o to 107.6^o. The distances and angles are in agreement with reported examples.[24,25,26,27] The value of the sum of the external angles

of the ring is 368.5°, which is much close to 360° (planar structure). Water molecules of crystallization not only take part in the water polymer formation but also form hydrogen bonds to the 1-MeC⁻ ligands and nitrate anions. For example, there are hydrogen bonds between O(3w)···O(2)(1-MeC⁻), O(1w)···O(23)(NO_3), O(5w)···O(22)(NO_3) and O(5w)···O(21)(NO_3). The water molecules O(2w) and O(6w) show hydrogen bond formation between each other and also form hydrogen bonds to 1-MeC⁻ nucleobases, e.g. O(2w)···O(2B) (2.53(2) Å) and O(6w)···N(4A) (2.94(2) Å). The relevance of water clusters in biological systems and chemical processes has been intensively studied in recent years.[25,28,29,30,31,32,33] Water pentamers have been reported before.[34]

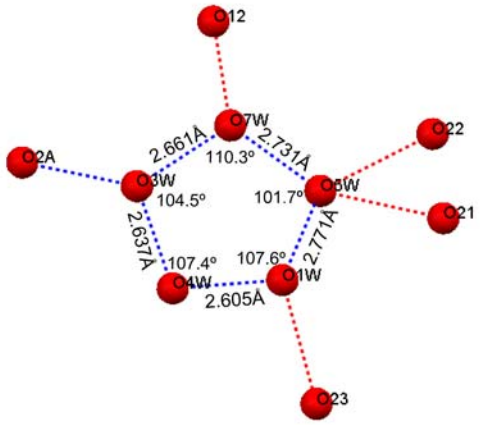

Figure 8. View of the water cluster found in compound **I-3**.

In the ^{1}H NMR spectrum, only two sets of methyl resonances are observed, despite four non-equivalent ones in solid-state structure. The methyl resonances are broader than those of 1-MeC, which could be due to a dynamic behavior. Chemical shifts of these resonances are 2.67 and 1.69 ppm.

Although the steric hindrance of the bipzp appears to be similar to that of the tmeda ligand (see the following section 4), we note that only a *head-tail* dimer was obtained, yet not a larger cyclic structure.

4 Cyclic trimer structures

4.1 Reactions of Pd^{II}(tmeda) with 1-MeC

Isolation of the cyclic Pd trimer was preceded by ^{1}H NMR spectroscopic studies on the interaction of the μ-OH dimer $[\{Pd(OH)(tmeda)\}_2]^{2+}$ with 1-MeC and that of $[Pd(tmeda)(1\text{-MeC-}N3)_2]^{2+}$ with $[Pd(tmeda)(D_2O)_2]]^{2+}$ at alkaline pD. In both cases, the region of the aromatic cytosine protons is rather complex at the beginning of the reaction, but simplifies greatly as the reaction proceeds. Eventually only a limited number of sets of resonances remains. In Figure 9, ^{1}H NMR spectra obtained by mixing $[Pd(tmeda)(1\text{-MeC-}N3)_2]^{2+}$ with $[Pd(tmeda)(D_2O)_2]^{2+}$ at alkaline pH are shown.

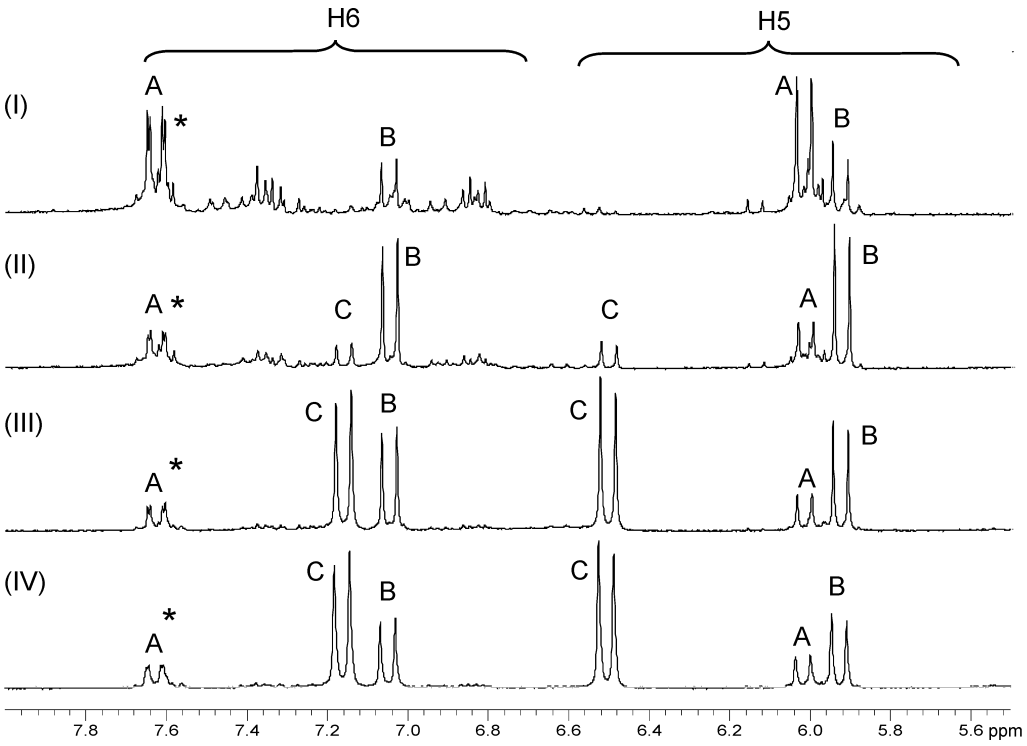

Figure 9. Low field section of ^{1}H NMR spectra (D_2O) obtained upon mixing $[Pd(tmeda)(1\text{-MeC-}N3)_2]^{2+}$ and $[Pd(tmeda)(H_2O)_2]^{2+}$ (1:1) and addition of NaOD: (I) Immediately after adjusting pD to 10.4. (II) After 3d at 25 °C; pD has dropped to 9.2. (III) After heating to 60 °C for 25h; pD 9.2. (IV) After additional heating to 60 °C for 3d; pD 9.2. For assignment of A-C, see text.

In sequence of relative intensities, the following cytosine resonances are eventually observed: Doublets (C) correspond to those of [{Pd(1-MeC$^-$-*N3,N4*)(tmeda)}$_3$](ClO$_4$)$_3$·5.5H$_2$O, as unambiguously confirmed by recording a spectrum of the isolated compound. Its 1-MeC$^-$ resonances (D$_2$O, pD 7.7) are observed at 7.17 ppm (H6, d, ^3J = 7.6 Hz), 6.56 ppm (H5, d, ^3J = 7.6 Hz) and 3.12 ppm (N(1)CH$_3$, s). Somewhat surprisingly, the N(4)H protons exchange only very slowly against ^{2}D (days) to give rise to a singlet at 5.20 ppm (not shown). The tmeda ligands of Pd$_3$(1-MeC$^-$)$_3$ display two CH$_2$ quartets centered at around 3.0 ppm and four individual methyl singlets at 2.85, 2.83, 2.75, and 2.40 ppm. In wet DMSO-d_6, the resonances are observed at 7.36 ppm (H6, d), 6.38 ppm (H5, d), 5.0 ppm (N(4)H, s), 3.16 ppm (N(1)CH$_3$, s), 2.9 ppm (tmeda-CH$_2$, m) as well as 2.77, 2.76, 2.65, and 2.33 ppm (tmeda-CH$_3$, s, each). Already prior to isolation of Pd$_3$(1-MeC$^-$)$_3$ and its X-ray crystallographic confirmation as a cyclic trimer, we had speculated that (C) must be a species in which the 1-methylcytosine base is anionic, bridging two Pd^{II} ions, and in particular is in an *anti* orientation relative to the Pd^{II} at N(3). Thus, the upfield shift of H(6) as compared to free 1-MeC (7.56 ppm) or typical Pd^{II}(1-MeC-*N3*) species (*ca.* 7.6 ppm) was consistent with an anionic 1-methylcytosine base being present. On the other hand, the remarkable downfield shift of the H(5) doublet relative to free 1-MeC (5.95 ppm) or Pd^{II}(1-MeC-*N3*) (*ca*. 6.0 ppm) could only be rationalized if a second metal was reasonably close to H(5), a situation realized only with this metal being bonded at N(4) and present in an *anti* arrangement with respect to N(3). Our group has previously reported an even larger downfield shift of H(5) resonances in pyrimidine nucleobase complexes, namely in complexes derived from Pt(tmeda)(1-MeU-*N3*)$_2$ (1-MeU = 1-methyluracilate).[35] This situation was interpreted in terms of a “face-back” arrangement of the two metals, hence an *anti* orientation of the metal at O(4). The steric bulk of the tmeda ligand obviously prevented an arrangement with the second metal being *syn*. It is proposed that the larger downfield shift of H(5) in the case of the 1-MeU compounds (1.64 ppm)[34] relative to 0.5 ppm in

$Pd_3(1\text{-}MeC^-)_3$ is largely due to the fact that in the 1-MeU complex the nucleobase was already anionic. In contrast, in the case of $Pd_3(1\text{-}MeC^-)_3$, binding of the second metal at N(4) is accompanied by deprotonation of the nucleobase. As the two effects of base deprotonation and metal binding counteract each other as far as the H(5) shift is concerned, this effect is smaller in the case of the 1-MeC^- compound.

The nature of the second compound (B) with its H(6) doublet at 7.05 ppm and its H(5) doublet at 5.93 ppm, was identified by analyzing the relative intensities of the 1-MeC^- and the methyl resonances of the tmeda ligands. Integrals of the various resonances gave a ratio of two tmeda ligands per 1-methylcytosine. As the H(5) and H(6) resonances are consistent with a μ(1-MeC^--*N3,N4*) mode, we assign this species a dinuclear structure, either $[\{Pd(OH)(tmeda)\}_2(\mu\text{-}1\text{-}MeC^-\text{-}N3,N4)]^+$ or $[\{Pd(tmeda)\}_2(\mu\text{-}OH)(\mu\text{-}1\text{-}MeC^-\text{-}N3,N4)]^{2+}$. Attempts to isolate this compound in pure form have not been successful. We originally also considered the possibility that (B) is the *head-tail* dimer (HT1) $[\{Pd(1\text{-}MeC^-\text{-}N3,N4)(tmeda)\}_2]^{2+}$, in analogy to the situation in the *cis*-$Pt^{II}(PMe_3)_2$/1-MeC system.[4,5] There it was shown that HT1 forms as the kinetic product, while the cyclic trimer Pt_3 only formed after long reactions times as the thermodynamic product. However, the chemical shifts of the cytosine resonances of (B), when compared with those of the closely related *ht* dimers $[\{Pd(1\text{-}MeC^-\text{-}N3,N4)(en)\}_2]^{2+}$ (H6, 6.89 ppm; H5, 5.69 ppm)[18] and *cis*-$[\{Pd(1\text{-}MeC^-\text{-}N3,N4)(NH_3)_2\}_2]^{2+}$ (H6, 6.91 ppm; H5, 5.71 ppm)[21a] do not agree with a dinuclear structure, even though there is general good agreement (≤ 0.04 ppm) in 1-MeC chemical shifts of 1:1 and 1:2 complexes of *cis*-$Pd^{II}a_2$ (a = NH_3, a_2 = en, a_2 = tmeda).

Resonances of the two species (A) and (*) are closely similar and overlap. Although in some of the spectra these sets look like doublets of doublets, addition of $[Pd(tmeda)(1\text{-}MeC\text{-}N3)_2]^{2+}$ leads to an intensity increase of only one

of the two doublets (A: H6, 7.63 ppm; H5, 6.02 ppm, ^3J = 7.4 Hz). The remaining doublet (*: H6, 7.62 ppm; H5, 6.00 ppm, ^3J = 7.4 Hz) is tentatively assigned to $[Pd(OH)(tmeda)(1\text{-MeC-}N3)]^+$.

Occasionally, yet not in the example given in Figure 9, also a fifth set of 1-MeC resonances is observed, which unambiguously can be assigned to free 1-MeC (H6, 7.56 ppm; H5, 5.95 ppm; $N(1)CH_3$, 3.36 ppm at pD 7.2).

The fact that, as demonstrated above, $Pd_3(1\text{-MeC}^-)_3$ also forms from the 1:2 complex $[Pd(tmeda)(1\text{-MeC-}N3)_2]^{2+}$ clearly demonstrates that the Pd-(1-MeC-*N3*) bond is labile and hence a self-assembly process is taking place.

4.2 Characterization of $PdCl_2$(tmeda) (I-4)

$PdCl_2$(tmeda) was prepared as a starting material for Pd^{II}(tmeda) which was assumed to cause a steric hindrance and prevent *head-tail* dimer structure formation.[36,37] Orange crystals were isolated and characterized by X-ray crystallography. A view of $PdCl_2$(tmeda) is given in Figure 10 and pertinent structural data are listed in Table 4.

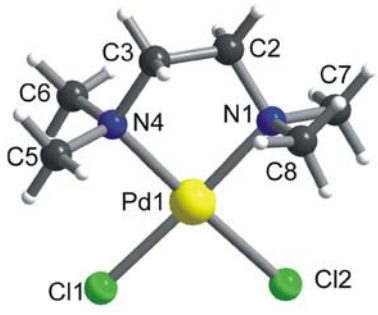

Figure 10. View of $PdCl_2$(tmeda) (**I-4**) with atom numbering scheme.

Like the en ligand, the tmeda ligand is also a chelate ligand, yet with four

methyl groups at the N(1) and N(4) positions. These four methyl groups are pointing out of the mean en plane with average C-N distances of 1.48 Å and average C-N-C angles of 109.0°. The bite angles of the tmeda ligand deviate markedly from 90° (85.7(3)°). Similar features are also observed in the crystal structure of the $PdCl_2$(en) complex.[38] The central methylene groups C(2) and C(3) are outside the PdN_2Cl_2 plane. Deviations of carbon atoms of the tmeda ligand from the plane formed by PdN_2Cl_2 are -0.46(1) Å (C2), 0.21(1) Å (C3). The chloride anions are involved in numerous hydrogen bonding interactions with the CH_3 and CH_2 groups of tmeda, C(2)-H···Cl(1), 3.604(7) Å, C(5)-H···Cl(1), 3.282(8)/3.695(8) Å, C(6)-H···Cl(1), 3.692(8) Å, and C(7)-H···Cl(2), 3.234(8) Å.

Table 4. Selected distances (Å) and angles (°) for compound **I-4**.

$PdCl_2$(tmeda) (I-4)			
Pd1-N1	2.072(6)	Pd1-Cl1	2.304(2)
Pd1-N4	2.073(7)	Pd1-Cl2	2.312(3)
N1-C7	1.49(1)	N4-C5	1.49(1)
N1-C8	1.464(9)	N4-C6	1.482(9)
Cl1-Pd1-Cl2	90.5(1)	N1-C2-C3	110.3(6)
Cl1-Pd1-N1	177.0(2)	N4-C3-C2	109.4(5)
Cl1-Pd1-N4	91.5(2)	Pd1-N1-C2	104.8(4)
Cl2-Pd1-N1	92.3(2)	Pd1-N4-C3	106.7(4)
Cl2-Pd1-N4	178.0(2)	N1-Pd1-N4	85.7(3)
C7-N1-C8	109.0(6)	C5-N4-C6	109.0(6)

4.3 Characterization of [Pd(tmeda)(1-MeC-*N3*)$_2$](NO$_3$)$_2$·2H$_2$O (I-5)

Displacement of the Cl ligands of $PdCl_2$(tmeda) by 1-MeC gave [Pd(tmeda)(1-MeC-*N3*)$_2$](NO$_3$)$_2$·2H$_2$O (**I-5**) in good yield. Compound **I-5** was characterized by X-ray crystallography. A view of the structure is given in Figure 11. Selected bond lengths and angles are listed in Table 5. The cation geometry is very similar to that of the corresponding Pt complex with the two

1-MeC rings adopting a *head-tail* orientation.[39] Dihedral angles between the 1-MeC ligands and the metal coordination plane are 83.2(9) and 81.7(8), similar to Pt^{II} and Pd^{II} analogues.[40] The cytosine rings are planar. The nitrate anions are intercalated between 1-MeC planes of adjacent cations in the solid state strucuture, which is similar to that of *trans*-$[Pt(NH_3)_2(1\text{-MeC})_2](NO_3)_2$[41] and *trans*-$[Pd(NH_3)_2(1\text{-MeC})_2](NO_3)_2$.[42]

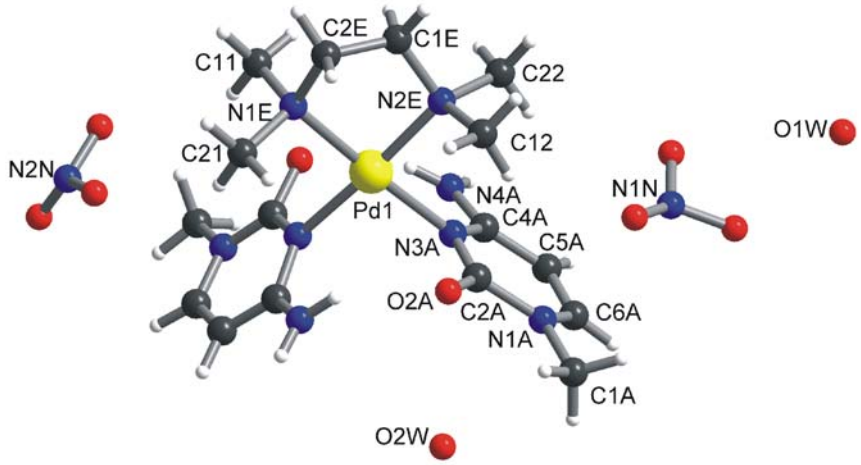

Figure 11. View of $[Pd(tmeda)(1\text{-MeC-}N3)_2](NO_3)_2\cdot 2H_2O$ (**I-5**) with atom numbering scheme.

Table 5. Selected distances (Å) and angles (º) for compound **I-5**.

$[Pd(tmeda)(1\text{-MeC-}N3)_2](NO_3)_2\cdot 2H_2O$ (I-5)			
Pd1-N1E	2.09(2)	Pd1-N3A	2.07(2)
Pd1-N2E	2.05(2)	Pd1-N3B	2.07(2)
N1E-Pd1-N2E	85.0(6)	N1E-C1E-C2E	102.3(17)
N1E-Pd1-N3B	93.2(7)	N2E-C2E-C1E	117.1(17)
N2E-Pd1-N3B	175.1(6)	Pd1-N1E-C1E	110.5(13)
N1E-Pd1-N3A	176.6(7)	Pd1-N2E-C2E	104.0(11)
N2E-Pd1-N3A	91.7(7)		
N3A-Pd1-N3B	90.2(7)		

The ^{1}H NMR spectrum of **I-5** in D_2O gives two sets of resonances of 1-MeC, which are assigned to a mixture of *head-tail* and *head-head* rotamers, with the

former predominating. The 1-MeC resonances of the *head-tail* rotamer are observed at 7.63 ppm (H6, d, ^3J = 7.4 Hz), 6.02 ppm (H5, d, ^3J = 7.4 Hz) and 3.44 ppm (CH_3, s), while the 1-MeC resonances of the *head-head* rotamer are observed at 7.57 ppm (H6, d, ^3J = 7.4 Hz), 6.01 ppm (H5, d, ^3J = 7.4 Hz), 3.37 ppm (CH_3, s). Both tmeda resonances are observed at 2.97 ppm (CH_2, d, ^3J = 3.0 Hz), 2.75 ppm (CH_3, s) and 2.53 ppm (CH_3, s). This agrees with the fact that every two of the four methyl groups of tmeda are pointing out in the same direction.

4.4 Characterization of [{Pd(*μ*-OH)(tmeda)}$_2$](ClO$_4$)$_2$ (I-6)

$[Pd(OH)(tmeda)(H_2O)]^+$, prepared in solution from the diaqua species upon addition of 1 equiv of NaOH, was isolated as a bis-*μ*-hydroxo bridged dimer, $[\{Pd(\mu\text{-}OH)(tmeda)\}_2]^{2+}$ and crystallized as its ClO_4^- salt. Two different views of the cation are shown in Figure 12. Selected interatomic distances and angles are listed in Table 6. The cation is closely analogous to similar bis-*μ*-hydroxo bridged dimers of Pd^{II} and Pt^{II}.[43] The four angles about the Pd centers and their immediate donor atoms deviate markedly (by 7 - 9^o in either direction) from the ideal 90^o angle in square-planar metal complexes, resulting in slight tetrahedral distortions about the metals (e.g.: N(1A)-Pd(1)-O(1A), 174.12(3)^o; N(2A)-Pd(1)-O(1), 175.10(2)^o). Similarly, the central Pd(1)-O(1)-Pd(1A)-O(1A) unit is not a square but rather a parallelogram, with the two halves N_2PdO_2 slightly bent and forming an angle of 6.6^o. The Pd···Pd distance is 3.11(5) Å. We note that there are other examples of bis(*μ*-hydroxo) dimers of Pt^{II} which display strongly bent butterfly structures with hinge angles of up to 43^o.[44] The hydroxyl protons point in different directions. They are involved in hydrogen bonding with oxygen atoms of the perchlorate anions (O(1)···O(14A)), 2.88(1) Å; Pd(1)-O(1)···O(14A), 117.4(3)^o).

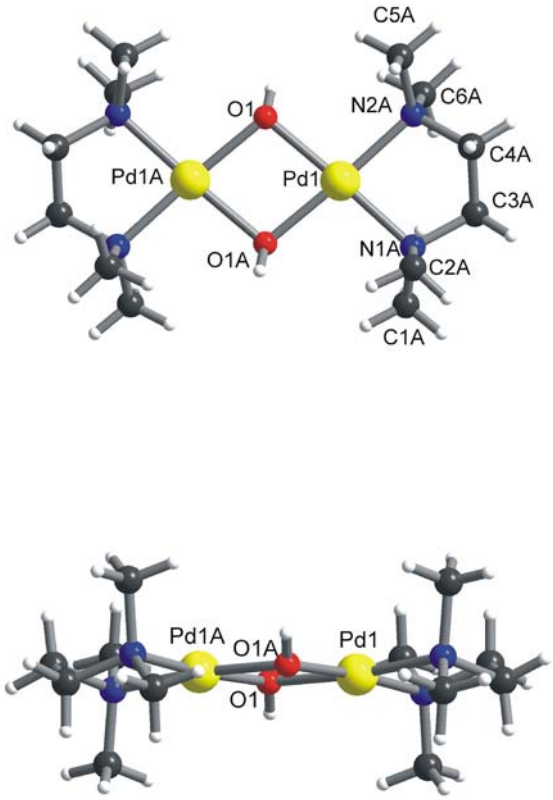

Figure 12. Top and side views of $[(tmeda)Pd(OH)_2Pd(tmeda)]^{2+}$ cation (**I-6**) with atom numbering scheme.

Table 6. Selected Bond Distances (Å) and Angles (º) for compound **I-6**[a].

$[Pd(\mu\text{-}OH)(tmeda)]_2(ClO_4)_2$ (I-6)			
Pd1-O1	2.029(4)	N1A-C1A	1.473(8)
Pd1-N1A	2.049(4)	N1A-C2A	1.489(8)
Pd1-N2A	2.052(5)	N1A-C3A	1.498(9)
Pd1-O1A	2.040(4)	N2A-C4A	1.481(9)
Pd1···Pd1A	3.11(5)		
O1-Pd1-N1A	97.59(2)	Pd1-N2A-C4A	105.8(4)
O1-Pd1-N2A	175.10(2)	Pd1-N2A-C5A	112.9(4)
O1-Pd1-O1A	80.38(2)	Pd1-N2A-C6A	108.9(4)
N1A-Pd1-N2A	85.62(2)	Pd1-N1A-C3A	106.7(3)
O1A-Pd1-N1A	174.12(3)	Pd1-N1A-C2A	108.1(7)
O1A-Pd1-N2A	96.78(2)	Pd1-N1A-C1A	114.1(3)
Pd1-O1-Pd1A	99.62(1)		

[a] Symmetry transformations used to generate equivalent atoms: -x, y, 1/2-z.

4.5 Characterization of [{Pd(1-MeC$^-$-*N3*,*N4*)(tmeda)}$_3$](ClO$_4$)$_3$·5.5H$_2$O (I-7)

[{Pd(1-MeC$^-$-*N3,N4*)(tmeda)}$_3$](ClO$_4$)$_3$·5.5H$_2$O was prepared by 1:2 ratio of the *μ*-OH dimer [{Pd(OH)(tmeda)}$_2$]$^{2+}$ with 1-MeC at alkaline conditions. Yellow crystals suitable for X-ray crystallography were successfully isolated. A view of the cation of the cyclic trimer [{Pd(1-MeC$^-$-*N3,N4*)(tmeda)}$_3$] (ClO$_4$)$_3$·5.5H$_2$O is provided in Figure 13, and pertinent structural data are listed in Table 7. The cyclic trimer cation is chiral, but only one of the two enantiomers present in the crystal is shown.

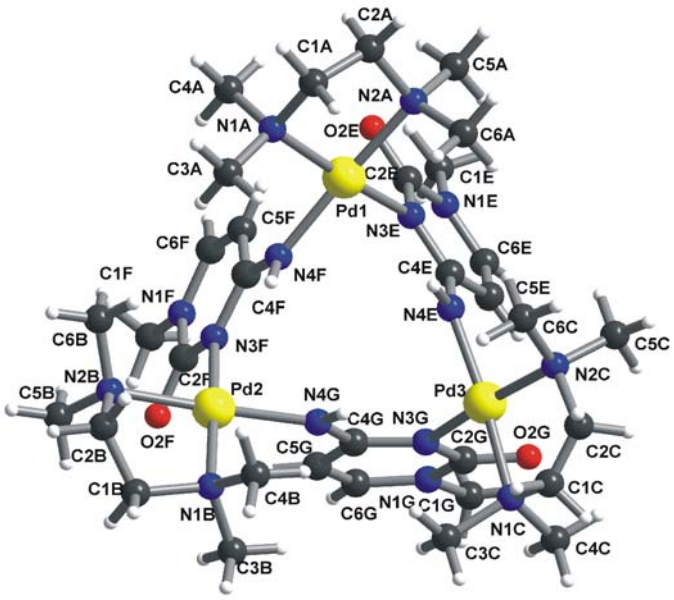

Figure 13. Perspective view of the trinuclear cation [{Pd(1-MeC$^-$-*N3,N4*)(tmeda)}$_3$]$^{3+}$ (**I-7**) and atom numbering scheme. The view is down the pseudo-threefold axis of the double cone.

The anionic 1-methylcytosine nucleobases act as bridging ligands, binding the Pd^{II} centers via N(3) and the deprotonated N(4) position. Relative orientations of two adjacent metal ions with regard to the bridging nucleobase are *anti*. The three Pd ions are at the corners of an almost ideal equilateral triangle, with Pd···Pd distances of 5.166(3) Å - 5.175(2) Å, and angles between 59.98(3)^o and 60.10(3)^o within the triangle. The three bases are inclined by 74.7(3)^o (ring E), 67.1(3)^o (ring F), and 71.8(2)^o (ring G) with respect to the Pd$_3$ plane. The

three N(4) atoms likewise form a triangle (3.329(8) - 3.427(8) Å), as do the N(3) atoms(4.443(8) - 4.522(8) Å) and the N(1)CH_3 groups (5.41(1) - 5.708(9) Å). These triangles are no longer equilateral as a consequence of the different inclinations of the three nucleobases relative to the Pd_3 plane. Overall, the three 1-MeC^- rings provide a cone of approximately threefold symmetry. The three tmeda entities likewise form a cone, which is wider than that formed by the three nucleobases. Thus, distances between equivalent amine-N atoms of the tmeda ligands are 6.98(1), 7.12(1) and 7.12(1) Å (N atoms of tmeda opposite to N(3) sites of 1-MeC^-) and 7.92(1), 8.01(1) and 8.10(1) Å (N atoms of tmeda opposite to N(4) sites of 1-MeC^-), and distances between methyl groups of the tmeda ligands furthest apart are 9.52(1), 9.78(1) and 10.19(1) Å (CH_3 groups at N(2) opposite to N(4) of 1-MeC^-, pointing away from 1-MeC^- ligands). The Pd_3(1-MeC^-)$_3$ cation has the shape of a double cone, which is wider at the tmeda Pd "bottom" than at the 1-methylcytosine "top" (Scheme 7). The structure of Pd_3(1-MeC^-)$_3$ is similar to that of *cis*-[{Pt(1-MeC^-)$(PMe)_3$}$_3$]$^{3+}$ reported by Longato et al.[5]

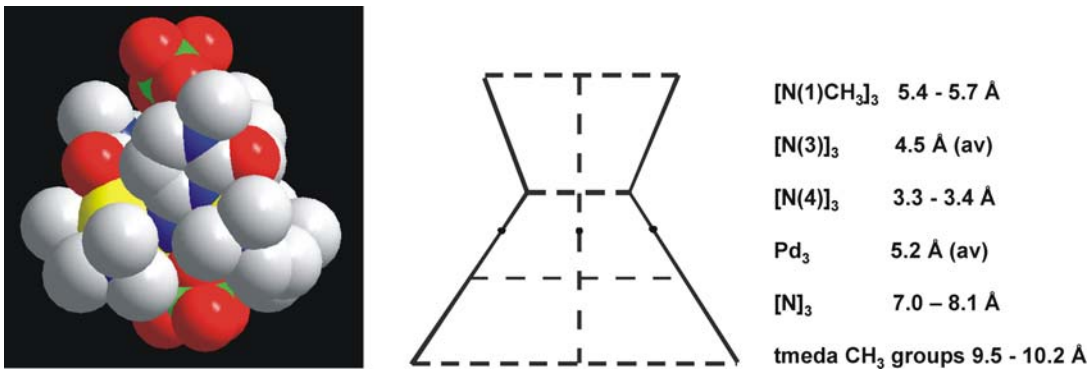

Scheme 7. Schematic representation of Pd_3(1-MeC^-)$_3$ double cone with separations within triangles of same atoms indicated.

Geometries about the Pd^{II} ions are normal. As expected, the bite angles of the tmeda ligands deviate markedly from 90° (*ca.* 85°, av.), but the N(3)-Pd-N(4) angles are virtually ideal (Table 7). The two other angles are consequently larger than 90°, *ca.* 92°. As to Pd-N bond lengths, they are normal (2.015(6) -

2.086(6) Å), displaying a trend of Pd-N(tmeda) > Pd-N(3)(1-MeC$^-$) > Pd-N(4)(1-MeC$^-$). There are no major changes in the cytosine rings of Pd_3 as compared to free 1-MeC, Pd-(1-MeC-*N3*), and HT1 of *cis*-$Pd^{II}(NH_3)_2$.[22a] This statement includes C(2)-O(2) and C(4)-N(4) bond lengths.

Table 7. Selected Distances (Å) and Angles (º) for compound **I-7**.

[{Pd(1-MeC$^-$-*N3,N4*)(tmeda)}$_3$](ClO$_4$)$_3$·5.5H$_2$O (I-7)			
Pd1-N1A	2.076(8)	Pd2-N3F	2.056(7)
Pd1-N2A	2.086(6)	Pd2-N4G	2.018(6)
Pd1-N3E	2.065(6)	Pd3-N1C	2.077(8)
Pd1-N4F	2.015(6)	Pd3-N2C	2.083(6)
Pd2-N1B	2.064(8)	Pd3-N3G	2.045(6)
Pd2-N2B	2.072(6)	Pd3-N4E	2.019(7)
Pd1···Pd2	5.166(3)	Pd1···Pd3	5.175(2)
Pd2···Pd3	5.169(1)		
N1A-Pd1-N2A	85.3(3)	N2B-Pd2-N3F	94.7(3)
N1A-Pd1-N3E	171.6(3)	N2B-Pd2-N4G	171.8(3)
N1A-Pd1-N4F	91.9(3)	N3F-Pd2-N4G	89.7(3)
N2A-Pd1-N3E	93.7(3)	N1C-Pd3-N2C	84.9(3)
N2A-Pd1-N4F	171.4(3)	N1C-Pd3-N3G	93.9(3)
N3E-Pd1-N4F	90.2(2)	N1C-Pd3-N4E	169.9(3)
N1B-Pd2-N2B	85.7(3)	N2C-Pd3-N3G	173.9(3)
N1B-Pd2-N3F	174.8(3)	N2C-Pd3-N4E	91.9(3)
N1B-Pd2-N4G	90.7(3)	N3G-Pd3-N4E	90.3(3)
Pd1-N1A-C1A	106.7(5)	Pd2-N2B-C2B	103.3(6)
Pd1-N1A-C3A	117.2(6)	Pd2-N2B-C5B	114.4(6)
Pd1-N1A-C4A	103.7(6)	Pd2-N2B-C6B	110.8(5)
Pd1-N2A-C5A	117.7(5)	Pd3-N1C-C3C	110.9(7)
Pd1-N2A-C6A	106.1(5)	Pd3-N1C-C4C	115.3(6)
Pd1-N2A-C2A	105.9(5)	Pd3-N1C-C1C	105.2(6)
Pd2-N1B-C3B	109.9(6)	Pd3-N2C-C6C	113.5(6)
Pd2-N1B-C4B	114.1(6)	Pd3-N2C-C2C	104.9(7)
Pd2-N1B-C1B	106.4(6)	Pd3-N2C-C5C	110.3(6)

As pointed out above, the major difference between the here described trinuclear species and the related dinuclear *cis*-[{M(1-MeC$^-$)L_2}$_2$]$^{2+}$ compounds with HT1 structure (L_2M = *cis*-$Pd^{II}(NH_3)_2$,[21a] *cis*-$Pt^{II}(NH_3)_2$,[45] *cis*-$Pt^{II}(PMe_3)_2$ [4]) is the *anti* orientation of the metal at N(4) with respect to the metal at N(3) of the

same nucleobase. It is this swing of the metal at N(4) around the C(4)-N(4) bond which enables the large M···M separation of *ca.* 5.175(2) Å and hence formation of a cyclic trimer. There are moderate deviations of the metal entities at N(4) from ideal *anti* arrangement, which are reflected by the distances of the three Pd ions from the best nucleobase planes, namely 0.19(2) Å (Pd(1) to ring E), 0.06(2) Å (Pd(2) to ring F), and 0.15(2) Å (Pd(3) to ring G). The values compare with estimated 1.7 - 2 Å values for the hypothetical HT2 dimer.

A major difference between the previously reported Pt_3 complex[5] and the here described $Pd_3(1\text{-}MeC^-)_3$ species refers, despite identical ClO_4^- anions, to the interactions between the trinuclear cations and the anions. While cations and anions are well separated in Pt_3, in the here described $Pd_3(1\text{-}MeC^-)_3$ species two distinct interaction patterns between $Pd_3(1\text{-}MeC^-)_3$ and ClO_4^- are seen (Figure 14). Thus in $Pd_3(1\text{-}MeC^-)_3$, two of the three counter anions approach the openings of the double cone: One ClO_4^- anion (Cl(1A)) interacts via O(11A) with the N(4)H triangle from the "bottom". While the protons at the N(4) groups were not located in the X-ray structure determination, inspection of a model clearly reveals, that the three protons of N(4)H are pointing toward the perchlorate oxygen atom, with distances of *ca.* 3.02 - 3.07 Å between N(4) sites and O(11A). There are additional weak contacts between the other three oxygen atoms of the ClO_4^- and protons of three out of the twelve methyl groups of the three tmeda chelate rings which are close to the lower cone C(3A), C(4B) and C(6C); see also Chapter V below. A second ClO_4^- anion (Cl(3A)) approaches the double cone from the "top". Comparison of the thermal ellipsoids of the atoms of the two anions clearly shows that the one approaching from the top is less fixed and more flexible. It appears that the interaction between one of the oxygen atoms of this second ClO_4^- (O(31A)) involves weak hydrogen bonds with the methyl group on N(1F) position of the nucleobase (3.33(1) Å). There are two additional positions for ClO_4^- anions: one has a 50% occupancy (Cl(2A)), and one has a 50% occupancy as well and

is at the same time disordered (Cl(5A) and Cl(5B)). Neither of these is immediately associated with the $Pd_3(1\text{-}MeC^-)_3$ cations but rather located in hydrophobic cavities between $Pd_3(1\text{-}MeC^-)_3$ cations formed by aromatic H(5) and H(6) protons as well as methyl groups of tmeda ligands. There is a weak hydrogen bond (3.18(2) Å) between O(24A) and C(6E) of the nucleobase.

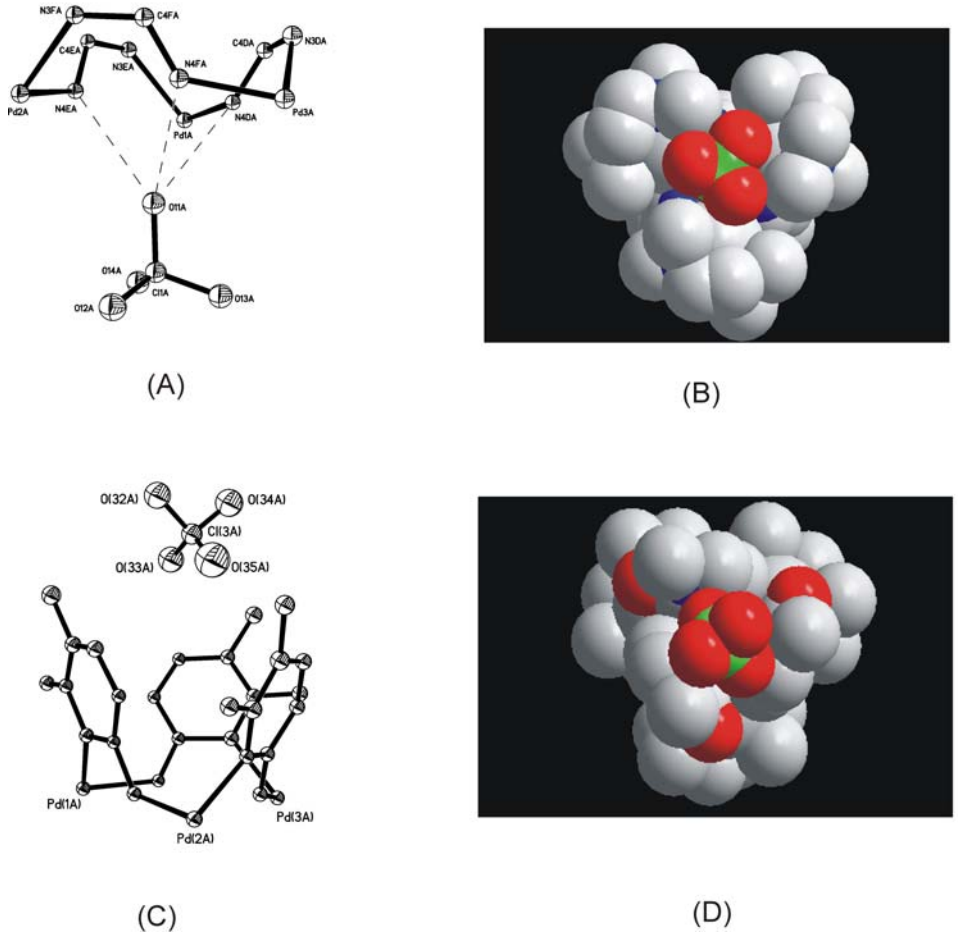

Figure 14. Interactions of two of the four positions of ClO_4^- anions with $Pd_3(1\text{-}MeC^-)_3$ cation: (A) Interaction of O(11A) with three N(4)H sites ("bottom" of double cone). Only the 12-membered ring is shown. (B) Space filling representation of interaction of this ClO_4^- with bottom cone. (C) Interaction of second ClO_4^- with top cone (tmeda ligands are omitted for clarity). (D) Space filling representation of top cone with ClO_4^-.

4.6 Characterization of $[Pt(\mu\text{-}OH)(tmeda)]_2X_2$ (X = ClO_4^-, I-8a or NO_3^-, I-8b)

$[\{Pt(\mu\text{-}OH)(tmeda)\}_2]^{2+}$, prepared in the same way as $[\{Pd(\mu\text{-}OH)(tmeda)\}_2]^{2+}$, was isolated as a bis-$\mu$-hydroxo bridged dimer, $[(tmeda)Pt(OH)_2Pt(tmeda)]^{2+}$ and crystallized as its ClO_4^- salt for **I-8a** and its NO_3^- salt for **I-8b**. The cations in **I-8a** and **I-8b** are almost identical. Two different views of the cation are shown in Figure 15. Selected interatomic distances and angles are listed in Table 8. The cation is closely analogous to bis-μ-hydroxo bridged dimers of Pd^{II}, Pt^{II} [43] and compound **I-6**. The four angles about the Pt centers and their immediate donor atoms deviate markedly (by 5 - 10° in either direction) from the ideal 90° angle in square-planar metal complexes, resulting in slight tetrahedral distortions about the metals (e.g.: N(1)-Pt(1)-O(1), 175.3(3); N(4)-Pt(1)-O(1'), 174.7(3)°). Similarly, the central Pt(1)-O(1)-Pt(1')-O(1') unit is not a square but rather a parallelogram, with the two halves N_2PtO_2 slightly bent and forming an angle of 5.8° for **I-8a** and 5.0° for **I-8b**. The distance between Pt(1)···Pt(1') is 3.16(3) Å for **I-8a**, and 3.14(4) Å for **I-8b**.

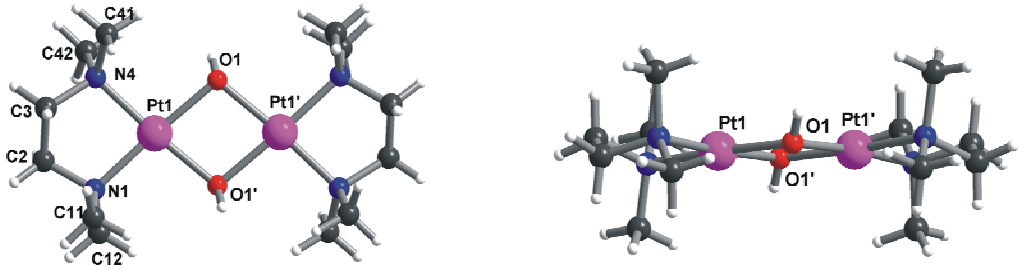

Figure 15. Top and side views of the $[Pt(\mu\text{-}OH)(tmeda)]_2^{2+}$ (**I-8**) cation with atom numbering scheme.

The OH ligands in **I-8a** are involved in hydrogen bonding with oxygen atoms of the perchlorate anions. The distance is (O(1)···O(41A)), 2.825(9) Å; Pt(1)-O(1)···O(14A), 114.8(3)°). However, the OH ligands in **I-8b** contain hydrogen bonds with free water molecule O(1w). (O(1w)···O(1), 2.76(1) Å, Pt(1)-O(1)···O(1w), 116.0(3)°). This free water molecule is involved in hydrogen bonding with oxygen atoms of the nitrate anions with O(1w)···O(11),

2.85(1) Å and O(1w)···O(12), 2.92(1) Å.

Table 8. Selected (bond) distances (Å) and angles (º) for compound **I-8a**[a] and **I-8b**[b].

	I-8a	**I-8b**
Pt1-O1	2.058(6)	2.044(6)
Pt1-N4	2.028(8)	2.025(8)
Pt1-N1	2.031(8)	2.043(8)
Pt1-O1'	2.047(6)	2.036(7)
Pt1···Pt1'	3.16(3)	3.14(4)
O1-Pt1-N4	98.5(3)	97.1(3)
O1-Pt1-N1	175.3(3)	175.4(3)
O1-Pt1-O1'	79.2(2)	79.3(3)
N1-Pt1-N4	85.3(3)	85.4(3)
O1'-Pt1-N4	174.7(3)	175.5(3)
O1'-Pt1-N1	97.2(3)	98.4(3)
Pt1-O1-Pt1'	100.8(3)	100.7(3)

Symmetry transformations used to generate equivalent atoms: [a]: 1-x, 1-y, 1-z; [b]: 1-x, -y, -z.

4.7 Reactions of $[\{Pt(\mu\text{-}OH)(tmeda)\}_2](ClO_4)_2$ with 1-MeC

The reaction of $[\{Pt(\mu\text{-}OH)(tmeda)\}_2](ClO_4)_2$ with 1-MeC in 1:1 ratio was performed in the same way as that leading to $[\{Pd(1\text{-}MeC^-\text{-}N3,N4)(tmeda)\}_3](ClO_4)_3$ (**I-7**). The reaction was monitored by ^1H NMR spectroscopy. The spectrum obtained three days after heating to 60 ^oC is given in Figure 16. Resonances C are observed at 7.09 ppm (H6, d, ^3J = 7.4 Hz) and 6.38 ppm (H5, d, ^3J = 7.4 Hz), in the same region of $[\{Pd(1\text{-}MeC^-\text{-}N3,N4)(tmeda)\}_3]^{3+}$ but with relatively low intensity. Subsequent heating is of no benefit to increase its yield. Rather it increases the yield of $[Pt(OH)(1\text{-}MeC)(tmeda)]^+$.

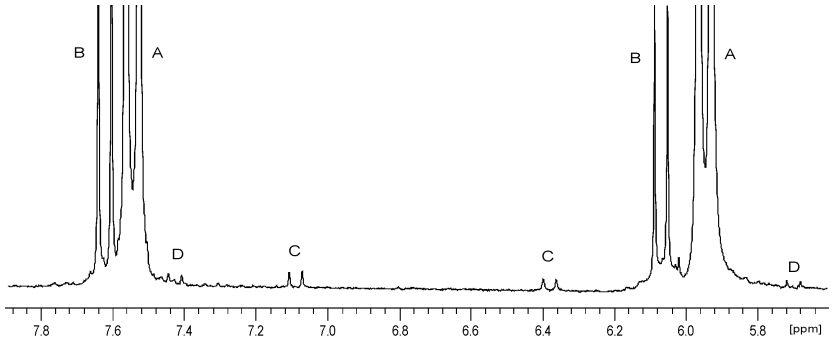

Figure 16. Low field section of ^{1}H NMR spectrum (D_2O) obtained upon mixing [{Pt(μ-OH)(tmeda)}$_2$](NO$_3$)$_2$ and 1-MeC (1:2), with pD kept at 8 after heating at 60 ^{o}C for three days. (A) correspond to 1-MeC resonances; (B) due to [Pt(OH)(1-MeC)(tmeda)]$^+$ resonances; (C) is proposed to be the analogue of Pd$_3$(1-MeC$^-$)$_3$; and D is assigned to [Pt(tmeda)(1-MeC)$_2$]$^{2+}$.

4.8 Reactions of Pd^{II}(tmeda) with cytidine

The reaction of [{Pd(μ-OH)(tmeda)}$_2$](ClO$_4$)$_2$ and cytidine was carried out in the same way as for compound **I-7**. The self-assembling process was followed by ^{1}H NMR spectroscopy. The region of the aromatic cytidine protons is rather complex as shown in Figure 17. Nevertheless, some interesting resonances were identified in the region reminiscent of products formed during the synthesis of **I-7**.

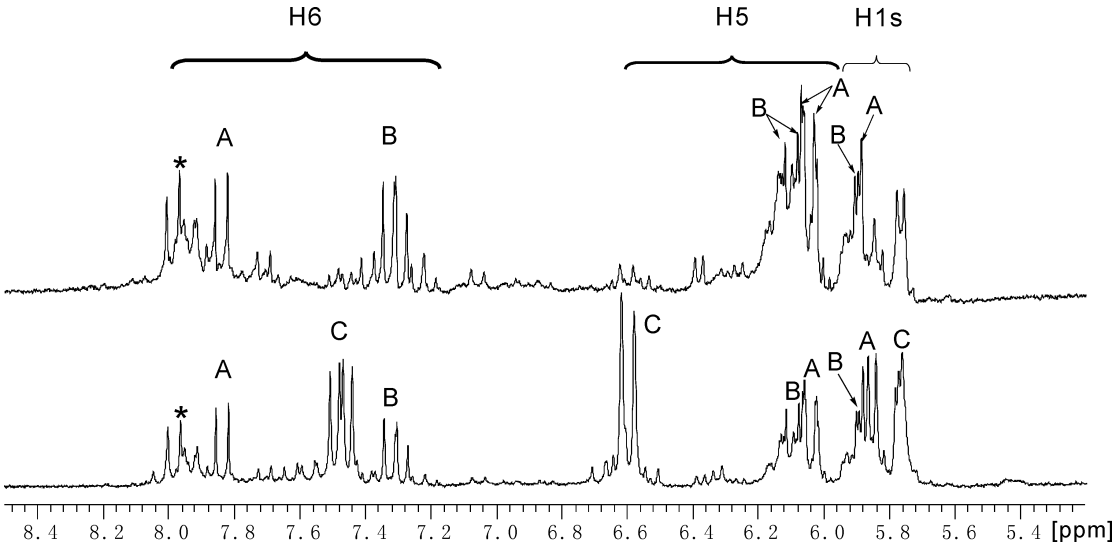

Figure 17. Low field section of ^{1}H NMR spectra (D_2O) obtained upon mixing [Pd(μ-OH)(tmeda)]$_2$(ClO$_4$)$_2$ and cytidine in 1:1 ratio, with pD adjusted to 8: (I) after 2 h stirring at room temperature; (II) after three days heating at 60 ^{o}C. For assignment of A-C, see text.

Spectrum (I) recorded after two hours stirring at room temperature, pD 8. Resonance A can be clearly assigned to cytidine with 7.83 ppm (H6, d, ^3J = 7.6 Hz), 6.04 ppm (H5, d, ^3J = 7.6 Hz), 5.89 ppm (H1S, d, ^3J = 4.0 Hz), 4.29 ppm (H2S, t, ^3J = 5.6 Hz), 4.19 ppm (H3S, t, ^3J = 5.6 Hz), 4.11 ppm (H4S, m) and 3.85 ppm (H5S, m). The intermediate product B is observed at 7.31 ppm (H6, d, ^3J = 7.6 Hz), 6.10 ppm (H5, d, ^3J = 7.6 Hz) and 5.90 ppm (H5, d, ^3J = 4.0 Hz). The ribose protons for product B overlap strongly and were not analysed. In comparison with the intermediate product of the $Pd_3(1\text{-}MeC^-)_3$ reaction, the H(6) and H(5) resonances are closely similar. Moreover, in spectrum (II), which is recorded after heating at 60 °C for three days, the resonances of compound C are observed at 7.46 ppm (H6, d, ^3J = 7.8 Hz), 6.61 ppm (H5, d, ^3J = 7.8 Hz), 5.77 ppm (H1S, d, ^3J = 4.2 Hz). This compound was later successfully isolated and characterized by X-ray crystallography and shown to have a $Pd_3(Cytd^-)_3$ cyclic structure. Somewhat surprisingly, the H(6) resonance occurs as a pair of doublets in the reaction process (spectrum (II)). This is a consequence of the presence of two diastereomers due to the presence of the chiral C(1) atom of the ribose group of cytidine. However, fractional crystallization of this reaction solution gave only one diastereomer (Figure 18). This phenomenon, the selective crystallization of one of two diastereomers under conditions of relatively rapid isomer equilibration in solution, is denoted second-order asymmetric transformation. [46] It has previously been observed in *fac*(*S*)-[Co{(*R*)-cysteinato-*N,S*}$_3$]$^{3-}$ [47] and [{Rh(adenosine)(Cp*)}$_3$]$^{3+}$ (Cp*: η^5-pentamethylcyclopentadienyl),[48] for example.

There are still several byproducts with relatively low intensity in the reaction mixture which are difficult to assign. The resonances (*) in (I) and (II) are tentatively assigned to [Pd(tmeda)(Cytd-*N3*)$_2$]$^{2+}$ or [Pd(OH)(Cytd-*N3*)(tmeda)]$^+$.

In Figure 18, the ^{1}H NMR spectrum obtained by dissolving crystals of [{Pd(Cytd$^-$-*N3*,*N4*)(tmeda)}$_3$](ClO$_4$)$_3$·6H$_2$O (**I-9**) compound is shown. The Cytd$^-$

resonances are observed at 7.46 ppm (H6, d, ^3J = 7.8 Hz), 6.61 ppm (H5, d, ^3J = 7.8 Hz), 5.77 ppm (H1S, d, ^3J = 4.2 Hz), 5.47 ppm (H(N4), s), 4.21 ppm (H2S, t, ^3J = 5.6 Hz), 4.19 ppm (H3S, t, ^3J = 5.6 Hz), 4.05 ppm (H4S, m), 3.80 ppm (H5S, t, ^3J = 12.6 Hz) and 3.76 ppm (H5S', t, ^3J = 12.6 Hz). The N(4)H protons exchange likewise very slowly against ^{2}D (days) reminiscent of $Pd_3(1\text{-}MeC)_3$ complex. The tmeda ligands of $Pd_3(Cytd^-)_3$ display two CH_2 quartets centered at approximately 3.01 ppm and four individual methyl singlets at 2.88, 2.84, 2.78 and 2.39 ppm. The upfield shift of H(6) and remarkable downfield shift of H(5) as compared to free cytidine (H6, 7.83 ppm; H5, 6.04 ppm), is consistent with a $Pd_3(1\text{-}MeC^-)_3$ structure and is only reasonable if a second metal bonded at N(4) of an anionic $Cytd^-$ ligand and present in an *anti* arrangement with respect to N(3).

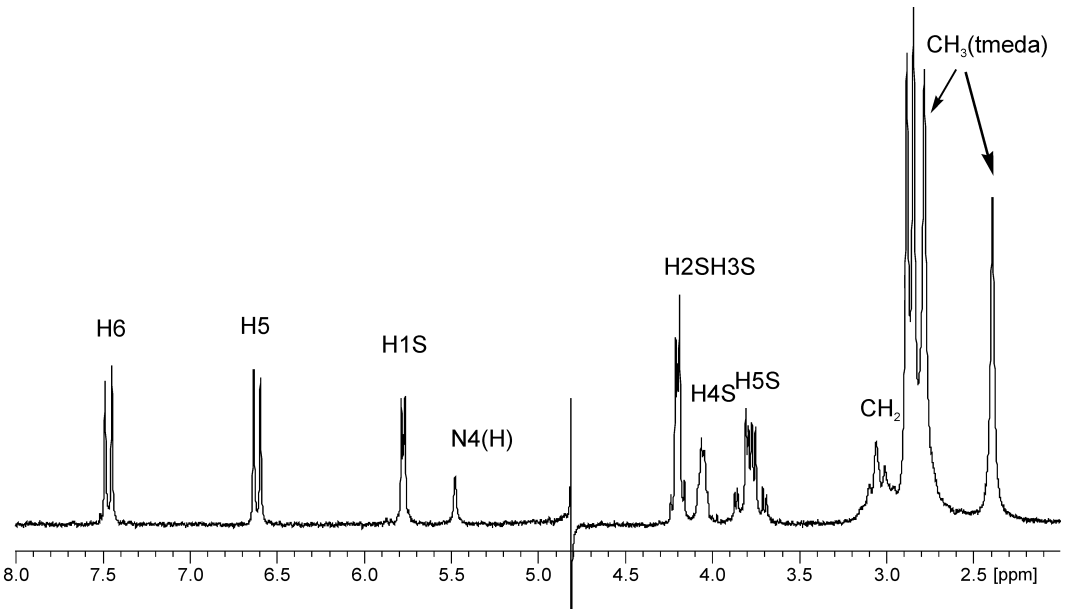

Figure 18. ^{1}H NMR spectrum (D_2O, pD 7.4) of compound **I-9**.

4.9 X-ray crystal structure of $[\{Pd(Cytd^-\text{-}N3,N4)(tmeda)\}_3](ClO_4)_3\cdot 6H_2O$ (I-9)

Crystals of $[\{Pd(Cytd^-\text{-}N3,N4)(tmeda)\}_3](ClO_4)_3\cdot 6H_2O$ (**I-9**) were obtained as the main product of the reaction of $[Pd(tmeda)(H_2O)_2]^{2+}$ with 1 equivalent cytidine at slightly alkaline conditions (pH 9). After a couple of days, yellow crystals were isolated and the structure was determined by X-ray

crystallography. A view of the cation of the cyclic complex $[\{Pd(Cytd^{-}\text{-}N3,N4)(tmeda)\}_3](ClO_4)_3 \cdot 6H_2O$ is provided in Figure 19, and pertinent structural data are listed in Table 9.

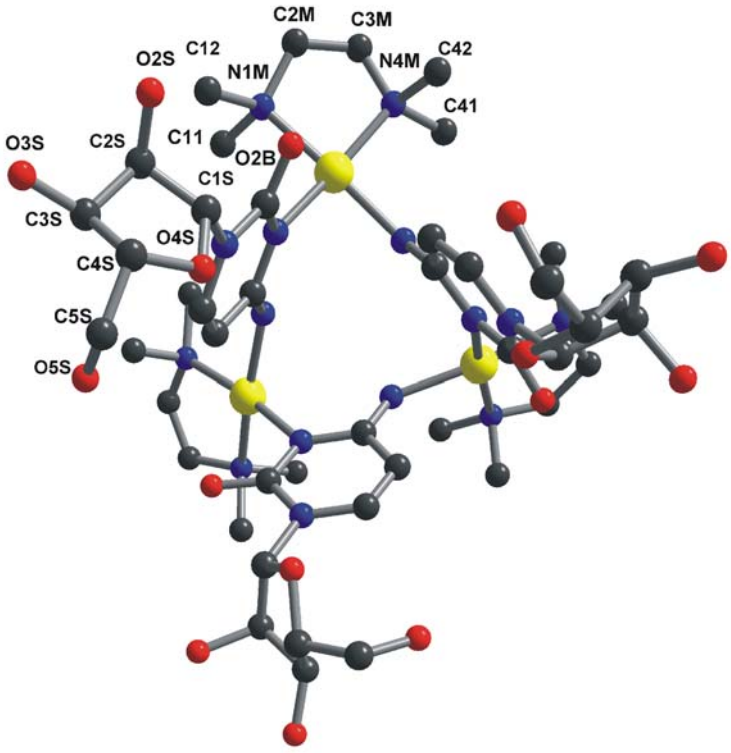

Figure 19. View of the trinuclear cation $[\{Pd(Cytd^{-}\text{-}N3,N4)(tmeda)\}_3]^{3+}$ and atom numbering scheme. The view is along the pseudo-threefold axis of the double cone.

The cation is cyclic, with the three Pd ions cross-linking N(3) and deprotonated N(4) positions of the cytidine nucleosides. As previously noted and described above,[49] the Pd at N(4) has to adopt an *anti* arrangement with respect to N(3) to enable formation of a cycle. A *syn* orientation would lead to a *head-tail* dinuclear species. When viewed from the side, the cation has the shape of a double cone. As compared to the related 1-methylcytosinato complex $[\{Pd(1\text{-}MeC^{-}\text{-}N3,N4)(tmeda)\}_3]^{3+}$ (**I-7**), the upper rim is considerably larger in the cytidine complex. The three deprotonated amino groups $N(4)H^{-}$ are located at the most narrow part of the double cone. The interatomic distances are about 3.369(1) Å. The three metal ions are located at the corners of an ideal equilateral triangle, with Pd···Pd distance of 5.187(1) Å and angles of 60°.

They are very similar to those of the 1-MeC$^-$ analogues and only slightly shorter than those of triangular adenine compounds.[50]

Table 9. Selected Distances (Å) and Angles (º) for compound **I-9**[a].

[{Pd(Cytd$^-$-*N3*,*N4*)(tmeda)}$_3$](ClO$_4$)$_3$·6H$_2$O (I-9)			
Pd1-N1M	2.087(5)	Pd1-N4[a]	2.020(5)
Pd1-N4M	2.066(6)	Pd1···Pd1[a]	5.187(1)
Pd1-N3	2.039(6)	Pd1···O11	3.119(1)
N1M-Pd1-N3	94.0(2)	N1-C1S-C2S	112.2(7)
N1M-Pd1-N4M	84.9(2)	O2S-C2S-C1S	106.2(9)
N1M-Pd1-N4[a]	170.2(2)	O2S-C2S-C3S	105.6(9)
N3-Pd1-N4M	171.5(2)	C1S-C2S-C3S	100.6(8)
N3-Pd1-N4[a]	89.8(2	C2S-C3S-C4S	103.9(9)
N4[a]-Pd1-N4M	92.6(2)	O3S-C3S-C2S	116.3(10)
C1S-O4S-C4S	106.8(6)	O3S-C3S-C4S	111.1(9)
C1S-N1-C6	119.8(6)	O4S-C4S-C3S	101.2(6)
C1S-N1-C2	118.2(6)	O4S-C4S-C5S	107.5(7)
O4S-C1S-N1	110.1(6)	C3S-C4S-C5S	114.3(10)
O4S-C1S-C2S	112.9(7)	O5S-C5S-C4S	117.7(8)
Cytosine plane/ribose	79.3(3)		

[a]: Symmetry transformations used to generate equivalent atoms: -x+y, 1-x, z.

The three bases are inclined by 69.2(2)^o with respect to the Pd_3 plane. The three N(3) atoms likewise form an equilateral triangle (4.498(1) Å), as do the N(1)CH_3 groups (5.763(1) Å). The three cytidine groups present a cone of 3-fold symmetry with a dihedral angle of 86.0(5)^o between the cytosine ring plane and the ribose plane. The three O(3S) atoms are furthest out with distances 12.116(2) Å. They likewise form an equilateral triangle. The three O(5S), although on the top of the methene groups C(5S) (the triangle for C(5S) with distance 7.710(1) Å), approach the center of the cone with shorter distances of 8.064(1) Å. The three tmeda entities likewise form a cone, which at its base is wider than that formed by the three nucleobases but narrower than that formed by three ribose groups. Thus, distances between equivalent amine-N atoms of the tmeda ligands are 7.175(1) Å (N atom of tmeda opposite to N(3) sites of cytidine) and 8.000(1) Å (N atom of tmeda opposite to N(4)

sites of cytidine), and distances between methyl groups of the tmeda ligands furthest apart are 9.594(2) Å (CH_3 groups at N(2) opposite to N(4) sites of cytidine) (Scheme 8).

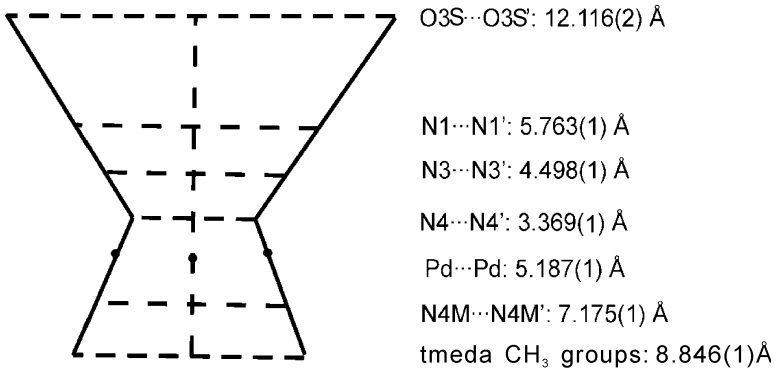

Scheme 8.

The ribose entities in this compound are so-called *β*-sugars, indicating that the nucleobase and C(5S)H_2-O(5S)H are pointing in the same direction as is the case in most of the natural products (Figure 20). The furanose rings are twisted out of the median plane of C(1S)-O(4S)-C(4S) by the major displacement of C(3S), so-called $C^{3'}$-*endo*. These sugar puckers are in the north (N) domains of the pseudorotation cycle of the furanose ring. Moreover, the H(6) atoms of $Cytd^-$ is present above the sugar ring, hence the nucleotide adopts the usual *anti* conformer. The distance between H(6) and O(5S) is 2.895(1) Å, suggesting a weak H bond.

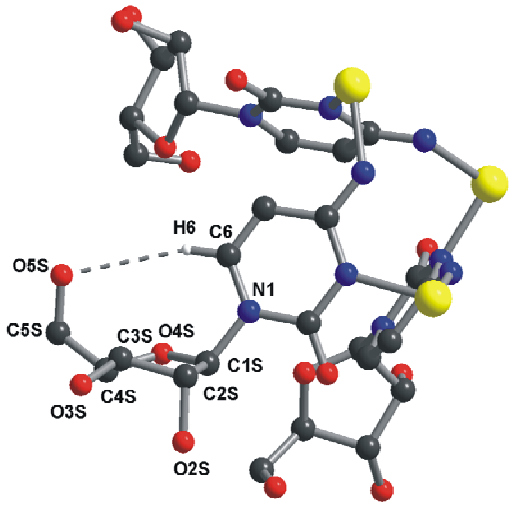

Figure 20. View of sugar pucker in compound **I-9**.

The location of the ClO_4^- anions is not as in the Pt_3 complex[50] and is not like in the Pd_3 complex **I-7** (see above). It is observed in the packing of **I-9** that one ClO_4^- anion is located at a position, which represents the "bottom" of the double cone of one $Pd_3(Cytd^-)_3$ cation, and at the same time close to the top of the double cone of the adjacent $Pd_3(Cytd^-)_3$ cation. The ClO_4^- anion (Cl(1)) interacts via O(11) with the N(4)H triangle from the "bottom" (Figure 21). While the protons at the N(4) groups were not located in the X-ray structure determination, inspection of a model clearly reveals that the three protons of N(4)H are pointing toward the perchlorate oxygen atom, with the distance of 3.119(1) Å between N(4) sites and O(11). Moreover, the ClO_4^- anion is close to the adjacent $Pd_3(Cytd^-)_3$ cation with the distance of 3.591(2) Å between C(5S) and O(12) and 3.549(1) Å between O(4S) and O(12). In this case, stacks of unidirectional trimeric molecules are built up; in these stacks, the trimers are related by the space group translation parallel to crystallographic axis z (Figure 22). A similar situation is found in the $[\{Pt(9\text{-}MeA^-)Me_3\}_3](ClO_4)_3$ compound.[51]

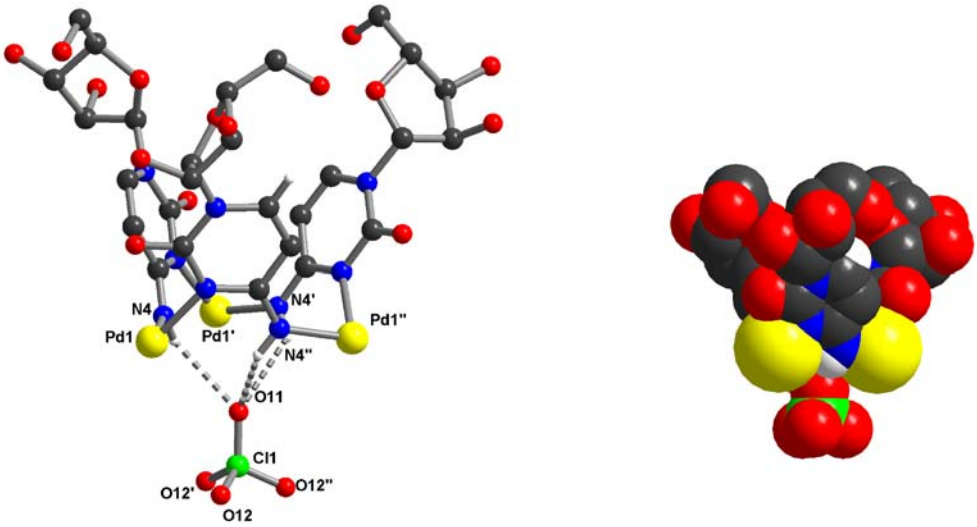

Figure 21. Interaction of ClO_4^- anion with $[Pd_3(Cytd^-)_3]^{3+}$ cation in **I-9**: Hydrogen bonds are found between O(11) with three N(4)H sites ("bottom" of the double cone). Only the 12-membered ring is shown. Space filling representation is shown to the right.

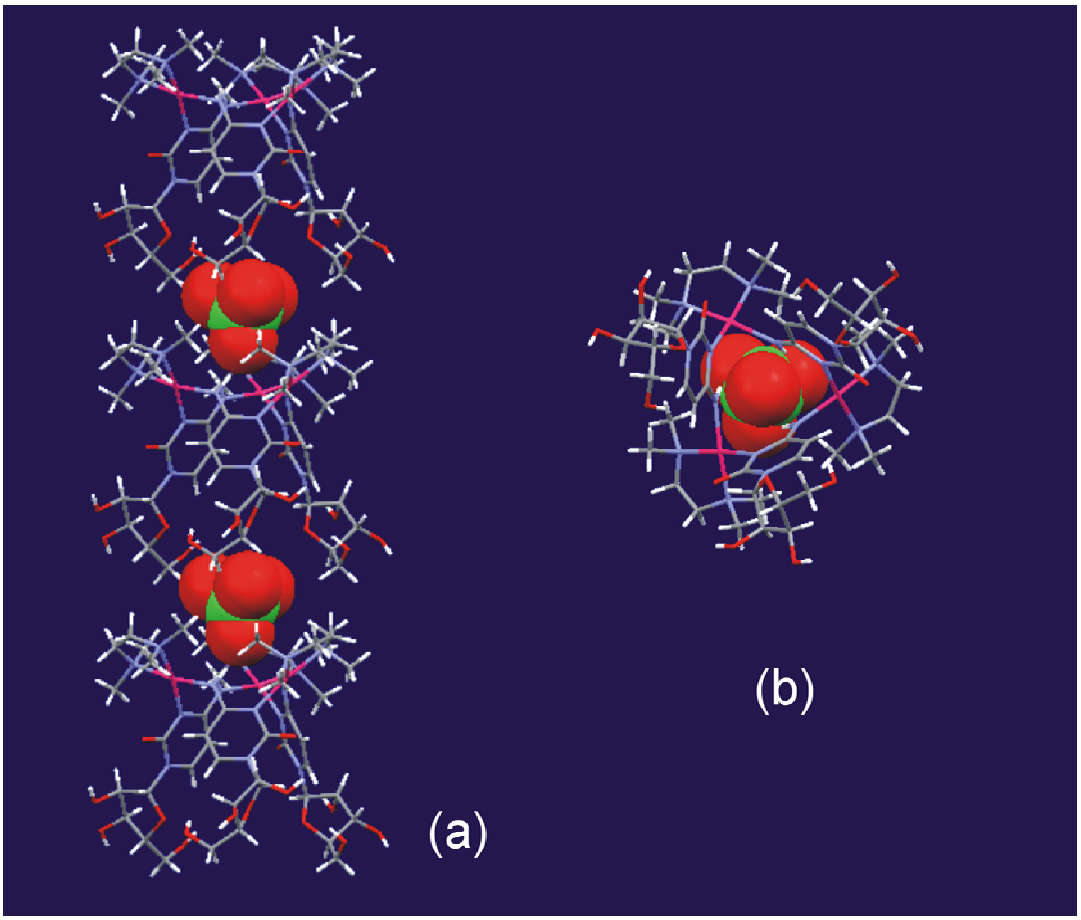

Figure 22. Packing view of the interaction of ClO_4^- anion with $Pd_3(Cytd^-)_3$ cation: (a) along x axis; (b) along the z axis.

4.10 Relationship of Pd_3 with cyclic adeninato complexes

The two cyclic cytosinato bridged Pd_3 compounds described here bear a close resemblance with a series of cyclic trinuclear complexes built from adenine nucleobases with six-coordinated metal entities such as $Rh^{III}(\eta^5\text{-}C_5\text{-}Me_5)$,[52,48] $Ru^{II}(\eta^6\text{-arene})$, [53] or *fac*-$Pt^{IV}(CH_3)_3$ [51] as well as the four-coordinated *cis*-$Pt^{II}(PMePh_2)_3$ entity.[50] Like in Pd_3, in all cases the metal bound to the exocyclic, deprotonated amino group is in an *anti* orientation relative to the metal at the endocyclic N(1) site. In the compounds with octahedral metal ions, this situation is reinforced by the additional chelating interaction of the metal with N(7) (Scheme 9). The metal triangles in the adeninato compounds containing octahedral metal ions have dimensions exceeding slightly those of the Pd triangle, with M···M distances of *ca.* 5.6 Å.[48] In the Pt triangle,[50] the Pt···Pt distances are between 5.20 and 5.38 Å and hence very similar to those of Pd_3. The intermetallic distances of a series of cyclic nucleobase complexes are listed in Table 10.

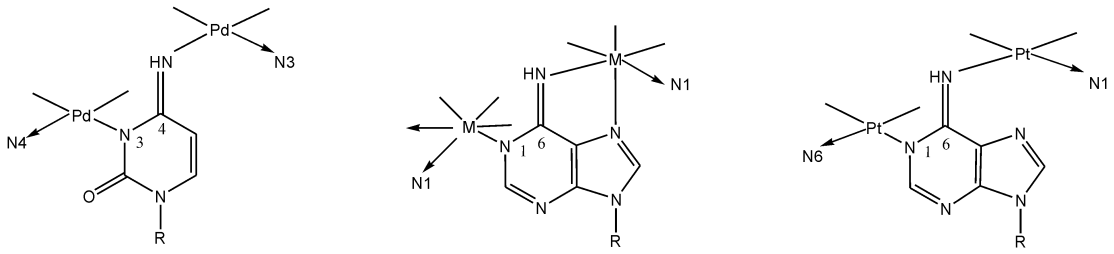

Scheme 9.

The host-guest chemistry of these adenine compounds has been studied (see also Chapter V). Compared to the cytosine (cytidine) complexes reported here, the π system is enlarged in the adenine compounds and gives rise to more versatile interactions with guests.

Table 10. Intermetallic distances (Å) in cyclic nucleobase complexes.

M	nucleobase	M···M	Ref
Pd^{II}(tmeda)	1-MeC	5,166(3) - 5.175(2)	this work
cis-$Pt^{II}(PMe_2Ph)_2$	1-MeC	5.174(2) - 5.308(1)	[54]
cis-$Pt^{II}(PMe_3)_2$	1-MeC	5.31 (av)	[5]
Pd^{II}(tmeda)	cytidine	5.187(1)	this work
cis-$Pt^{II}(PMePh_2)_2$	9-MeA	5.202(1) - 5.382(1)	[50]
Rh^{III}Cp*	9-MeA	5.587(1)	[52]
fac-$Pt^{IV}(Me_3)$	9-MeA	5.71(2)-5.789(2)	[51]
Rh^{III}Cp*	Adenosine	5.6037(6) – 5.6353(6)	[48]

4.11 Analogy of Pd_3 with metallacrowns

There is a close conceptional analogy between the classical crown ethers and the azacrowns, in which some or all of the oxygen atoms are replaced by NH functionalities.[55, 56] This analogy has lately been extended by Pecoraro et al. to cyclic metal complexes termed “metallacrowns” (Figure 23). They represent inorganic analogues of crown ethers.[39] According to this concept, CH_2 groups are substituted by heteroatoms such as N atoms and transition metal ions. For example, [12]crown-3 can be converted into the [12]metallacrown-3 by taking advantage of the self-assembly process of a Ru halfsandwich complex and 3-hydroxy-2-pyridone ligands (Figure 23).[57] This compound displays a high affinity for Li^+ cations, for example.[57a, 57b, 58] Following similar considerations, the here described Pd_3 compounds could be regarded a [12]metallaazacrown-3 ([12]mac-3). It is obvious that its receptor properties no longer are those of a crown ether and likewise not those of an azacrown in that the NH group, originating from N(4)H of 1-MeC^-, has no available electron lone pair. Consequently, no receptor chemistry of Pd_3 toward metal ions is to be expected, but both the positive charge of Pd_3 and the presence of NH functions make this compound a potential anion receptor (see Chapter V).

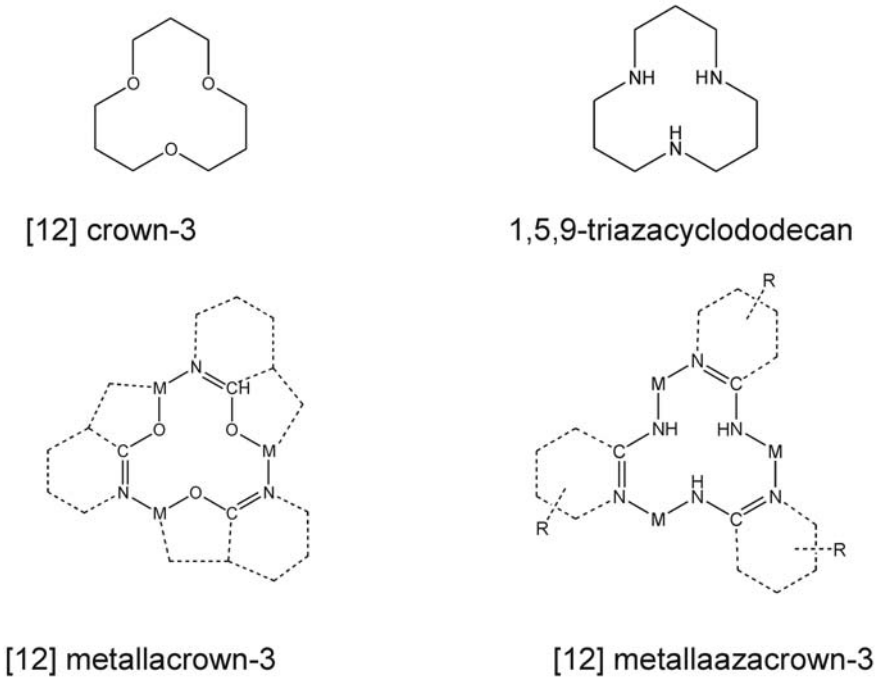

Figure 23. Analogy between crowns, azacrowns, metallacrowns, and metallaazacrowns.

5 Summary

Three *cis*-$Pd^{II}a_2$ entities, Pd^{II}(bpy), Pd^{II}(bipzp) and Pd^{II}(tmeda), were allowed to react with 1-methylcytosine at alkaline pH. Two *head-tail* dinuclear complexes (**I-1**) and (**I-2**) containing 1-methylcytosinato ligands with *N3,N4-syn*-bridging modes and two trinuclear cyclic complexes (**I-7**) and (**I-9**) containing 1-methylcytosinato and cytidinato ligands with *N3,N4-anti*-bridging modes have been synthesized and characterized. Formation of cyclic trimers rather than *head-tail* dimmers is attributed to the steric bulk exercised of the tmeda ligands, and unfavorable angles about the exocyclic N(4) donor, respectively.

References

[1] Review: Lippert, B. *Prog. Inorg. Chem.* **1989**, *37*, 1.

[2] (a) Lock, C. J. L.; Peresie, H. J.; Rosenberg, B.; Turner, G. *J. Am. Chem. Soc.* **1978**, *100*, 3371. (b) Faggiani, R.; Lock, C. J. L.; Pollock, R. J.; Rosenberg, B.; Turner, G. *Inorg. Chem.* **1981**, *20*, 804.

[3] (a) Grehl, M.; Krebs, B. *Inorg. Chem.* **1994**, *33*, 3877. (b) Paschke, N.; Röndigs, A.; Popenborg, H.; Wolff, J. E. A.; Krebs, B. *Inorg. Chim. Acta* **1997**, *264*, 239.

[4] Trovó, G.; Bandoli, G.; Casellato, U.; Corain, B.; Nicolini, M.; Longato, B. *Inorg. Chem.* **1990**, *29*, 4616.

[5] Schenetti, L.; Bandoli, G.; Dolmella, A.; Trovó, G.; Longato, B. *Inorg. Chem.* **1994**, *33*, 3169.

[6] Lippert, B. In *Cisplatin-Chemistry and Biochemistry of a Leading Anticancer Drug*; Lippert, B.; Ed.; VHCA: Zürich and Wiley-VCH: Weinheim, **1999**; pp. 379 - 403.

[7] O'Halloran, T. V.; Lippard, S. J. *J. Am. Chem. Soc.* **1983**, *105*, 3341.

[8] (a) Hollis, L. S.; Lippard, S. J. *J. Am. Chem. Soc.* **1981**, *103*, 6761. (b) Hollis, L. S.; Lippard, S. J. *J. Am. Chem. Soc.* **1981**, *103*, 1230.

[9] Schöllhorn, H.; Thewalt, U.; Lippert, B. *Inorg. Chim. Acta* **1984**, *93*, 19.

[10] (a) Kistenmacher, T. J.; Rossi, M.; Marzilli, L. G. *Inorg. Chem.* **1979**, *18*, 240. (b) Marzilli, L. G.; Kistenmacher, T. J.; Rossi, M. *J. Am. Chem. Soc.* **1977**, 2797.

[11] Biagini, M. C.; Ferri, M.; Lanfranchi, M.; Marchiò, L.; Pellinghelli, M. A. *Dalton Trans.* **1999**, 1575.

[12] See, e.g.: (a) Cramer, R. E.; Dahlstrom, P. L. *J. Am. Chem. Soc.* **1979**, *101*, 3679. (b) Cramer, R. E.; Dahlstrom, P. L. *Inorg. Chem.* **1985**, *24*, 3420.

[13] Natile, G.; Marzilli, L. G. *Coord. Chem. Rev.* **2006**, *250*, 1315, and refs. cited.

[14] Schröder, G.; Sabat, M.; Baxter, I.; Kozelka, J.; Lippert, B. *Inorg. Chem.* **1997**, *36*, 490, and refs. cited.

[15] Weinkötter, T.; Sobat, M.; Fusch, G.; Lippert, B. *Inorg. Chem.* **1995**, *34*, 1022.

[16] Matsumoto, K.; Harashima, K.; Moriyama, H.; Sato, T. *Inorg. Chim. Acta* **1992**,*197*, 217.

[17] Sakai, K.; Takeshita, M.; Tsubomura, T. 43rd Symposium on Coordination Chemistry of Japan, **1993**, Paper No. 2, P32.

[18] Krumm, M. *Dissertation*, University of Dortmund, **1992**.

[19] Minghetti, G.; Cinellu, M. A. *J. Organomet. Chem.* **1986**, *315*, 387.

[20] Tsuji, S.; Swenson, D. C.; Jordan, R. F. *Organometallics* **1999**, *18*, 4758-4764.

[21] (a) Krumm, M.; Mutikainen, I.; Lippert, B. *Inorg. Chem.* **1991**, *30*, 884. (b) Zangrado, E.; Pichierri, F.; Randaccio, L.; Lippert, B. *Coord. Chem. Rev.* **1996**, *156*, 275.

[22] Pauling, L. The Nature of the Chemical Bond, Cornell University Press, Ithaca, 2nd Edn., **1944**, p.180.

[23] Bondi, A. *J. Phys. Chem.* **1964***, 68*, 441.

[24] Rother, I. B.; Willermann, M.; Lippert, B. *Supramolecular Chemistry* **2002**, *14*, 189.

[25] Ludwig, R. *Angew. Chem. Int. Ed.* **2001**, *40*, 1808.

[26] Custelcean, R.; Afloroaei, C.; Vlassa, M.; Polverejan, M. *Angew. Chem. Int. Ed.* **2000**, *39*,

3094.

[27] Randaccio, L.; Zangrando, E.; Cesàro, A.; Holthenrich, D.; Lippert, B. *J. Mol. Struct.* **1998**, *440*, 221.

[28] (a) Liu, K.; Brown, M. G.; Carter, C.; Saykally, R. J.; Gregory, J. K.; Clary, D. C. *Nature* **1996**, *381*, 501.

[29] Nauta, K.; Miller, R. E. *Science* **2000**, *287*, 293.

[30] Weinhold, F. *J. Chem. Phys.* **1998**, *109*, 367.

[31] Ugalde, J. M.; Alkorta, I.; Elguero, J. *Angew. Chem. Int. Ed.* **2000**, *39*, 717.

[32] Kim, J.; Majumdar, D.; Lee, H. M.; Kim, K. S. *J. Chem. Phys.* **1999**, *110*, 9128.

[33] Liu, K.; Cruzan, J. D.; Saykally, R. J. *Science* **1996**, *271*, 929.

[34] Ma, B. Q.; Sun, H. L.; Gao, S. *Chem. Commun.* **2004**, 2220.

[35] Frommer, G.; Lianza, F.; Albinati, A.; Lippert, B. *Inorg. Chem.* **1992**, *31*, 2434.

[36] Reily, M. D.; Marzilli, L. G. *J. Am. Chem. Soc.* **1986**, *108*, 6785.

[37] De Graaf, W.; Boersma, J.; Smeets, J. J. W.; Spek, A. L.; Van Koten, G. *Organometallics* **1989**, *8*, 2907.

[38] Wiesner, J. R.; Lingafelter, E. C. *Inorg. Chem.* **1996**, *5*, 1770.

[39] (a) Lah, M. S.; Pecoraro, V. L. *Comments Inorg. Chem.* **1990**, *11*, 59. (b) Pecoraro, V. L.; Stemmler, A. J.; Gibney, B. R.; Bodwin, J. J.; Wang, H.; Kampf, J. W.; Barwinski, A. *Prog. Inorg. Chem.* **1997**, *45*, 83. (c) Bodwin, J. J.; Cutland, A. D.; Malkani, R. G.; Pecoraro, V. L. *Coord. Chem. Rev.* **2001**, *216-217*, 489.

[40] Preut, H.; Frommer, G.; Lippert, B. *Acta Cryst.* **1991**, *C47*, 852.

[41] Lippert, B.; Lock, C. J. L.; Speranzini, R. A. *Inorg. Chem.* **1981**, *20*, 808.

[42] Krumm, M.; Mutikainen, I.; Lippert, B. *Inorg. Chem.* **1991**, *30*, 884.

[43] (a) Getty, A. D.; Goldberg, K. L. *Organometallics* **2001**, *20*, 2545. (b) Schnebeck, R.-D.; Freisinger, E.; Lippert, B. *Eur. J. Inorg. Chem*. **2000**, 1193. (c) Faggiani, R.; Lippert, B.; Lock, C. J. L.; Rosenberg, B. *J. Am. Chem. Soc.* **1977**, *99*, 777.

[44] Fekl, U.; van Eldik, R.; Richardson, C.; Robinson, W. T. *Inorg. Chem*. **2001**, *40*, 3247 and refs. cited.

[45] Faggiani, R.; Lippert, B.; Lock, C. J. L.; Speranzini, R. A. *J. Am. Chem. Soc.* **1981**, *103*, 1111.

[46] Turner, E. E.; Harris, M. M. *Quart. Rev. (London)*, **1947**, *1*, 299.

[47] Kita; M.; Yamanari, K. *J. Chem. Soc., Dalton Trans.* **1999**, 1221.

[48] (a) Yamanari, K.; Ito, R.; Yamamoto, S.; Fuyuhiro, A. *Chem. Commun.* **2001**, 1414. (b) Yamanari, K.; Ito, R.; Yamamoto, S.; Konno, T.; Fuyuhiro, A.; Kobayashi, M.; Arakawa, R. *Dalton Trans.* **2003**, 380.

[49] Shen, W.-Z.; Gupta, D.; Lippert, B. *Inorg. Chem.* **2005**, *44,* 8249.

[50] Longato, B.; Pasquato, L.; Mucci, A.; Schenetti, L.; Zangrando, E. *Inorg. Chem.* **2003**, *42*, 7861.

[51] Zhu, X.; Rusanov, E.; Kluge, R.; Schmidt, H.; Steinborn, D. *Inorg. Chem.* **2002**, *41*, 2667.

[52] (a) Smith, D. P.; Baralt, E.; Morales, B.; Olmstead, M. M.; Maestre, M. F.; Fish, R. H. *J. Am.*

Chem. Soc. **1992**, *114*, 10647. (b) Fish, R. H. *Coord. Chem. Rev.* **1999**, *185-186*, 569.

[53] (a) Korn, S.; Sheldrick, W. S. *Inorg. Chim. Acta* **1997**, *254*, 85. (b) Korn, S.; Sheldrick, W. S. *J. Chem. Soc., Dalton Trans.* **1997**, 2191.

[54] Longato, B.; Montagner, D.; Zangrando, E. *Inorg. Chem.* **2006**, *45*, 8179

[55] Steed, J. W.; Atwood, J. L. *Supramolecular Chemistry*, John Wiley & Sons, Ltd. Chichester **2000**.

[56] With all oxygen atoms replaced by NH groups, these ligands are also termed polyamine macrocycles or azacorands.

[57] (a) Piotrowski, H.; Severin, K *Proc. Natl. Acad. Sci USA* **2002**, *99*, 4997. (b) Grole, Z.; Lehaire, M-. L.; Scopelliti, R.; Severin, K. *J. Am. Chem. Soc.* **2003**, *125*, 13638. (c) Piotrowski, H.; Hilt, G.; Schulz, A.; Mayer, R.; Polborn, K.; Severin, K. *Chem. Eur. J.* **2001**, *7*, 3197. (d) Lehaire, M.-L.; Scopelliti, R.; Herdeis, L.; Polborn, K.; Mayer, P.; Severin, K. *Inorg. Chem.* **2004**, *43*, 1609.

[58] Mimassi, L.; Guyard-Duhayon, C.; Rager, M. N.; Amouri, H. *Inorg. Chem.* **2004**, *43*, 6644.

Chapter II

Pd_2Ag triangle supported by two μ_3-amidopyridine ligands

1 Aim of the project

The original aim of the work was to prepare a cyclic Pd_3 species with *N1*,*N2*-binding ampy ligands and a structure analogous to the 1-methylcytosinato complexes reported in the previous section.[1,2] To this end we tried to achieve the condensation of the mononuclear $[Pd(tmeda)(Hampy\text{-}N1)(H_2O)]^{2+}$ species, which had been prepared by treating $[PdCl(tmeda)(Hampy\text{-}N1)]NO_3$ with $AgNO_3$ in water. The compound actually isolated from solution proved not to be the compound aimed for, but rather $[\{(tmeda)Pd(N2\text{-}ampy^{-}\text{-}N1)\}_2Ag]^{3+}$, a compound formally obtained by intramolecular condensation reactions between $[Ag(Hampy\text{-}N1)_2]^{+}$ and two $[Pd(OH)_2(tmeda)]$ entities (Scheme 1). Moreover, Pd^{II}(bpy), when reacted with Hampy, leads to a *head-tail* dimer structure, the same as in the case of 1-MeC.

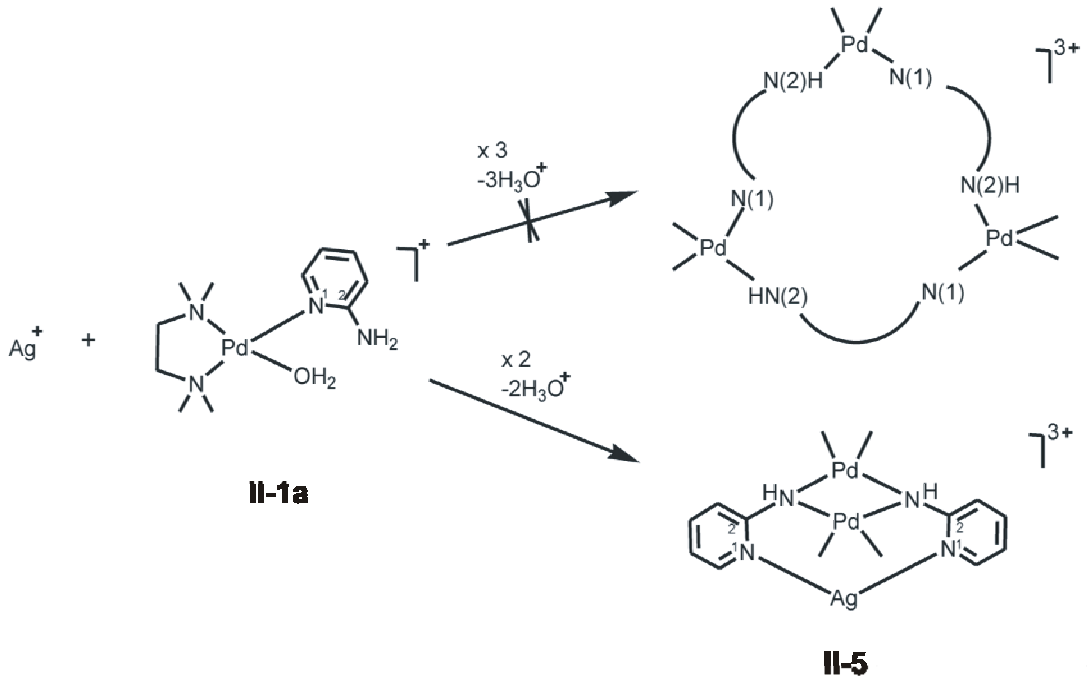

Scheme 1.

Related to this work, the reactivity patterns of *trans*-$[Pta_2(Hampy\text{-}N1)_2]^{2+}$ (a = NH_3 [3,4] or $MeNH_2$ [5]) with Pd^{II}(en) and $[Pd(H_2O)_4]^{2+}$, have been previously studied. As a result, the formation of species with Pd^{II} binding either exclusively to the exocyclic amino group of the Hampy ligand with deprotonation of the latter,[4,5] or in addition with condensation between the Pt-NH_3 ligand and the Pd-OH_2 entity,[3] have been observed. In the former case, reaction between the Pt complex and Pd^{II}(en) occurred in an intermolecular fashion, leading to rectangular Pt_2Pd_2 cage compounds. In the latter case an intramolecular reaction took place, yielding a product of $PtPd_3$ stoichiometry displaying a Pt→Pd dative bond, and two μ-NHpy as well as two μ-NH_2 groups.

2 NMR spectra of 2-aminopyridine

The ^{1}H NMR spectrum of the free ligand Hampy was recorded in order to have a direct comparison with spectra of the various metal complexes. At high resolution (600 MHz), the proton resonances of H(6), H(4) and H(5) represent eight-line signals, whereas H(3) displays six lines only due to superposition of two lines (Figure 1). Analysis of the individual signals gives the following coupling constants: H6: ^3J(H6, H5), 5.4 Hz, ^4J(H6, H4), 2.0 Hz, ^5J(H6, H3), 1.0 Hz; H5: ^3J(H5, H6), 5.4 Hz, ^3J(H5, H4), 7.3 Hz, ^4J(H5, H3), 2.0 Hz; H4: ^3J (H4, H5), 7.3 Hz, ^3J(H4, H3), 8.3 Hz, ^4J(H4, H6), 2.0 Hz; H3: ^3J(H3, H4), 8.3 Hz, ^4J (H3, H5), 2.0 Hz, ^5J(H3, H6), 1.0 Hz.

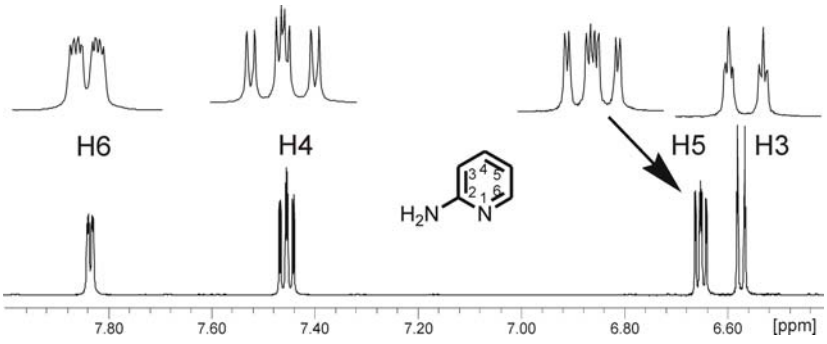

Figure 1. ^{1}H NMR spectrum of Hampy in D_2O, pD = 9.

As expected, the ^{1}H NMR resonances of the Hampy are pD dependent due to protonation[6]/deprotonation[6,7] equilibria of the following types:

$$H_2ampy^+ \rightleftharpoons Hampy \rightleftharpoons ampy^-$$
$$pK_{a1} = 6.71 \qquad pK_{a2} \geq 23.5$$

In aqueous solution, only pK_{a1} is relevant.

The ^{13}C NMR spectrum of Hampy (D_2O, pD = 9) is not unusual, with the five carbon atoms displaying the following shifts (δ, ppm): C2, 158.5, C6, 146.8, C4, 139.3, C5, 114.8 and C3, 110.4. The assignment of the ^{1}H NMR resonances used above is based on a HSQC spectrum.

3 1:1 and 1:2 complexes of M^{II}(tmeda) (M = Pd, Pt) with Hampy

Reactions of $PdCl_2$(tmeda) and $PtCl_2$(tmeda), and their aqua species, respectively, with Hampy gave the following compounds: [PdCl(tmeda)(Hampy-*N1*)](NO_3) (**II-1**), [Pd(tmeda)(Hampy-*N1*)$_2$](NO_3)$_2$ (**II-2**), [PtCl(tmeda)(Hampy-*N1*)](NO_3) (**II-3**), and [Pt(tmeda)(Hampy-*N1*)$_2$](NO_3)$_2$ (**II-4**). The compounds were characterized by elemental analysis and ^{1}H NMR spectroscopy. Of compound **II-2**, an X-ray crystal structure analysis was performed.

The ^{1}H NMR spectra of **II-1**-**II-4** in D_2O contain three (**II-1**, **II-3**, **II-4**) and more (**II-2**) sets of multiplets attributed to H(6), H(4), as well as H(3)/H(5) (overlapping) signals (Table 1).

The two sets of resonances of **II-2**, present in a ratio of *ca.* 3:1, are due to the presence of two rotamers in solution, *head-tail* (major rotamer) and *head-head* (minor rotamer). This assignment is based on the observation that immediately after dissolving crystals of **II-2** in D_2O, the ^{1}H NMR spectrum displays a predominant doublet centered at 8.44 ppm, whereas the lower intensity doublet centered at 8.51 ppm reaches its full intensity only later.

Table 1. Chemical shifts (δ centre of multiplet of aromatic resonance) of free ligand Hampy and of Hampy/ampy resonances of **II-1** – **II-5** in D_2O (200 MHz).

	H6	H4	H3/H5	pD
Hampy	7.96	7.58	6.77,6.70	7.0
II-1	8.16	7.60	6.79	6.1
II-1a	8.27	7.61	6.78	9.0
II-2	8.44 *ht*/8.51 *hh*	7.56 *ht*/7.58 *hh*	6.76	6.9
II-3	8.16[a]	7.59	6.76	7.0
II-4	8.34 *hh*/8.35 *ht*[a,b]	7.54	6.71	7.0
II-5	8.72	7.82	7.43	6.9

[a] $^3J(^{195}Pt–^1H)$ ~ 31 Hz;

[b] assignment of *ht* and *hh* may be reversed.

The H(6) resonance of Hampy in the Pt complex **II-3** is readily identified because of its ^{195}Pt satellites of *ca.* 31 Hz due to ^3J coupling. A similar situation is realized with **II-4,** with a stronger overlap of the individual H(6) resonances and Pt satellites, however.

The CH_3 resonances of the tmeda ligands (Table 2) are observed in the range δ = 2.6 – 3.0 ppm. In the bis(Hampy) complexes **II-2** and **II-4** two pairs of individual CH_3 singlets of the two rotamers can be readily distinguished on the basis of their different intensities. In the mono(Hampy) complexes **II-1** and **II-3** the four methyl groups occur as four singlets, grouped in two pairs.

Table 2. Chemical shifts of CH_2 and CH_3 resonances of **II-1** – **II-5** in D_2O (200 MHz).

	CH_2	CH_3	pD
II-1	2.99	2.80, 2.79, 2.62, 2.61	6.1
II-1a	2.87	2.75, 2.72, 2.52	9.0
II-2	3.13	2.83(*hh*), 2.79(*ht*), 2.77(*ht*), 2.71(*hh*)	6.9
II-3	2.99	2.93, 2.91, 2.80, 2.77	7.0
II-4	3.10	2.94(*hh*)[a], 2.89(*ht*)[a], 2.85(*ht*)[a], 2.77(*hh*)[a]	7.0
II-5	2.61	2.46, 1.43	6.9

[a] assignment of *ht* and *hh* may be reversed.

4 Characterization of [Pd(tmeda)(Hampy-*N1*)$_2$](NO$_3$)$_2$ (II-2)

The cation of **II-2** is depicted in Figure 2. The two Hampy ligands are bonded to Pd via the endocyclic N(1) positions and adopt a *head-tail* arrangement. Bond distances and angles about the metal ion are not unusual (Table 3).

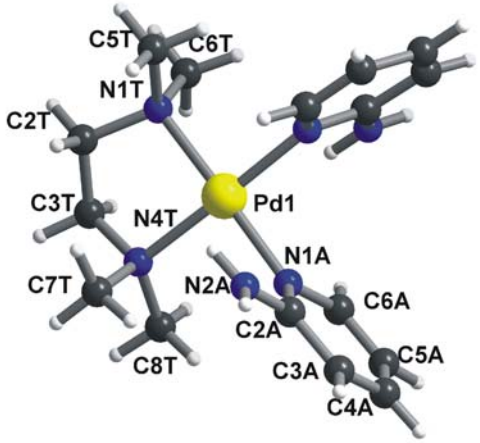

Figure 2. Side view of cation of [Pd(tmeda)(Hampy-*N1*)$_2$](NO$_3$)$_2$ (**II-2**) with atom numbering scheme. The two Hampy ligands adopt a *head-tail* orientation.

Geometries of the Hampy ligands are normal.[4,8] As compared to the free ligand,[9] the internal ring angle at N(1) in **II-2** is expected to increase upon metal coordination. However, due to the relatively large standard deviation in **II-2** (118.7(6)^o) this difference (117.5(3)^o in free ligand) is not significant. The dihedral angles between the Hampy and the Pd coordination plane is 89.6(3)^o and 86.9(2)^o, similar as Pt^{II} and Pd^{II} analogues.[10]

Table 3. Selected bond distances (Å) and angles (^{o}) for compound **II-2**.

[Pd(tmeda)(Hampy-*N1*)$_2$](NO$_3$)$_2$ (II-2)			
Pd1-N1A	2.027(5)	Pd1-N4T	2.064(4)
Pd1-N1B	2.047(6)	C2A-N2A	1.288(9)
Pd1-N1T	2.050(4)	C2B-N2B	1.34(1)
N1A-Pd1-N1B		87.5(2)	
Pd plane/2-ampy plane		89.6(3)/86.9(2)	

5 Interaction of Hampy with Ag^+

Additon of increasing amounts of $AgNO_3$ to a solution of Hampy in D_2O (0.1 M, pD 7) causes downfield shifts of most of the Hampy resonances and in particular those of H(3) and H(4) (Figure 3), tentatively suggesting a primary binding of Ag^+ at the exocyclic amino group of Hampy. The fact that only single sets of resonances are observed is in agreement with labile Ag-N bonds and fast exchange on the NMR time scale. At higher absolute concentrations of Hampy and $AgNO_3$, formation of a colorless precipitate is observed, presumably of $[Ag_3(Hampy)_4](NO_3)_3$, as previously reported by Uhlig and Mädler[11] and later confirmed in an X-ray crystal structure analysis by Charland and Beauchamp.[12]

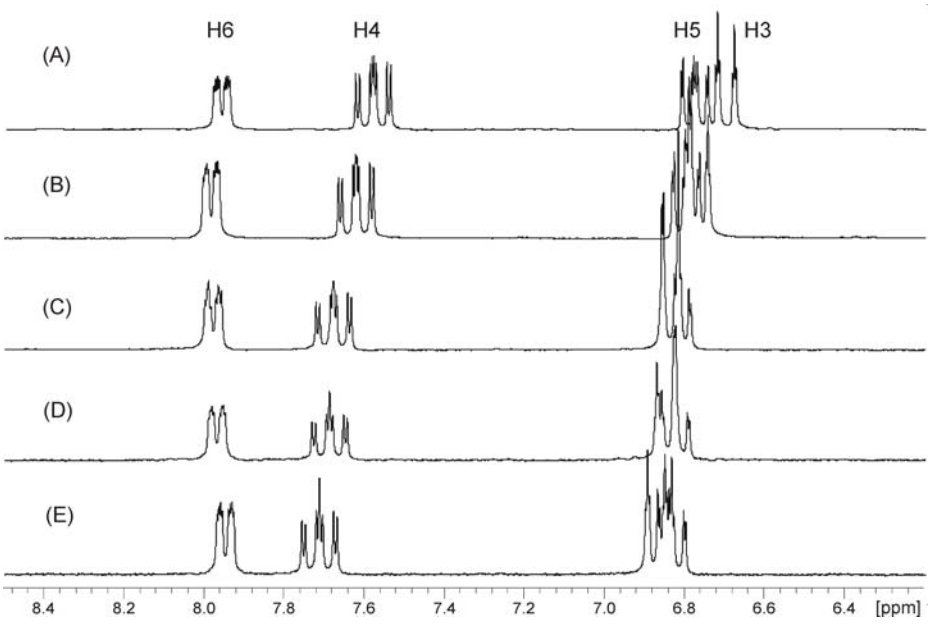

Figure 3. Low field section of ^1H NMR spectra of mixtures of Hampy and $AgNO_3$ in D_2O (pD = 7): (A) Hampy ligand. (B) $AgNO_3$: Hampy 1:0.2. (C) $AgNO_3$: Hampy 1:0.5. (D) $AgNO_3$: Hampy 1:0.8. (E) $AgNO_3$: Hampy 1:1.

6 Reaction of [PdCl(tmeda)(Hampy-*N1*)]NO_3 with $AgNO_3$

Treatment of [PdCl(tmeda)(Hampy-*N1*)]NO_3 (**II-1**) with two equiv of $AgNO_3$, hence an excess of Ag^+, filtration of AgCl, and addition of NaOH (pH 8-9)

leads to an orange-coloured solution from which orange-brown crystals of composition [{(tmeda)Pd(*N2*-ampy-*N1*)}$_2$Ag(μ-NO_3)$_2$Ag(NO_3)$_2$] (**II-5**) crystallized.

In Figure 4 the low field sections of ^{1}H NMR spectra recorded upon combining [PdCl(tmeda)(Hampy-*N1*)]$^+$ (**II-1**) and $AgNO_3$ are presented. Initially $AgNO_3$ reacts with **II-1** to give the aqua species [Pd(tmeda)(Hampy-*N1*)(H_2O)]$^{2+}$ (**II-1a**), which undergoes partial hydrolysis to give the corresponding hydroxo species (pK_a of aqua ligand estimated 5 – 6) and causes a drop in pD of the solution (H(6) signal). As can be seen from the H6 resonances in the shift range 8.2-8.5 ppm (spectra (B)-(D)), formation of the hydrolysis product **II-1a** is accompanied by the appearance of resonances of the two rotamers of the 2:1-complex [Pd(tmeda)(Hampy-*N1*)$_2$]$^{2+}$ (**II-2**). This feature is indicative of a symmetrization reaction of the 1:1-complex to give the 2:1-complex and $Pd(OH)_2$(tmeda)/[Pd(tmeda)(H_2O)$_2$]$^{2+}$. Eventually formation of the Pd_2Ag complex **II-5** is apparent from its highly characteristic H(6) multiplet at 8.72 ppm, see also discussion below.

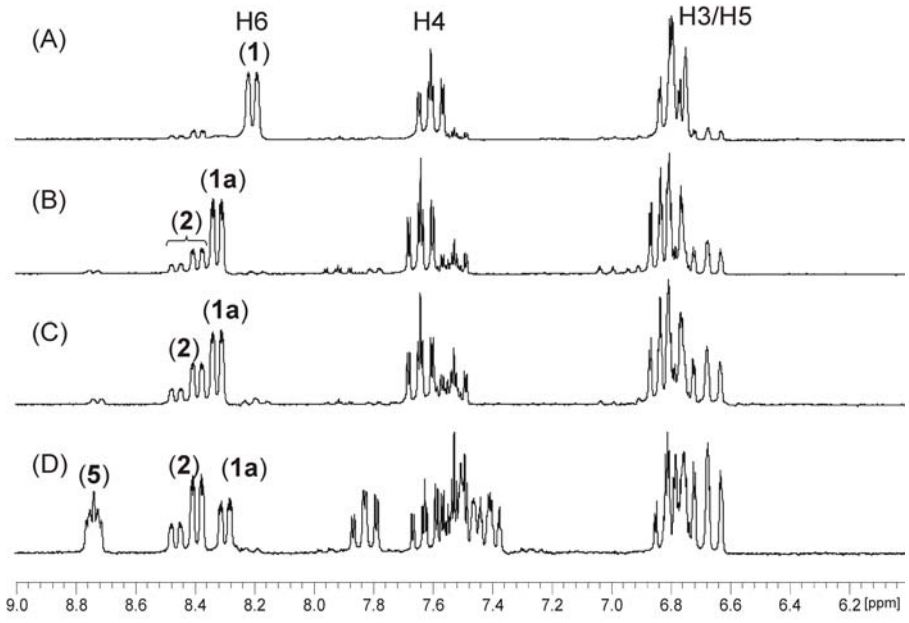

Figure 4. Low field section of ^{1}H NMR spectra (D_2O) of (A) Compound **II-2** dissolved in D_2O, pD 7.0. (B) After 3 h stirring with excess $AgNO_3$ (1.5 equiv) and filtration of AgCl, pD 4.0. (C) After adjusting the pD to 5 with NaOD. (D) After adjusting the pD to 7.5 with NaOD and stirring the solution at 50 °C for one day. H6 resonances correspond to **II-1**, **II-1a**, **II-2**, and **II-5**.

7 Characterization of [{(tmeda)Pd(*N2*-ampy$^-$-*N1*)}$_2$Ag(μ-NO_3)$_2$Ag(NO_3)$_2$] (II-5) and [{(tmeda)Pd(*N2*-ampy$^-$-*N1*)}$_2$Ag(ClO_4)$_2$](ClO_4)·2H_2O (II-5a)

Compound **II-5a** was synthesized in the same way as compound **II-5** except that $AgClO_4 \cdot xH_2O$ was used instead of $AgNO_3$. Figure 5 and Figure 6 provide the views of compound **II-5** and compound **II-5a**, respectively. Both compounds consist of trinuclear Pd_2Ag cores (Pd(1), Pd(1'), Ag(1)) which are almost identical in their coordination modes. A crystallographic plane of symmetry disects the Pd_2Ag plane at Ag(1). The Pd_2Ag triangle is covered at both faces by triply bridging amidopyridine ($ampy^-$) anions, with the Ag^+ chelated by two N(1) positions of the heterocyclic rings and the two Pd centres bridged via the exocyclic N(2) sites. The exocyclic amino group of each Hampy has thus lost a proton, giving the ampy ligands a –1 charge each. The Pd_2Ag triangle in compound **II-5** is isolateral with a Pd···Pd separation of 3.088(1) Å and Pd···Ag distances of 3.088(1) Å, while in compound **II-5a** it is more distorted with a Pd···Pd separation of 3.070(2) Å and Pd···Ag distances of 3.15(5) Å. Selected interatomic distances and angles of **II-5** and **II-5a** are compiled together in Table 4 for better comparison. The coordination patterns of the ampy ligand seen in **II-5** and **II-5a** are not unprecedented and realized, for example, also in trinuclear clusters of Os[13] and Ru[10,14], albeit with a single face of the metal triangle covered by the ampy ligand only. The two Pd^{II} ions and the amido functions of the ampy ligands form a diamond-shaped, planar entity with angles of 81.1(3)° at the metals and 98.3(3)° at the amide-N atoms for **II-5**, and with angles of 80.6(3)° at the metals and 80.6(2)° at the amide-N atoms for **II-5a**. Pd-N(amide) distances are 2.073(7) Å for **II-5** and 2.085(8) Å for **II-5a**. The diagonals of the diamond are 2.68(1) Å (**II-5**) and 2.69(2) (**II-5a**) between the amide-N atoms and 3.088(1) Å (**II-5**) and 3.15(5) Å (**II-5a**) between the two metals. The four-membered PdN_2Pd metallacycles are *syn*-planar according to the classification of Ciriano and Oro et al.[15] and, as far as their size concerned, similar to related metallacycles.[16,17] The PdN_2Pd plane and the ampy plane are almost perpendicular, the dihedral angle being 85.9(6)^o for **II-5** and 87.4(3)^o for **II-5a**. The coordination spheres of Ag(1) are

both tetrahedrally distorted (with Pd atoms ignored). Thus, the angle N(1A)-Ag(1)-N(1A') amounts to 153.6(4)^o in **II-5** and 148.4(4)^o in **II-5a**, and the angle O(13)-Ag(1)-O(13') is 82.2(5)^o in **II-5** and 78.3(3)^o in **II-5a**. Ag-N and Ag-O distances in **II-5** are 2.167(7) Å and 2.58(1) Å, while in **II-5a** are 2.179(9) Å and 2.69(1) Å, respectively.

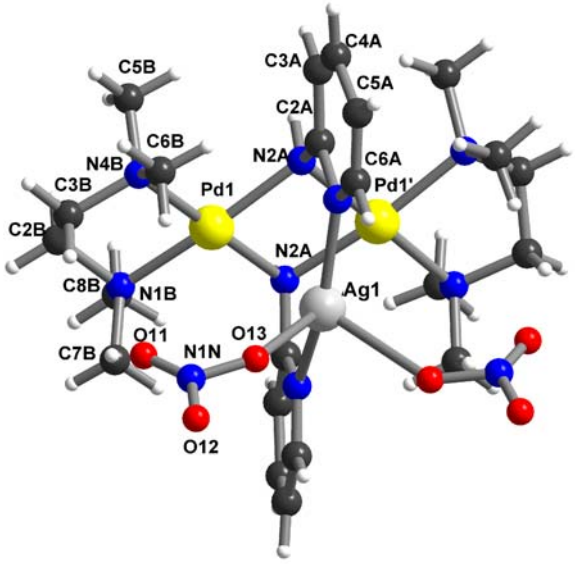

Figure 5. View of central core of [{(tmeda)Pd(*N2*-ampy$^-$-*N1*)}$_2$Ag(μ-NO$_3$)$_2$Ag(NO$_3$)$_2$] (**II-5**) with atom numbering scheme. The co-crystallized AgNO$_3$ was omitted for the sake of clarity. For a schematic view of **II-5** see Scheme 2.

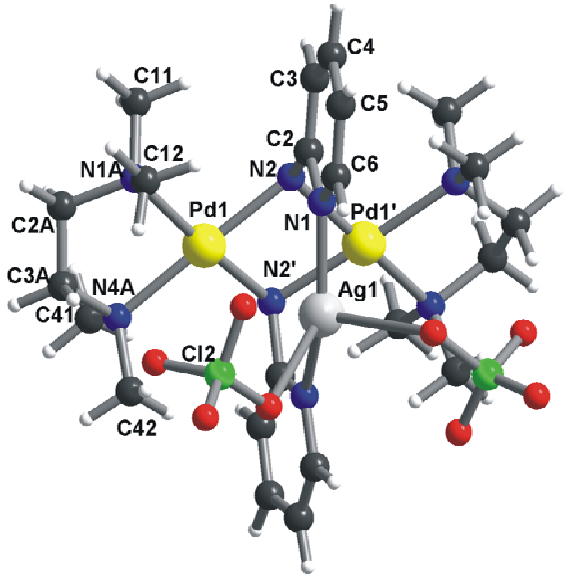

Figure 6. View of central core of [{(tmeda)Pd(*N2*-ampy$^-$-*N1*)}$_2$Ag(ClO$_4$)$_2$](ClO$_4$)·2H$_2$O (**II-5a**) with atom numbering scheme. For a schematic view of **II-5a** see Scheme 2.

Table 4. Selected (bond) distances (Å) and angles (º) for compound **II-5**[a] and **II-5a**[b].

(II-5)		**(II-5a)**	
Pd1-N2A	2.073(7)	Pd1-N2	2.085(8)
Pd1-N1B	2.095(7)	Pd1-N1A	2.103(8)
Pd1-N4B	2.080(9)	Pd1-N2[b]	2.075(6)
Ag1-N1A	2.167(7)	Pd1-N4A	2.113(6)
Ag1-O13	2.59(1)	Ag1-N1	2.179(9)
Ag2-O12	2.64(1)	Ag1-N1[b]	2.179(9)
Ag2-O13	2.17(1)	Ag1-O21	2.69(1)
Ag2-O21	2.523(7)	Ag1···Pd1	3.070(2)
Ag2-O23	2.658(8)	Pd1···Pd1[b]	3.15(5)
C2A-N2A	1.42(1)	N2···N2[b]	2.69(2)
Ag1···Pd1	3.088(1)		
Ag1···Ag2	3.724(2)		
Pd1···Pd1[a]	3.088(1)		
N2A···N2A[a]	2.68(1)		
N1A-Ag1-N1A[a]	153.6(4)	N1-Ag1-N1[b]	148.4(4)
O13-Ag1-O13[a]	82.2(5)	O21-Ag1-O21[b]	78.3(3)
N2A-Pd1-N2A[a]	81.1(3)	N2-Pd1-N2[b]	80.6(3)
O13-Ag2-O21	138.2(3)		
N1B-Pd1-N4B	84.6(3)	N1A-Pd1-N4A	85.0(3)
N1B-Pd1-N2A[a]	96.3(3)	N1A-Pd1-N2[b]	96.7(3)
N2A-Pd1-N4B	98.1(3)	N2-Pd1-N4A	97.6(3)
N2A-Pd1-N2A[a]	81.1(3)	N2-Pd1-N2[b]	80.6(3)
N1B-Pd1-N2A	171.0(3)	N1A-Pd1-N2	171.7(3)
Pd1-N2A-Pd1[a]	98.3(3)	Pd1-N2-Pd1[b]	80.6(2)
Ag1-O13-Ag2	102.9(4)		
Pd1···Ag1···Pd1[a]	60.65(4)	Pd1···Ag1···Pd1[b]	61.66(2)
Pd1···Pd1[a]···Ag1	59.67(2)	Pd1···Pd1[b]···Ag1	59.17(2)
Pd1[a]···Pd1···Ag1	59.67(2)	Pd1[b]···Pd1···Ag1	59.17(2)
Pd plane/ampy plane	85.9(6)	Pd plane/ampy plane	87.4(3)

[a]: Symmetry transformations used to generate equivalent atoms: -x,y,1/2-z;

[b]: Symmetry transformations used to generate equivalent atoms: 1-x,y,1/2-z

The main difference between compounds **II-5** and **II-5a** is an additional $AgNO_3$ co-crystallized in the former case with an attachment via bridging nitrate anions. The second Ag ion is symmetrically disordered over two positions, Ag(2) and Ag(2A). It is linked to Ag(1) via bridging nitrate anions and completes its coordination sphere by two terminal oxygen atoms of nitrate anions (Scheme 2). The Ag(1)···Ag(2)(Ag2A) distance is 3.724(2) Å.

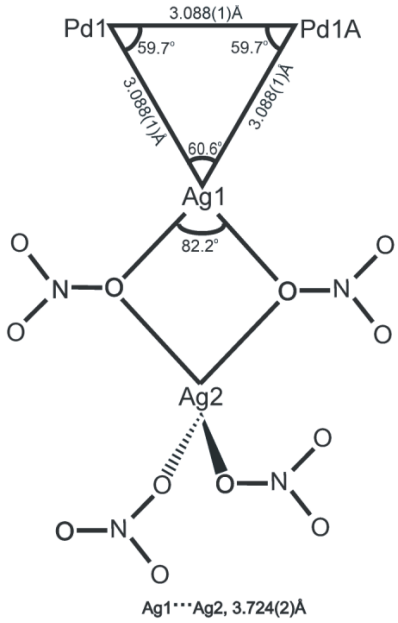

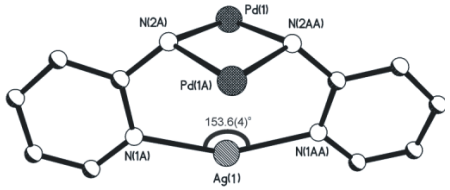

II-5

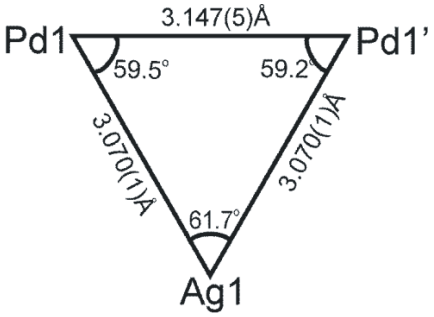

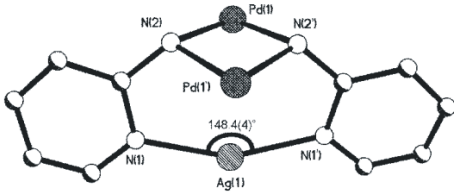

II-5a

Scheme 2.

8 ^{1}H NMR spectrum of [{(tmeda)Pd(*N2*-ampy$^-$-*N1*)}$_2$Ag(μ-NO_3)$_2$Ag$(NO_3)_2$] (II-5) and decomposition by Cl^-

The ^{1}H NMR spectrum of **II-5** in D_2O, pD 6.9 is given in Figure 7. There are two features worth while discussing: First, the H(6) resonance represents a symmetrical multiplet, which contrasts in appearance with those of the free Hampy (Figure 1) as well as those of **II-1**-**II-4**. In those cases, this resonance appears as doublet-of-doublet-of-doublet, hence as an eight-line signal due to vicinal coupling with the adjacent H(5) (^3J), and long range coupling with H(4) (^4J) as well as with H(3) (^5J). For the free Hampy, these values are 5.39 Hz, 1.95 Hz, and 0.97 Hz, respectively. Because of its width and the number of lines we initially considered the unexpected pattern of H(6) in **II-5** to be due to a rare case of proton coupling with ^{109}Ag and ^{107}Ag isotopes,[18] but eventually homo decoupling experiments unambiguously proved this resonance to be a 12-line-superposition of two H(6) signals due to two non-equivalent ampy ligands (Figure 7, (B), (C)). The ^{13}C NMR spectrum of **II-5** likewise confirms the non-equivalence of the two ampy ligands. Three of the five carbon resonances (C(3), C(5), C(6)) are doubled, even though separated by 0.01-0.02 ppm only and therefore seen in the 150 MHz- spectrum only. The reason as to why the two coordinating ampy ligands are non-equivalent is not immediately clear. It may be due to interactions between the coordinated Ag^+ ion and solvent molecules and/or anions leading to a slightly unsymmetrical arrangement. Second, the methyl resonances of the tmeda ligand are split in two signals, at 2.46 and 1.43 ppm, thus differing markedly. Inspection of the crystal structure of **II-5** reveals that four of the eight methyl groups are pointing onto the π-system of the ampy ligands, whereas the four other methyl groups are pointing outside.

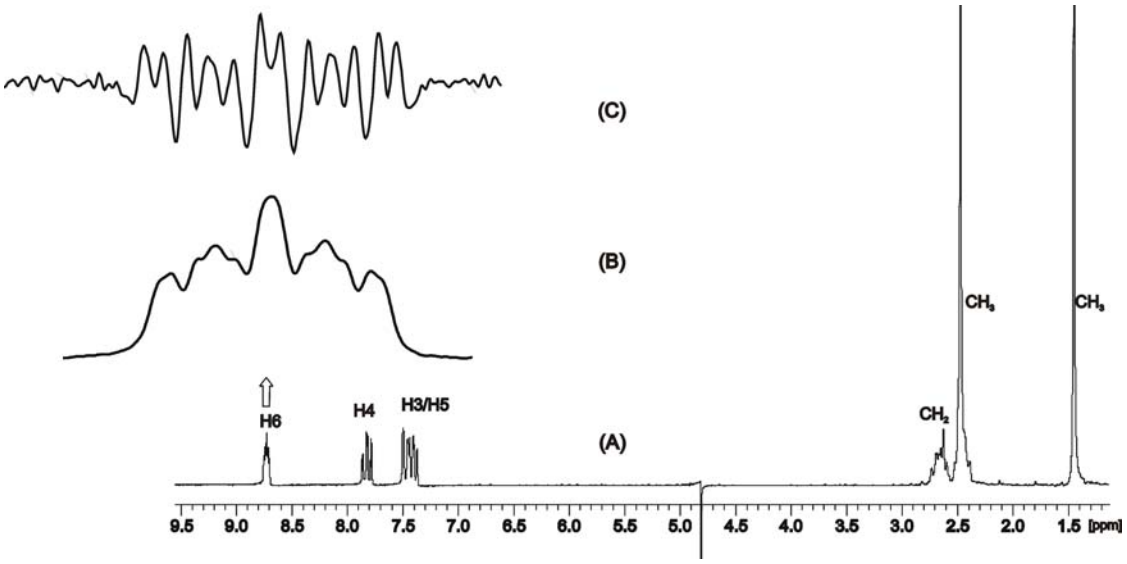

Figure 7. ^{1}H NMR spectrum of **II-5** in D_2O, pD 6.9 (A) and expanded sections of H(6) signal (B) as well as of H(6) signal transformed with a sinus function in order to determine its individual components (C).

Addition of an excess of NaCl to a solution of **II-5** in D_2O (pD 6.9) causes a rapid change in the ^{1}H NMR spectrum, which can be particularly well followed for the H6 resonances furthest downfield (Figure 8).

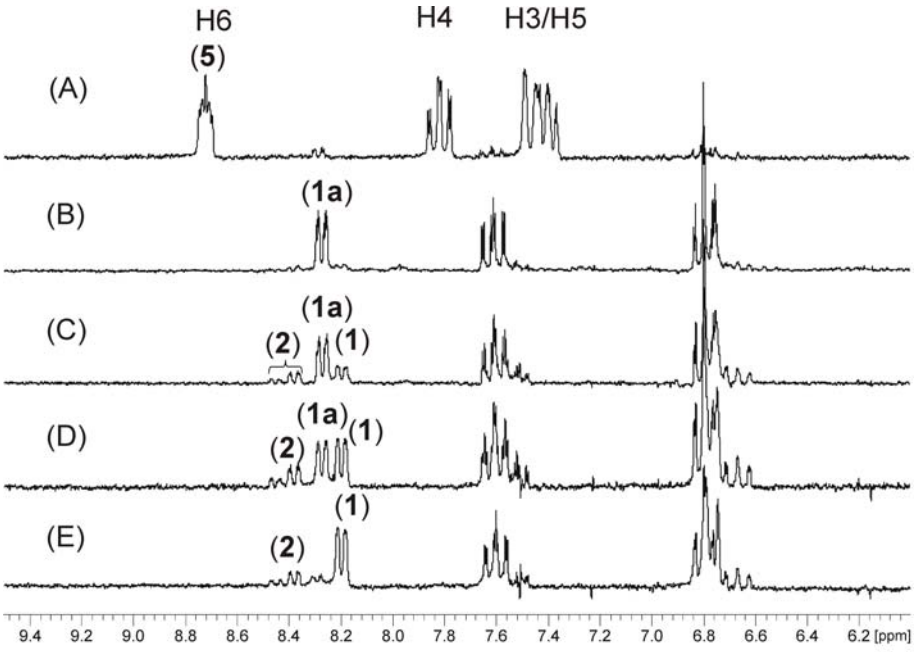

Figure 8. Low field section of ^{1}H NMR spectra (D_2O):(A) **II-5** after dissolving in D_2O; pD 6.9. (B) After 3h stirring with excess NaCl and subsequent filtration of AgCl, pD now risen to 9.3. (C) pD of solution adjusted to 8 with DNO_3. (D) pD adjusted to 7.5. (E) pD adjusted to 6.1.

Resonances due to **II-5** disappear completely, and those of $[Pd(OD)(tmeda)(Hampy\text{-}N1)]^+$/$[Pd(tmeda)(Hampy\text{-}N1)(D_2O)]^{2+}$ appear rapidly (signal (**II-1a**) in spectrum (B)). This change is accompanied by a rise in pD, from 6.9 to 9.3. Lowering of the pD to 8, 7.5, and 6.1 by addition of DNO_3 (spectra (C)-(E)) eventually produces $[PdCl(tmeda)(Hampy\text{-}N1)]^+$ (**II-1**) as well as the two rotamers of $[Pd(tmeda)(Hampy\text{-}N1)_2]^{2+}$ (**II-2**). These changes are interpreted in terms of a linkage isomerization process as indicated in Scheme 3. Obviously there is a symmetrization reaction of the 1:1 complex according to

$[PdX(tmeda)(Hampy\text{-}N1)]^+ \rightleftharpoons 0.5\ [Pd(tmeda)(Hampy\text{-}N1)_2]^{2+} + 0.5\ PdX_2(tmeda)$

(with X = OH or Cl)

also going on, but it takes place only following the decomposition of **II-5** into AgCl and mononuclear Pd species. On the other hand, addition of excess $AgNO_3$ to these resultant mononuclear Pd species causes reformation of **II-5**.

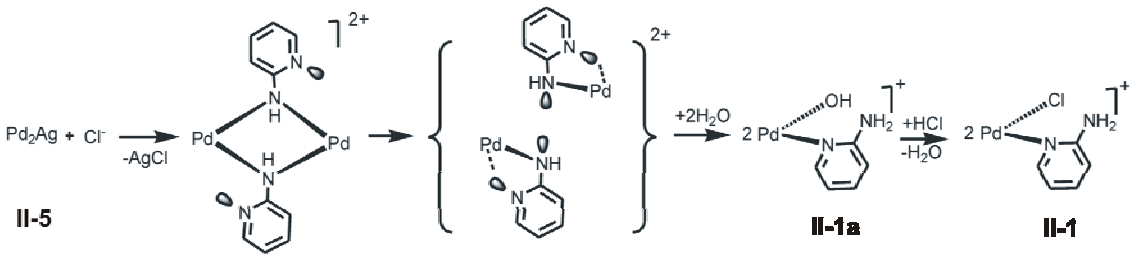

Scheme 3.

9 Attempts to prepare related Pd_2M complexes

Attempts to substitute Ag^+ in **II-5** by other transition metal ions or metal fragments failed. Thus, removal of Ag^+ by means of NaCl and subsequent addition of either $ZnSO_4$, $CdSO_4$, or $Hg(NO_3)_2$ did not yield, according to ^1H NMR spectroscopy, heteronuclear Pd_2M compounds. Similarly, reactions of *trans*-$[Pta_2(Hampy\text{-}N1)_2]^{2+}$ (a = NH_3 or $MeNH_2$)[3-5] with $[Pd(tmeda)(H_2O)_2]^{2+}$, which were followed by ^1H NMR spectroscopy (D_2O, pD 9), did not yield compounds analogous to **II-5** and neither did they lead to analogues of the previously described Pt_2Pd_4[4] and $PtPd_3$[3] compounds. In fact there was no

reaction at all. This tentatively suggests that the steric bulk of the tmeda ligand is too large to allow formation of Pt_2Pd_4 and $PtPd_3$ analogues and that the linearity of the Pt fragment in *trans*-$[Pta_2(Hampy\text{-}N1)_2]^{2+}$ prevents the exocyclic amino group from coming sufficiently close to permit ring Pd_2N_2 formation as seen in **II-5** (Scheme 4).

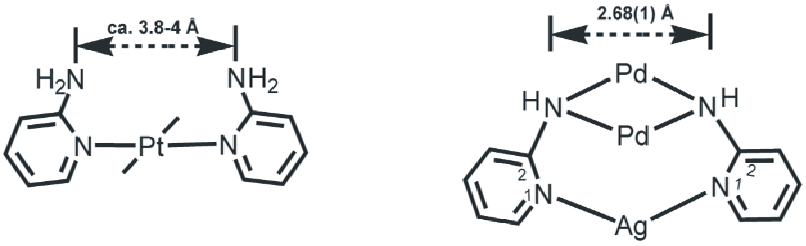

II-5

Scheme 4.

10 Characterization of $[\{Pd(ampy^{-}\text{-}N1,N2)(bpy)\}_2](NO_3)_2$ (II-6)

Pd^{II}(bpy) and Hampy were reacted in a 1:1 ratio. Somewhat surprisingly, even in slightly acid solution (pH = 6), the *head-tail* dimer **II-6** was obtained as the main product. Orange red crystals suitable for X-ray crystallography were isolated. A view of the cation is depicted in Figure 9. Table 5 contains selected bond lengths and angles.

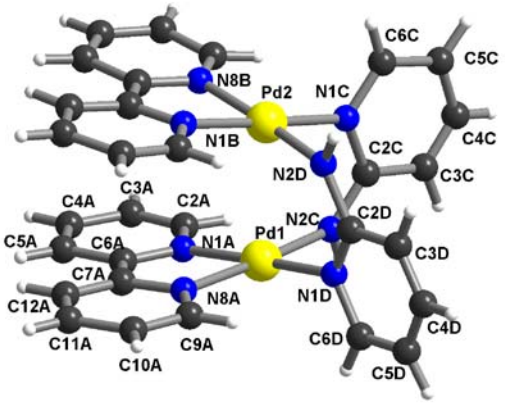

Figure 9. View of $[Pd(ampy^{-}\text{-}N1,N2)(bpy)]^{2+}$ (**II-6**) with atom numbering scheme.

Table 5. Selected distances (Å) and angles (º) for compound **II-6**.

[{Pd(ampy$^-$-*N1,N2*)(bpy)}$_2$](NO$_3$)$_2$ (II-6)			
Pd1-N1A	2.009(8)	Pd1-N2C	1.983(8)
Pd1-N8A	2.030(6)	Pd1-N1D	2.026(8)
Pd2-N1B	1.995(8)	Pd2-N1C	2.043(8)
Pd2-N8B	2.013(8)	Pd2-N2D	1.947(8)
Pd1···Pd2	2.866(1)		
N1A-Pd1-N2C	96.1(3)	N1B-Pd2-N2D	94.6(3)
N1A-Pd1-N8A	78.9(3)	N1B-Pd2-N8B	79.6(3)
N1D-Pd1-N2C	89.2(3)	N1C-Pd2-N2D	90.4(3)
N1D-Pd1-N8A	95.8(3)	N1C-Pd2-N8B	95.4(3)
N8B-Pd2-Pd1-N1A	-8.27(1)	N1B-Pd2-Pd1-N8A	-7.03(1)
N1C-Pd2-Pd1-N2C	-7.12(1)	N2D-Pd2-Pd1-N1D	-8.78(1)

Two Pd^{II}(bpy) units are bridged by two ampy ligands in a *head-tail* fashion. The mean-plane calculations performed for the four coordinated atoms reveal that the two Pd coordination spheres are planar, with mean deviations of four atoms N(1A)/N(8A)/N(1D)/N(2C) being 0.0016 Å and N(1B)/N(8B)/N(1C) /N(2D) being 0.0054 Å. The dihedral angle between the two Pd coordination planes within the dimeric unit is 20.7(4)^o and the average torsional twist about the Pd···Pd axis is 7.8(1)^o. Within the dimer unit, the tilt angle between the two bpy planes (10.9(2)^o) is 9.8(2)^o smaller than that between the two Pd coordination planes, indicating that a relatively strong π-stacking interaction is achieved within the unit. The intramolecular distance between these bpy planes is 3.6(2) Å, while the intermolecular distance is 3.8(2) Å, slightly longer (Figure 10). The intradimer Pd···Pd distance (2.866(7) Å) is quite similar to the previously reported Pd···Pd distance (2.8511(9) Å) in [{Pd(1-MeC$^-$-*N3,N4*)(bpy)}$_2$](ClO$_4$)$_2$·2H$_2$O (**I-1**) (see Chapter I).

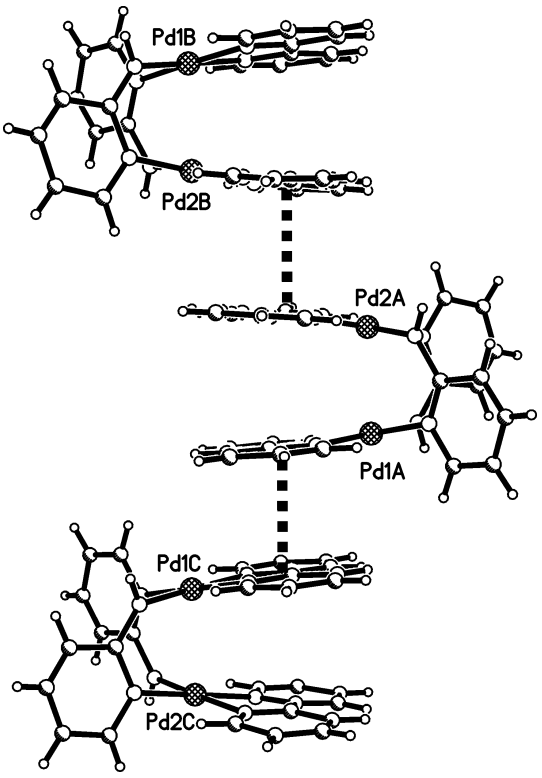

Figure 10. A view showing the packing of the different enantiomers of the *head-tail* dimeric compound **II-6**. [Symmetry codes: (2A to 2B) -x, 1-y. -z (1A to 1C) 1-x, 1-y, -z.]

As *head-tail* dimers are inherently chiral, the cation of compound **II-6** is present in its two enantiomeric forms. As shown in Figure 10, both enantiomers stack along the x axis in a 1:1 ratio to give one-dimensional stacks of bpy units. The interdimer Pd(1A)···Pd(1C) (6.54(8) Å) and Pd(2A)···Pd(2B) (6.29(5) Å) distances are much too long to imply metal-metal interactions. The interplanar spacing between the stacked bpy planes is 3.68(2) Å for the stack Pd(1)···Pd(1) (1-x, 1-y, -z), and Pd(2)···Pd(2) (-x, 1-y. –z). The Pt^{II} analog of this compound has been reported by Sakai.[19]

To analyze the 2,2'-bpy resonances of this compound in more detail 1D TOCSY experiments were carried out, since TOCSY spectra can be used to obtain information on all protons within a ring system. The spectra (irradiated signals indicated) are shown in Figure 11.

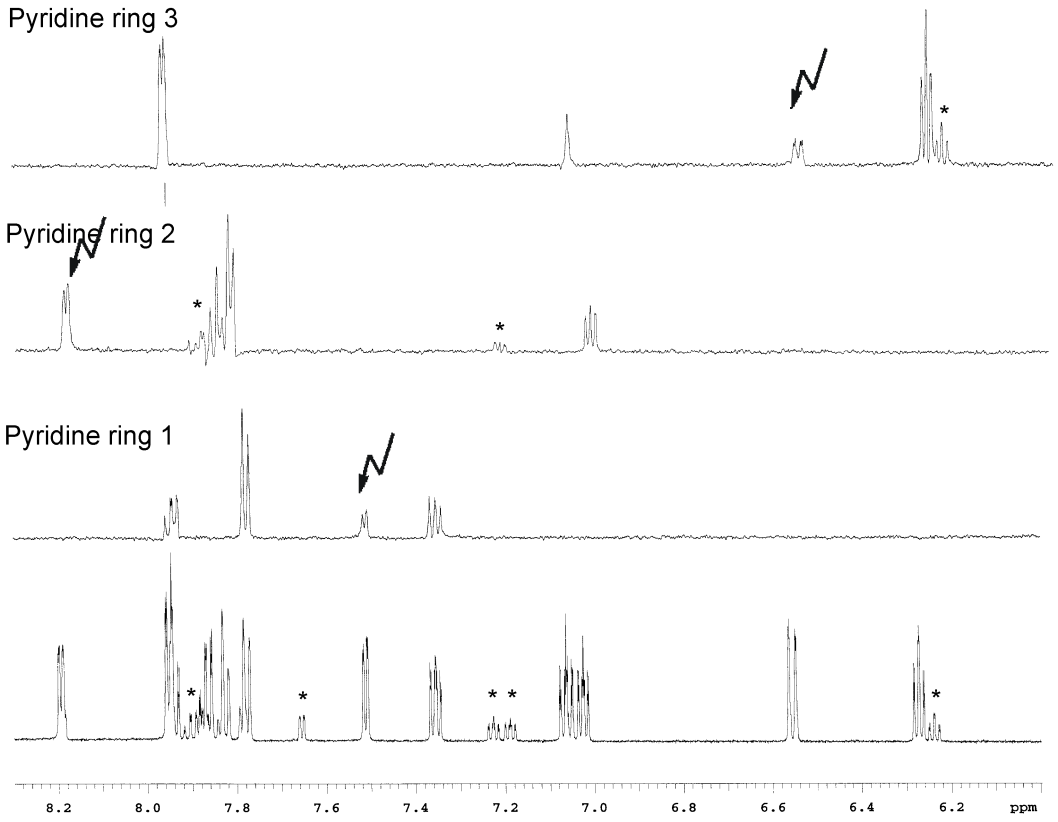

Figure 11. Low field section of the ^{1}H NMR spectrum (600 MHz) of **II-6** (bottom) and 1D TOCSY experiments (top) applied to the pyridine resonances (pD = 6.9). Resonances (*) are assigned to an unknown impurity in the solution.

As expected, three sets of pyridine resonances are observed. One set corresponds to the 2-ampy rings. The other two sets are due to the two non-equivalent pyridine "halves" of bpy as a consequence of different *trans*-positioned Pd donor atoms (N(1), N(2)). In Figure 11, pyridine rings 1 and 2 correspond to the resonances of the bpy entities, while pyridine ring 3, which is more upfield shifted, corresponds to the resonances of 2-ampy. When comparing resonances of pyridine ring 1 and 2, H(6) of pyridine ring 1 is at higher field than that of ring 2. This is a consequence of the *trans*- positioned donor atoms $N(2)H^-$. Resonances of ring 1 are observed at 7.95 ppm (H4, t, ^3J = 4.8 Hz), 7.78 ppm (H6, d, ^3J = 4.8 Hz), 7.51 ppm (H3, d, ^3J = 4.8 Hz) and 7.36 ppm (H5, d, ^3J = 4.8 Hz). Pyridine ring 2 corresponds to the other "half" which is in *trans*-position of the Pd donor atom N(1). The resonances of ring 2 are observed at 8.20 ppm (H6, d, ^3J = 4.8 Hz), 7.85 ppm (H4, t, ^3J = 4.8 Hz),

7.82 ppm (H3, d, ^3J = 4.8 Hz) and 7.02 ppm (H5, t, ^3J = 4.8 Hz). As pointed out, the H(5) signal of ring 2 exhibits the highest upfield shift, possibly due to the bpy stacking. Moreover, the resonances for 2-ampy are observed at 7.95 ppm (H6, d, ^3J = 4.8 Hz), 7.06 ppm (H4, t, ^3J = 4.8 Hz), 6.56 ppm (H3, d, ^3J = 4.8 Hz) and 6.28 ppm (H5, t, ^3J = 4.8 Hz). The resonances (*) are assigned to an unknown impurity in the solution.

11 Open Questions

It is common practice among coordination chemists to prepare aqua/hydroxo complexes of Pt^{II} and Pd^{II} by abstracting Cl^- from Cl-containing precursor complexes with the help of soluble Ag^+ salts. The aspect of an absolutely *exact* stoichiometric reaction in most cases is not a serious one, but it can be, as demonstrated here, namely if excess Ag^+ undergoes a reaction with the Pd/Pt aqua species. We admit that, despite several attempts, which included also an IR-spectroscopic analysis of the AgCl precipitate, among others, we are not certain whether it was a slight excess of $AgNO_3$ over **II-1**, which led us to the original observation of the highly characteristic H(6) resonance of **II-5** in the ^{1}H NMR spectra, or whether it was possibly the propensity of the aminopyridine ligand to partly solubilize AgCl. In any case, we soon realized that the deliberate use of an excess of Ag^+ over Pd in **II-1** increased the yield of **II-5** drastically.

Concerning the way of formation of the Pd_2Ag triangle present in **II-5**, it appears that Pd migration from N(1) of the aminopyridine to N(2) at basic pH is the first step. It is less obvious, how the second step takes place. Two scenarios are feasible. In the first one, dimerization of the N(2) linkage isomer creates a Pd_2 entity, which is capable of chelating an Ag^+ ion to give Pd_2Ag. Alternatively, Ag^+ could cross–link the two mononuclear Pd–N(2) linkage isomers, and pre-organize their dimerization. Whatever the exact mechanism of formation of **II-5** is, it is obvious from the decomposition reaction of **II-5** with excess Cl^-, that the bis(μ-amidopyridine) complex of Pd^{II}(tmeda) itself requires the presence of Ag^+ to be isolated from aqueous solution. Consistent with this

view is our observation that **II-1**, in the complete absence of Ag^+, yet at alkaline pD (8-9), shows no signs of reactivity whatsoever. Concerning the metal-metal distances in **II-5** of slightly over 3 Å, we do not feel that these reflect dative bond interactions, e.g. Pd – Ag, or Pd – Pd bonds. We are aware, that Pd···Pd separations which are shorter than the sum of the van der Waals radii have been discussed in terms of weak attractive interactions, for example,[20] but in these cases the interacting metal orbitals are arranged differently. Moreover, donor-acceptor bonds between Pd and Ag are expected to be considerably shorter, very much as in the case of related Pt, Ag compounds,[21] with Ag^+ interacting strongly with the d_z^2 orbital of Pt or Pd.

References

[1] Shen, W.-Z.; Gupta, D.; Lippert, B. *Inorg. Chem.* **2005**, *44*, 8249.

[2] For compounds with an analogous structure, see: (a) Longato, B.; Pasquato, L.; Mucci, A.; Schenetti, L.; Zangrando, E. *Inorg. Chem.* **2003**, *42*, 7861. (b) Longato, B.; Montagner, D.; Zangrando, E. *Inorg. Chem.* **2006**, *45*, 8179.

[3] Schneider, A.; Freisinger, E.; Beck, B.; Lippert, B. *J. Chem. Soc., Dalton Trans*. **2000**, 837.

[4] Beck, B.; Schneider, A.; Freisinger, E.; Holthenrich, D.; Erxleben, A.; Albinati, A.; Zangrando, E.; Randaccio, L.; Lippert, B. *Dalton Trans*. **2003**, 2533.

[5] Rauter, H.; Mutikainen, I.; Blomberg, M.; Lock, C. J. L.; Amo-Ochoa, P.; Freisinger, E.; Randaccio, L.; Zangrando, E.; Chiarparin, E.; Lippert, B. *Angew. Chem. Int. Ed*. **1997**, *36*, 1296.

[6] Stewart, A R.; Harris, M. G. *J. Org. Chem.* **1978**, *43*, 3123.

[7] Bordwell, B. F. G.; Singer, D. L.; Satish, A. V. *J. Am. Chem. Soc.* **1993**, *115*, 3543.

[8] Krizanovic, O.; Sabat, M.; Beyerle-Pfnür, R.; Lippert, B. *J. Am. Chem. Soc.* **1993**, *115*, 5538.

[9] Bordwell, B. F. G.; Singer, D. L.; Satish, A. V. *J. Am. Chem. Soc.* **1993**, *115*, 3543.

[10] (a) Preut, H.; Frommer, G.; Lippert, B. *Acta Cryst.* **1991**, *C47*, 852. (b) See Chapter I, compound **I-5**.

[11] Uhlig, E.; Mädler, M. *Z. Anorg. Allg. Chem.* **1965**, *338*, 199.

[12] Charland, J.-P.; Beauchamp, A. L. *J. Crystallogr. Spectrosc. Res.* **1985**, *15*, 581.

[13] Deeming, A. J.; Peters, R.; Hursthouse, M. B.; Backer-Dirks, J. D. J. *J. Chem. Soc.*, *Dalton Trans*. **1982**, 1205.

[14] Cabeza, J. A.; del Río, I.; Llammazares, A.; Riera, V.; García-Grande, S.; Van der Maelen, J. F. *Inorg. Chem*. **1995**, *34*, 1620.

[15] Tejel, C.; Ciriano, M. A.; Bordonaba, M.; López, J. A.; Lahoz, F. J.; Oro, L. A. *Chem. Eur. J.* **2002**, *8*, 3128.

[16] Li, J. J.; Li, W.; James, A. J.; Holbert, T.; Sharp, T. R.; Sharp, P. R. *Inorg. Chem.* **1999**, *38*, 1546.

[17] Ragaini, F.; Cenini, S.; Demartin, F. *J. Chem. Soc., Dalton Trans*. **1997**, 2855.

[18] Albinati, A.; Lehner,H.; Venanzi, L. M.; Wolfer, M. *Inorg. Chem.* **1987**, *26*, 3933.

[19] Mizota, M.; Sakai, K. *Acta Cryst.* **2004**, *E60*, m473.

[20] Xia, B.-H.; Che, C. -M.; Zhou, Z. -Y. *Chem. Eur. J.* **2003**, *9*, 3055, and references therein.

[21] See, e.g.: Usón, R.; Forniés, J. *Inorg. Chim. Acta* **1992**, *198-200*, 165.

Chapter III

Pyrazine as a Building Block for Molecular Architectures with Pt^{II}

1 Aim of the project

Our interest in the pyrazine (pz) ligand stems from its usefulness as a building block to generate distinct molecular architectures in combination with suitable transition metal ions. A few examples of such compounds exist, e.g. open Re boxes with luminescence properties,[1] a mixed-valence Creutz-Taube square, $[Ru_4(cyclen)_4(pz)_4]^{9+}$,[2] a titanocene box,[3] molecular triangles obtained from *cis*-$Pt^{II}(PMe_3)_2$ [4] and *cis*-$Rh^{I}(PPh_3)_2$,[5] and molecular squares obtained from Pt^{II}(en).[6] In our group, a series of compounds containing Pt^{II} entities and pz have been obtained: For example, pz as a monotopic ligand, *cis*-$[Pt(NH_3)_2(pz)_2]^{2+}$ and *trans*-$[Pt(NH_3)_2(pz)_2]^{2+}$; pz as a bridging ligand, *cis*-$[\{PtCl(NH_3)_2\}_2(pz)]^{2+}$; pz as a bridging ligand in the box *cis*-$[\{Pt(NH_3)_2(pz)\}_4]^{8+}$, and a mixed Pt, Ag polymer $[\{Pt(tmeda)(pz)_2\}_2Ag]^{5+}$.[7] The formation of a pz box conforms to expections of the "molecular library approach"[8], which predicts a molecular box when two ditopic building blocks with 90° and 180° angles, respectively, are combined.

In continuation of this work, the reaction between Pt^{II}(tmeda), a ~90° angular fragment, and pyrazine (pz) was performed; *trans*- and *cis*-conformation building blocks were prepared by using 2,3-dimethylpyrazine (dmpz).

2 Pyrazine

2.1 Reactions of Pt^{II}(tmeda) with pyrazine

NMR scale reactions with a 1:1 ratio of Pt^{II}(tmeda) and pyrazine were performed. The spectrum given in Figure 1 was recorded after one day of stirring at room temperature. The resonances of A and B reveal that pz

ligands are in unsymmetrical coordination modes, which could belong to 1:1 or 1:2 compounds (Pt^{II} per pz), while C is a highly symmetrical product, which could be a bridged dinuclear complex, a triangle or a box. The subsequent crystallization confirmed that resonances A and C are due to $[PtCl(tmeda)(pz)]^+$ (9.07 ppm, H2&H6, ^3J = 4.6 Hz; 8.90 ppm, H3&H5, ^3J = 4.6 Hz) and $[\{Pt(tmeda)(pz)\}_3]^{6+}$ (9.48 ppm), respectively. Therefore, resonances B are assigned to $[Pt(tmeda)(pz)_2]^{2+}$ (9.14 ppm, H2&H6, ^3J = 4.6 Hz; 8.82 ppm, H3&H5, ^3J = 4.6 Hz). ^{195}Pt satellites are present for the aromatic protons (*) in C. The coupling constant is ^3J ~ 38.0 Hz.

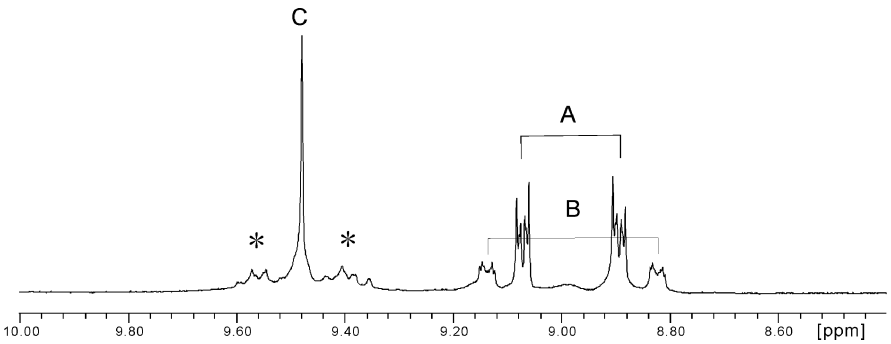

Figure 1. ^{1}H NMR spectrum (D_2O, pD 4.0, endocyclic proton resonances only) of reaction mixture (1:1) of $[Pt(tmeda)(D_2O)]^{2+}$and pz after one day stirring at room temperature. For assignment of resonances (A)–(C), see text.

In addition, at very high concentration a second singlet resonance (5%) could be observed by ^{1}H NMR spectroscopy with a chemical shift close to resonance C (9.36 ppm), which is most likely attributable to a square.

2.2 Characterization of $[PtCl(tmeda)(pz)](ClO_4)$ (III-1)

Compound **III-1**, which contains pz as a monotopic ligand, was isolated as one of the products of the previous reaction after anions were exchanged to ClO_4^-. An X-ray crystal structure analysis was performed. A view of **III-1** is given in Figure 2, and salient structural features are listed in Table 1.

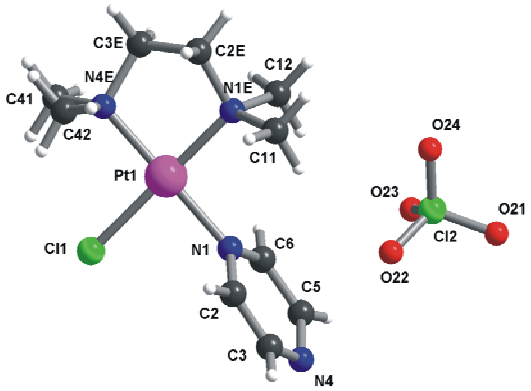

Figure 2. View of [PtCl(tmeda)(pz)](ClO_4) (**III-1**) with atom numbering scheme.

In compound **III-1**, the Pt coordination geometry is slightly distorted square-planar because of the chelating tmeda ligand. Pt-N and Pt-Cl distances are normal. The pz plane is tilted with respect to the PtN_3Cl coordination plane with an angle of 80.1(5)°. There are no unusual features in the pz rings. The cations of **III-1** interact with each other through weak hydrogen bonds (N(4)···H, 2.581 Å and N(4)···C, 3.492 Å) between the noncoordinating ring N atom of pz (N(4)) and the proton of one of the methyl groups of tmeda. A view of the packing is shown in Figure 3. The cations form an infinite helix along the z axis. The perchlorate anions are located between the helices and form multiple H bonds to the aromatic protons and the methyl groups of tmeda.

Table 1. Selected bond distances (Å) and angles (°) for compound **III-1**.

[PtCl(tmeda)(pz)](ClO_4) (III-1)			
Pt1-N1	2.02(2)	Pt1-N1E	2.030(10)
Pt1-Cl1	2.283(6)	Pt1-N4E	1.972(9)
Cl1-Pt1-N1	85.9(6)	N1-Pt1-N1E	94.1(6)
Cl1-Pt1-N4E	93.9(3)	N1E-Pt1-N4E	86.0(4)
C2-N1-C6	116.4(19)	Pt plane/pz plane	80.1(5)
C3-N4-C5	116(2)		

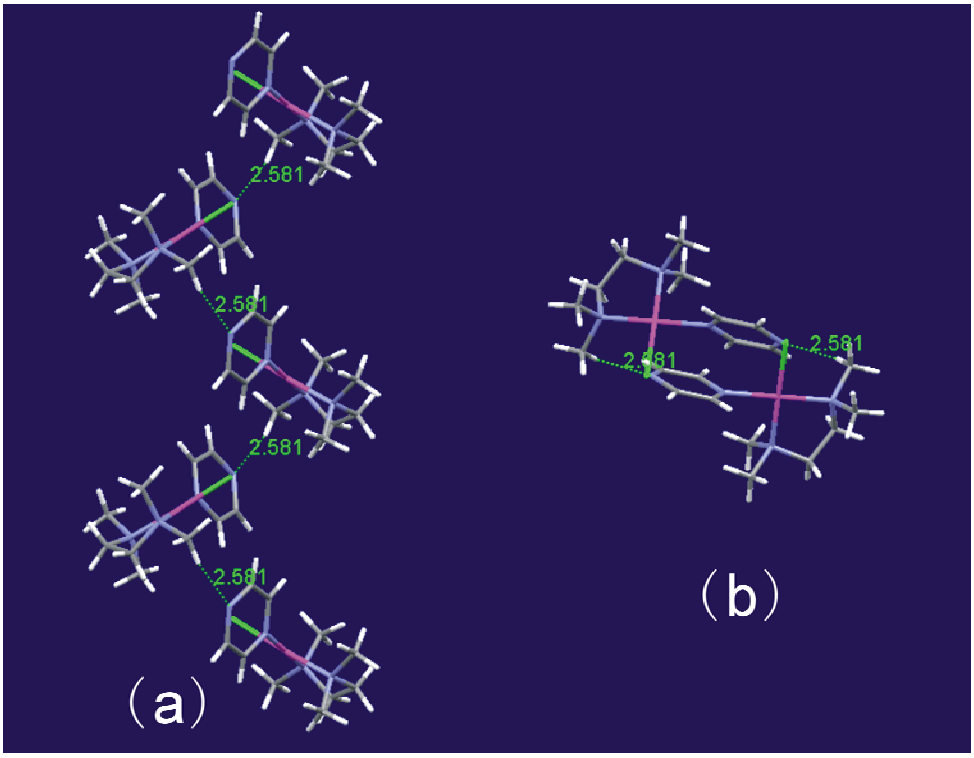

Figure 3. Packing view of compound **III-1:** (a) view along the y axis, (b) view along the z axis. Each molecular unit is connected by a weak hydrogen bond between N(4) and a proton of methyl group of tmeda. The distance of the hydrogen bond (N(4)···H) is 2.581 Å.

2.3 Characterization of $[\{Pt(tmeda)(pz)\}_3](NO_3)_6 \cdot 2.5H_2O$ (III-2)

Compound **III-2** was isolated as the main product in the above reported reaction. Light yellow crystals of poor quality for X-ray crystallography were obtained. However, the structure confirmed **III-2** to be a triangle (Figure 4), with Pt···Pt distances of ca. 6.7 Å. Because of the poor crystallographic data, we do not wish to discuss details of the structure. Elemental analysis showed compound **III-2** to contain 2.5 water molecules per unit.

Formation of **III-2** was a quite unexpected result. Pyrazine is the smallest, and hence most rigid, linear aromatic linker available for self-assembly processes, while the Pt^{II}(tmeda) entity, with its two bonding sites oriented approximately 90^o to one another, is also quite compact. Following the "molecular library approach",[8] the combination of Pt^{II}(tmeda) and pz would predict to yield a square as the final aggregate, but the triangle **III-2** is formed instead. This occurrence, where inflexible linkers lead to unexpected products, is rare but has been observed before by Stang in the case of pz and *cis*-$Pt^{II}(PMe_3)_2$,

which likewise produce a molecular triangle.[4] Moreover, it is interesting to note that with Pt^{II}(en) the expected formation of a square complex is observed.[6] We agree with Stang that there are likely limitations and exceptions to the coordination-directed synthetic strategy of a "rational design".[9]

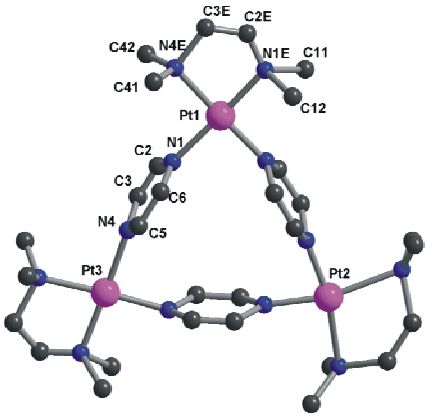

Figure 4. View of the cation $[\{Pt(tmeda)(pz)\}_3]^{3+}$ (**III-2**) with atom numbering scheme. This view is obtained from X-ray crystallographic data. Pt···Pt distances are 6.7 Å.

3 Dimethylpyrazine

3.1 Solution studies with 2,3-dimethylpyrazine (dmpz)

Pyrazine is weakly basic, having a pK_{a1} between 0.6[10] and 1.1[11]. Compared to pyrazine, 2,3-dimethylpyrazine (dmpz) is expected to be more basic because of the presence of two electron donating groups. pK_a values of dmpz were determined by using pD dependent ^{1}H NMR spectroscopic measurements (Figure 5). The pK_a values for the protonated $dmpzH_2^{2+}$ and $dmpzH^+$ were determined as 1.93 ± 0.09 (pK_{a1}) and 3.2 ± 0.2 (pK_{a2}). Scheme 1 depicts the two acid-base equilibria. This result suggests that dmpz may be a better ligand for metal ions than pz.

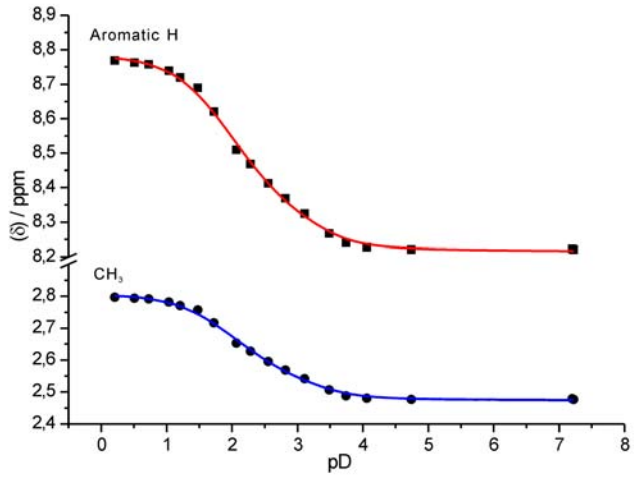

Figure 5. pD dependence (δ , ppm) of aromatic H and CH_3 resonances of dmpz in D_2O, fitted to two pK_a values.

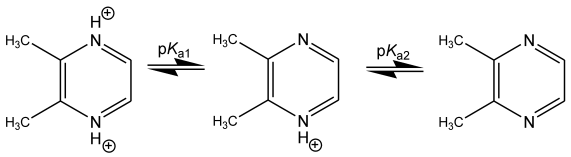

Scheme 1. Acid-base equilibria.

3.2 Synthesis of *trans*-$[Pt(NH_3)_2(dmpz)_2](NO_3)_2$ (III-3) as a potential building block

The initial idea was to synthesize the building block *trans*-$[Pt(NH_3)_2(dmpz)_2]^{2+}$, in which Pt is bonded to the N(1) positions of two dmpz ligands and forms a linear, rodlike subunit. It possesses two reactive sites which are opposite to each other (180°). Once the building blocks are obtained, these can be joined with other 90° angular fragments, e.g. *cis*-$M^{II}(NH_3)_2$ and M^{II}(en) (M = Pt and Pd), to form boxes or/and triangles (Scheme 2).

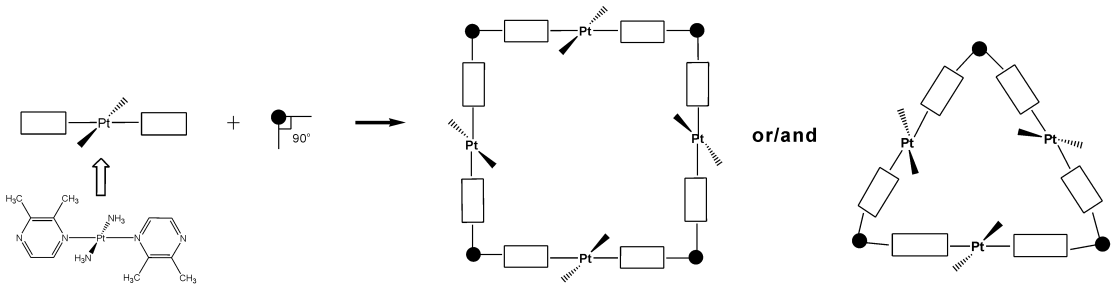

Scheme 2. The *trans*-$[Pt(NH_3)_2(dmpz)_2]^{2+}$ complex as potential building block in supramolecular chemistry.

trans-$[Pt(NH_3)_2(H_2O)_2]^{2+}$ and an excess amount of dmpz were warmed at 40°C for two days. Only a single product, *trans*-$[Pt(NH_3)_2(dmpz)_2](NO_3)_2$, was formed. It was easily isolated because of the low evaporation point of dmpz, which allowed removal of the excess ligand. Unfortunately, the compound could not be obtained as single crystals. The ^1H NMR spectrum is shown in Figure 6. There are two rotamers (1:1) for *trans*-$[Pt(NH_3)_2(dmpz)_2](NO_3)_2$, *head-tail* and *head-head* with respect to the methyl substituents. The resonances for the two rotamers are observed at 8.92 and 8.91 ppm (H6, d, ^3J = 3.4 Hz), 8.50 ppm (H5, d, ^3J = 3.4 Hz), 3.35 and 3.32 ppm (C(2)H_3, s), and 2.69 ppm (C(3)H_3, s). The two H(5) doublets are not resolved in the 200 MHz NMR spectrum. In contrast, the two resonances of H(6) (doublet of doublet each; long-range coupling, ^5J = 0.6 Hz) are resolved. ^{195}Pt satellites are observed for the H(6) proton (*) in Figure 6. The coupling constant is ^3J ~ 36.0 Hz.

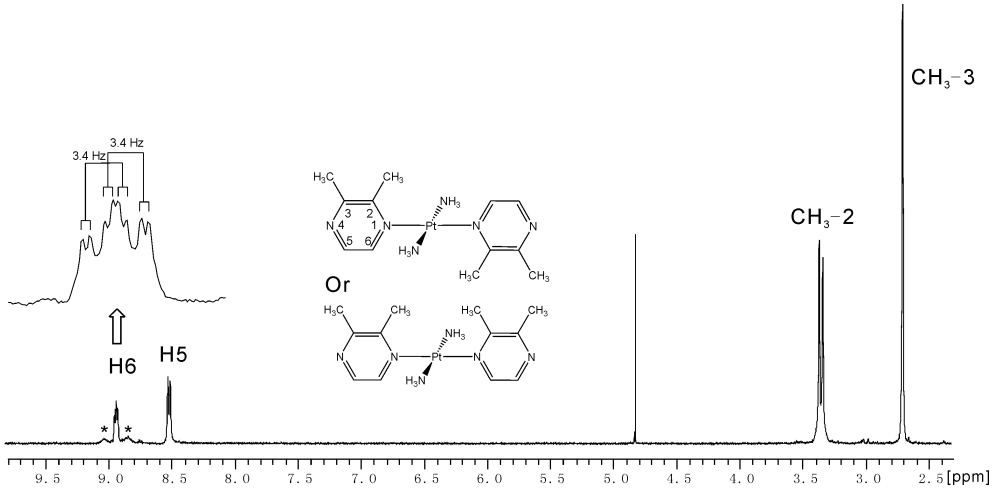

Figure 6. ^1H NMR spectrum (D_2O, pD 4.3) of *trans*-$[Pt(NH_3)_2(dmpz)_2](NO_3)_2$ (**III-3**).

3.3 Synthesis of *cis*-$[Pt(NH_3)_2(dmpz)_2](NO_3)_2$ (III-4) as potential building blocks

The other idea was to synthesize building blocks *cis*-$[Pt(NH_3)_2(dmpz)_2]^{2+}$, in which Pt is binding to the N(1) positions of two equivalents dmpz and forming 90° angular fragments. This building block can join with 90° angular fragments, e.g. *cis*-$M^{II}(NH_3)_2$ and M^{II}(en) (M = Pt and Pd), to form boxes, or with 180° linear subunits, to form larger boxes or/and triangles (Scheme 3).

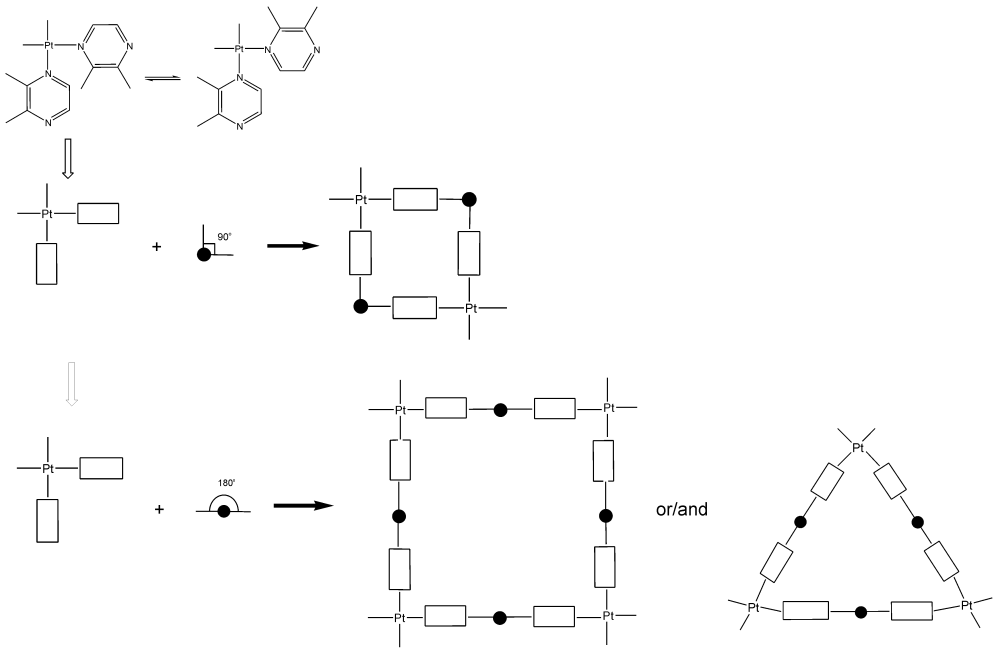

Scheme 3. The *cis*-$[Pt(NH_3)_2(dmpz)_2]^{2+}$ complex **III-4** as a potential building block in supramolecular chemistry.

cis-$[Pt(NH_3)_2(dmpz)_2](NO_3)_2$ (**III-4**) can be easily obtained by the same method used to synthesize *trans*-$[Pt(NH_3)_2(dmpz)_2](NO_3)_2$. The excess ligand is likewise readily removed because of its low evaporation point. The ^1H NMR spectrum of complex **III-4** is shown in Figure 7. Two rotamers with 1:1 ratio can be clearly distinguished by their different chemical shifts. The resonances are observed at 8.97 ppm (H6, d, ^3J = 3.4 Hz), 8.85 ppm (H6, d, ^3J = 3.4 Hz), 8.44 ppm (H5, d, ^3J = 3.4 Hz), 8.41 ppm (H5, d, ^3J = 3.4 Hz), 3.42 ppm ($C(2)H_3$, s), 3.27 ppm ($C(2)H_3$, s) and 2.61 ppm ($C(3)H_3$, s). ^{195}Pt satellites (*) are present for the H(6) protons as seen in Figure 7. The coupling constant is ^3J ~ 36.0 Hz.

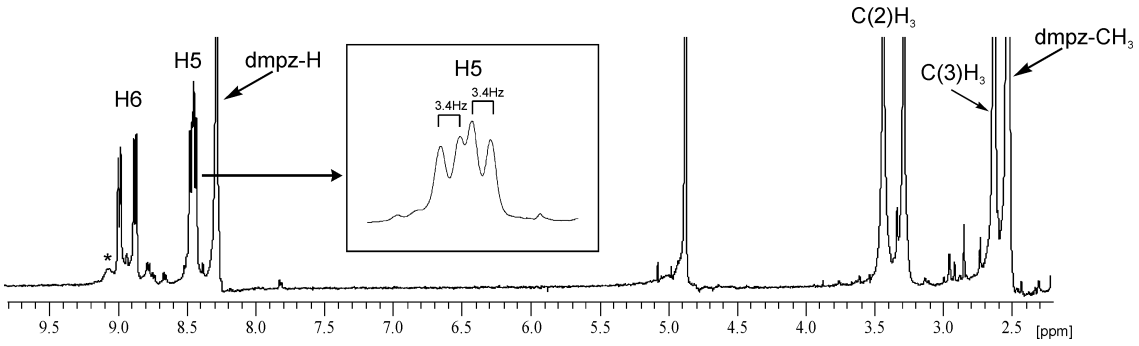

Figure 7. ^1H NMR spectrum (D_2O, pD 5.7) of *cis*-$[Pt(NH_3)_2(dmpz)_2](NO_3)_2$ (**III-4**) with an excess amount of dmpz.

3.4 Generation of molecular assemblies

The reactions of the *trans*-$[Pt(NH_3)_2(dmpz)_2]^{2+}$ building block with the 90° angular fragments Pt^{II}(en) and *cis*-$Pt^{II}(NH_3)_2$, in 1:1 ratio, were performed. The reactions were followed by ^{1}H NMR spectroscopy. Relatively simple spectra were obtained in both cases. However, an examination of relative signal intensities of en resonances (of Pt^{II}(en)) vs. dmpz resonances did not answer the question whether 1:1- or 1:2-products are formed. Attempts to crystallize a product were unsuccessful.

It probably has to be ruled out that the relative simplicity of the spectra is due to rapid (on NMR scale) equilibration following dissociation of Pt-N(dmpz) bonds. Also, the small line width of the low field resonances of the product(s) point against an oligomeric mixture but rather to the existence of discrete species.

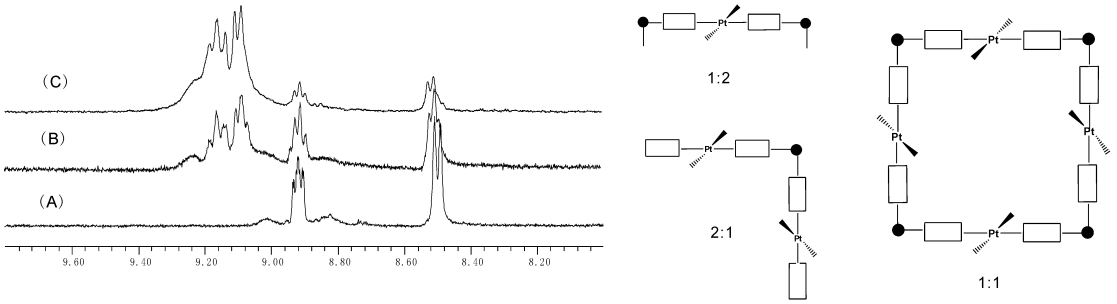

Figure 8. The reaction of the *trans*-$[Pt(NH_3)_2(dmpz)_2]^{2+}$ building block with Pt^{II}(en) was followed by ^{1}H NMR spectroscopy (left). The small line width of the low field resonances of the products suggests that discrete species are formed (right).

Similarly, reactions were also carried out by mixing *cis*-$[Pt(NH_3)_2(dmpz)_2]^{2+}$ with *cis*-$Pt^{II}(NH_3)_2$ and Pt^{II}(en). Again, relatively simple spectra were obtained. The problem is that both rotamers can, in principle, form an open or a cyclic structure.

4 Summary and outlook

Two Pt^{II} complexes with monodentate and bidentate bridging metal binding patterns of pyrazine have been isolated. Formation of the cyclic trimer **III-2** is somewhat unexpected considering the "molecular library approach" which predicts a molecular box when two ditopic building blocks with 90° and 180° angles are combined. It should be noted that formation of a similar cyclic trimer was likewise observed with the *cis*-$Pt^{II}(PMe_3)_2$ entity. The reason is tentatively assigned to the steric repulsion between methyl groups and pz ligands.

The pK_a values (calculated for H_2O) of dmpz were found to be 3.18 and 1.93, indicating that dmpz is substantially more basic than pyrazine. Therefore, dmpz could be a potential good bridging ligand. Two building blocks, with *trans*- and *cis*- geometries, were prepared by using dmpz. Unfortunately, the reaction products with additional metal entities have not been identified as yet.

References

[1] (a) Slone, R. V.; Hupp, J. T.; Stern, C. L.; Albrecht-Schmitt, T. E. *Inorg. Chem.* **1996**, *35*, 4096. (b) Rajendran, T.; Manimaran, B.; Lee, F.-Y.; Lee, G.-H.; Peng, S.-M.; Wang, C. M.; Lu, K.-L. *Inorg. Chem.* **2000**, *39*, 2016.

[2] Lau, V. C.; Berben, L. A.; Long, J. R. *J. Am. Chem. Soc.* **2002**, 124, 9042.

[3] Kraft, S.; Hanuschek, E.; Beckhaus, R.; Haase, D.; Saak, W. *Chem. Eur. J.* **2005**, *11*, 969.

[4] Schweiger, M.; Seidel, S. R.; Arif, A. M.; Stang, P. J. *Angew. Chem. Int. Ed.* **2001**, *40*, 3467.

[5] Yu, X.-Y.; Maekawa, M.; Kondo, M.; Kitagawa, S.; Jin, G.-X. *Chem. Lett.* **2001**, 168.

[6] Kumazawa, K.; Biradha, K.; Kusukawa, T.; Okano, T.; Fujita, M. *Angew. Chem. Int. Ed.* **2003**, *42*, 3909-3913.

[7] Willermann, M.; Mulcahy, C.; Sigel, R. K. O.; Morell, M.; Freisinger, E.; Sanz Miguel, P. J.; Roitzsch, M.; Lippert, B. *Inorg. Chem.* **2006**, *45*, 2093-2099.

[8] (a) Stang, P. J.; Olenyuk, B. *Acc. Chem. Res.* **1997**, *30*, 502. (b) Olenyuk, B.; Fechtenkötter, A.; Stang, P. J. *J. Chem. Soc., Dalton Trans*. **1998**, 1707.

[9] Leininger, S.; Olenyuk, B.; Stang. P. *J. Chem. Rev.* **2000**, *100*, 853

[10] Albert, A.; Phillips, J. N. *J. Chem. Soc.* **1956**, 1294

[11] Keyworth, D. A. *J. Org. Chem.* **1959**, *24*, 1355.

Chapter IV

Solution and Solid State Studies of a Triangle-Square System

1 Aim of the project

Transition-metal-mediated, coordination-driven self-assembly can allow for the synthesis of a series of predesigned macrocycles and cages.[1] Variations of ligand structure and coordination geometry give rise to the variety of structures, and it is now possible to predict the product structures in many cases.[2] There have been certain instances in which the stoichiometric combination of ~90° corners with linear linking units has led to a mixture of two, highly symmetrical products, instead of the anticipated supramolecular square.[3] This phenomenon has been postulated to be an equilibrium between differently sized entities in solution. Recently an increasing number of examples which crystallographically prove the existence of such equilibria, has been reported.[4] These systems have been a topic of interest in recent years due to their deviation from the directional-bonding approach[2b,c] and, more importantly, due to the insight that they may provide into the mechanism of self-assembly.

The linear 2,2'-bipyrazine ligand has proven to enable a large number of different metal binding patterns due to the availability of four ring N donor atoms and its structural flexibility about the central C(2)-C(2') bond.[5] With the Pt^{II}(en) angular fragment, it forms a cyclic trinuclear structure, [{Pt(en)(2,2'-bpz-*N4,N4'*)}$_3$]$^{6+}$, while with the Pd^{II}(en) angular fragment, it forms a mononuclear chelate, [Pd(en)(2,2'-bpz-*N1,N1'*)]$^{2+}$.[6] Both can be applied as building blocks for larger aggregates by combining them with suitable metal fragments.[7] For example, [Pd(en)(2,2'-bpz-*N1,N1'*)]$^{2+}$ and *trans*-$Pt^{II}(NH_3)_2$ units can be connected through N4,N4' donor atoms to form a flat triangle [{*trans*-$(NH_3)_2$Pt(*N4,N4'*-2,2'-bpz-*N1,N1'*)Pd(en)}$_3$]$^{12+}$ with Pd^{II} at the corners and Pt^{II} in the middle of the sides of the triangle.[7] On the other hand, the combination of the Pt triangle [{Pt(en)(2,2'-bpz-*N4,N4'*)}$_3$]$^{6+}$ with three more

Pd^{II}(en) yields a hexanuclear molecular vase or, with three Ag^{+}, a container compound.[8] Anion inclusion is a general phenomenon found in all these compounds.

In continuation of this work, *cis*-$Pt^{II}(NH_3)_2$, another ~90° angular fragment was reacted with 2,2'-bpz. A crystalline compound was obtained by Dr. Hussein H. Alkam, when visiting our laboratory in 2005. As demonstrated by the writer of this thesis, by applying X-ray crystallography, the compound represents a cyclic tetranuclear square. Own ^{1}H NMR work further proved that the molecular square co-exists in solution with a triangular species. The details will be discussed in below.

2 ^{1}H NMR resonances of the ligand 2,2'-bpz

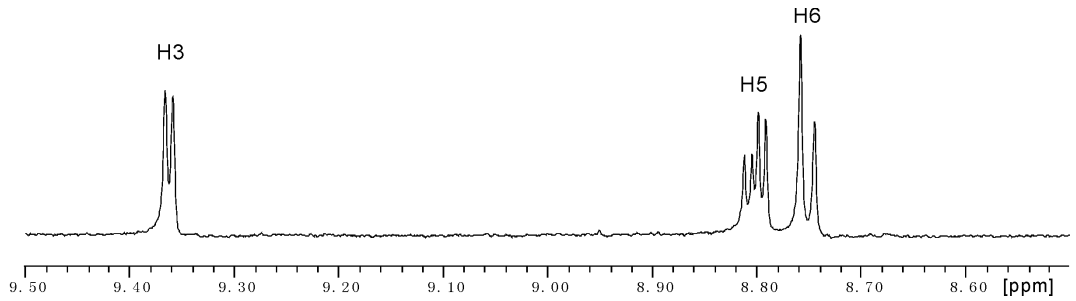

Figure 1. ^{1}H NMR spectrum of free 2,2'-bpz ligand in D_2O (pD = 6.7).

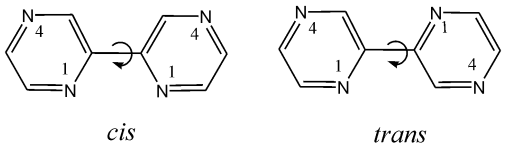

Scheme 1. *trans*- and *cis*-conformation of 2,2'-bipyrazine.

The ^{1}H NMR spectrum of free 2,2'-bpz in D_2O is shown in Figure 1. The simplicity of the spectrum suggests both pyrazine rings are equivalent. The *cis* conformation is expected to be less stable due to steric repulsion of the H(3) protons. 2,2'-bpz is known to be in the *trans* conformation in the solid state (Scheme 1).[9,10] The H(3) protons of bipyrazine in solution are expected to be deshielded by either the nonbonding electrons of nitrogen in the *trans* form and/or the diamagnetic anisotropy of the opposing pyrazine ring. The protons of each pyrazine ring form an ABX system. $J_{5,6}$ and $J_{3,5}$ couplings are

observed but not $J_{3,6}$ coupling; so H(5) can be distinguished readily from H(6). Thus, proton H(3) is assigned to the doublet resonance at 9.36 ppm, $^4J_{3,5}$ = 1.4 Hz, proton H(5) is assigned to the doublet-of-doublet resonance at 8.80 ppm, with $^4J_{3,5}$ = 1.4 Hz and $^3J_{5,6}$ = 2.6 Hz, and proton H(6) is assigned to the doublet resonance at 8.75 ppm, $^3J_{5,6}$ = 2.6 Hz.

3 Reactions of *cis*-$Pt^{II}(NH_3)_2$ with 2,2'-bpz

The reaction of *cis*-$Pt^{II}(NH_3)_2$ and 2,2'-bpz in 1:1 ratio was followed by ^{1}H NMR spectroscopy. In Figure 2, the low field sections of ^{1}H NMR spectra obtained by mixing *cis*-$Pt^{II}(NH_3)_2$ and 2,2'-bpz (1:1) at neutral pH are given. The region of the aromatic pyrazine protons is quite complex. Isolation of the cyclic Pt tetramer **IV-1** and Pt trimer **IV-2** helps to make the assignment of some of the resonances.

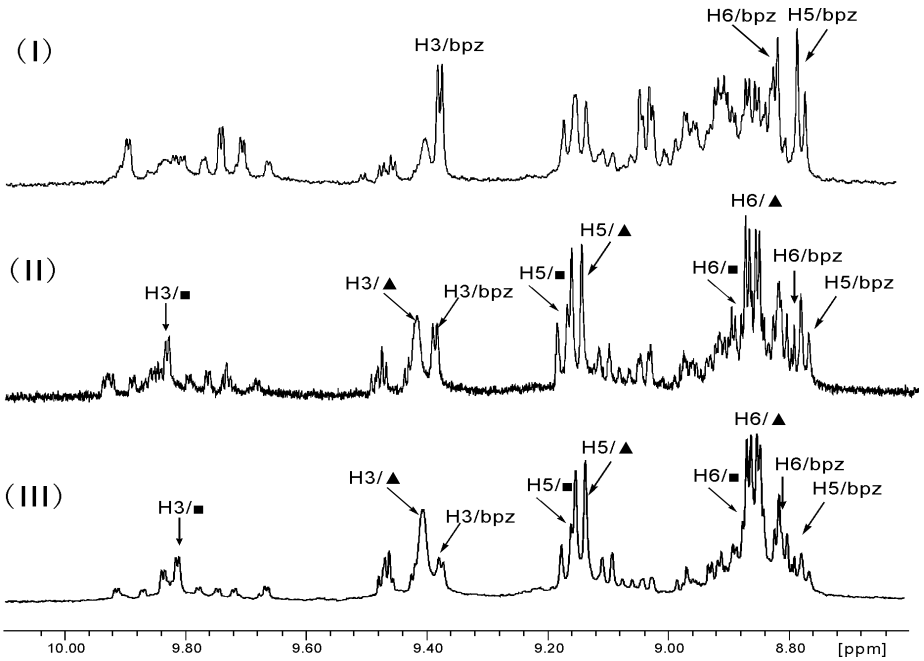

Figure 2 Low field section of ^{1}H NMR spectra (D_2O, pD = 6.8) obtained upon mixing *cis*-$Pt^{II}(NH_3)_2$ and 2,2'-bpz (1:1), and stirring at room temperature: (I) after one day. (II) after three days. (III) after five days. ▲ is assigned to [{*cis*-$Pt(NH_3)_2$(2,2'-bpz-*N4,N4'*)}$_3$]$(NO_3)_6$ (**IV-2**), ■ is assigned to [{*cis*-$Pt(NH_3)_2$(2,2'-bpz-*N4,N4'*)}$_4$]$(NO_3)_8 \cdot 4H_2O$ (**IV-1**)

Compound **IV-2** is the main product of this reaction. The integration of the signals of **IV-1** and **IV-2** give a ratio of 1:3. However, there are still several resonances with relative low intensity, which could be monomer, trimer, tetramer, even oligomeric products. Moreover, because of the possibility of

rotation about the C(2)-C(2') bond of the 2,2'-bpz ligands, additional conformations and hence resonances of such rotamers in solution can be expected.

4 Characterization of [{*cis*-Pt$(NH_3)_2$(2,2'-bpz-*N4,N4'*)}$_4$]$(NO_3)_8$·4H_2O (IV-1)

Compound **IV-1** was isolated as crystals suitable for X-ray crystallography. A view of cation is depicted in Figure 3. The selected bond lengths and angles are compiled in Table 1.

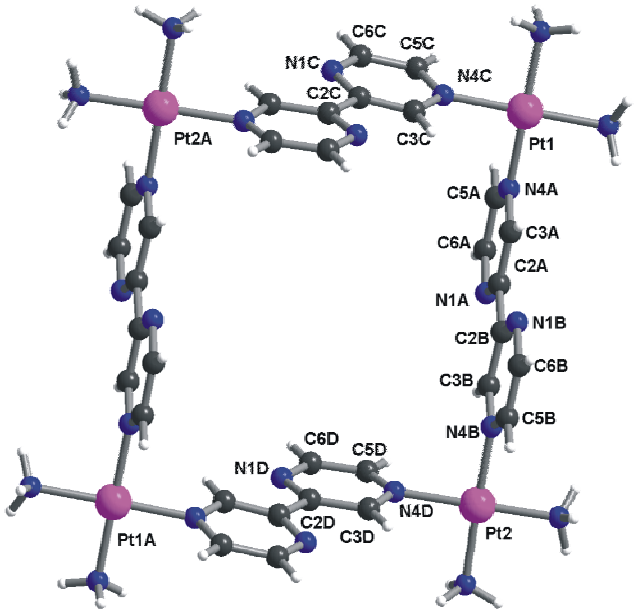

Figure 3. Perspective view of tetranuclear cation [{*cis*-Pt$(NH_3)_2$(2,2'-bpz-*N4,N4'*)}$_4$]$^{8+}$ (**IV-1**) and atom numbering scheme.

The solid-state structure of the nitrate salt of **IV-1** displays *trans* conformations for all four 2,2'-bpz ligands with respect to the C(2)-C(2') bonds. Inspection of the model reveals that this is just one structure (I) out of four possible ones for all-*trans* conformations (Scheme 2). The Pt coordination geometries are square planar with all bonding sites oriented approximately 90^o to each other. The Pt-N bond distances are in a normal region from 2.01(1) to 2.064(9) Å. The four Pt atoms form a parallelogram arrangement, with Pt(1)···Pt(2) distance 9.670(2) Å and Pt(1)···Pt(2A) distance 9.643(4) Å. The angles between the Pt centers are 96.90(1)^o for Pt(1)···Pt(2)···Pt(1A) and and

83.10(1)^{o} for Pt(2)···Pt(1)···Pt(2A). The structure of **IV-1** could be a consequence of the specific sequence of *trans*-bpz ligands in the cycle. It is (-+)(+-)(+-)(-+) (III)* (+ means pyridine ring higher than the metal position, while – means pyridine ring lower than the metal position). Other sequences are feasible (Scheme 2). From model building it appears that a sequence $(+-)_4$ generates a true square.

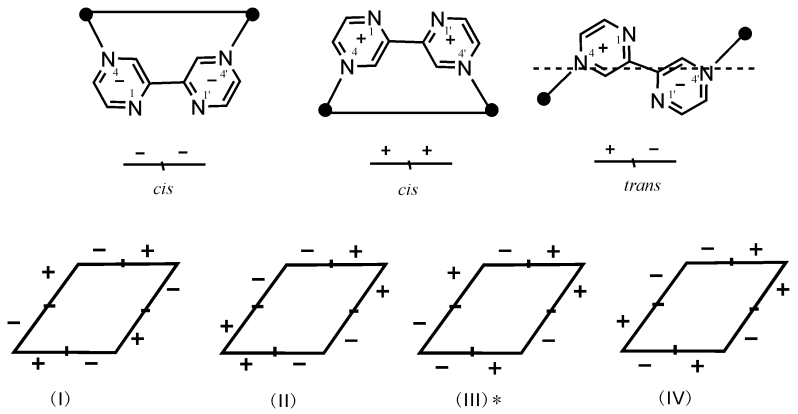

All-*trans* orientations of 2,2'-bpz in molecular "square"

* = observed in this work

Scheme 2.

Table 1. Selected Distances (Å) and angles (^{o}) for compound **IV-1**[a].

[{*cis*-Pt(NH$_3$)$_2$(2,2'-bpz-*N4,N4'*)}$_4$](NO$_3$)$_8$·4H$_2$O (IV-1)			
Pt1-N1M	2.064(9)	Pt2-N3M	2.012(10)
Pt1-N2M	2.039(9)	Pt2-N4M	2.046(11)
Pt1-N4A	2.033(8)	Pt2-N4B	2.027(8)
Pt1-N4C	2.033(9)	Pt2-N4D[a]	2.049(8)
Pt1···Pt2	9.670(2)	Pt1···Pt2[a]	9.643(4)
Pt1···Pt1[a]	14.454(3)	Pt2···Pt2[a]	12.808(6)
N1M-Pt1-N2M	90.7(3)	N3M-Pt2-N4M	89.5(5)
N1M-Pt1-N4A	89.6(3)	N3M-Pt2-N4B	89.4(4)
N2M-Pt1-N4C	88.8(4)	N4B-Pt2-N4D[a]	90.1(3)
N4A-Pt1-N4C	90.9(3)	N4D[a]-Pt2-N4M	91.1(4)
N1M-Pt1-N4C	179.0(3)	N3M-Pt2-N4D[a]	179.4(5)
N2M-Pt1-N4A	177.7(3)	N4B-Pt2-N4M	178.7(4)
Pt1···Pt2···Pt1[a]	96.90(1)	Pt2···Pt1···Pt2[a]	83.10(1)
Pz(A)/Pz(B)	2.5(1)	Pz(C)/Pz(D)	7.0(1)
Pz(A)/Pz(D)	85.6(2)	Pz(A)/Pz(C)	89.2(1)
Pz(B)/Pz(D)	84.1(3)	Pz(B)/Pz(C)	90.9(2)

[a]: Symmetry transformations used to generate equivalent atoms: 2-x,-y,1-z.

The comparison of **IV-1** with the [{Pt(en)(2,2'-bpz-*N4,N4'*)}$_3$](NO$_3$)$_6$ triangular cations, which have been reported by our group before,[5] reveals surprising similarities, but also a number of major structural differences. First, both of the compounds form cyclic structures via all-*trans* 2,2'-bpz-*N4,N4'* positions. Second, compound **IV-1** can be formally obtained by combining two sets of [{Pt(en)(2,2'-bpz-*N4,N4'*)}$_3$](NO$_3$)$_6$ (Scheme 3). Third, the two halves of 2,2'-bpz in [{Pt(en)(2,2'-bpz-*N4,N4'*)}$_3$](NO$_3$)$_6$ are markedly twisted (torsional angles ca. 15-39^o), whereas in compound **IV-1** all 2,2'-bpz ligands are closer to planar (ca. 2.5-7^o).

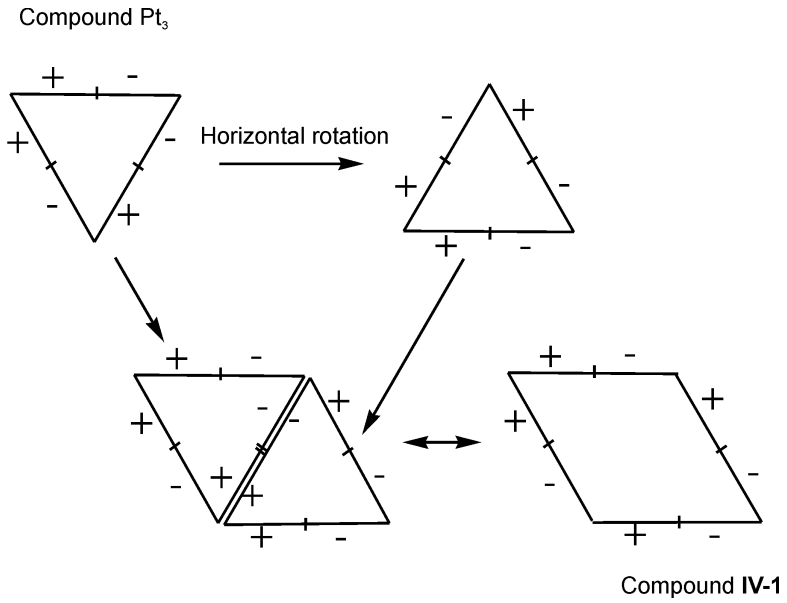

Scheme 3.

As a consequence of this particular arrangement of the bpz ligands, there are differences in intramolecular distances between aromatic protons. Thus, at the corners with (++) or (--) orientation, the shortest H···H distance, namely between H(5) and H(5'), is 3.187 Å, whereas in the (+-) corner, the distance between H(3') and H(5'') is significantly shorter, 2.845 Å.

As evident from the space filling representation, compound **IV-1** represents an open box with two nitrate anions and four water molecules inside. The volume of this box is roughly 9.7×9.6×5.0 Å^3. O(43) of the nitrate anion and the water molecule O(1w) with their symmetry related O(43') and O(1w') (-x, -y, -1-z) form a tetramer through hydrogen bonds with distances of 2.787 Å

(O(1w)···O(43)) and 2.938 Å (O(1w)···O(43')). Two more hydrogen bonds are formed by O(41)···O(1w) (2.949 Å), O(41)···O(2w) (2.676 Å). The open box thus behaves as a host for two nitrate anions and four water molecules, bearing some similarity with the situation in a recently described Pt_4 compound containing four triflate anions.[11]

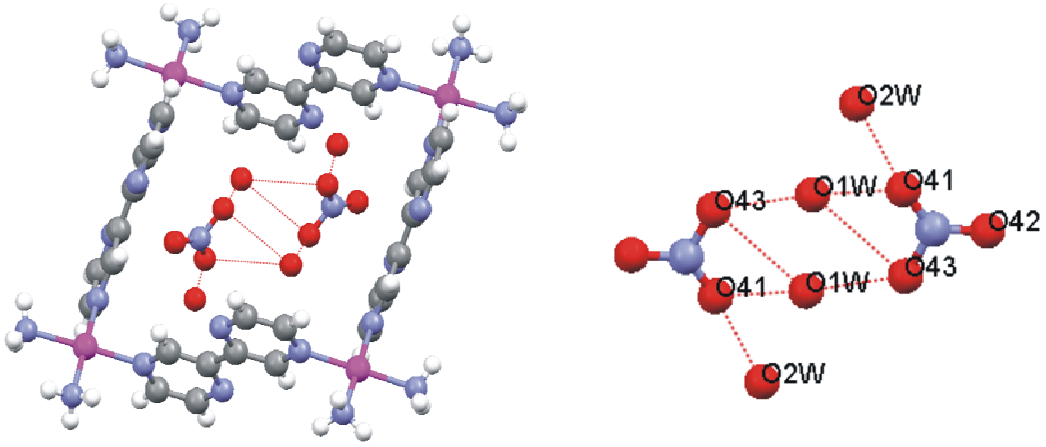

Figure 4. View of compound **IV-1** with two nitrate anions and four water molecules cluster encapsulated.

The packing of the cations of **IV-1** is such that they form a stair which is inclined by *ca*. 60° and has treads separated by *ca.* 7.5 Å (Figure 5). In the interior of this stair, a channel is formed, which hosts two nitrate anions and four water molecules per tread. This situation is in a way reminiscent of self-assembling ion channels that generate pore structures.[1a] The interaction between the layered, flat triangles is likewise *via* stacking.[7] However, in the present case, there is no direct H bonding between the steps, unlike in nanotubes generated by cyclic peptides, for example.[12] Rather NO_3^- anions and water molecules engage in H bonding with the NH_3 group of the adjacent positively charged tetramers, reinforced by NO_3^- anions at the periphery of the boxes, all of which are involved in multiple H bonding interactions with NH_3 ligands.

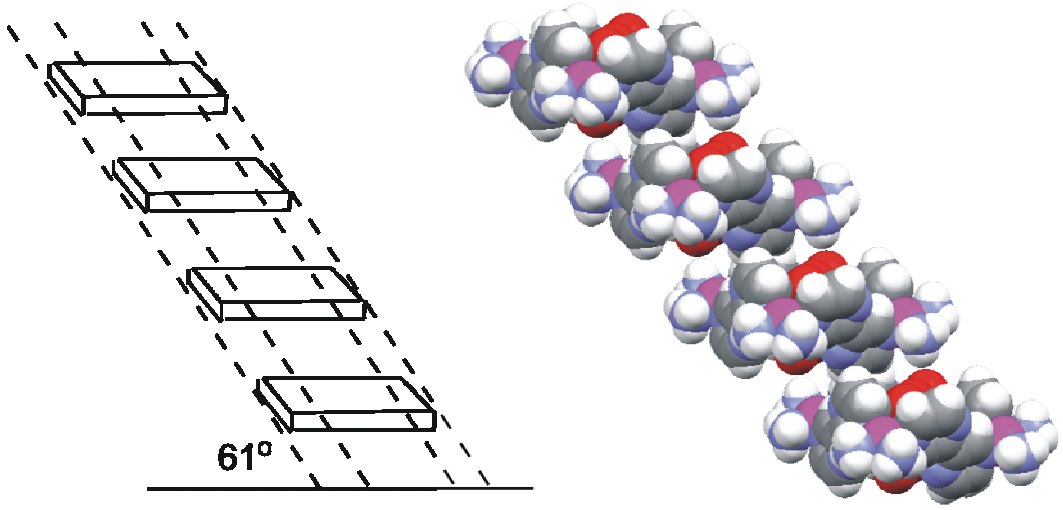

Figure 5. Schematic representation and space filling of the layered tetramers **IV-1** forming a 'stair'. Two NO_3^- anions and four H_2O molecules are encapsuled in the tetramers and form multiple H bonds with adjacent NH_3 groups of *cis*-$Pt^{II}(NH_3)_2$ entities (not shown). At the periphery the other six NO_3^- anions interact *via* H bonds with NH_3 groups of *cis*-$Pt^{II}(NH_3)_2$ entities (not shown), thereby generating a very compact structure that resembles a pipe rather than a stair.

The ^{1}H NMR spectrum of **IV-1** in D_2O is shown in Figure 6. All the pyrazine rings are in *trans* conformation in solution. No *cis* conformation rotamer is detected. The resonances consist of a doublet for H(3) at 9.83 ppm ($^5J_{3,6}$ = 1.1 Hz), a doublet for H(5) at 9.18 ppm ($^3J_{5,6}$ = 3.2 Hz) and a doublet of doublet for H(6) at 8.89 ppm ($^5J_{3,6}$ = 1.1 Hz, $^3J_{5,6}$ = 3.2 Hz).

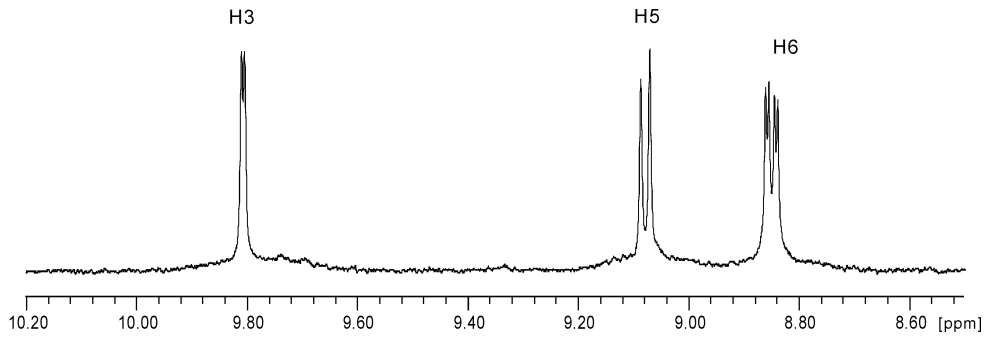

Figure 6. ^{1}H NMR spectrum of [{*cis*-Pt$(NH_3)_2$(2,2'-bpz-*N4,N4'*)}$_4$]$(NO_3)_8 \cdot 4H_2O$ (**IV-1**) in D_2O (pD = 6.3).

5 Characterization of [{*cis*-Pt(NH$_3$)$_2$(2,2'-bpz-*N4,N4'*)}$_3$](NO$_3$)$_6$ (IV-2)

Following crystallization of **IV-1**, a second compound, **IV-2**, was found to crystallize from solution. Unfortunately, these new crystals proved unsuitable for X-ray crystallography. However, the ^{1}H NMR spectrum was obtained by dissolving the crystals in D_2O (Figure 7). The resonances of compound **IV-2** consist of a singlet for H(3) at 9.36 ppm, a doublet for H(5) at 9.13 ppm ($^3J_{5,6}$ = 3.2 Hz) and a doublet of doublet for H(6) at 8.87 ppm ($^5J_{3,6}$ = 1.1 Hz, $^3J_{5,6}$ = 3.2 Hz), which are almost identical with those of [{Pt(en)(2,2'-bpz-*N4,N4'*)}$_3$]$^{6+}$.[5] The second species **IV-2** is consequently assigned to a trimer structure.

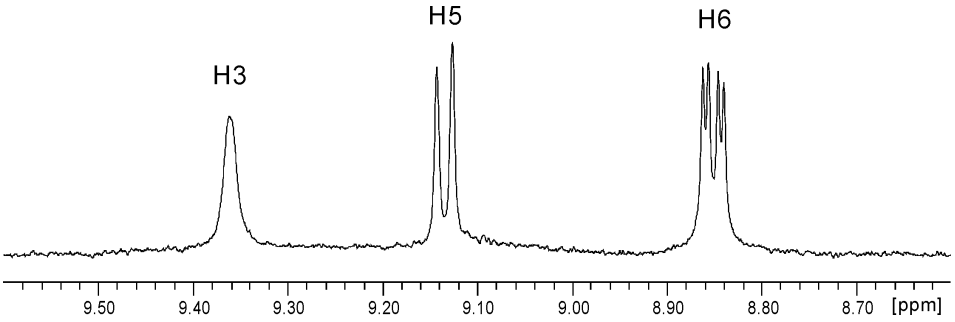

Figure 7. ^{1}H NMR spectrum of [{*cis*-Pt(NH$_3$)$_2$(2,2'-bpz-*N4,N4'*)}$_3$](NO$_3$)$_6$ (**IV-2**) in D_2O (pD = 6.3).

These findings imply that in solution both **IV-1** and **IV-2** exist in (slow) equilibrium. Heating the solution of compound **IV-1** at 50 °C for one day leads to 50% of compound **IV-2**. No further changes have been found upon continued heating at 50 °C. However, increasing the temperature to 100 °C leads to decomposition of both **IV-1** and **IV-2**. Then only resonances of 2,2'-bpz were found in solution. Attempts to isolate compound **IV-1** and compound **IV-2** by using different potential anion templates, such as $[Pt(CN)_4]^{2-}$, PF_6^-, ClO_4^- and terephthalate, were unsuccessful.

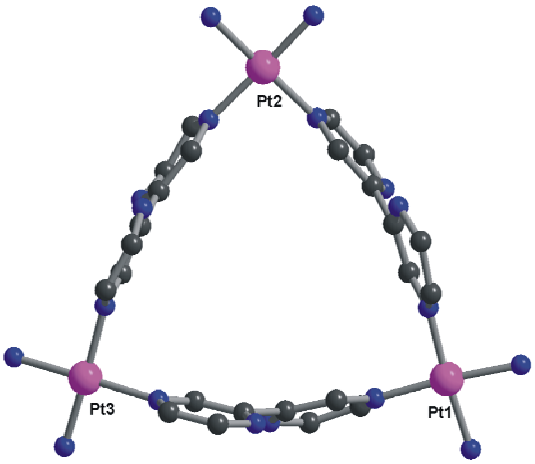

Figure 8. A view of cation [{*cis*-Pt(NH_3)$_2$(2,2'-bpz-*N4,N4'*)}$_3$]$^{6+}$ (**IV-2**) simulated from the known structure of [{Pt(en)(2,2'-bpz-*N4,N4'*)}$_3$]$^{6+}$.

6 Reaction of IV-1 and IV-2 with *cis*-a$_2$M^{II} (M = Pt or Pd) entity

Three different reactions were carried out, namely mixing compound **IV-1** with Pd^{II}(en), compound **IV-2** with Pd^{II}(en), and reacting a mixture of compound **IV-1** and compound **IV-2** with Pd^{II}(en). In all cases, the same phenomenon was observed, namely that the color of the solution turned to distinctly red after a mixing time of 5 min. Slow evaporation at 4 ^{o}C led to a dark green, highly concentrated solution. Meanwhile a small amount of KPF_6 was added to the solution. Within two weeks, green cubes had formed, which showed decay during the X-ray crystallographic measurements, however. The ^{1}H NMR spectrum of the green crystals in D_2O is shown in Figure 9. Resonances due to 2,2'-bpz are observed at 10.62 ppm (H3, s), 9.83 ppm (H5, d, $^{3}J_{5,6}$ = 3.8 Hz) and 8.84 ppm (H6, d, $^{3}J_{5,6}$ = 3.8 Hz). These shifts are almost identical with the resonances observed for [{(en)Pt(*N4,N4'*-2,2'-bpz-*N1,N1'*)Pd(en)}$_3$]$^{12+}$ (H3,H3', s, 10.66 ppm; H5,H5', d, 9.79 ppm, $^{3}J_{5,6}$ = 3.4 Hz; H6,H6', d, 8.83 ppm, $^{3}J_{5,6}$ = 3.4 Hz). As expected from binding of two metal entities to 2,2'-bpz via N1,N1' and N4,N4', the chemical shifts of the aromatic protons are furthest downfield with respect to those of **IV-1** and **IV-2**. By adding NaCl to the solution, a yellow precipitate of $PdCl_2$(en) formed within 2 hours of stirring. The ^{1}H NMR

spectrum of the filtrate showed it to contain compound **IV-2**. Therefore, the green crystals are tentatively assigned to the [{*cis*-$(NH_3)_2$Pt(*N4,N4'*-2,2'-bpz-*N1,N1'*)Pd(en)}$_3$]$^{12+}$ (**IV-3**) cation. Elemental analysis suggests that there are eleven NO_3^-, one PF_6^- and six water molecules per unit. No decomposition is observed in solution.

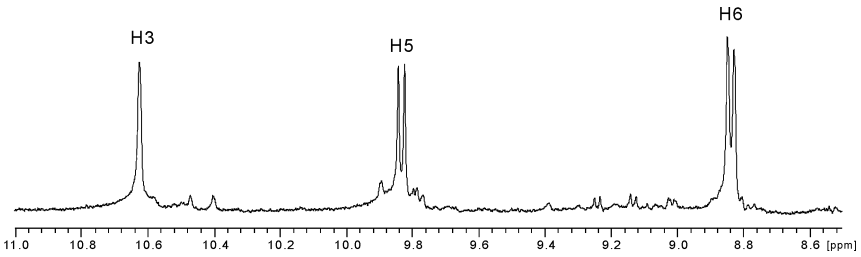

Figure 9. ^{1}H NMR spectrum of [{*cis*-$(NH_3)_2$Pt(*N4,N4'*-2,2'-bpz-*N1,N1'*)Pd(en)}$_3$]$(NO_3)_{12}$ (**IV-3**) in D_2O (pD = 7.3).

In addition, reactions of compound **IV-1** with other *cis*-square planar entities, such as Pd^{II}(bpy), Pd^{II}(tmeda) and *cis*-$Pt^{II}(NH_3)_2$, were conducted and followed by ^{1}H NMR spectroscopy (D_2O, pD ~ 9). They did not yield compounds analogous to **IV-3.** In fact there were no reactions at all. This tentatively suggests that either the π-stacking of bpy to 2,2'-bpz (confirmed by upfield shift of the resonances of bpy), the steric bulk of the tmeda ligand, and/or the low reactivity of Pt^{II} are the factors which impede further reactions.

8 Summary

This study represents one of the few cases[13] in which both products of a square-triangle equilibrium are detected in solution by ^{1}H NMR spectroscopy. The crystal structure of the "square" compound **IV-1** has been solved. It shows an interesting box structure with two nitrate anions and four water molecules incorporated in the interior. It remains to be seen whether this observation may have further implications in host-guest chemistry.

References

[1] (a) Lehn, J.-M. *Supramolecular Chemistry: Concepts and Perspectives;* VCH: New York, **1995**. (b) Steed, J. W.; Atwood, J. L. *Supramolecular Chemistry;* VCH: New York, **2000**.

[2] Recent review: (a) Fujita, M.; Umemoto, K.; Yoshizawa, M.; Fujita, N.; Kusukawa, T.; Biradha, K. *Chem. Commun.* **2001**, 509. (b) Holliday, B. J.; Mirkin, C. A. *Angew. Chem. Int. Ed.* **2001**, *40*, 2022. (c) Leininger, S.; Olenyuk, B.; Stang, P. J. *Chem. Rev.* **2000**, *100*, 853 and references therein.

[3] (a) Fujita, M.; Sasaki, O.; Mitsuhashi, T.; Fujita, T.; Yazaki, J.; Yamaguchi, K.; Ogura, K. *Chem. Commun.* **1996**, 1535. (b) Lee, S. B.; Hwang, S.; Chung, D. S.; Yun, H.; Hong, J.-I.; *Tetrahedron Lett.* **1998**, *39*, 873. (c) Romero, F. M.; Ziessel, R.; Dupont-Gervais, A.; van Dorsselaer, A. *Chem. Commun.* **1996**, 551. (d) Satter, A.; Schmid, D. G.; Jung, G.; Würthner, F. *J. Am. Chem. Soc.* **2001**, *123*, 5424. (e) Cotton, F. A.; Lin, C.; Murillo, C. A. *Inorg. Chem.* **2001**, *40*, 575.

[4] (a) Sautter, A.; Schmid, D. G.; Jung, G.; Würthner, F. *J. Am. Chem. Soc.* **2001**, *123*, 5424. (b) Schweiger, M.; Seidel, S. R.; Arif, A. M.; Stang, P. J. *Inorg. Chem.* **2002**, *41,* 2556. (c) Berben, L. A.; Faia, M. C.; Crawford, M.; Long, J. R. *Inorg. Chem.* **2006**, *45*, 6378. (d) Baxter, P. N. W.; Lehn, J.-M.; Rissanen, K. *Chem. Comm.* **1997**, 1323. (e) Chi, X.; Guerin, A. J.; Haycock, R. A.; Hunter, C. A.; Sarson, L. D. *J. Chem. Soc., Chem. Commun.* **1995**, 2567. (f) Ferrer, M.; Mounia, M.; Rossell, O.; Ruiz, E.; Maestro, M. A. *Inorg. Chem.* **2003**, *42*, 5890. (g) Cotton, F. A.; Murillo, C. A.; Yu, R. *Dalton Trans.* **2006**, 3900. (h) Cotton, F. A.; Daniels, L. M.; Lin, C.; Murillo, C. A. *J. Am. Chem. Soc.* **1999**, *121*, 4538.

[5] Schnebeck, R.-D.; Freisinger, E.; Lippert, B. *Eur. J. Inorg. Chem.* **2000**, 1193.

[6] Schnebeck, R.-D.; Randaccio, L.; Zangrando, E.; Lippert, B. *Angew. Chem. Int. Ed.* **1998**, *37*, 119.

[7] Schnebeck, R.-D.; Freisinger, E.; Lippert, B. *J. Chem. Soc. Chem. Commun.* **1999**, 675.

[8] (a) Schnebeck, R.-D.; Freisinger, E.; Glahé, F.; Lippert, B. *J. Am. Chem. Soc.* **2000**, *122*, 1381. (b) Schnebeck, R.-D.; Freisinger, E.; Lippert, B. *Angew. Chem. Int. Ed.* **1999**, *38,* 168.

[9] Bertinotti, F.; Liquori, A. M.; Parisi, R. *Gazz. Chim. Ital.* **1956**, *86*, 893.

[10] Merritt, L. L. Jr.; Schroeder, E. D. *Acta Crystallogr.* **1956**, *9*, 801.

[11] Janzen, D. E.; Patel, K. N.; VanDerveer, D. G.; Grant, G. *J. Chem. Commun.* **2006**, 3540.

[12] Hartgerink, J. D.; Clark, T. D.; Ghadiri, M. R. *Chem. Eur. J.* **1998**, *4*, 1367.

[13] (a) Cotton, F. A.; Daniels, L. M.; Lin, C.; Murillo, C. A. *J. Am. Chem. Soc.* **1999**, *121*, 4538. (b) Cotton, F. A.; Daniels, L. M.; Lin, C.; Murillo, C. A.; Yu, S.-Y. *J. Chem. Soc., Dalton Trans.* **2001**, 502. (c) Cotton, F. A.; Lin, C.; Murillo, C. A. *J. Am. Chem. Soc.* **2001**, *123*, 2670. (d) Bera, J. K.; Angaridis, P.; Cotton, F. A.; Petrukhina, M. A.; Fanwick, P. E.; Walton, R. A. *J. Am. Chem. Soc.* **2001**, *123*, 1515. (e) Cotton, F. A.; Lin, C.; Murillo, C. A. *Chem. Commun.* **2001**, 11. (f) Cotton, F. A.; Lin, C.; Murillo, C. A. *Inorg. Chem.* **2001**, *40*, 478.

Chapter V

Host-guest Interaction Studies with Cyclic Metal Compounds

1 Introduction

The synthetic approach via metal-directed self-assembly[1] has led to the rapid development of supramolecular coordination compounds in the past decade. There is a variety of geometrically and topologically elegant structures such as molecular triangles,[2] squares,[3,2f] pentagons and hexagons,[4] cuboctahedra and dodecahedra, bowls, cages, boxes, catenanes and tubes.[5] These metallosupramolecular systems display attractive properties in molecular recognition, catalysis, redox activity, magnetism, luminescence, and electron transfer.

In this chapter, a series of cyclic compounds, which have structures such as double cone, triangle and box, will be presented that function as anion receptors or for molecular encapsulation. The affinity of a host for a guest is assessed by means of the association constant for the binding process, which is established by NMR titration methods.

2 Host-guest chemistry study with [{Pd(1-MeC$^-$-*N3*,*N4*)(tmeda)}$_3$](ClO$_4$)$_3$·5.5H$_2$O (I-7)

2.1 [{Pd(1-MeC$^-$-*N3*,*N4*)(tmeda)}$_3$](ClO$_4$)$_3$·5.5H$_2$O: Structure

Considering the volumes of the cavities of the [{Pd(1-MeC$^-$-*N3*,*N4*)(tmeda)}$_3$](ClO$_4$)$_3$·5.5H$_2$O (**I-7**) (Pd$_3$(1-MeC$^-$)$_3$) double cone (Figure 1), halide anions were chosen as potential guests due to their size and spherical shape (Table 1).

Table1 Ionic radius

	r(pm)
F^-	133
Cl^-	181
Br^-	196
I^-	220
ClO_4^-	250

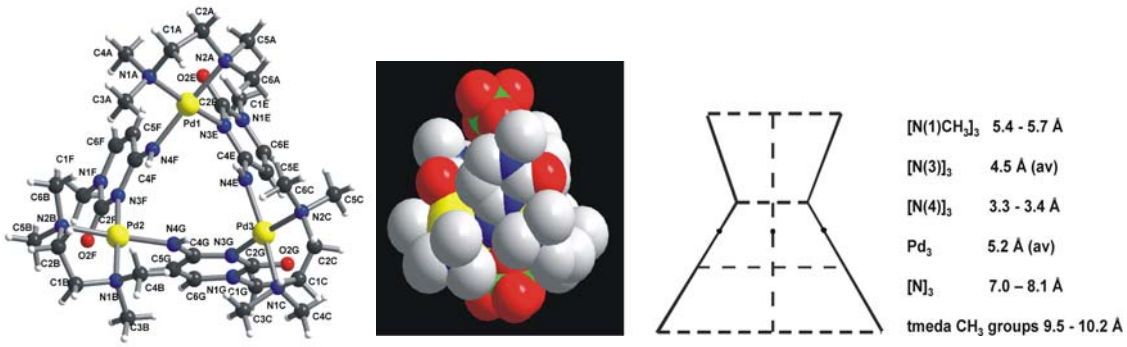

Figure 1. Perspective view of trinuclear cation $[\{Pd(1\text{-}MeC^{-}\text{-}N3,N4)(tmeda)\}_3]^{3+}$ and atom numbering scheme. Schematic representation of Pd_3 double cone with separations within triangles of same atoms indicated.

2D $^1H,^1H$ NOESY experiments were carried out with the $Pd_3(1\text{-}MeC^{-})_3$ compound in order to assign individual methyl groups of the tmeda ligands. Figure 2 displays the chemical shift region which rationalizes the relationship between the aromatic protons of 1-MeC$^-$ and the methyl groups of tmeda ligand. The signal of the proton H(5) at 6.38 ppm gives an intense cross-peak with the signal of methyl group (2) located at 2.76 ppm, but only a weak cross-peak with the signal of methyl group (4) located at 2.33 ppm. Moreover, the signal of the proton of N(4) at 5.03 ppm gives intense cross-peaks with the signals of methyl group (1) and methyl group (3) located at 2.78 ppm and 2.65 ppm, respectively. Space filling representations of particular sections of the $Pd_3(1\text{-}MeC^{-})_3$ compound are shown in Figure 3. Concerning the structure, the resonance at 2.78 ppm is assigned to methyl group (1), which is closest to the cavity and likewise close to N(4)H proton. The resonance at 2.76 ppm is assigned to methyl group (2), which is opposite to methyl group (1) and close to the H(5) proton. The resonance at 2.65 ppm is assigned to methyl group (3), which is also pointing to the center of cavity and therefore is close to the N(4)H proton. The resonance at 2.33 ppm is assigned to methyl group (4), which is opposite to methyl group (3) but close to the H(5) proton.

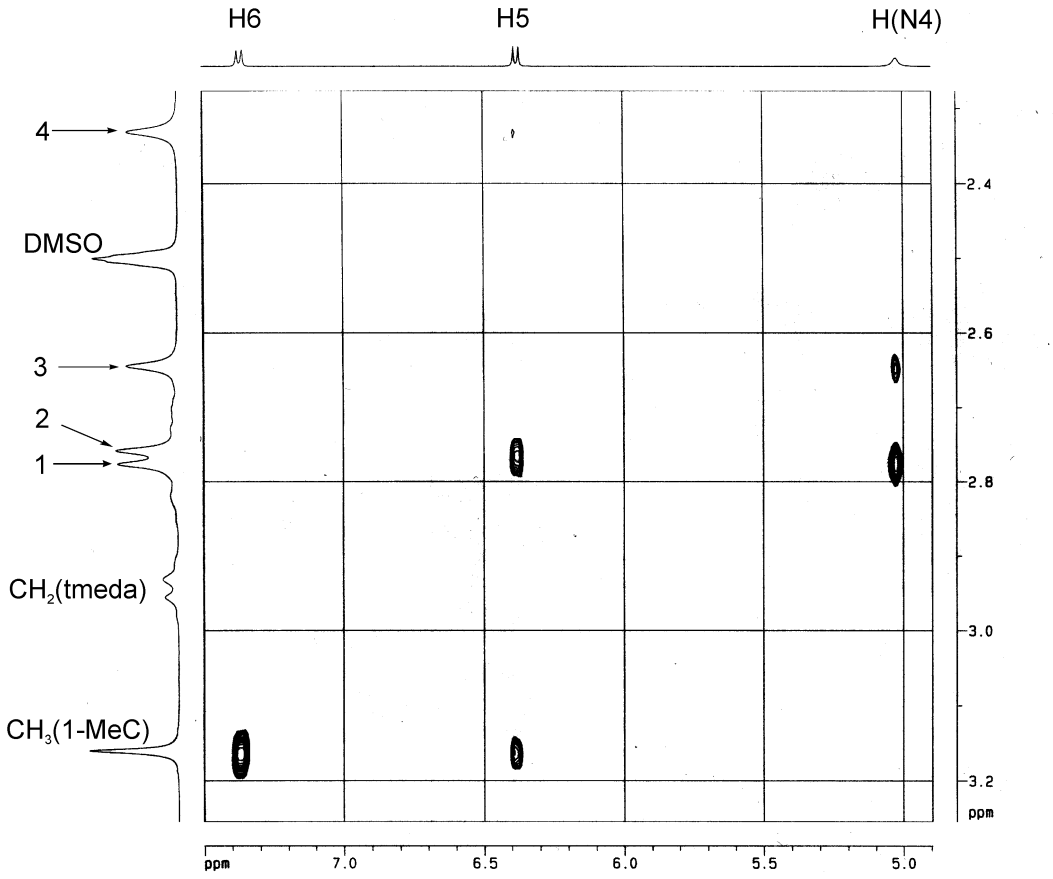

Figure 2. 2D ^{1}H,^{1}H NOESY experiment with [{Pd(1-MeC^{-}-*N3,N4*)(tmeda)}$_3$](ClO$_4$)$_3$·5.5H$_2$O (**I-7**), rationalizing the relationship between the aromatic protons of 1-MeC and the methyl groups of tmeda.

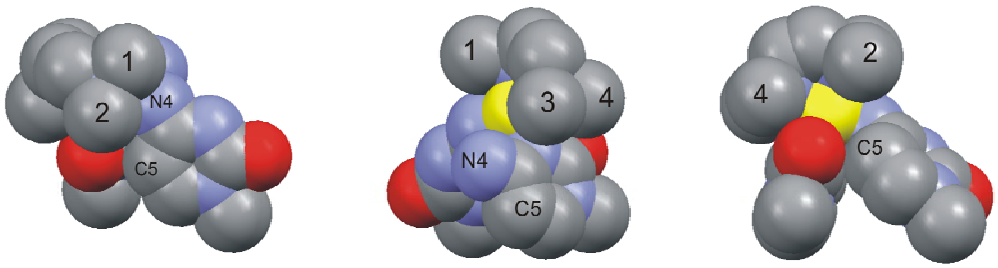

Figure 3. Space filling representation of sections of [{Pd(1-MeC^{-}-*N3,N4*)(tmeda)}$_3$]$^{3+}$ seen from different directions. 1, 2, 3, and 4 are the four methyl groups of the tmeda ligand.

2.2 [{Pd(1-MeC$^-$-*N3*,*N4*)(tmeda)}$_3$](ClO$_4$)$_3$·5.5H$_2$O as receptor for fluoride

Applying ^{1}H NMR spectroscopy and concentrating on the N(4)H resonance, no evidence for any host-guest chemistry between Pd$_3$(1-MeC$^-$)$_3$ and F$^-$ was found in D$_2$O as the solvent, presumably as a consequence of efficient solvation of host and guest. In DMSO-*d*$_6$, however, shifts of several ^{1}H resonances of the trinuclear Pd$_3$(1-MeC$^-$)$_3$ cation in the presence of F$^-$ were detected (Figure 4). Thus, addition of increasing amounts of [NMe$_4$]F to a solution of Pd$_3$(1-MeC$^-$)$_3$ resulted in a marked downfield shift of the N(4)H resonance, moderate downfield shifts of two of the four CH$_3$ resonances of the tmeda ligand, and minor upfield shifts of the aromatic protons of the 1-MeC$^-$ ligand. A saturation behavior was seen with more than 2 equiv. of F$^-$ added. For example, chemical shift changes of Pd$_3$(1-MeC$^-$)$_3$ (4 mmol/l) in the presence of 4 equiv of [NMe$_4$]F amounted to $\Delta\delta$ = 3.75 ppm for N(4)H, 0.20 and 0.10 ppm, respectively, for (tmeda)-CH$_3$, –0.18 ppm for H(6), and –0.04 ppm for H(5) (Figure 4). Attempts to analyze the chemical shift data and to determine an association constant were hampered by the fact that water was introduced into DMSO-*d*$_6$ by both the Pd$_3$(1-MeC$^-$)$_3$ compound (water of crystallization) as well as the hygroscopic [NMe$_4$]F salt and the fact that the N(4)H resonance proved quite sensitive to the presence of water.[50] Deliberate additon of D$_2$O to DMSO-*d*$_6$ solutions of Pd$_3$(1-MeC$^-$)$_3$ and F$^-$ indeed caused a partial reversal of the chemical shifts mentioned above. Consequently, the slope of $\Delta\delta$ for N(4)H as a function of the ratio (r) between F$^-$ guest and Pd$_3$(1-MeC$^-$)$_3$ receptor is artificially lowered with the change of slope reached near r ≈ 2 (Figure 5). This behavior is not considered evidence for a 2:1 stoichiometry (two F$^-$ bound per Pd$_3$(1-MeC$^-$)$_3$) but rather a consequence of the introduction of water into the system.

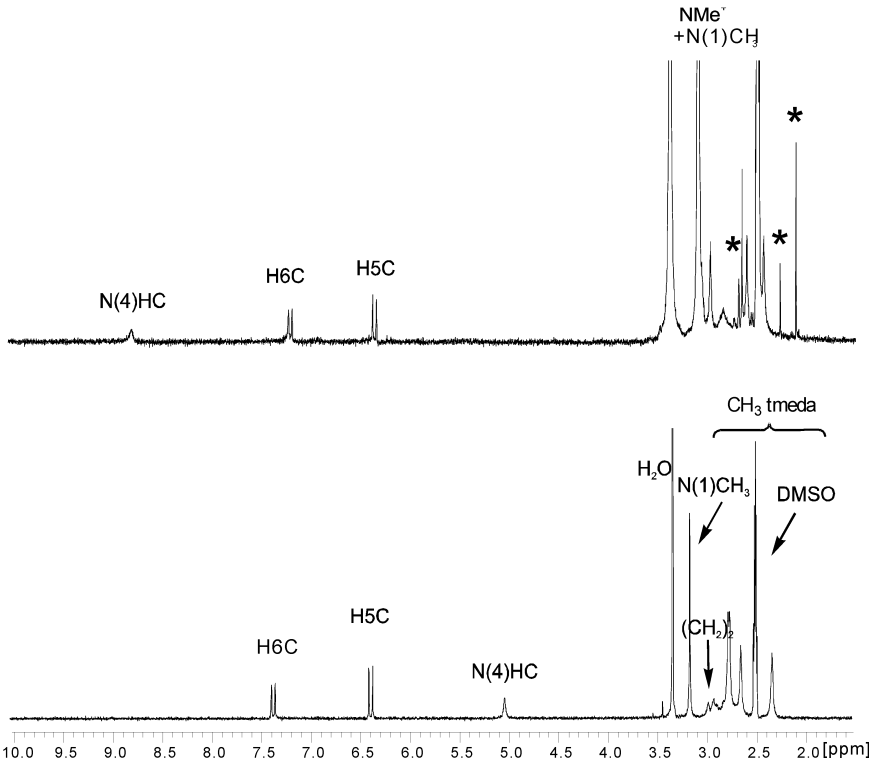

Figure 4. ^{1}H NMR spectra (DMSO-d_6, c = $4 \cdot 10^{-3}$ M) of $Pd_3(1\text{-}MeC^{-})_3$ compound (bottom) and in presence of 4 equiv of $[NMe_4]F$ (top). Note that the water peak increases strongly upon addition of the fluoride salt. Signals with asterisks refer to unknown species.

As pointed out above, only two of the four methyl resonances of the tmeda ligands proved sensitive to F^-. It was the one furthest downfield (2.77 ppm in DMSO-d_6) and the one furthest upfield (2.33 ppm) which underwent downfield shifts with increasing F^- amounts. This either reflects CH···F hydrogen bonding, averaged over the protons of CH_3 groups involved, or is due to a reorganization of the lower cone in the presence of fluoride. From the structure provided in Figure 1, it appears that at least the methyl groups C(3A), C(4B) and C(6C), which are closest to the cavity with the three N(4)H's at its bottom, are affected by F^- binding.

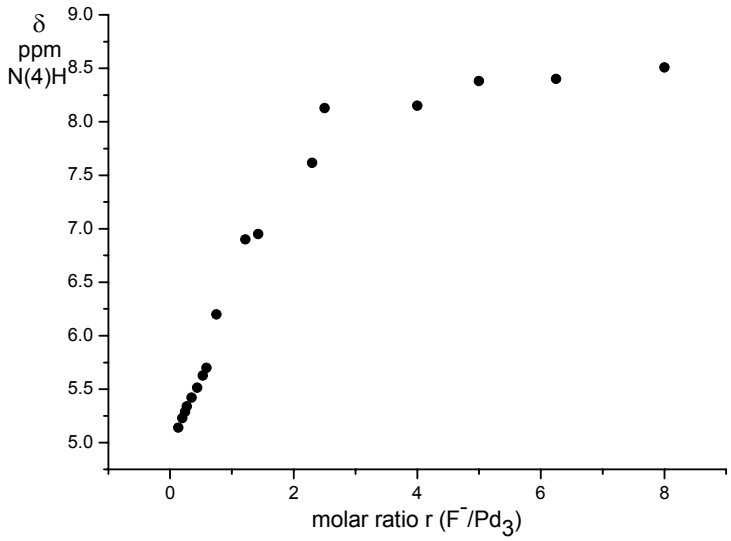

Figure 5. Dependence of downfield shift of N(4)H resonance of $Pd_3(1\text{-}MeC^-)_3$ (DMSO-d_6) in dependence of molar ratio of $[NMe_4]F$ to host. The presence of H_2O in DMSO-d_6 reduces the downfield shift of this resonance. Assuming a 1:1 stoichiometry between F^- and $Pd_3(1\text{-}MeC^-)_3$ and the absence of water, a steeper inclination of the curve would have been expected.

Concerning the long term stability of the $Pd_3(1\text{-}MeC^-)_3\text{-}F^-$ adduct in DMSO-*d*$_6$, gradual ^{1}H NMR spectroscopic changes were observed within days at 25 °C only in cases of high F^- excess ($r \geq 4$). A sign of secondary reactions taking place was the appearance of sharp resonances in the 2.1 – 2.7 ppm region of the spectrum (see Figure 4).

2.3 [{Pd(1-MeC$^-$-*N3*,*N4*)(tmeda)}$_3$](ClO$_4$)$_3$·5.5H$_2$O as receptor for chloride, bromide and iodide

In DMSO-*d*$_6$, the chemical shifts of proton resonances of the $Pd_3(1\text{-}MeC^-)_3$ cation in the presence of chloride, bromide and iodide were likewise observed. Similar to fluoride, increasing amounts of $[NMe_4]X$ (X = Cl, Br, I) to a solution of $Pd_3(1\text{-}MeC^-)_3$ led to a marked downfield shift of the N(4)H resonance, and minor upfield shifts of the aromatic protons of the 1-MeC$^-$ ligands. As an example, ^{1}H NMR spectra of $Pd_3(1\text{-}MeC^-)_3$ with increasing amounts of Br^- are shown in Figure 6. In contrast, the shifts of the CH_3 resonances of the tmeda ligand are different (not shown). For chloride and bromide, two of the four CH_3 resonances of the tmeda ligand, namely methyl groups (1) and (3), undergo downfield shifts, while the other two (methyl groups (2) and (4)) are upfield

shifted. For iodide, three of the four CH_3 resonances of the tmeda ligand, methyl groups (1), (2) and (3) are downfield shifted, while the other one (methyl group (4)) is upfield shifted. These findings strongly suggest that the interactions for chloride and bromide are different from iodide. It possibly reflects the difference in CH···X hydrogen bonding and/or differences in the way the halide ions approach the double cone.

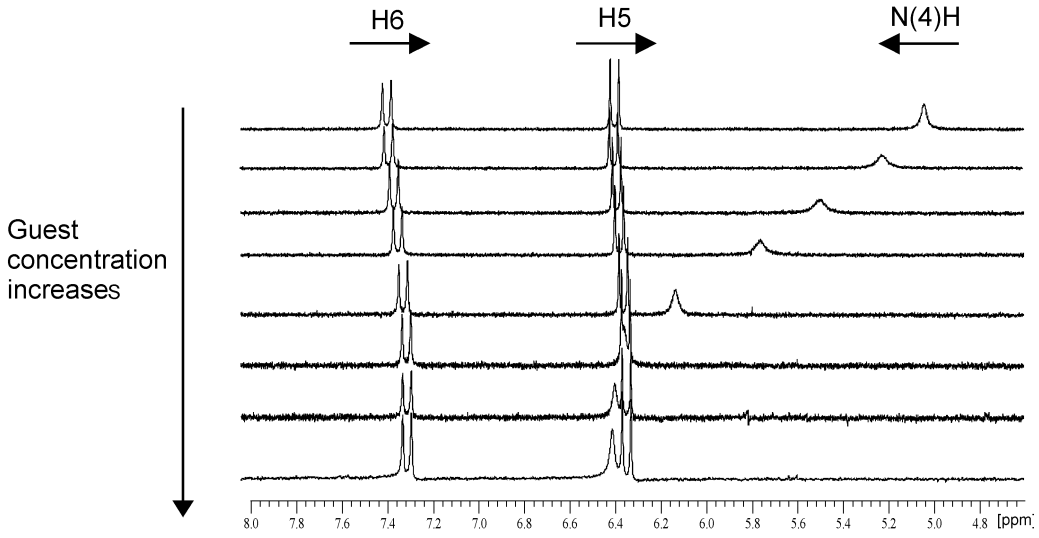

Figure 6. Stackplot of ^{1}H NMR spectra of mixtures of $Pd_3(1\text{-}MeC^-)_3$ and Br^-. Increasing amounts of bromide result in marked downfield shifts of the N(4)H resonance and minor upfield shifts of the aromatic protons of the 1-MeC^- ligands.

In all cases, the downfield shift of N(4)H resonance is the largest, which reflects the fact the halide anions approach the double cone from the bottom (tmeda side). Hydrogen bonds between the N(4)H protons and halide anions are formed. The maximum chemical shifts caused by chloride, bromide and iodide are presented in Table 2. The stoichiometry of the host-guest complexes was established by the Job plots method of continuous variations.[6] The Job plots for the studied systems are shown in Figure 7. The complexation-induced shift of the ^{1}H NMR resonance for the guest moiety is shown as a function of the host mole fraction, with the total concentrations kept constant. In all cases, a 1:1 stoichiometry was found.

The association constants were determined by ^{1}H NMR titration (DMSO-d_6 solution) from the dependencies of the proton (N(4)) resonance of the host molecule on the ratio of the guest/host concentrations. The association

constants (K_{assoc}) were obtained from simultaneous fits of Equation (1) (see Appendix) to the experimental data with the assumption that the observed frequencies are the molar-fraction-weighted averages of the respective frequencies in the free guest molecules and those for the host-guest complexes (Figure 8).

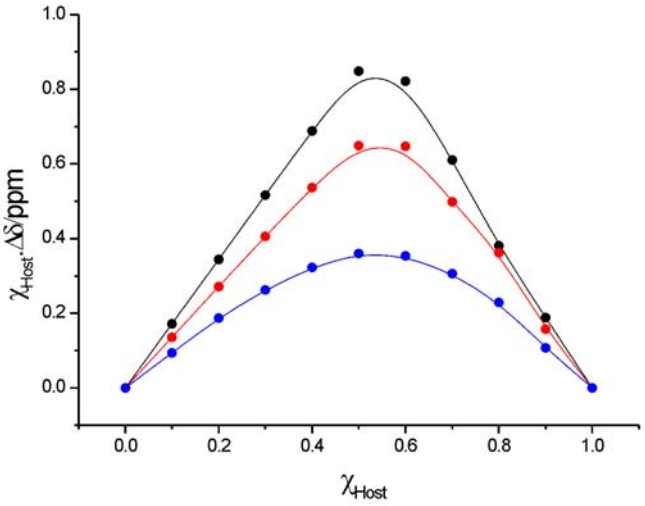

Figure 7. Job plots for the host $Pd_3(1\text{-}MeC^-)_3$ and guest Cl^-(black), Br^-(red) and I^-(blue).

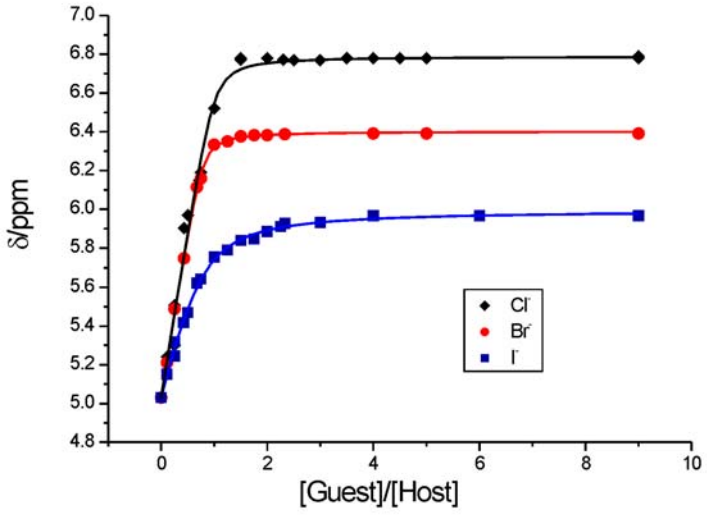

Figure 8. Dependence of downfield shift of N(4)H resonance of $Pd_3(1\text{-}MeC^-)_3$ (DMSO-d_6) on the molar ratio of $[NMe_4]X$ (X: Cl, Br and I) to host.

The association constants for the three host-guest complexes are compiled in Table 2. The association constants for chloride and bromide are larger than the one for iodide. This also confirms that the spatial relationships are different.

Table 2. Association constants for chloride, bromide and iodide with $Pd_3(1\text{-}MeC^-)_3$.

	Cl^-	Br^-	I^-
$\Delta\delta_{max}$/ppm	1.75	1.37	0.96
K/M^{-1}	47 ± 15	56 ± 13	6 ± 1
log K	1.7(2)	1.8(1)	0.78(9)

2.4 The interactions between $Pd_3(1\text{-}MeC^-)_3$ and amino acids

Recently, Fish et al. reported the molecular recognition of aromatic and aliphatic amino acid guests by cyclic trinuclear host molecules derived from Cp^*Rh-adenine (Cp^*: η^5-pentamethylcyclopentadienyl) in aqueous solution at physiological pH.[7,8,9]

In a similar way, eight amino acids were tested with $Pd_3(1\text{-}MeC^-)_3$ by ^1H NMR spectroscopy in D_2O. No evidence for any host-guest interaction was found. This was surprising considering the fact that the intermetallic distances in both types of compounds are almost identical. However, the π-system of the adenine ligands is larger than that of cytosine, which could be an explanation for the difference in behavior. Nevertheless an interesting difference between the various amino acids was found. For alanine, valine, leucine and isoleucine, there were no interactions at all, while for phenylalanine, aspartic acid, glycine and histidine the $Pd_3(1\text{-}MeC^-)_3$ compound was found to decompose with formation of free 1-MeC and Pd(tmeda)(amino acid) species. This difference is tentatively proposed to be due to a particular orientation of the “reactive” amino acid at the $Pd_3(1\text{-}MeC^-)_3$ cone, which permits rapid substitution reactions at Pd^{II}. However, no specific orientation can be proposed at this point.

3 Host-guest chemistry studies of [{*cis*-Pt(NH_3)$_2$(2,2'-bpz-*N4,N4'*)}$_4$](NO_3)$_8$·4H_2O (IV-1) and [{*cis*-Pt(NH_3)$_2$(2,2'-bpz-*N4,N4'*)}$_3$](NO_3)$_6$ (IV-2)

3.1 [{*cis*-Pt(NH_3)$_2$(2,2'-bpz-*N4,N4'*)}$_4$]$^{8+}$ and [{*cis*-Pt(NH_3)$_2$(2,2'-bpz-*N4,N4'*)}$_3$]$^{6+}$ as receptors for terephthalate

The tetramer [{*cis*-Pt(NH_3)$_2$(2,2'-bpz-*N4,N4'*)}$_4$](NO_3)$_8$·4H_2O (Pt_4), due to the cyclic square shape and its high positive charge, should in principle be in the position to accept large anionic guests. Several guest molecules have been applied in a host-guest interaction study with the Pt_4 compound, including the square-planar anions $[PtCl_4]^{2-}$, $[PdCl_4]^{2-}$ and $[Pt(CN)_4]^{2-}$. However, there was no evidence from ^{1}H NMR spectroscopy for any host-guest interaction with these anions. Rather there was formation of precipitation with time which caused a strong reduction in NMR signal intensities. It is unclear if a simple anion exchange is responsible or if there are slow reactions involving the 2,2'-bpz ligands. Nucleosides such as CMP^- and TMP^- neither led to changes in chemical shifts, nor to formation of precipitation from solution. These findings permit the conclusion that none of the above-mentioned anions do engage in host-guest interactions with Pt_4.

Considering the hydrophobic interior of the Pt_4 box, and the potential of π-π interactions that 2,2'-bpz could become engaged in, terephthalate was selected as the next anion. It was anticipated that the benzene ring could interact with the hydrophobic pyrazine rings, while the two carboxylate groups could be exposed outwards to have the opportunity to interact with solvent molecules by hydrophilic and dipole-ion forces.

Changes in chemical shifts of 2,2'-bpz and guest resonances were indeed observed upon adding terephthalate to a Pt_4 solution (D_2O, pD 6.7) (Figure 9). Addition of increasing amounts of terephthalate to a solution of Pt_4 resulted in a major downfield shift of the aromatic proton of terephthalate, a moderate upfield shift of the H(3) resonance of 2,2'-bpz, as well as minor upfield shifts of H(5) and H(6) resonances. As to the terephthalate resonance, it is highest

upfield relative to the free species when present in low concentration, hence when largely bonded to the host. The upfield shift then is consistent with stacking. The effect on H(3) is largest for the host compound. Job plots established the stoichiometry of the host-guest complex as 1:2 (host : guest) as seen from Figure 10.[6] The origin of the bump in the curve of the Job plot is unclear at present. However, similar features have been observed before,[10] indicating that they are by no means unique. The association constant was determined from the dependencies of the H(3) resonance shifts of the host molecules and the ratio of the guest/host concentration (Figure 11). Appling the EQNMR programme,[11] an overall binding constant of β_{12} = 3.0 ± 0.9 M^{-2} is obtained for the stepwise formation of the 1:2 complex (see Appendix).

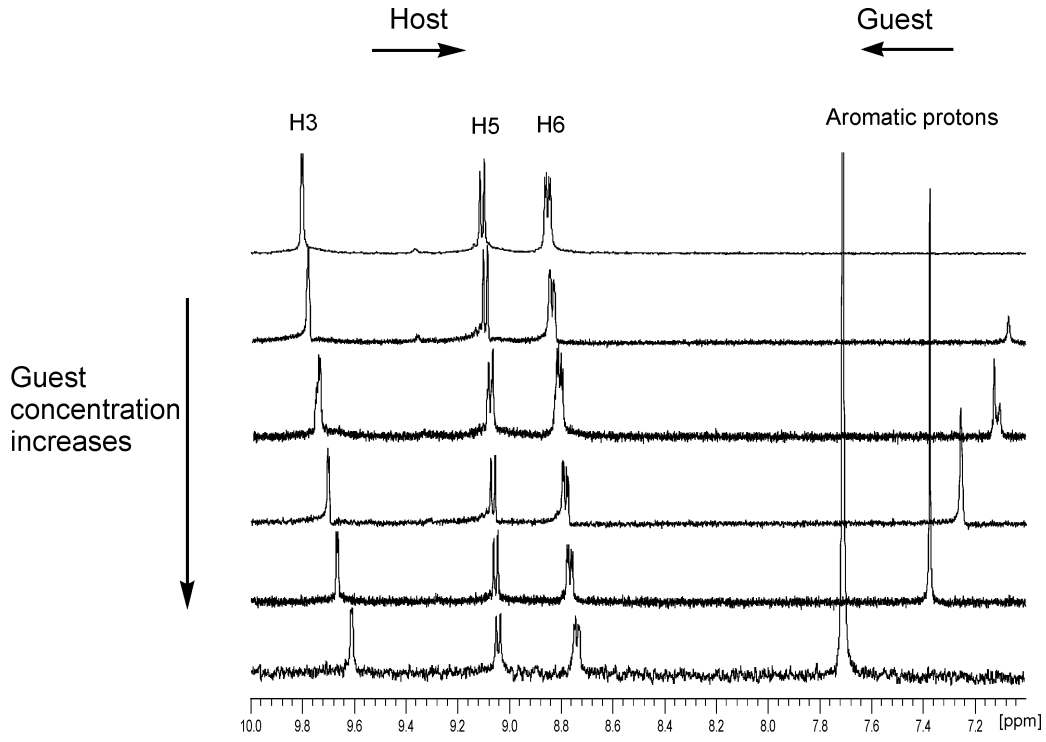

Figure 9. ^{1}H NMR spectra (D_2O, pD 6.7) of equilibrium mixtures of host complex Pt_4 and guest terephthalate. Increasing amounts of terephthalate relative to Pt_4 result in minor upfield shift of proton resonances of Pt_4 and moderate downfield shifts of the aromatic protons of terephthalate.

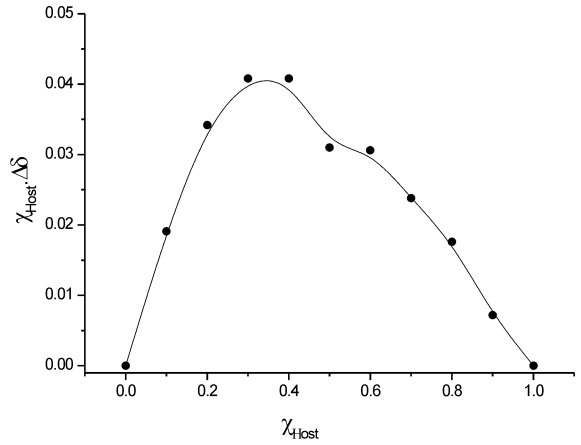

Figure 10. Job plot for the interaction of Pt_4 and terephthalate.

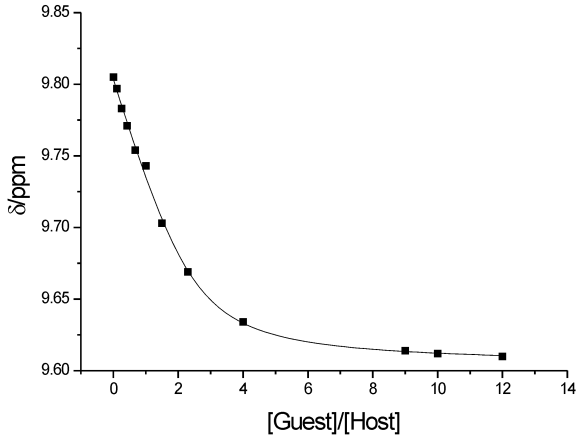

Figure 11. Dependence of H(3) chemical shift of 2,2'-bpz from [Guest]/[Host] ratio. From this curve, an overall binding constant β_{12} = 3.0 ± 0.9 M^{-2} was calculated.

Analogous host-guest interaction studies were also performed with [{*cis*-$Pt(NH_3)_2$(2,2'-bpz-*N4,N4'*)}$_3$]$^{6+}$ (Pt_3) and terephthalate. The changes of the chemical shifts were similar except that the interaction is weaker (Figure 12). The stoichiometry of the complex formed from Pt_3 and terephthalate is likewise 1:2, established by a Job plot (Figure 13).[6] The overall association constant is calculated from the EQNMR programme as 1.8 ± 0.2 M^{-2} (Figure 14).

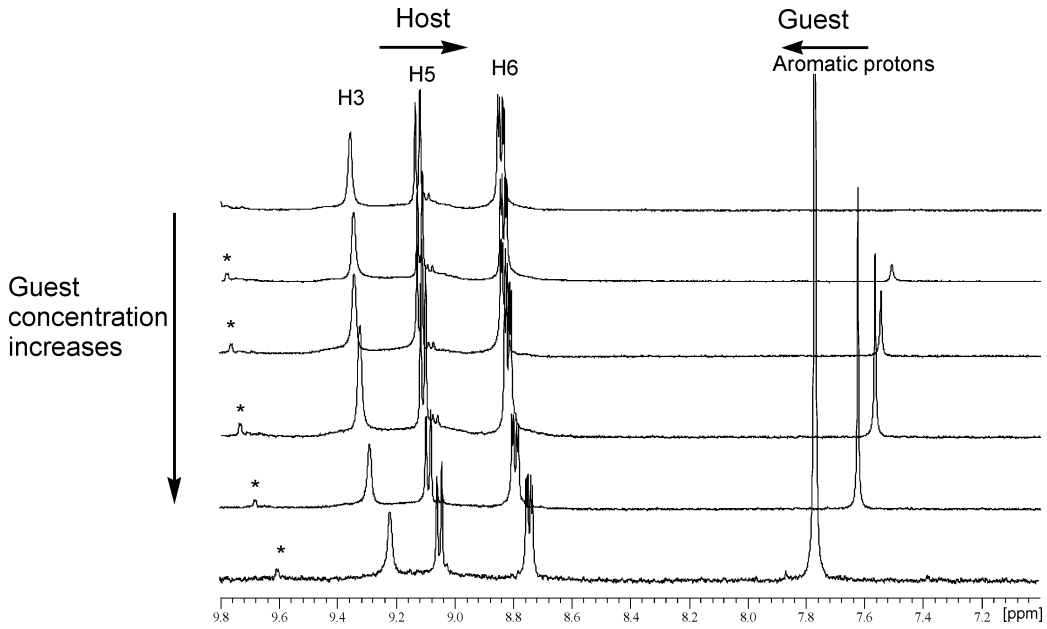

Figure 12. ^{1}H NMR spectra (D_2O, pD 6.5) of equilibrium mixtures of host complex Pt_3 and terephthalate. * is the unpurity of compound Pt_4.

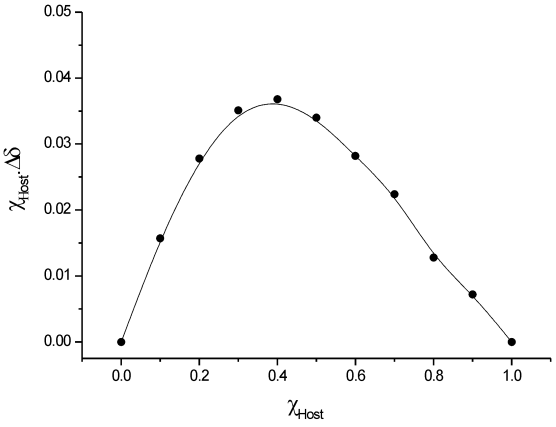

Figure 13. Job plot for the interaction of Pt_3 and terephthalate.

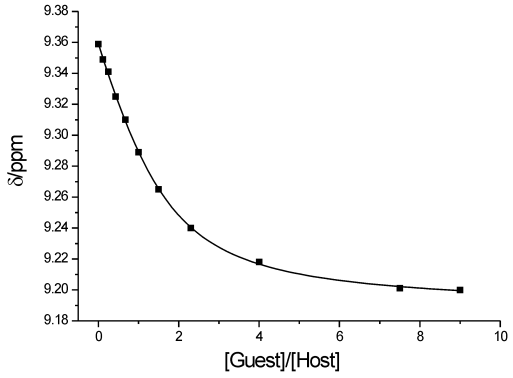

Figure 14. Dependence of H(3) chemical shift of 2,2'-bpz from [Guest]/[Host] ratio. From this curve, an overall binding constant β_{12} = 1.8 ± 0.2 M^{-2} was determined.

3.2 Discussion

In both cases low overall binding constants with anions are obtained in the solvent water. This is not unexpected considering the fact that the anions are strongly hydrated and that the cavities of the host molecules are likewise expected to contain water molecules and NO_3^- anions.[12] With +12 charged Pt_3Pd_3 complexes of 2,2'-bpz association constants with inorganic anions are of similar magnitude, except for SO_4^{2-}, which binds more efficiently.[13]

The 1:2 (host to guest) stoichiometry of the Pt_4/terephthalate system suggests that a pair of stacked terephthalate ions enters into the cavity of Pt_4. In fact, the available space (viz. Pt···Pt distance minus thickness of 2,2'-bpz ligands, hence ca. 9.7 Å – 2(1.7 Å) = 6.3 Å) is just sufficient for a pair of aromatic rings. The carboxylate functions could then extend into the solvent and could become hydrated. A similar π stacking phenomena was observed by Liu et al. with two 1,10-phenanthrolinium cations inside a molecular capsule.[14]

Pt_3 can adopt two different 3D structures, namely all-*trans* and all-*cis*, due to the flexibility of bpz ligands, as first detected by R. D. Schnebeck et al. in our group. The all-*trans* compound is a triangle with Pt···Pt distances of 9.4 Å, while the all-*cis* compound looks more like a vase or a double cone with Pt···Pt distances of 7.7-8.0 Å. In solution, the existence of the both rotamers can lead to a quite complicated environment for guest molecules.

4 Summary

Pd_3(1-MeC$^-$)$_3$ with its double cone structure functions as a halide anion receptor in DMSO-d_6 solution as deteced by ^{1}H NMR spectroscopy. The proton of N(4) of 1-MeC$^-$ is most sensitive to the concentration of the halide anions, which suggests that the halide anions approach the double cone in a specific direction. A comparison of the association constants for chloride, bromide and iodide reveals that iodide binds with the lowest affinity. Most likely this is due to the size of iodide, which is too large to be accommodated in the lower cone. Attempts to verify a defined host-guest interaction between Pd_3(1-MeC$^-$)$_3$ and amino acids in water failed.

The cyclic tetramer Pt_4 and the cyclic trimer Pt_3 were studied with regard to their affinities for $[PtCl_4]^{2-}$, $[PdCl_4]^{2-}$, $[Pt(CN)_4]^{2-}$, CMP^-, TMP^- and terephthalate. With the exception of terephthalate, no evidence for host-guest interaction was found. The stoichiometry in the latter case, established by a Job plot analysis, is 1:2 of host per guest. However, the overall association constants in water are quite small for both Pt_4 and Pt_3, indicating weak host-guest interactions in this solvent.

References

[1] (a) Lehn, J.-M. *Supramolecular Chemistry: Concepts and Perspectives* (VCH, New York), **1995**. (b) Service, R. F.; Szuromi, P.; Uppenbrink, J. *Science* **2002**, *295*, 2395. (*Supramolecular Chemistry and Self-Assembly, Special Issue)*. (c) Lindoy, L. F.; Atkinson, I. In *Self-Assembly in Supramolecular Systems (Monographs on Supramolecular Chemistry)*; Stoddart, J. F., Ed.; The Royal Society of Chemistry: London, **2000**. (d) Fujita, M. *Molecular Self-Assembly Organic versus Inorganic Approach (Structure and Bonding)*; Springer: New York, **2000**; Vol. 96. (e) Sauvage, J.-P. *Transition Metals in Supramolecular Chemistry, Perspectives in Suppramolecular Chemisty*; Wiley: New York, **1999**; Vol. 5. (f) Lehn, J.-M. *Templating, Self-Assembly, and Self-organization.* In *Comprehensive Supramolecular Chemistry*; Sauvage, J.-P., Hosseini, M. W., Eds.; Pergamon: New York, **1996**.

[2] (a) Chen, H.; Ogo, S.; Fish, R. H. *J. Am. Chem. Soc.* **1996**, *118*, 4993. (b) Longato, B.; Pasquato, L.; Mucci, A.; Schenetti, L.; Zangrando, E. *Inorg. Chem.* **2003**, *42*, 7861. (c) Zhu, X.; Rusanov, E.; Kluge, R.; Schmidt, H.; Steinborn, D. *Inorg. Chem.* **2002**, *41*, 2667. (d) Smith, D. P.; Baralt, E.; Morales, B.; Olmstead, M. M.; Maestre, M. F.; Fish, R. H. *J. Am. Chem. Soc.* **1992**, *114*, 10647. (e) Longato, B.; Montagner, D.; Zangrando, E. *Inorg. Chem.* **2006**, *45*, 8179. (f) Yamanari, K.; Ito, R.; Yamamoto, S.; Fuyuhiro, A. *Chem. Commun.* **2001**, 1414. (g) Yamanari, K.; Ito, R.; Yamamoto, S.; Konno, T.; Fuyuhiro, A.; Kobayashi, M.; Arakawa, R. *Dalton Trans.* **2003**, 380. (h) Schenetti, L.; Bandoli, G.; Dolmella, A.; Trovó, G.; Longato, B. *Inorg. Chem.* **1994**, *33*, 3169. (f) Roitzsch, M.; Lippert, B. *Angew. Chem. Int. Ed.* **2006**, *45*, 147.

[3] (a) Rother, I. B.; Willermann, M.; Lippert, B. *Supramol. Chem.* **2002**, *14*, 189. (b) Purohit, C. S.; Verma, S. *J. Am. Chem. Soc.* **2006**, *128*, 400. (c) Janzen, D. E.; Patel, K. N.; VanDerveer, D. G.; Grant, G. J. *Chem. Commun.* **2006**, 3540.

[4] (a) Schnebeck, R.-D.; Freisinger, E.; Glahé, F.; Lippert, B. *J. Am. Chem. Soc.* **2000**, *122*, 1381. (b) Stang. P. J.; Persky, N. E.; Manna, J. *J. Am. Chem. Soc.* **1997**, *119*, 4777. (c) Matsumoto, N.; Motoda, Y.; Matsuo, T.; Nakashima, T.; Re, N.; Dahan, F.; Tuchagues, J.-P. *Inorg. Chem.* **1999**, *38*, 1165.

[5] Fujita, M.; Tominaga, M.; Hori, A.; Therrien, B. *Acc. Chem. Rev.* **2005**, *38*, 371. and references therein.

[6] Connors, K. A. *Binding Constants: The Measurement of the Complex Stability*, Wiley, New York, **1987**.

[7] Chen, H.; Maestre, M. F.; Fish, R. H. *J. Am. Chem. Soc.* **1995**, *117*, 3631.

[8] Smith, D. P.; Baralt, E.; Morales, B.; Olmstead, M. M.; Maestre, M. F.; Fish, R. H. *J. Am. Chem. Soc.* **1992**, *114*, 10647.

[9] Smith, D. P.; Kohen, E.; Maestre, M. F.; Fish, R. H. *Inorg. Chem.* **1993**, *32*, 4119.

[10] Kruppa, M.; Mandl, C.; Miltschitzky, S.; König, B. *J. Am. Chem. Soc.* **2005**, *127*, 3362.

[11] Hynes, M. J. *J. Chem. Soc., Dalton Trans.* **1993**, 311.

[12] Steed, J. W.; Atwood, J. L. *Supramolecular Chemistry*, (Wiley, New York), **2000**.

[13] Schnebeck, R.-D.; Freisinger, E.; Lippert, B. *Angew. Chem. Int. Ed.* **1999**, *38*, 168.

[14] Liu, Y.; Guo, D. S.; Zhang, H. Y.; Ding. F.; Chen, K.; Song, H. B. *Chem. Eur. J.* **2007**, *13*, 466.

Chapter VI

DNA Condensation and Aggregation with a Pd^{II} 1-Methylcytosine Complex

1 Introduction

Metal complexes such as Cisplatin, interacting with DNA through formation of metal-ligand bonds, have been extensively studied. In all these cases, a clear focus has been on binding to N(7) sites of guanine and adenine nucleobases.[1] In contrast, non-covalent binding of metal complexes to DNA is a less well-developed area and has primarily centered around ruthenium polypyridyl complexes that have planar intercalating units.[2,3]

Supramolecular chemistry provides an excellent methodology for designing noncovalent DNA recognition agents.[4] This is so not only because of the cationic charge the metallo-centers impart, and which will afford an electrostatic interaction to the noncovalent binding to anionic DNA, but also because it is possible to take advantage of the shape. For example, a tetracationic triple helical cylinder $[Fe_2(C_{25}H_{20}N_4)_3]^{4+}$ can lead to remarkable effects on DNA structure, as observed by CD, LD, and AFM. The intermolecular NOEs between the complex and DNA confirm that the cylinder can bind to DNA in the major groove.[5] Moreover, this metal helicate is capable of binding to the central hydrophobic cavity of a DNA three-way junction.[6] This finding was interpreted in terms of the metal helicate being able to recognize a naturally occurring three-way junction and bind to it. It opens up an entirely new range of possible DNA-binding therapeutic agents based on metal complexes.[7]

DNA condensation occurs naturally, among others, in virus capsids and sperm cells.[8] It is postulated that condensation occurs when 90% of the negative charge of DNA from the phosphate backbone is neutralized.[9] However, the electrostatic effect has not been found to be sufficient to completely account for the condensation forces.[10] DNA condensation is accomplished also *in vitro* by a variety of compounds including multivalent cations, such as $[Co(NH_3)_6]^{3+}$ [11]and protonated polyamines such as spermidine.[12]

The aim of this work was to investigate the interaction between $[\{Pd(1\text{-}MeC^{-}\text{-}N3,N4)(tmeda)\}_3](ClO_4)_3 \cdot 5.5H_2O$ (**I-7**, $Pd_3(1\text{-}MeC^{-})_3$) and DNA.

2 Atomic Force Microscopy

Atomic Force Microscopy (AFM) is the method which allows the direct observation of interactions of compounds with individual DNA molecules without stains and under natural conditions with simple sample preparation. It can measure the three-dimensional surface profile, as opposed to just providing a two-dimensional image. The main disadvantages of AFM are its limited image size, inability to detect chemical bonds, and requirement that sample molecules are securely immobilized on a solid surface.

3 Results and Disscusions

3.1 AFM study of complex-DNA adducts

The initial research work was performed following the accidental observation of DNA precipitation with a small amount of $Pd_3(1\text{-}MeC^{-})_3$ compound. Applying the AFM technique, DNA compact pictures were observed (Figure 1). The concentration of DNA solution was 0.01 mg/mL, while the concentration of the $Pd_3(1\text{-}MeC^{-})_3$ complex was 0.02 mg/mL, with a ratio of DNA-bp per metal

complex of 10:1. Under these conditions, the $Pd_3(1\text{-}MeC^-)_3$ complex condensed and aggregated the linear DNA (5690 bp) into molecular clusters, which is observed all over the mica surface. Obviously, this concentration was too high to study the interaction between the complex and DNA.

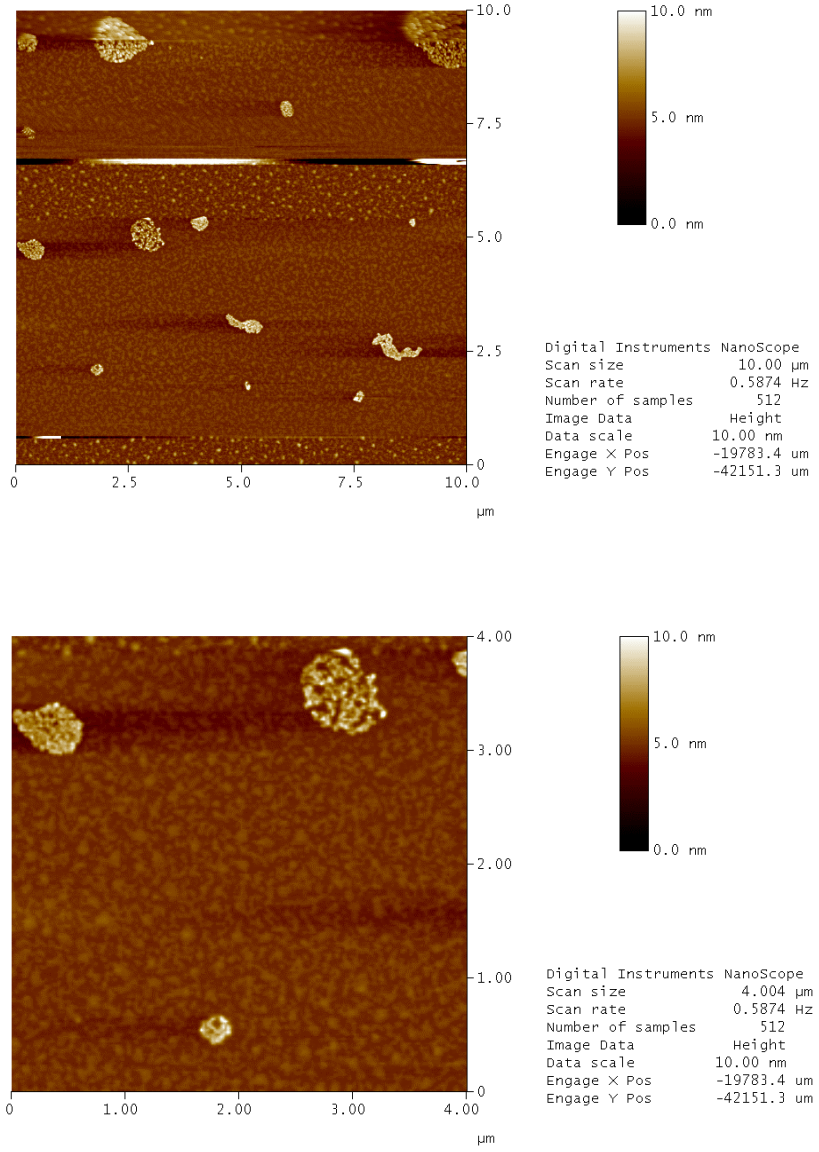

Figure 1. AFM images of linear DNA (5690 bp) on mica with $Pd_3(1\text{-}MeC^-)_3$ (DNA bp : $Pd_3(1\text{-}MeC^-)_3$ complex ratio is 10:1)

Gel electrophoresis and UV-vis spectroscopy of the $Pd_3(1\text{-}MeC^-)_3$-DNA adduct in different concentration ratios were performed separately for long linear DNA (~20,000 bp) and short linear DNA (~500 bp). Normally, both methods can assist to find out the most suitable concentration to perform the AFM. However, applying UV-vis spectroscopy, the $Pd_3(1\text{-}MeC^-)_3$ compound's absorption regions ($1\text{-}MeC^-$ ligands) are overlapping with those of DNA. Applying gel electrophoresis, compound-DNA adducts in different ratios were observed at the end of the gel, which could be due to the compound-DNA compacted to a big volume. Thus, both of these analytical techniques have the same disadvantages of averaging the results of numerous molecules in a sample instead of looking at interactions between individual molecules and of requiring interpretation of the interactions from indirect evidence.

Without the assistance of UV-vis spectroscopy and gel electrophoresis, the concentration ratio was tested by directly applying AFM. At a concentration of DNA of 0.001mg/mL and a concentration of $Pd_3(1\text{-}MeC^-)_3$ of $1.5*10^{-8}$ mg/mL, two interesting images were obtained (Figure 2).

The measured height of the DNA is ~1.0 nm. The height of the coiling part is ~2.5 nm, which thus reveals the phenomenon called "coil-globule" transition.[13] It is known that AFM measurements of DNA give strand heights that are lower than the theoretical height of DNA. A recent study by Moreno-Herrero et al.[14] explored this anomaly and concluded that the molecules may be embedded in a salt layer covering the mica surface which could account for part of the height difference, while the force exerted by the oscillating tip during imaging could further distort the apparent height.[15]

Figure 2 reveals that the $Pd_3(1\text{-}MeC^-)_3$ compound condenses and aggregates the DNA into intermolecular clusters, i.e. the binding appears to be cooperative with clusters observed in the presence of uncoiled DNA strands. These images

are very similar to those previously reported for the interaction of $[Co(NH_3)_6]^{3+}$ with DNA.[5]

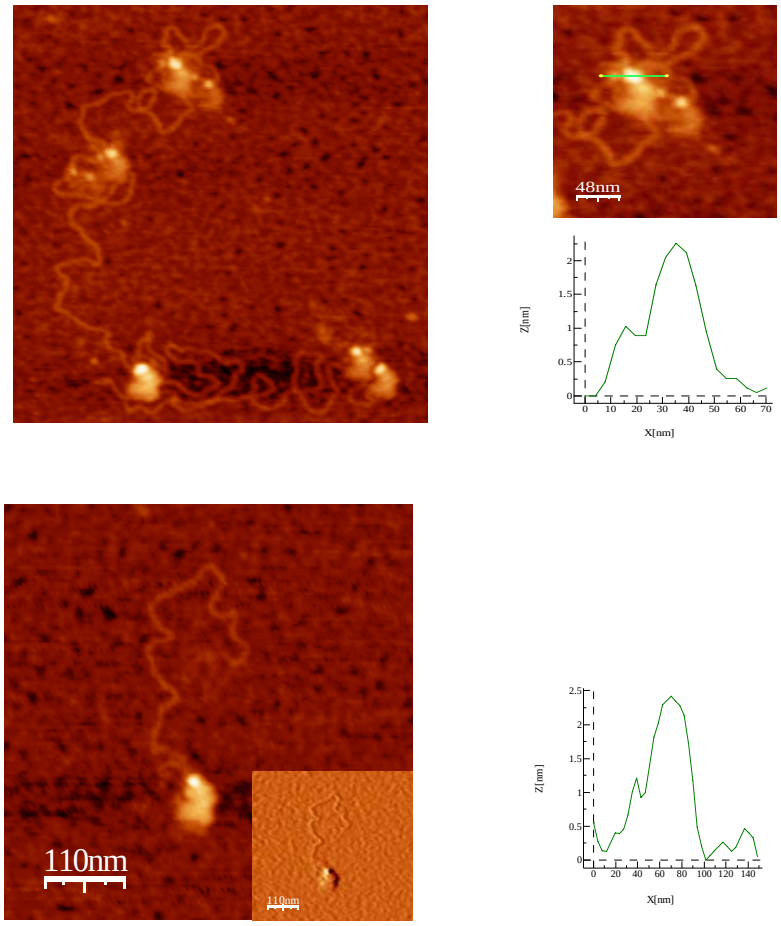

Figure 2. DNA coiling by $Pd_3(1\text{-}MeC^-)_3$ was found with DNA (0.001 mg/mL) in the presence of $Pd_3(1\text{-}MeC^-)_3$ ($1.5*10^{-8}$ mg/mL)

3.2 NMR study of complex-oligonucleotide adducts

Preliminary work was performed by applying ^1H NMR spectroscopy to investigate the interaction between the single stranded DNA oligonucleotide, 5'-d(TAGGGTTA) (S-8er), and $Pd_3(1\text{-}MeC^-)_3$. The concentration of the S-8er was 0.295 mM. Under these conditions the S-8er is a single strand.[16]

The NMR spectra, which are given in Figure 3, represent the solution behavior

of S-8er upon the addition of the $Pd_3(1\text{-}MeC^-)_3$ compound. The chemical shifts of the resonances of S-8er are listed in Table 1.

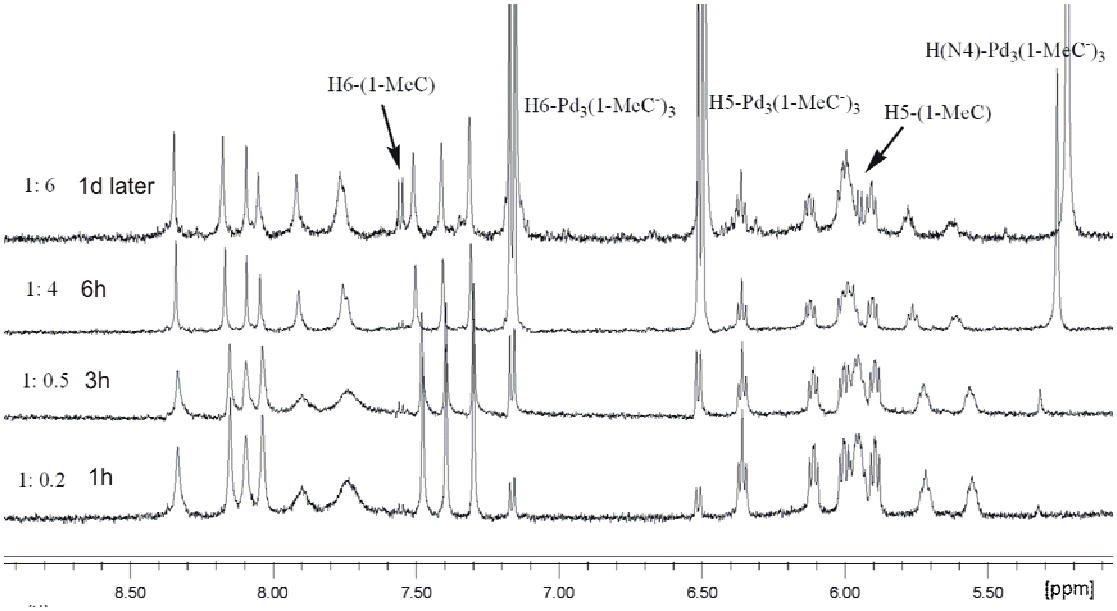

Figure 3. Lowfield section of ^1H NMR spectra (D_2O pD 6.8) obtained upon mixing $Pd_3(1\text{-}MeC^-)_3$ and S-8er at different ratios. These spectra were obtained after 1 h, 3 h, 6 h and 1 day.

Table 1. The aromatic protons resonances of the nucleobases of S-8er ($T^1AGG^4GTTA^8$) in D_2O, pD 6.8 and in the presence of 6 equivalents of $Pd_3(1\text{-}MeC^-)_3$.

Singlet	A2-H^8	A8-H^8	G3-H^8	A2-H^2	A8-H^2	G4-H^8	G5-H^8	T6-H^6	T7-H^6	T1-H^6
δ/ppm	8.33	8.15	8.09	8.04	7.89	7.74	7.71	7.48	7.40	7.30
6eq	8.35	8.18	8.10	8.06	7.92	7.77	7.76	7.52	7.42	7.32

A comparison of the resonances of S-8er without $Pd_3(1\text{-}MeC^-)_3$ and with 6 equivalents of $Pd_3(1\text{-}MeC^-)_3$ present, reveals hardly any changes of chemical shifts of the aromatic protons. However, the solution studies provide the clear information that the $Pd_3(1\text{-}MeC^-)_3$ complex is stable in the presence of this oligonucleoside for at least one day. After long incubation times, free 1-MeC is observed in the ^1H NMR spectra (see Figure 3).

The fact that ^1H NMR spectra of the single-stranded octamer do not reveal any distinct changes does not rule out an interaction with DNA, in principle. One possibility is that the single-stranded 8-mer is too short to coil around the metal complex. Another possibility is that the interaction happens just for the double-stranded DNA, or some special sequences of DNA.

4. Summary

DNA condensation and aggregation was observed with the $Pd_3(1\text{-}MeC^-)_3$ complex applying Atomic Force Microscopy. In contrast, UV-visible titration and gel electrophoresis experiments did not permit an unambiguous proof for an interaction between the $Pd_3(1\text{-}MeC^-)_3$ complex and DNA. Attempts to determine local aspects of the interaction between the single stranded DNA oligonucleotide 5'-d(TAGGGTTA) with $Pd_3(1\text{-}MeC^-)_3$ were likewise unsuccessful but provided clear evidence that the $Pd_3(1\text{-}MeC^-)_3$ complex is stable in the presence of this oligonucleotide for at least one day. The interaction between DNA and the $Pd_3(1\text{-}MeC^-)_3$ complex requires additional studies to be fully understood.

References

[1] Lippert, B. ed. *Cisplatin, Chemistry and Biochemistry of a Leading Anti-Cancer Drug* (Wiley-VCH, Weinheim, Germany), **1999** (and references therein).

[2] Coggan, D. Z.; Haworth, I. S.; Bates, P. J.; Robinson, A.; Rodger, A. *Inorg. Chem.* **1999**, *38*, 4486.

[3] Erikkila, K. E.; Odom, D. T.; Barton, J. K. *Chem. Rev.* **1999**, *99*, 2777.

[4] Schoentjes, B.; Lehn, J.-M. *Helv. Chim. Acta* **1995**, *79*, 1.

[5] Hannon, M. J.; Moreno, V.; Prieto, J. M.; Moldrheim, E.; Sletten, E.; Meistermann, I.; Isaac, C. J.; Sanders, K. J.; Rodger, A. *Angew. Chem. Int. Ed.* **2001**, *40*, 880.

[6] Oleksi, A.; Blance, A. G.; Boer, R.; Usón, I.; Aymamí, J.; Rodger, A.; Hannon, M. J.; Coll, M. *Angew. Chem. Int. Ed.* **2006**, *45*, 1227.

[7] Müller, J.; Lippert, B. *Angew. Chem. Int. Ed.* **2006**, *45*, 2.

[8] Bloomfield, V. A. *Biopolymers* **1998**, *44*, 269.

[9] Wilson, R. W.; Bloomfield, V. A. *Biochemistry* **1979**, *18*, 2192.

[10] Conwell, C. C.; Hud, N. V. *Biochemistry* **2004**, *43*, 5380.

[11] Arscott, P. G.; Ma, C.; Wenner, J.; Bloomfield, V. A. *Biopolymers* **1995**, *36*, 345.

[12] Fang, Y.; Hoh, J. H. *J. Am. Chem. Soc.* **1998**, *120*, 8903.

[13] Fink, T. R.; Crothers, D. M. *Biopolymers* **1968**, *6*, 863-871.

[14] Moreno-Herrero, F.; Colchero, J.; Baro, A. M. *Ultramicroscopy* **2003**, *96*, 167.

[15] Allen, M. J.; Hud, N. V.; Balooch, M.; Tench, R. J.; Siekhaus, W. J.; Balhorn, R. *Ultramicroscopy* **1992**, *42*, 1095.

[16] Lax, P. *Dissertation*, University of Dortmund, **2006**.

D SUMMARY

English Version

This thesis is dealing with metal compounds and interactions relevant to both supramolecular chemistry with all its possible architectures, built of metal ions and N-heterocyclic ligands, and to chemical biology. It has its roots in the interest in a detailed understanding of interactions of antitumor active complexes of platinum with nucleobases of DNA, and consequently deals (in part) with model nucleobase complexes. More recently, this field expanded into interactions of discrete multinuclear metal-nucleobase complexes with anions (host-guest chemistry) and - in a sense closing the circle - to interactions between such multinuclear complexes and DNA.

— Molecular architecture

Square-planar *cis*-$Pd^{II}L_2$ (L = bpy and bipzp) entities form, with deprotonated 1-methylcytosine anions (1-MeC^-), in most cases *head-tail* dimer structures. These *head-tail* dimers containing two identical 1-MeC^- ligands via *N3,N4-syn*-bridging modes display the phenomenon of chirality. Depending on the spatial disposition of the two ligands, the enantiomers are named Λ-form or Δ-form, both of which are present in the crystal lattice in a 1:1 ratio. A convention is proposed to differentiate the two forms.

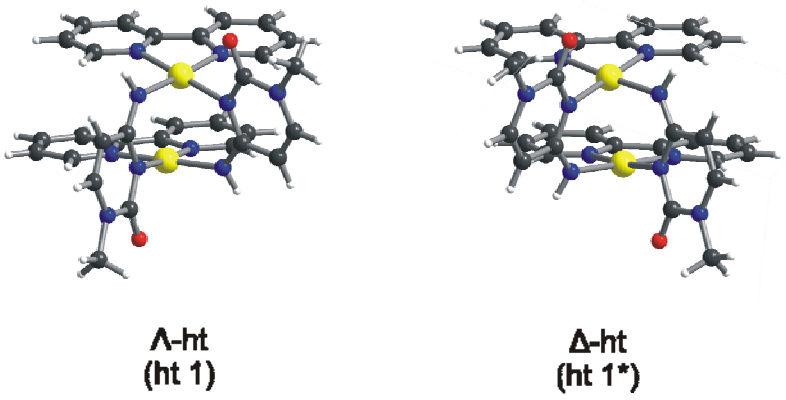

Two enantiomers of head-tail dimer $[\{Pd(1\text{-}MeC^-\text{-}N3,N4)(bpy)\}_2]^{2+}$ ***(I-1)***

During the analysis of the X-ray crystal structures of two *head-tail* dimers, it became obvious that increasing the steric hindrance of the co-ligand (L) increases the distance between the metal entities. By applying the Pd^{II}(tmeda) (tmeda: *N,N,N',N'*-tetramethylethylenediamine) entity and reacting it with 1-MeC$^-$, the system "escapes" to a trinuclear cyclic complex [{Pd(1-MeC$^-$-*N3,N4*)(tmeda)}$_3$](ClO$_4$)$_3$·5.5H$_2$O (**I-7**) containing 1-MeC$^-$ ligands in *N3,N4-anti*-bridging modes. The Pd···Pd distances are about 5.2 Å. This cyclic complex has the shape of a double cone.

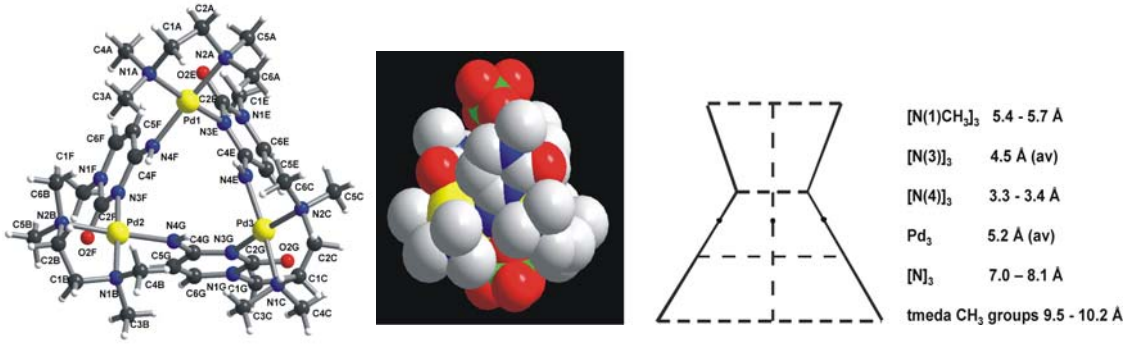

*Trinuclear cation [{Pd(1-MeC$^-$-N3,N4)(tmeda)}$_3$]$^{3+}$ (**I-7**) displaying a double cone structure*

In an extension of this work, a similar trinuclear cyclic complex [{Pd(Cytd$^-$-*N3,N4*)(tmeda)}$_3$](ClO$_4$)$_3$·6H$_2$O (**I-9**) containing cytidine with identical *N3,N4-anit*-bridging modes was likewise obtained. Compared to the 1-MeC$^-$ complex (**I-7**), the "top" of the double cone structure is substantially enlarged by the ribose groups, however.

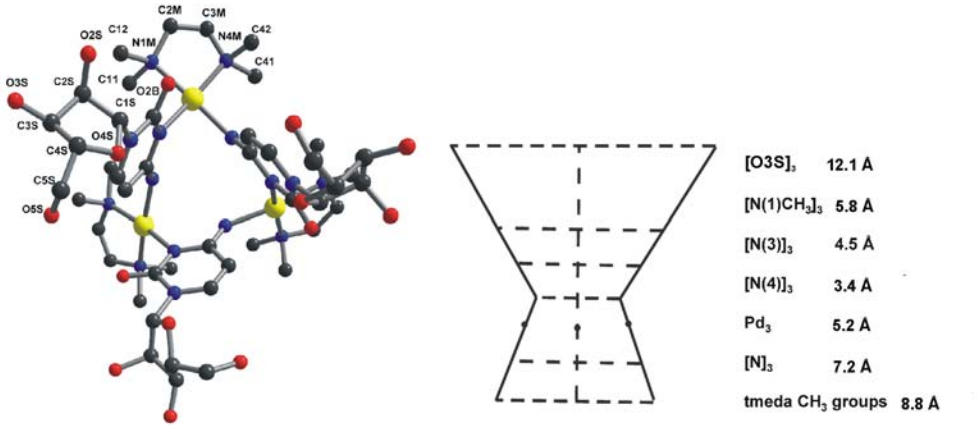

*Trinuclear cation [{Pd(Cydt$^-$-N3,N4)(tmeda)}$_3$]$^{3+}$(**I-9**) with double cone structure*

2-Aminopyridine as a ligand for Pd^{II} was selected because of the similar structure but different electron distribution as compared to 1-methylcytosine, i.e. the lone electron pair of the amino group is located at the exocyclic N atom rather than being delocalized into the pyridine ring as in cytosine residues. The reaction between the Pd^{II}(tmeda) entity and 2-aminopyridine was performed under similar conditions with the aim of forming a *N1,N2*-bridged cyclic structure. However, an almost equilateral metal triangular structure, $[\{(tmeda)Pd(\mathit{N2}\text{-}ampy^{-}\text{-}\mathit{N1})\}_2Ag]^{3+}$ (**II-5**), was obtained, in which two Pd^{II}(tmeda) entities bridge via two N2 donor atoms and Ag^{+} is bonded to two N1 donor atoms.

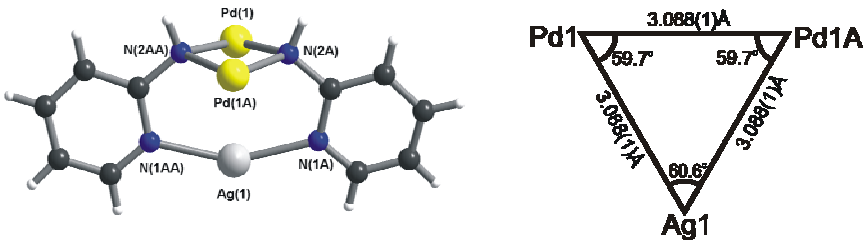

*Molecular Pd_2Ag triangle of $[\{(tmeda)Pd(N2\text{-}ampy^{-}\text{-}N1)\}_2Ag]^{3+}$ (**II-5**)*

Another cyclic triangle structure $[\{Pt(tmeda)(pz)\}_3](NO_3)_3\cdot(H_2O)_{2.25}$ (**III-2**) was obtained by mixing the Pt^{II}(tmeda) entity with pyrazine. The formation is unexpected considering the "molecular library approach" which predicts a molecular box with two ditopic 90^{o} and 180^{o} building blocks. The reason is not clear, but it is tentatively believed that the steric repulsion between the methyl groups of the tmeda ligands and the pyrazine ligands is responsible for the fact that the "expected" square is not realized.

Furthermore, the reaction between *cis*-$Pt^{II}(NH_3)_2$, a 90^{o} angular fragment, and 2,2'-bipyrazine was performed. A square complex $[\{cis\text{-}Pt(NH_3)_2(2,2'\text{-}bpz\text{-}\mathit{N4,N4'})\}_4](NO_3)_8\cdot 4H_2O$ (**IV-1**) and a triangle complex $[\{cis\text{-}Pt(NH_3)_2(2,2'\text{-}bpz\text{-}\mathit{N4,N4'})\}_3](NO_3)_6$ (**IV-2**) were detected by ^{1}H NMR spectroscopy in the solution. The square complex (**IV-1**) was successfully isolated and its structure was confirmed by X-ray crystallography. In aqueous solution the square and the triangle exist in an equilibrium.

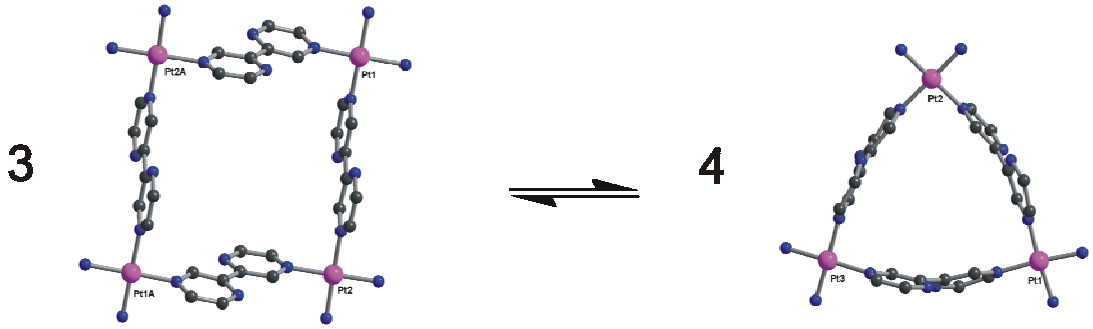

*A square-triangle equilibrium of [{cis-Pt(NH$_3$)$_2$(2,2'-bpz-N4,N4')}$_4$]$^{8+}$ (**IV-1**) and [{cis-Pt(NH$_3$)$_2$(2,2'-bpz-N4,N4')}$_3$]$^{6+}$(**IV-2**)*

— Host-guest chemistry

Three of the compounds mentioned above were chosen to study possible host-guest interactions in solution, namely Pd$_3$(1-MeC$^-$)$_3$ (**I-7**), Pt$_4$(**IV-1**) and Pt$_3$(**IV-2**).

In DMSO-*d*$_6$, Pd$_3$(1-MeC$^-$)$_3$ (**I-7**) interacts with halide anions, as demonstrated by ^{1}H NMR spectroscopy. Specifically, it was found that the N(4)H resonance of the cytosinate ligand is sensitive to the presence of halide anions, being shifted to lower field with increasing concentrations of the guest ions. This suggests that these anions approach the cationic host from the "lower" cone. A quantitative determination of the interaction between (**I-7**) and F$^-$ was hampered by the hygroscopic nature of the fluoride salt employed and the sensitivity of the N(4)H resonance toward the presence of water. For the three other halide ions weak binding was found (Table), which in addition suggests a clear dependence on the size of the anion, as expected.

Table: Association constants for halide ions with Pd$_3$(1-MeC$^-$)$_3$ in DMSO

	Cl$^-$	**Br$^-$**	**I$^-$**
$\Delta\delta_{max}$/ppm	1.75	1.37	0.96
***K*/M^{-1}**	47 ± 15	56 ± 13	6 ± 1
log *K*	1.7(2)	1.8(1)	0.78(9)

The cyclic tetramer Pt_4 (**IV-1**) and the trimer Pt_3 (**IV-2**) displayed encapsulation of terephthalate anions in water. The 1:2 stoichiometry of the Pt_4/terephthalate system suggests that a pair of stacked terephthalate ions enters the cavity of Pt_4. The available space inside Pt_4 is just sufficient to accommodate a pair of aromatic rings. In addition, the hydrophilic carboxylate functions can extend into the solvent. Pt_3, due to its potential of existing in different conformations, provides a quite versatile environment for guest molecules. The 1:2 stoichiometry of the Pt_3/terephthalate could possibly imply that two terephthalate ions enter from both sides into the cavity of Pt_3. In both cases low overall binding constants are observed. This is not unexpected considering the fact that the anions are strongly hydrated and that the cavities of the host molecules are likewise expected to contain water molecules and nitrate anions, which compete with the anions added.

— Metal complex and DNA interaction

DNA condensation and aggregation was observed with the $Pd_3(1\text{-}MeC^-)_3$ complex applying Atomic Force Microscopy. In contrast, UV-visible titration and gel electrophoresis experiments did not permit an unambiguous proof for an interaction between the $Pd_3(1\text{-}MeC^-)_3$ complex and DNA. Attempts to determine local aspects of the interaction between the single stranded DNA oligonucleotide 5'-d(TAGGGTTA) with $Pd_3(1\text{-}MeC^-)_3$ were likewise unsuccessful but provided the clear information that the $Pd_3(1\text{-}MeC^-)_3$ complex is stable in the presence of this oligonucleotide for at least one day. The interaction between DNA and the $Pd_3(1\text{-}MeC^-)_3$ complex requires additional studies to fully understand it.

German Version

Diese Arbeit befasst sich mit Metallkomplexen und ihren Wechselwirkungen, die sowohl in der Supramolekularen Chemie (mit all ihren möglichen Architekturen aus Metallionen und Stickstoff-Heterozyklen als Liganden) als auch in der Chemischen Biologie relevant sind. Die Ursprünge dieser Arbeit liegen in dem Interesse, die Wechselwirkungen von antitumor-aktiven Komplexen des Platins mit Nukleobasen der DNA detailliert zu verstehen, und daher befasst sie sich (in Teilen) mit Komplexen von Modellnukleobasen. Dieses Gebiet wurde um das Themenfeld der Wechselwirkungen mehrkerniger Metall-Nukleobase-Komplexe mit Anionen (Wirt-Gast-Chemie) sowie mit DNA erweitert.

— Molekulare Architektur

Quadratisch-planare *cis*-$Pd^{II}L_2$ (L = bpy und bipzp) Einheiten bilden mit deprotoniertem 1-Methylcytosinat (1-MeC^-) in den meisten Fällen *head-tail*-Dimer-Strukturen. Diese *head-tail*-Dimere enthalten zwei identische über *N3,N4*-verbrückende 1-MeC^--Liganden und weisen das Phänomen der Chiralität auf. Abhängig von der räumlichen Orientierung der beiden Liganden entstehen so die Λ- und die Δ-Spezies. Beide Enantiomere treten im Kristallgitter im Verhältnis 1:1 auf. Eine Konvention zur Unterscheidung beider Spezies wird vorgeschlagen.

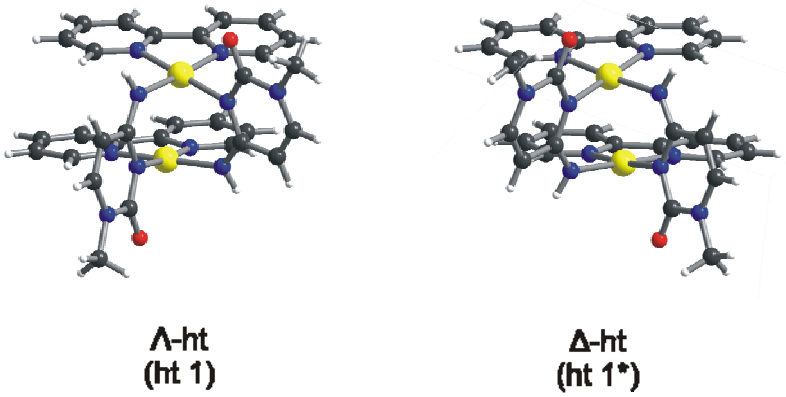

Zwei Enantiomere des head-tail-Dimers $[\{Pd(1\text{-}MeC^-\text{-}N3,N4)(bpy)\}_2]^{2+}$ ***(I-1)***

Während der Untersuchung der Kristallstrukturen der beiden *head-tail*-Dimere wurde deutlich, dass eine Erhöhung des sterischen Anspruchs der Koliganden (L) den Abstand zwischen den Metallzentren erhöht. Setzt man das Pd^{II}(tmeda)-Fragment (tmeda: *N,N,N',N'*-Tetramethylethylendiamin) mit 1-MeC^- um, so "weicht" das System in einen dreikernigen zyklischen Komplex [{Pd(1-MeC^--*N3,N4*)(tmeda)}$_3$](ClO_4)$_3$·5.5H_2O (**I-7**) aus, in dem die 1-MeC^--Liganden *N3,N4-anti*-verbrückend sind. Die Pd···Pd-Abstände betragen ca. 5.2 Å. Dieser zyklische Komplex hat die Gestalt eines Doppelkegels.

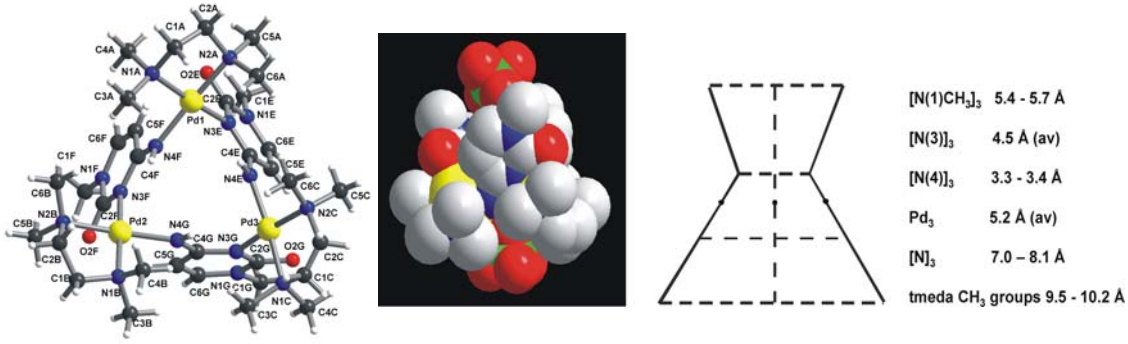

*Dreikerniges Kation [{Pd(1-MeC^--N3,N4)(tmeda)}$_3$]$^{3+}$ (**I-7**) mit der Gestalt eines Doppelkegels.*

Zudem wurde ein vergleichbarer dreikerniger zyklischer Komplex [{Pd($Cytd^-$-*N3,N4*)(tmeda)}$_3$](ClO_4)$_3$·6H_2O (**I-9**) erhalten, in dem das Cytidin in einem analogen *N3,N4-anti*-verbrückenden Koordinationsmodus vorliegt. Verglichen mit dem 1-MeC^--Komplex (**I-7**) ist hierin die "Spitze" des Doppelkegels durch die Ribose-Gruppen deutlich aufgeweitet.

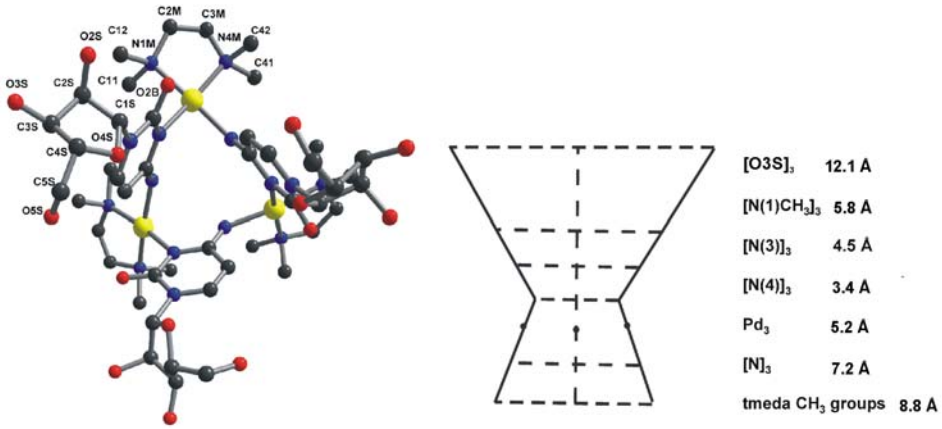

*Dreikerniges Kation [{Pd($Cydt^-$-N3,N4)(tmeda)}$_3$]$^{3+}$(**I-9**) mit der Gestalt eines Doppelkegels*

2-Aminopyridin wurde als Ligand für Pd^{II} ausgewählt, weil es eine mit 1-Methylcytosin vergleichbare Struktur aufweist, aber eine unterschiedliche Elektronendichteverteilung besitzt. 2-Aminopyridin weist ein freies Elektronenpaar am exozyklischen Stickstoffatom auf, während dieses Elektronenpaar in Cytosin-Derivaten in den Pyridin-Ring delokalisiert ist. 2-Aminopyridin wurde unter vergleichbaren Bedingungen mit Pd^{II}(tmeda) umgesetzt, um *N1,N2*-verbrückte zyklische Strukturen zu erhalten. Überraschenderweise wurde auf diesem Weg jedoch ein nahezu gleichschenkliges Dreieck erhalten, $[\{(tmeda)Pd(\mathit{N2}\text{-}ampy^{-}\text{-}\mathit{N1})\}_2Ag]^{3+}$ (**II-5**), in dem zwei Pd^{II}(tmeda)-Fragmente über zwei N2-Donoratome koordinieren und Ag^{+} an zwei N1-Atome bindet.

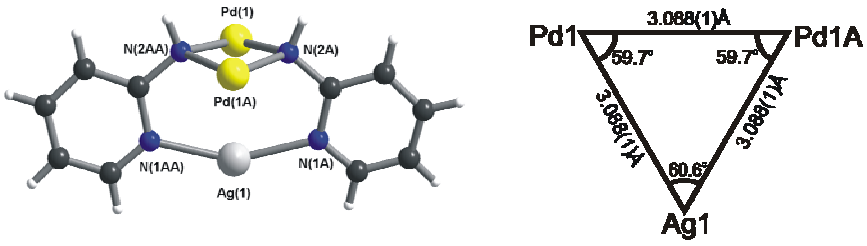

*Molekulares Pd_2Ag Dreieck des $[\{(tmeda)Pd(N2\text{-}ampy^{-}\text{-}N1)\}_2Ag]^{3+}$ (**II-5**)*

Eine weitere Dreiecksstruktur $[\{Pt(tmeda)(pz)\}_3](NO_3)_3\cdot(H_2O)_{2.25}$ (**III-2**) wurde nach Umsetzung von Pt^{II}(tmeda) mit Pyrazin erhalten. Die Bildung eines Dreiecks ist unerwartet, da gemäß der Methode der "Molekularen Bibliotheken" ein molekulares Rechteck aus ditopen 90°- und 180°-Bausteinen entstehen sollte. Die Ursache hierfür ist noch unbekannt, aber wir nehmen an, dass die sterische Abstoßung zwischen den Methylgruppen der tmeda-Liganden und den Pyrazin-Liganden verantwortlich dafür ist, dass das "erwartete" Rechteck nicht realisiert wird.

Des weiteren wurde *cis*-$Pt^{II}(NH_3)_2$, ein Baustein für 90°-Winkel, mit 2,2'-Bipyrazin umgesetzt. Ein quadratischer Komplex $[\{cis\text{-}Pt(NH_3)_2(2,2'\text{-}bpz\text{-}\mathit{N4,N4'})\}_4](NO_3)_8\cdot 4H_2O$ (**IV-1**) und ein dreieckiger Komplex $[\{cis\text{-}Pt(NH_3)_2(2,2'\text{-}bpz\text{-}\mathit{N4,N4'})\}_3](NO_3)_6$ (**IV-2**) wurden in der Lösung mittels ^{1}H-NMR-Spektroskopie nachgewiesen. Der quadratische Komplex (**IV-1**) wurde

erfolgreich abgetrennt und seine Struktur röntgenkristallografisch bestätigt. In wässriger Lösung stehen die quadratische und die dreieckige Spezies im Gleichgewicht.

3 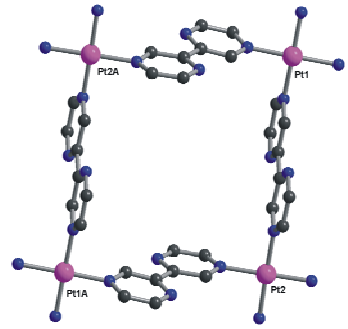 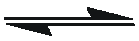 4 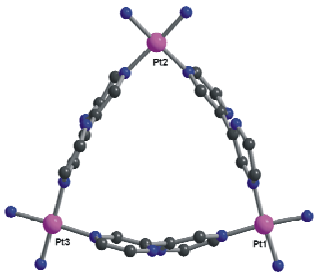

*Ein Gleichgewicht zwischen quadratischem [{cis-Pt(NH$_3$)$_2$(2,2'-bpz-N4,N4')}$_4$]$^{8+}$ (**IV-1**) und dreieckigem [{cis-Pt(NH$_3$)$_2$(2,2'-bpz-N4,N4')}$_3$]$^{6+}$(**IV-2**)*

— Wirt-Gast-Chemie

Drei der bereits erwähnten Komplexe wurden daraufhin untersucht, ob sie Wirt-Gast-Chemie in Lösung zeigen, nämlich Pd$_3$(1-MeC$^-$)$_3$ (**I-7**), Pt$_4$(**IV-1**) und Pt$_3$(**IV-2**).

In DMSO-*d$_6$* wechselwirkt Pd$_3$(1-MeC$^-$)$_3$ (**I-7**) mit Halogenid-Anionen, wie ^{1}H-NMR-spektroskopisch gezeigt werden konnte. Speziell konnte gezeigt werden, dass die N(4)H Resonanz des Cytosinato-Liganden sensitiv auf die Anwesenheit von Halogenid-Anionen reagiert und zu tiefem Feld verschoben wird, wenn die Konzentration der Gast-Anionen zunimmt. Dies läßt darauf schließen, dass sich diese Anionen dem kationischen Wirt vom unteren Kegel her nähern. Eine quantitative Untersuchung zwischen der Wechselwirkung von (**I-7**) und F$^-$ wurde durch die hygroskopische Natur des eingesetzten Fluoridsalzes und die Empfindlichkeit der N(4)H-Resonanz gegenüber Wasser behindert. Die drei anderen Halogenid-Anionen binden schwach (Tabelle), was -wie vorausgesehen- für eine eindeutige Abhängigkeit der Bindungsstärke von der Größe des Anions spricht.

Tabelle: Assoziationskonstanten der Halogenid-Anionen mit $Pd_3(1\text{-}MeC^-)_3$ in DMSO

	Cl^-	Br^-	I^-
$\Delta\delta_{max}$/ppm	1.75	1.37	0.96
K/M^{-1}	47 ± 15	56 ± 13	6 ± 1
log K	1.7(2)	1.8(1)	0.78(9)

Das zyklische Tetramer Pt_4 (**IV-1**) und das Trimer Pt_3 (**IV-2**) können Terephthalat-Anionen in wässriger Lösung einschließen. Die 1:2-Stöchiometrie des Pt_4/Terephthalat-Systems suggeriert, dass ein Paar stapelnder Terephthalat-Ionen in den Hohlraum des Pt_4 eindringt. Der zur Verfügung stehende Raum innerhalb von Pt_4 reicht gerade aus, um ein Paar aromatischer Moleküle aufzunehmen. Zusätzlich können so die hydrophilen Carboxylatgruppen in das Lösungsmittel weisen. Pt_3 stellt eine vergleichsweise vielseitige Umgebung für Gastmoleküle dar, da es in verschiedenen Konformationen vorliegen kann. Die 1:2-Stöchiometrie des Pt_3/Terephthalat-Systems könnte darauf hindeuten, dass zwei Terephthalat-Ionen von beiden Seiten in den Hohlraum des Pt_3 eindringen. In beiden Fällen werden nur schwache Gesamtbindungskonstanten beobachtet. Dies ist nicht unerwartet, da die Anionen stark hydratisiert vorliegen und auch die Hohlräume der Wirtverbindungen Wassermoleküle und Nitrat-Anionen enthalten, die mit den Anionen konkurrieren.

—Wechselwirkung zwischen Metallkomplex und DNA

Die Zugabe von $Pd_3(1\text{-}MeC^-)_3$ zu DNA bewirkt die Kondensation und Aggregation der Nukleinsäure, wie mittels Rasterkraftmikroskopie gezeigt werden konnte. Im Gegensatz dazu ließen UV/vis-Titrationen und Gel-Elektrophorese-Experimente keinen eindeutigen Beleg dafür zu, dass der $Pd_3(1\text{-}MeC^-)_3$-Komplex mit DNA wechselwirkt. Versuche, lokale Aspekte der Wechselwirkung zwischen dem Nukleinsäure-Einzelstrang 5'-d(TAGGGTTA) und dem $Pd_3(1\text{-}MeC^-)_3$-Komplex zu untersuchen, blieben erfolglos, wiesen zugleich aber darauf hin, dass der Komplex in Gegenwart von Nukleinsäuren für mindestens einen Tag stabil ist. Die Wechselwirkung zwischen dem Komplex und DNA benötigt noch weitere Studien, um verstanden zu werden.

E EXPERIMENTAL SECTION

1 Instrumentation and Methods

1.1 NMR Spectroscopy

1.1.1 General aspects

One- and two-dimensional ^{1}H NMR spectra were recorded on Varian Mercury 200, on Bruker DRX 500, and/or Varian Inova 600 instruments. One-dimensional ^{13}C NMR spectra were recorded on the Varian Inova 600 instrument. In D_2O, TSP (sodium 3-trimethylsilyl-propanesulfonate) (δ = 0 ppm) or TMAB (tetramethylammonium tetrafluoroborate) (δ = 3.18 ppm) were used as internal standards. Spectra in DMSO-d_6 were recorded without presaturation of the water signal using the resonance of DMSO-d_5 (δ = 2.50 ppm relative to tetramethylsilane (TMS)) as reference. The samples were measured in collaboration with Prof. Dr. Burkhard Costisella and were processed using MestReC.[1]

1.1.2 pK_a values determination

The pH* (uncorrected pH) of a D_2O solution was measured by use of a glass electrode Typ “SenTix Mic” on a pH meter WTW Walheim “Ino-Lab pH Level 1”. The pD values were obtained by adding 0.4 units to the value displayed on the pH meter.[2] Measurement of the pD dependences were carried out using identical samples, in which the pD of the solutions was modified in small increments by addition of small amounts of DNO_3 and/or NaOD. Due to the limitations of the AgCl glass electrodes, it was not possible to get reliable measurements at pH values close to 14. The pK_a values were evaluated with a

Newton-Gauss non-linear least-squares curve fitting procedure that deals with the chemical shift (δ) data at different pD.[3]

In this thesis, the 2,3-dimethylpyrazine molecule was studied which has two deprotonation sites, thus two pK_a values were calculated according to Equation 1:

$$\delta = \frac{\delta_B + \delta_1 \times 10^{(pK_{a1} - pD)} + \delta_2 \times 10^{(pK_{a2} + pK_{a1} - 2\times pD)}}{1 + 10^{(pK_{a1} - pD)} + 10^{(pK_{a2} + pK_{a1} - 2\times pD)}} \qquad (1)$$

With:

δ = measured chemical shift; pD = established pD; K_a = dissociation constant, δ_B = chemical shift of the unprotonated form B; δ_1 = chemical shift of the protonated form BH; δ_2 = chemical shift of the protonated form BH_2.

The pK_a values obtained for D_2O were then converted into pK_a values for H_2O by using Equation 2:[4]

$$pK_a(H_2O) = \frac{pK_a(D_2O) - 0.45}{1.015} \qquad (2)$$

1.1.3 Association constant determination for host-guest interactions

In the host-guest chemistry studies of this thesis, association constants of the host guest adducts were established by titration methods via ^{1}H NMR spectroscopy. For the Pd_3(1-MeC$^-$)$_3$-halide anions systems, the ^{1}H NMR spectra were recorded in DMSO-d_6 solutions. From a plot of the chemical shift of N(4)H against the increasing concentration of the halide anions, the curve best fitting these experimental data was computed.

Job plot determined that the stoichiometry is 1:1, namely one host molecule

per one guest molecule, the reaction follows the general equation:

$$H + G \overset{K}{\rightleftharpoons} HG$$

The association constant *K* is defined as the concentration of the host-guest complex [HG] divided by the concentration of the host molecule [H] times the concentration of the guest molecule [G], the concentration was established when the host guest interaction reach the equilibrium.

$$K = \frac{[HG]}{[H]\cdot[G]} \quad (1)$$

$$\delta_{obs} = \frac{[H]\cdot\delta_H + [HG]\cdot\delta_{HG}}{[H^0]} \quad (2)$$

With:

δ_{obs} = observed chemical shift; δ_H = the chemical shift of the free host molecule; δ_{HG} = the chemical shift of the host-guest adduct; $[H^0]$ = the initial concentration of the host compound.

$$[H^0] = [H] + [HG] \quad (3)$$

and

$$[G^0] = [G] + [HG] \quad (4)$$

with: $[G^0]$ = the initial concentration of the host compound.

therefore, equation 5 is obtained as,

$$\delta_{obs} = \delta_H + \frac{\left(1 + K\cdot[G^0] + K\cdot[H^0] - \sqrt{-4\cdot K^2\cdot[G^0]\cdot[H^0] + \left(1 + K\cdot[G^0] + K\cdot[H^0]\right)^2}\right)\cdot\left(-\delta_H + \delta_{HG}\right)}{2\cdot K\cdot[H^0]}$$

Equation 5 gives an expression which contains only two unknown parameters, δ_{HG} and *K,* and these were determined by starting an iterative calculation with estimated values, and varying these until the standard deviation reached a minimum (least-squares regression).

For the Pt_4 and Pt_3-terephthalate systems, the ^1H NMR spectra were recorded in D_2O solutions. From a plot of the chemical shift of H(3) against the increasing concentration of the terephthalate anions, the curve best fitting these experimental data was computed.

Job plot determined that the stoichiometries are both 1:2, namely one host molecule per two guest molecules. In these cases, a sequential process involving the binding of more than one guest molecular was involved, then two *K* values were established: K_{11} and K_{12}. The association of the host with the first guest was denoted K_{11}, while the association of the resulting 1:1 complex with a further guest to produce a 1:2 complex has the equilibrium constant K_{12}. A computer program EQNMR was used for the computation of association constants for these host-guest compounds.

In an easy way, an overall binding constant, β_{12} was defined for the stepwise process:

$$\beta_{12} = K_{11} * K_{12}$$

1.2 IR Spectroscopy

IR spectra were recorded on a Bruker IFS 28 spectrometer. Measurements (KBr pellets) were carried out from 250 to 4000 cm^{-1}. The spectra were processed with Opus-IR. UV-vis spectra were recorded on an UNICAM Modell UV-410 spectrometer.

1.3 Elemental Analysis

Elemental analyses were performed on a CHNS-932 Element Analyzer by Markus Hüffner in the Chemistry Department.

1.4 X-Ray Crystallography

Intensity data were collected on an Enraf-Nonius KappaCCD diffractometer[5] using graphite-monochromated Mo Kα radiation (λ = 0.7107 Å) at low temperature (150 K) or at room temperature. None of the crystals reported in this thesis showed evidence of crystal decay during data collection. For data reduction and cell refinement, the programs DENZO and SCALEPACK (Nonius, 2000) were used.[6] Corrections for incident and diffracted beam absorption effects were applied using SADABS.[7] The structures were solved by either standard conventional direct methods or Patterson methods and refined by full-matrix least squares based on F^2 using the SHELXTL-PLUS[8] and SHELXL-97[9] programs. The positions of all non-hydrogen atoms were deduced from difference Fourier maps and were refined anisotropically, except for the disordered atoms. Hydrogen atoms except those of the water molecules were generated geometrically and given isotropic thermal parameters equivalent to 1.2 or 1.5 times those of the atom to which they were attached. The distances and angles were calculated by using PLATON[10] and the CIF files[11] were generated using the Software WinGX.[12] The graphics were generated using Diamond programs. Relevant crystal data and data collection parameters are summarized in X-ray Tables.

1.5 Atom Force Microscopy

The AFM instrument used was a Nanotec Electronica System and the images were acquired in dynamic mode. The Olympus cantilevers that we used have a nominal force constant 0.75 N/m.

Sample solutions were prepared in plastic microcentrifuge tubes with the following order of addition: $Pd_3(1\text{-}MeC^-)_3$ compound, deionised water, DNA. Solution were mixed using an Eppendorf micropipette and allowed to incubate at room conditions for one hour to assure sufficient time for complete compound/DNA interactions to take place. Solutions were mixed using the pipette periodically throughout the incubation. Half inch diameter disks of mica (New York Mica Company, New York, NY) were freshly cleaved using transparent tape to peel off the top mica planes. Mica has a high negative charge on the surface. Poly-L-Lysine was applied to the mica within five minutes after cleavage for pre-treating the mica surface and neutralizing the negative charge. The pre-treatment took about 2 min under ambient conditions. Then the mica surface was washed by deionised water. Ten microliters of sample solution were pipetted into the center of the mica disk and allowed to stand in the open air for 10 min. After that, the mica disk was rinsed in 20 mL deionised water and was thoroughly dried using a stream of nitrogen at approximately 60^o angle to the sample surface (without putting sample under too much stress). The mica was firmly attached to a 15 mm diameter metal shim using an adhesive tab. The metal shim served to mount the sample on the magnetic holder of the AFM piezo stack. The measurements were done in collaboration with the group of Dr. Félix Zamora (Madrid, Spain).

2 General Work Descriptions

2.1 Starting Materials

The following compounds were purchased: K_2PtCl_4 and K_2PdCl_4 (Heraeus), $PdCl_2$ (Sigma), cytidine (Merck), 2-aminopyridine (Aldrich), pyrazine (Fluka), 2,3-dimethylpyrazine (Aldrich), 2,2'-bipyridine (Aldrich), pyrazole (Aldrich), 2,2'-dimethoxypropane (Aldrich), N,N,N',N'-tetramethylethylenediamine (Fluka), $[Me_4N]Cl$, $[Me_4N]Br$ and $[Me_4N]I$ (Fluka), terephthalate disodium salt (Aldrich), Deoxyribonucleic acid sodium salt from calf thymus (Sigma), poly-L-lysine (Sigma), 8-mer oligonucleotide 5'-d(TAGGGTTA) (Eurogentech Deutschland GmbH, Köln). Deuterated solvents DMSO-d_6, D_2O were obtained from Deutero GmbH, Kastellaun (Germany). The following starting compounds were synthesized according to published methods: 1-methylcytosine, [13] $PdCl_2$(tmeda) (**I-4**),[14] $PtCl_2$(tmeda),[14] *cis*-$PtCl_2(NH_3)_2$,[15] *trans*-$PtCl_2(NH_3)_2$,[16] $PdCl_2$(bpy),[17] and $PdCl_2$(bipzp).[18]

2.2 Synthesis of compounds

$[Pd(1\text{-}MeC^{-}\text{-}N3,N4)(bpy)]_2(ClO_4)_2 \cdot 4H_2O$ (I-1)

An aqueous suspension (40 mL) of $PdCl_2$(bpy) (335 mg, 1.00 mmol) and $AgNO_3$ (340 mg, 2.00 mmol) was stirred for 12 h at 40 °C with daylight excluded. The resultant AgCl precipitate was filtered off, the pH of the solution was adjusted to 9.5 by adding NaOH (1 M) solution. 1-Methylcytosine (125 mg, 1.00 mmol) was added to the clear filtrate and this solution was first stirred for two days at room temperature, then heated at 80 °C for three days. The resulting solution was concentrated to a volume of 5 mL at 40 °C on a rotary evaporator. Cube-shaped yellow crystals were obtained after anion exchange to ClO_4^-**.** The yield was 180 mg (0.172 mmol), 34 %.

Elemental analysis:

(calc. for 4 molecules of crystal water)

$C_{30}H_{28}N_{10}Pd_2Cl_2O_8 \cdot 4H_2O$, M = 1044.41 g·mol^{-1}

Calculated: C 34.5 %, H 3.5 %, N 13.4 %

Obtained: C 34.2 %, H 3.6 %, N 13.3 %

^{1}H NMR:

(200 MHz, D_2O, pD = 8.1, δ/ppm): Resonances of bpy: 8.24 (H6', d, $^3J_{H\text{-}H}$ = 5.6 Hz), 8.13 (H6'', d, $^3J_{H\text{-}H}$ = 5.6 Hz), 8.00 (H4',H4'',H3',H3'', m) and 7.30 (H5',H5'', m); resonances of 1-MeC$^-$: 7.18 (H6, d, $^3J_{H\text{-}H}$ = 7.6 Hz), 5.98 (H5, d, $^3J_{H\text{-}H}$ = 7.6 Hz) and 3.35 (CH_3, s).

$PdCl_2$(bipzp) (I-2)

A mixture of pyrazole (13.6 g, 200 mmol), 2,2'-dimethoxypropane (10.4 g, 100 mmol) and *p*-toluenesulphonic acid (0.1 g, 0.6 mmol) was heated to 110 °C. After methanol (*ca.* 8 mL, 200 mmol) was collected in Dean-Stark apparatus, the reaction mixture was poured into cold heptane (40 mL) and cooled down to room temperature. Recrystallisation of the resulting solid for three times from heptane and further purification by column chromatograph (silica gel, CH_2Cl_2/MeOH = 60:1) yielded 9.54 g, 53.6 mmol of bis(pyrazol-1-yl)propane (54 %) as a crystalline solid.

$PdCl_2$ (285 mg, 1.60 mmol) was dissolved in CH_3CN (15 mL) under reflux at 100^{o}C. After $PdCl_2$ (dark red) had been fully converted into $Pd(CH_3CN)_2Cl_2$ (yellow), the reaction mixture was cooled to RT, then brought to dryness. The resulting yellow powder $Pd(CH_3CN)_2Cl_2$ (*ca.* 1.60 mmol) and bis(pyrazol-1-yl)propane (285 mg, 1.60 mmol) were dissolved in CH_2Cl_2 (40 mL) at room temperature. The reaction mixture was stirred for 3 hours. Filtration of the reaction mixture yielded 500 mg, 1.41 mmol of $PdCl_2$(bipzp) (88%) as an orange solid.

Elemental analysis:

$C_9H_{12}N_4PdCl_2$, M = 353.54 g·mol^{-1}

Calculated: C 30.6 %, H 3.4 %, N 15.9 %

Obtained: C 30.4 %, H 3.5 %, N 16.0 %

^{1}H NMR:

(200 MHz, $CDCl_3$, δ/ppm): 8.32 (H3, d, $^3J_{H\text{-}H}$ = 3.0 Hz), 7.74 (H5, d, $^3J_{H\text{-}H}$ = 3.0 Hz), 6.46 (H4, t, $^3J_{H\text{-}H}$ = 3.0 Hz) and 2.78 (CH_3, s).

[Pd(1-MeC$^-$-*N3,N4*)(bipzp)]$_2$(NO_3)$_2$·7H_2O (I-3)

An aqueous suspension (40 mL) of $PdCl_2$(bipzp) (354 mg, 1.00 mmol) and $AgNO_3$ (340 mg, 2.00 mmol) was stirred for 12 h at room temperature with daylight excluded. The resultant AgCl precipitate was filtered off, the pH of the solution was adjusted to 9 by adding NaOH (1 M) solution. 1-Methylcytosine (125 mg, 1.00 mmol) was added to the clear filtrate and this solution was stirred for one day at 60 °C. The resulting solution was concentrated to a volume of 5 mL at 40 °C by rotary evaporatoration. Yellow crystals were obtained two days later**.** The yield was 280 mg (0.288 mmol), 58 %. X-ray crystal structure analysis showed that the water content of freshly prepared **I-3** is higher (7 H_2O) than the one obtained by elemental analysis.

Elemental analysis:

(calc. for 2 molecules of crystal water)

$C_{28}H_{36}N_{16}O_8Pd_2$·2$H_2O$, M = 973.55 g·mol^{-1}

Calculated: C 34.5 %, H 4.1 %, N 23.0 %

Obtained: C 34.2 %, H 4.0 %, N 22.9 %

^{1}H NMR:

(200 MHz, D_2O, pD = 7.5, δ/ppm): Resonances of bipzp : 8.13 (H3', d, $^3J_{H\text{-}H}$ = 3.0 Hz), 8.09 (H3', d, $^3J_{H\text{-}H}$ = 3.0 Hz), 7.78 (H5', d, $^3J_{H\text{-}H}$ = 3.0 Hz), 7.44 (H5', d,

$^3J_{H\text{-}H}$ = 3.0 Hz), 6.44 (H4', t, $^3J_{H\text{-}H}$ = 3.0 Hz), 6.37 (H4', t, $^3J_{H\text{-}H}$ = 3.0 Hz), 2.66 and 1.68 (C(1)CH_3, s); resonances of 1-MeC$^-$: 7.13 (H6, d, $^3J_{H\text{-}H}$ = 7.6 Hz), 5.98 (H5, d, $^3J_{H\text{-}H}$ = 7.6 Hz) and 3.35 (N(1)CH_3, s).

[Pd(tmeda)(1-MeC-*N3*)$_2$](NO$_3$)$_2$·2H$_2$O (I-5)

$AgNO_3$ (340 mg, 2.00 mmol) was added to a suspension of $PdCl_2$(tmeda) (294 mg, 1.00 mmol) in 20 mL of water and the mixture was stirred at room temperature in the dark for 2 h and then filtered from AgCl. 1-MeC (250 mg, 2.00 mmol) was added to the filtrate and stirred for 1 h. The resulting solution was subsequently concentrated in vacuo to a volume of 5 mL. Yellow crystals were obtained after two days. The yield was 417 mg (0.668 mmol), 67 %.

Elemental analysis:

(calc. for 2 molecules of crystal water)

$C_{16}H_{30}N_{10}O_8Pd·2H_2O$, M = 623.92 g·mol^{-1}

Calculated: C 30.4 %, H 5.4 %, N 22.1 %

Obtained: C 30.4 %, H 5.3 %, N 22.4 %

^{1}H NMR:

(200 MHz, D_2O, pD = 7.0, δ/ppm): (*head-tail* rotamer) 7.63 (H6, d, $^3J_{H\text{-}H}$ = 7.4 Hz), 6.02 (H5, d, $^3J_{H\text{-}H}$ = 7.4 Hz) and 3.44 (CH_3, s); (*head-head* rotamer) 7.57 (H6, d, $^3J_{H\text{-}H}$ = 7.4 Hz), 6.01 (H5, d, $^3J_{H\text{-}H}$ = 7.4 Hz) and 3.37 (CH_3, s); both tmeda resonances are observed at 2.97 (CH_2, d, $^3J_{H\text{-}H}$ = 3.0 Hz), 2.75 (CH_3, s) and 2.53 (CH_3, s).

IR:

(cm^{-1}) 3243 vs, 3085 vs, 1666 vs, 1544 s, 1506 s, 1465 m, 1383 vs, 1064 w, 1041 m, 958 s, 787 vs and 643 vs.

[{Pd(μ-OH)(tmeda)}$_2$](ClO$_4$)$_2$ (I-6)

Addition of $AgNO_3$ (340 mg, 2.00 mmol) to a suspension of $PdCl_2$(tmeda) (294 mg, 1.00 mmol) in 20 mL of water resulted in the immediate precipitation of AgCl. The mixture was stirred at room temperature in the dark for 2 h and then filtered from AgCl. One equiv of aqueous NaOH (0.5 M) and $NaClO_4$ (245 mg, 2.00 mmol) were added to the filtrate. The resulting solution was subsequently concentrated in vacuo to a volume of 5 mL. Yellow crystals were obtained upon cooling the solution in ice water. The yield was 224 mg (0.330 mmol), 66 %.

Elemental analysis:

$C_{12}H_{34}N_4O_{10}Cl_2Pd_2$, M = 678.16 g·mol^{-1}

Calculated: C 21.3 %, H 5.1 %, N 8.3 %

Obtained: C 20.9 %, H 5.0 %, N 8.2 %

^{1}H NMR:

(200 MHz, D_2O, pD = 8.4, δ/ppm): 2.58 (CH_3, s) and 2.72 (CH_2, s).

IR:

(cm^{-1}) 3438 vs, 3334 s, 2923 w, 1464 vs, 1408 w, 1385 w, 1285 m, 1107 vs, 1065 vs, 956 m, 931 w, 811 m, 773 w, 624 s, 513 m, 489 w and 456 w.

[{Pd(1-MeC$^-$-*N3,N4*)(tmeda)}$_3$](ClO$_4$)$_3$·5.5H$_2$O (I-7)

A solution of [Pd(μ-OH)(tmeda)]$_2$(ClO_4)$_2$ (134 mg, 0.197 mmol) and 1-MeC (49.2 mg, 0.394 mmol) in 10 mL of H_2O was stirred at room temperature for 48 h and then warmed to 80 ^{o}C for three days. The solution was centrifuged from some black powder (presumably Pd) and then evaporated under vacuum. Crystals suitable for X-ray crystallography were obtained upon slow cooling of a saturated (at 80 ^{o}C) aqueous solution of the complex. The yield was 150 mg (0.104 mmol), 79 %.

Elemental analysis:

$C_{33}H_{68}N_{15}O_{15}Cl_3Pd_3 \cdot 5.5H_2O$, M = 1439.68 g·mol^{-1}

Calculated: C 27.5 %, H 5.5 %, N 14.6 %

Obtained: C 27.5 %, H 5.3 %, N 14.7 %

^{1}H NMR:

(400 MHz, D_2O, pD = 3.5, δ/ppm): 7.17 (H6, d, $^3J_{H\text{-}H}$ = 7.6 Hz), 6.51 (H5, d, $^3J_{H\text{-}H}$ = 7.6 Hz), 5.20 (N(4)H, s; slow isotopic exchange; c.f. text page 39), 3.21 (CH_3, s), 2.72 (CH_2, m) and 2.62 (CH_3, m).

IR:

(cm^{-1}) 3788 vw, 3659 w, 3434 s, 3229 m, 2924 w, 1651 vs, 1537 vs, 1493 s, 1467 m, 1383 s, 1341 s, 1270 s, 1089 vs, 1016 w, 957 w, 810 m, 770 m, 697 w, 625 m, 572 w and 476 w.

[{Pt(μ-OH)(tmeda)}$_2$](ClO$_4$)$_2$ (I-8a) and [{Pt(μ-OH)(tmeda)}$_2$] (NO$_3$)$_2$ (I-8b)

An aqueous suspension (15 mL) of $PtCl_2$(tmeda) (382 mg, 1.00 mmol) and $AgNO_3$ (170 mg, 1.00 mmol) was stirred for 24 h at 40 ^{o}C with daylight excluded. The resultant AgCl precipitate was filtered off. Colorless prismatic crystals were recovered after slow evaporation of the solution at room temperature for two days. Addition of $NaClO_4$ to a solution of the nitrate salt gave the corresponding perchlorate salt. The yield for **I-8a** was 172 mg (0.201 mmol), 40 %, while for **I-8b**, it was 60.8 mg (0.0779 mmol), 16 %.

For **I-8a**:

Elemental analysis:

$C_{12}H_{34}N_4O_{10}Cl_2Pt_2$, M = 855.48 g·mol^{-1}

Calculated: C 16.8 %, H 4.0 %, N 16.8 %

Obtained: C 16.7 %, H 4.1 %, N 16.7 %

^{1}H NMR:

(200 MHz, D_2O, pD = 8.0, δ/ppm): 2.59 (CH_3, s) and 2.70 (CH_2, s).

IR:

(cm^{-1}) 3438 vs, 3334 s, 2923 w, 1464 vs, 1408 w, 1385 w, 1285 m, 1107 vs, 1065 vs, 956 m, 931 w, 811 m, 773 w, 624 s, 513 m, 489 w and 456 w.

I-8b was characterized by ^{1}H NMR spectroscopy (identical with **I-8a**) and X-ray crystallography.

[{Pd(Cytd$^-$-*N3,N4*)(tmeda)}$_3$](ClO$_4$)$_3$·6H$_2$O (I-9)

A solution of [Pd(μ-OH)(tmeda)]$_2$(ClO_4)$_2$ (134 mg, 0.198 mmol) and cytidine (96.8 mg, 0.398 mmol) in 10 mL of H_2O was stirred at room temperature for 48 h and then warmed to 80 ^{o}C for three days. The solution was centrifuged from some black powder (presumably Pd) and then evaporated under vacuum. Crystals suitable for X-ray crystallography were obtained upon slow cooling of a saturated (at 80 ^{o}C) aqueous solution of the complex. The yield was 20.2 mg (0.0113 mmol), 34 %.

Elemental analysis:

(calc. for 6 molecules of crystal water)

$C_{45}H_{78}N_{15}O_{27}Cl_3Pd_3·6H_2O$, M = 1794.89 g·mol^{-1}

Calculated: C 30.1 %, H 5.1 %, N 11.7 %

Obtained: C 30.1 %, H 5.5 %, N 11.8 %

^{1}H NMR:

(200 MHz, D_2O, pD = 7.4, δ/ppm): 7.46 (H6, d, $^3J_{H\text{-}H}$ = 7.8 Hz), 6.61 (H5, d, $^3J_{H\text{-}H}$ = 7.8 Hz), 5.77 (H1S, d, ^3J = 4.2 Hz), 5.47 (N(4)H, s; slow isotopic exchange; c.f. text page 55), 4.21-3.75 (H from sugar part, m), 2.86 (CH_3, s), 2.84 (CH_3, s), 2.77 (CH_3, s) and 2.41 (CH_3, s).

[PdCl(tmeda)(Hampy-*N1*)](NO_3) (II-1)

Addition of $AgNO_3$ (170 mg, 1.00 mmol) to a suspension of $PdCl_2$(tmeda) (294 mg, 1.00 mmol) in 20 mL of water resulted in the immediate precipitation of AgCl. The mixture was stirred at room temperature in the dark for 12 h and then filtered from AgCl. 2-Aminopyridine (94.1 mg, 1.00 mmol) was added to the filtrate, which was stirred for one day at room temperature. The resulting solution was concentrated in vacuo to a volume of 5 mL. Several days later, yellow crystals were obtained by slow evaporation of the solution in air. The yield was 285 mg (0.688 mmol), 69 %.

Elemental analysis:

$C_{11}H_{22}N_5O_3ClPd$, M = 414.19 g·mol^{-1}

Calculated: C 31.9 %, H 5.4 %, N 16.9 %

Obtained: C 31.6 %, H 5.2 %, N 17.2 %

^{1}H NMR:

(200 MHz, D_2O, pD = 6.1, δ/ppm): 8.16 (H6, d, $^3J_{H\text{-}H}$ = 7.0 Hz), 7.60 (H4, t, $^3J_{H\text{-}H}$ = 7.0 Hz), 6.79 (H3/H5, m), 2.99 (CH_2, m), 2.80 (CH_3, s), 2.79 (CH_3, s), 2.62 (CH_3, s) and 2.61 (CH_3, s).

[Pd(tmeda)(Hampy-*N1*)$_2$](NO_3)$_2$·2H_2O (II-2)

Addition of $AgNO_3$ (340 mg, 2.00 mmol) to a suspension of $PdCl_2$(tmeda) (294 mg, 1.00 mmol) in 20 mL of water resulted in the immediate precipitation of AgCl. The mixture was stirred at room temperature in the dark for 2 h and then filtered from AgCl. 2-Aminopyridine (188 mg, 2.00 mmol) was added to the filtrate, which was stirred overnight. The resulting solution was concentrated in vacuo to a volume of 5 mL. Two days later, yellow cubes were obtained upon slow evaporation of the solution at room temperature. The yield was 482 mg (0.831 mmol), 83 %.

Elemental analysis:

(calc. for 2 molecules of crystal water)

$C_{16}H_{28}N_8O_6Pd \cdot 2H_2O$, M = 579.90 g·mol^{-1}

Calculated: C 33.1 %, H 5.7 %, N 19.3 %

Obtained: C 33.6 %, H 5.6 %, N 19.6 %

^{1}H NMR:

(200 MHz, D_2O, pD = 6.9, δ/ppm): 8.44 (H6, d, $^3J_{H\text{-}H}$ = 7.0 Hz), 7.56 (H4, t, $^3J_{H\text{-}H}$ = 7.0 Hz), 6.76 (H3/H5, m), 3.13 (CH_2, m), 2.79 (CH_3, s) and 2.77 (CH_3, s).

[PtCl(tmeda)(Hampy-*N1*)](NO$_3$) (II-3)

This compound was prepared strictly analogous to **II-1** with $AgNO_3$ (170 mg, 1.00 mmol), $PtCl_2$(tmeda) (382 mg, 1.00 mmol) and 2-Aminopyridine (94.1 mg, 1.00 mmol) were employed. Following concentration to a volume of 5 mL, the solution was allowed to slowly evaporate in air with colorless crystals harvested after four days. The yield was 82.9 mg, 0.165 mmol, 16.5 %.

Elemental analysis:

$C_{11}H_{22}N_5O_3ClPt$, M = 502.85 g·mol^{-1}

Calculated: C 26.3 %, H 4.4 %, N 13.9 %

Obtained: C 26.0 %, H 4.2 %, N 13.8 %

^{1}H NMR:

(200 MHz, D_2O, pD = 7.0, δ/ppm): 8.16 (H6, d, $^3J_{H\text{-}H}$ = 7.0 Hz, $^3J_{Pt\text{-}H}$ = 31 Hz), 7.59 (H4, t, $^3J_{H\text{-}H}$ = 7.0 Hz), 7.76 (H3/H5, m), 2.99 (CH_2, t), 2.93 (CH_3, s), 2.91 (CH_3, s), 2.80 (CH_3, s) and 2.77 (CH_3, s).

[Pt(tmeda)(Hampy-*N1*)$_2$](ClO$_4$)$_2$ (II-4)

Addition of $AgNO_3$ (340 mg, 2.00 mmol) to a suspension of PtI_2(tmeda) (566 mg, 1.00 mmol) in 20 mL of water resulted in the immediate precipitation of AgI.

The mixture was stirred at 40 °C in the dark for 12 h and then filtered from AgI. Excess 2-aminopyridine (200 mg, 2.13 mmol) was added to the filtrate, which was stirred for one day at 50 °C. The resulting solution was concentrated in vacuo to a volume of 5 mL. The anions were changed to ClO_4^- by using an anion exchange column. After five days, colorless crystals were obtained by slow evaporation of the solution at 4 °C. The yield was 50.2 mg (0.0719 mmol), 7.2 %.

Elemental analysis:

$C_{16}H_{28}N_6O_8PtCl_2$, M = 698.41 g·mol^{-1}

Calculated: C 27.5 %, H 4.0 %, N 12.0 %

Obtained: C 27.7 %, H 4.2 %, N 12.3 %

^{1}H NMR:

(200 MHz, D_2O, pD = 7.0, δ/ppm): 8.35 (H6, d, $^3J_{H\text{-}H}$ = 7.0 Hz, $^3J_{Pt\text{-}H}$ = 31 Hz), 7.54 (H4, t, $^3J_{H\text{-}H}$ = 7.0 Hz), 6.71 (H3/H5, m), 3.10 (CH_2, t), 2.89 (CH_3, s) and 2.85 (CH_3, s).

[{(tmeda)Pd(*N2*-ampy$^-$-*N1*)}$_2$Ag(μ-NO$_3$)$_2$Ag(NO$_3$)$_2$] (II-5)

Addition of $AgNO_3$ (33.7 mg, 0.198 mmol) to a 10 mL solution of compound **1** (42.2 mg, 0.102 mmol) resulted in the immediate precipitation of AgCl. The mixture was stirred at room temperature in the dark for 12 h and then filtered from AgCl. NaOH (7.89 mg, 0.197 mmol) in 5 mL water was added to the filtrate dropwise. An orange colored solution was obtained within 2 h stirring, pH 8.6. The resulting solution was concentrated in vacuo to a volume of 5 mL. Orange brown crystals were obtained after one day. The yield was 28.5 mg (0.0260 mmol), 51 %.

Elemental analysis:

$C_{22}H_{42}N_{12}O_{12}Pd_2Ag_2$, M = 1095.21 g·mol^{-1}

Calculated: C 24.3 %, H 3.9 %, N 14.8 %

Obtained: C 24.0 %, H 3.8 %, N 15.1 %

^{1}H NMR:

(200 MHz, D_2O, pD = 6.9, δ/ppm): 8.72 (H6, ddd), 7.82 (H4, t), 7.43 (H3/H5, m), 2.61 (CH_2, m), 2.46 (CH_3, s) and 1.43 (CH_3, s).

[{(tmeda)Pd(*N2*-ampy$^-$-*N1*)}$_2$Ag(ClO$_4$)$_2$](ClO$_4$)·2H$_2$O (II-5a)

This compound was synthesized in the same way with same amount of starting materials as compound **5** except using $AgClO_4 \cdot xH_2O$ (40.6 mg, 0.196 mmol). The yield was 33 mg (0.0307 mmol), 60 %.

Elemental analysis:

(calc. for 2 molecules of crystal water)

$C_{22}H_{46}N_8O_{14}Cl_3Pd_2Ag$, M = 1073.71 g·mol^{-1}

Calculated: C 24.6 %, H 4.3 %, N 10.4 %

Obtained: C 24.6 %, H 4.2 %, N 10.4 %

^{1}H NMR:

(200 MHz, D_2O, pD = 6.9, δ/ppm): 8.72 (H6, ddd), 7.82 (H4, t), 7.43 (H3/H5, m), 2.61 (CH_2, m), 2.46 (CH_3, s) and 1.43 (CH_3, s).

[Pd(ampy$^-$-*N1,N2*)(bpy)]$_2$(NO$_3$)$_2$ (II-6)

An aqueous suspension (40 mL) of $PdCl_2$(bpy) (340 mg, 1.00 mmol) and $AgNO_3$ (340 mg, 2.00 mmol) was stirred for 12 h at 40 ^{o}C with daylight excluded. The resultant AgCl precipitate was filtered off, and 2-aminopyridine (94.2 mg, 1.00 mmol) was added to the clear filtrate. The resulting orange color solution was concentrated to a volume of 5 mL at 40 ^{o}C on a rotary

evaporator. Yellow cube-shaped crystals were obtained after one day**.** The yield was 310 mg (0.371 mmol), 74 %.

Elemental analysis:

$C_{30}H_{26}N_{10}O_6Pd_2$, M = 835.43 g·mol^{-1}

Calculated: C 43.1 %, H 3.1 %, N 16.8 %

Obtained: C 43.2 %, H 3.0 %, N 16.7 %

^{1}H NMR:

(200 MHz, D_2O, pD = 6.9, δ/ppm): 7.95 (H4, t, $^3J_{H\text{-}H}$ = 4.8 Hz), 7.78 (H6, d, $^3J_{H\text{-}H}$ = 4.8 Hz), 7.51 (H3, d, $^3J_{H\text{-}H}$ = 4.8 Hz) and 7.36 (H5, d, $^3J_{H\text{-}H}$ = 4.8 Hz) for the pyridine ring *trans* to N(2); 8.20 (H6, d, $^3J_{H\text{-}H}$ = 4.8 Hz), 7.85 (H4, t, $^3J_{H\text{-}H}$ = 4.8 Hz), 7.82 (H3, d, $^3J_{H\text{-}H}$ = 4.8 Hz) and 7.02 (H5, t, $^3J_{H\text{-}H}$ = 4.8 Hz) for the pyridine ring *trans* to N(1); 7.95 (H6, d, $^3J_{H\text{-}H}$ = 4.8 Hz), 7.06 (H4, t, $^3J_{H\text{-}H}$ = 4.8 Hz), 6.56 (H3, d, $^3J_{H\text{-}H}$ = 4.8 Hz) and 6.28 (H5, t, $^3J_{H\text{-}H}$ = 4.8 Hz) for the pyridine ring of ampy$^-$.

[PtCl(tmeda)(pz)](ClO$_4$) (III-1)

An aqueous suspension (15 mL) of $PtCl_2$(tmeda) (382 mg, 1.00 mmol) and $AgNO_3$ (170 mg, 1.00 mmol) was stirred for 24 h at 40 ^{o}C with daylight excluded. The resultant AgCl precipitate was filtered off, pyrazine (80.1 mg, 1.00 mmol) was added to the clear filtrate and this solution was stirred at room temperature for 24 h. The resulting solution was concentrated to a volume of 5 mL at 40 ^{o}C on a rotary evaporator. The pH of the solution was adjusted to 9 by adding NaOH (0.1 M) solution. Following anion exchange to ClO_4^- and slow evaporation, yellow cube-shaped crystals were obtained. The yield was 120 mg (0.228 mmol), 23 %.

Elemental analysis:

$C_{10}H_{20}N_4O_4Cl_2Pt$, M = 526.27 g·mol^{-1}

Calculated: C 22.8 %, H 3.8 %, N 10.7 %

Obtained: C 22.3 %, H 4.1 %, N 10.8 %

^{1}H NMR:

(200 MHz, D_2O, pD = 4.0, δ/ppm): 9.07 (H2/H6, d, $^3J_{H\text{-}H}$ = 4.6 Hz), 8.90 (H3/H5, d, $^3J_{H\text{-}H}$ = 4.6 Hz), 3.02 (CH_2, m), 2.88 (CH_3, s) and 2.79 (CH_3, s).

[{Pt(tmeda)(pz)}$_3$](NO$_3$)$_6$·2.5H$_2$O (III-2)

An aqueous suspension (15 mL) of $PtCl_2$(tmeda) (500 mg, 1.31 mmol) and $AgNO_3$ (440 mg, 2.59 mmol) was stirred for 24 h at 40 ^{o}C with daylight excluded. The resultant AgCl precipitate was filtered off, pyrazine (105 mg, 1.31 mmol) was added to the clear filtrate and this solution was stirred at room temperature for 24 h. The resulting solution was concentrated to a volume of 5 mL at 40 ^{o}C on a rotary evaporator. The pH of the solution was adjusted to 6.3 by adding NaOH (0.1 M) solution. Yellow needles were obtained after one week. The yield was 180 mg (0.113 mmol), 26 %.

Elemental analysis:

(calc. for 2.5 molecules of crystal water)

$C_{30}H_{60}N_{18}O_{18}Pt_3$·2.5$H_2O$, M = 1591.18 g·mol^{-1}

Calculated: C 22.7 %, H 4.1 %, N 15.9 %

Obtained: C 22.6 %, H 4.1 %, N 15.8 %

^{1}H NMR:

(200 MHz, D_2O, pD = 4.0, δ/ppm): 9.48 (aromatic H, s) and 2.83 (CH_3, s).

***trans*-[Pt(NH$_3$)$_2$(dmpz)$_2$](NO$_3$)$_2$ (III-3)**

An aqueous suspension of *trans*-$PtCl_2(NH_3)_2$ (300 mg, 1.00 mmol) and $AgNO_3$ (326 mg, 1.92 mmol) was stirred for 24 h at 40 ^oC with daylight excluded. After 1 h in an ice bath, the resultant AgCl precipitate was filtered off, 2,3-dimethylpyrazine (211.6 mL, 2.00 mmol) was added to the clear filtrate, and this solution was stirred at 40 ^oC for 48 h. The solution was then evaporated to dryness. A white solid was obtained as 546 mg (0.889 mmol), 89 %.

^{1}H NMR:

(200 MHz, D_2O, pD = 4.3, δ/ppm): Resonances assigned to two rotamers were observed at 8.92 and 8.91 (H6, d, $^3J_{H\text{-}H}$ = 3.4 Hz, $^3J_{Pt\text{-}H}$ ~ 36.0 Hz); 8.50 (H5, d, $^3J_{H\text{-}H}$ = 3.4 Hz); 3.35 and 3.32 (C(2)H_3, s) and 2.69 (C(3)H_3, s).

***cis*-[Pt(NH$_3$)$_2$(dmpz)$_2$](NO$_3$)$_2$ (III-4)**

An aqueous suspension of *cis*-$PtCl_2(NH_3)_2$ (300 mg, 1.00 mmol) and $AgNO_3$ (326 mg, 1.92 mmol) was stirred for 24 h at 40 ^oC with daylight excluded. After 1 h in ice bath, the resultant AgCl precipitate was filtered off, 2,3-dimethylpyrazine (211.6 mL, 2.00 mmol) was added into the clear filtrate, and this solution was stirred at 40 ^oC for 48 h. The solution was then evaporated to dryness. The yield was 506 mg (0.889 mmol), 89 %.

^{1}H NMR:

(200 MHz, D_2O, pD = 4.3, δ/ppm): 8.97 (H6, d, $^3J_{H\text{-}H}$ = 3.4 Hz, $^3J_{Pt\text{-}H}$ ~ 36.0 Hz), 8.85 (H6, d, $^3J_{H\text{-}H}$ = 3.4 Hz), 8.44 (H5, d, $^3J_{H\text{-}H}$ = 3.4 Hz), 8.41 (H5, d, $^3J_{H\text{-}H}$ = 3.4 Hz), 3.42 (C(2)H_3, s), 3.27 (C(2)H_3, s) and 2.61 (C(3)H_3, s).

[{*cis*-Pt(NH_3)$_2$(2,2'-bpz-*N4,N4'*)}$_4$](NO_3)$_8$·4H_2O (IV-1) and [{*cis*-Pt(NH_3)$_2$(2,2'-bpz-*N4,N4'*)}$_3$](NO_3)$_6$ (IV-2)

cis-$PtCl_2(NH_3)_2$ (300 mg, 1.00 mmol) was suspended in 30 mL of water, $AgNO_3$ (3.40 mg, 2.00 mmol) was added, and the mixture was stirred for one night at 40 °C with light excluded. After the mixture was cooled and AgCl removed by filtration, bpz (159 mg, 1.00 mmol) was added, and the mixture was stirred for three days at 45 °C. The reaction mixture was filtered then and concentrated to 5 mL under vacuum. $NaNO_3$ (85.1 mg, 1.00 mmol) was then added to the light red solution. Pale crystals (**IV-1**) had formed after five days at 4 °C. The yield was 60.2 mg (0.0259 mmol), 10 %. Continued evaporation of the solution at 4 °C led to colorless micro-crystals **IV-2**, as a second fraction. The yield was 100 mg (0.0557 mmol), 17 %. According to elemental analysis data, both compounds contain also two $NaNO_3$, although X-ray analysis of **IV-1** does not confirm their presence.

The result of elemental analysis showed that the products have two more water molecules and two more $NaNO_3$ entities.

Elemental analysis:

For **IV-1**, $C_{32}H_{48}N_{32}O_{24}Pt_4·6(H_2O)·2(NaNO_3)$, M = 2323.32 g·mol^{-1}

Calculated: C 16.5 %, H 2.6 %, N 20.5 %

Obtained: C 16.6 %, H 2.5 %, N 20.5 %

For **IV-2**, $C_{24}H_{36}N_{24}O_{18}Pt_3·5(H_2O)·2(NaNO_3)$, M = 1793.99 g·mol^{-1}

Calculated: C 16.1 %, H 2.6 %, N 20.3 %

Obtained: C 16.1 %, H 2.4 %, N 20.3 %

^{1}H NMR:

For **IV-1**, (200 MHz, D_2O, pD = 6.3, δ/ppm): 9.83 (H3, d, $^5J_{H-H}$ = 1.1 Hz), 9.18 (H5, d, $^3J_{H-H}$ = 3.2 Hz) and 8.89 (H6, dd, $^3J_{H-H}$ = 3.2 Hz, $^5J_{H-H}$ = 1.1 Hz).

For **IV-2**, (200 MHz, D_2O, pD = 6.3, δ/ppm): 9.36 (H3, s), 9.13 (H5, d, $^3J_{H\text{-}H}$ = 3.2 Hz) and 8.87 (H6, dd, $^3J_{H\text{-}H}$ = 3.2 Hz, $^5J_{H\text{-}H}$ = 1.1 Hz).

[*cis*-$(NH_3)_2$Pt(*N1,N1'*-bpz-*N4,N4'*)Pd(en)]$_3(NO_3)_{11}(PF_6)(H_2O)_6$ (IV-3)

$PdCl_2$(en) (14.2 mg, 0.0598 mmol) was mixed with $AgNO_3$ (20.4 mg, 0.120 mmol) in 10 mL of water. The solution was stirred for one night at RT with light excluded. After the mixture had been cooled at 0 ^oC for 2 h, AgCl was removed by filtration. Then, compound **IV-2** (36.4 mg, 0.0203 mmol) was dissolved in the filtrate, and the mixture stirred for 4 h. A bright red color solution was obtained just after 5 min stirring. Then a small amount of KPF_6 was added to solution. The resulting solution was concentrated to 5 mL under vacuum and then kept at 4 ^oC to crystallize. After one week, the color of the solution had turned dark green. Two weeks later, dark green cubes were recovered from the solution. The yield was 30.2 mg (0.0116 mmol), 58 %.

Elemental analysis:

$C_{30}H_{60}N_{35}O_{33}Pd_3Pt_3F_6P\cdot 6H_2O$, M = 2596.56 g·mol^{-1}

Calculated: C 13.9 %, H 2.8 %, N 18.9 %

Obtained: C 13.7 %, H 2.8 %, N 18.9 %

^{1}H NMR:

(200 MHz, D_2O, pD = 7.3, δ/ppm): 10.62 (H3, s), 9.83 (H5, d, ^3J = 3.8 Hz), 8.84 (H6, d, ^3J = 3.8 Hz) and 2.97 (CH_2, s).

References

[1] MESTRELAB RESEARCH, M.: Rúa Xosé Pasín 6-5c, Santiago de Compostela, A Corunia, CP: 15706, Spain.

[2] Lumry, R.; Smitz, E. L.; Glantz, R. *J. Am. Chem. Soc.* **1951**, *73*, 4336.

[3] Tribolet, R.; Sigel, H. *Eur. J. Biochem*. **1987**, *163*, 353.

[4] Martin, R. B. *Science* **1963**, 1198.

[5] KappaCCD package, Nonius, Delft, The Netherlands, **1997**.

[6] Otwinowsky, Z.; Minor, W. DENZO and SCALEPACK, *Methods Enzymol.* **1997**, *276*, 307.

[7] *SADABS: Area-Detector Absorption Correction.*; Siemens Industrial Automation, Inc.: Madison, Wisconsin, U.S.A.

[8] Sheldrick, G. M. *SHELXTL-PLUS (VMS)*.

[9] Sheldrick, G. M. *SHELXL-97, Program for Crystal Structure Refinement*; University of Göttingen: Germany.

[10] Spek, A. L. *Acta Crystallogr.* **1990***, A46*, C34.

[11] Hall, S. R.; Allen, F. H.; Brown, I. D. *Acta Crystallogr.* **1991***, A47*, 655-685.

[12] Farrugia, L. J. *J. Appl. Cryst.* **1999***, 32*, 837-838.

[13] Kistenmacher, T. J.; Rossi, M.; Caradonna, J. P.; Marzilli, L. G. *Adv. Mol. Relax. Interact. Proc.* **1979**, *15*, 119.

[14] De Graaf, W.; Boersma, J.; Smeets, J. J. W.; Spek, A. L.; Van Koten, G. *Organometallics* **1989**, *8*, 2907.

[15] a) Dhara, S. C. *Indian. J. Chem.* **1970**, *8*, 193. b) Raudaschl-Sieber, G.; Lippert, B.; Hoeschele, J. D.; Howard-Lock, H. E.; Lock, C. J. L.; Pilon, P. *Inorg. Chim. Acta* **1985**, *106*, 141.

[16] Kaufman, G. B.; Cowan, D. O. *Inorg. Synth.* **1963***, 7*. 239

[17] McCormick, B. J.; Jaynes Jr., E. N.; Kaplan, R. I. *Inorg. Synth.* **1972***, 13*, 216.

[18] Minghetti, G.; Cinellu, M. A. *J. Organomet. Chem.* **1986**, *315*, 387.

F X-RAY TABLES

Table I-1: Crystallographic data for compound **I-1**.

Compound	[{Pd(1-MeC^{-}-*N3,N4*)(bpy)}$_2$](ClO$_4$)$_2$·4H$_2$O
Formula	$C_{30}H_{36}Cl_2N_{10}O_{14}Pd_2$
Formula weight (g mol^{-1})	1044.41
Crystal color and habit	Yellow prisms
Crystal system	Monoclinic
Space group	C2/c
a (Å)	13.762(3)
b (Å)	24.089(5)
c (Å)	11.850(2)
α (º)	90
β (º)	112.13(3)
γ (º)	90
Z	4
V (Å^3)	3639(1)
ρ_{calc}(g cm^{-1})	1.892
μ (Mo Kα) (mm^{-1})	1.219
F(000)	2064
Temperature (K)	150(2)
θ range (º)	2.12-24.41
No. reflections collected	2994
No. reflections observed I>2σ(I)	1733
No. parameters refined	283
R_1 (obs. data)	0.0422
wR_2 (obs. data)	0.1012
Goodness-of-fit, S	0.847
Residual ρ_{max}, ρ_{min} (e Å^{-3})	0.595, -0.531

Table I-2: Crystallographic data for compound **I-2**.

Compound	$PdCl_2$(bipzp)
Formula	$C_9 H_{12} Cl_2 N_4 Pd$
Formula weight (g mol^{-1})	353.53
Crystal color and habit	Yellow cubes
Crystal system	Orthorhombic
Space group	Pbca
a (Å)	13.909(3)
b (Å)	12.910(3)
c (Å)	14.018(3)
α (º)	90
β (º)	90
γ (º)	90
Z	8
V ($Å^3$)	2517.1(9)
ρ_{calc}(g cm^{-1})	1.866
μ (Mo Kα) (mm^{-1})	1.877
F(000)	1392
Temperature (K)	293(2)
θ range (º)	2.6-25.02
No. reflections collected	2224
No. reflections observed I>2σ(I)	1249
No. parameters refined	145
R_1 (obs. data)	0.0293
wR_2 (obs. data)	0.0523
Goodness-of-fit, S	0.77
Residual ρ_{max}, ρ_{min} (e $Å^{-3}$)	0.558, -0.307

Table I-3: Crystallographic data for compound **I-3**.

Compound	[{Pd(1-MeC$^-$-*N3,N4*)(bipzp)}$_2$]$(NO_3)_2 \cdot 7H_2O$
Formula	$C_{28} H_{50} N_{16} O_{15} Pd_2$
Formula weight (g mol^{-1})	1063.63
Crystal color and habit	Yellow cubes
Crystal system	Triclinic
Space group	P-1
a (Å)	9.497(2)
b (Å)	13.960(3)
c (Å)	16.920(3)
α (º)	79.72(3)
β (º)	75.65(3)
γ (º)	81.67(3)
Z	2
V ($Å^3$)	2126.5(7)
ρ_{calc}(g cm^{-1})	1.639
μ (Mo Kα) (mm^{-1})	0.928
F(000)	1056
Temperature (K)	150(2)
θ range (º)	2.49-24.1
No. reflections collected	6677
No. reflections observed I>2σ(I)	3263
No. parameters refined	536
R_1 (obs. data)	0.0566
wR_2 (obs. data)	0.1368
Goodness-of-fit, S	0.855
Residual ρ_{max}, ρ_{min} (e $Å^{-3}$)	1.379, -0.56

Table I-4: Crystallographic data for compound **I-4**.

Compound	$PdCl_2$(tmeda)
Formula	$C_6 H_{16} Cl_2 N_2 Pd$
Formula weight (g mol^{-1})	293.51
Crystal color and habit	Yellow cubes
Crystal system	Monoclinic
Space group	Cc
a (Å)	16.039(3)
b (Å)	5.959(1)
c (Å)	11.855(2)
α (º)	90
β (º)	113.94(3)
γ (º)	90
Z	4
V ($Å^3$)	1035.6(4)
ρ_{calc}(g cm^{-1})	1.883
μ (Mo Kα) (mm^{-1})	2.253
F(000)	584
Temperature (K)	293(2)
θ range (º)	2.78-27.46
No. reflections collected	1187
No. reflections observed	883
I>2σ(I)	293(2)
No. parameters refined	100
R_1 (obs. data)	0.0286
wR_2 (obs. data)	0.053
Goodness-of-fit, S	0.805
Residual ρ_{max}, ρ_{min} (e $Å^{-3}$)	0.809, -0.642

Table I-5: Crystallographic data for compound **I-5**.

Compound	[Pd(tmeda)(1-MeC-*N3*)$_2$]$(NO_3)_2 \cdot 2H_2O$
Formula	$C_{16} H_{34} N_{10} O_{10} Pd$
Formula weight (g mol^{-1})	632.92
Crystal color and habit	Yellow cubes
Crystal system	Monoclinic
Space group	Cc
a (Å)	19.721(4)
b (Å)	12.119(2)
c (Å)	11.961(2)
α (º)	90
β (º)	112.99(3)
γ (º)	90
Z	4
V ($Å^3$)	2631.6(9)
ρ_{calc}(g cm^{-1})	1.547
μ (Mo Kα) (mm^{-1})	0.768
F(000)	1256
Temperature (K)	293(2)
θ range (º)	2.43-27.14
No. reflections collected	2833
No. reflections observed I>2σ(I)	1895
No. parameters refined	324
R_1 (obs. data)	0.0479
wR_2 (obs. data)	0.1142
Goodness-of-fit, S	0.941
Residual ρ_{max}, ρ_{min} (e $Å^{-3}$)	0.787, -0.589

Table I-6: Crystallographic data for compound **I-6**.

Compound	$[\{Pd(\mu\text{-}OH)(tmeda)\}_2](ClO_4)_2$
Formula	$C_{12}\ H_{34}\ Cl_2\ N_4\ O_{10}\ Pd_2$
Formula weight (g mol^{-1})	678.13
Crystal color and habit	Yellow blocks
Crystal system	Monoclinic
Space group	P2(1)/c
a (Å)	5.993(1)
b (Å)	9.632(2)
c (Å)	21.324(5)
α (º)	90
β (º)	105.48(3)
γ (º)	90
Z	2
V ($Å^3$)	1186.3(4)
ρ_{calc}(g cm^{-1})	1.898
μ (Mo Kα) (mm^{-1})	1.794
F(000)	680
Temperature (K)	293(2)
θ range (º)	3.53-26
No. reflections collected	2300
No. reflections observed I>2σ(I)	1456
No. parameters refined	137
R_1 (obs. data)	0.0448
wR_2 (obs. data)	0.0872
Goodness-of-fit, S	1.058
Residual ρ_{max}, ρ_{min} (e $Å^{-3}$)	0.611, -0.58

Table I-7: Crystallographic data for compound **I-7**.

Compound	$[\{Pd(1\text{-}MeC^{-}\text{-}N3,N4)(tmeda)\}_3](ClO_4)_3 \cdot 5.5H_2O$
Formula	$C_{33}\ H_{77}\ Cl_3\ N_{15}\ O_{20.50}\ Pd_3$
Formula weight (g mol^{-1})	1426.56
Crystal color and habit	Yellow blocks
Crystal system	Triclinic
Space group	P-1
a (Å)	12.621(3)
b (Å)	13.074(3)
c (Å)	19.722(4)
α (º)	78.22(3)
β (º)	86.87(3)
γ (º)	65.56(3)
Z	2
V ($Å^3$)	2899(1)
ρ_{calc}(g cm^{-1})	1.634
μ (Mo Kα) (mm^{-1})	1.138
F(000)	1444
Temperature (K)	150(2)
θ range (º)	3.05-26
No. reflections collected	11366
No. reflections observed I>2σ(I)	6349
No. parameters refined	688
R_1 (obs. data)	0.0636
wR_2 (obs. data)	0.151
Goodness-of-fit, S	1.069
Residual ρ_{max}, ρ_{min} (e $Å^{-3}$)	1.463, -1.005

Table I-8a: Crystallographic data for compound **I-8a**.

Compound	$[Pt(\mu\text{-}OH)(tmeda)]_2(ClO_4)_2$
Formula	$C_{12}\ H_{34}\ Cl_2\ N_4\ O_{10}\ Pt_2$
Formula weight (g mol^{-1})	855.48
Crystal color and habit	Yellow prisms
Crystal system	Monoclinic
Space group	P2(1)/n
a (Å)	5.813(1)
b (Å)	9.810(2)
c (Å)	20.361(4)
α (º)	90
β (º)	92.52(3)
γ (º)	90
Z	2
V ($Å^3$)	1160.0(4)
ρ_{calc}(g cm^{-1})	2.444
μ (Mo Kα) (mm^{-1})	12.331
F(000)	804
Temperature (K)	293(2)
θ range (º)	2.3-25.37
No. reflections collected	2112
No. reflections observed I>2σ(I)	1656
No. parameters refined	131
R_1 (obs. data)	0.0638
wR_2 (obs. data)	0.1654
Goodness-of-fit, S	1.054
Residual ρ_{max}, ρ_{min} (e $Å^{-3}$)	5.196,-4.349

Table I-8b: Crystallographic data for compound **I-8b**.

Compound	$[Pt(\mu\text{-}OH)(tmeda)]_2(NO_3)_2$
Formula	$C_{12}\ H_{34}\ N_6\ O_{10}\ Pt_2$
Formula weight (g mol^{-1})	812.59
Crystal color and habit	Colorless cubes
Crystal system	Monoclinic
Space group	P2(1)/n
a (Å)	5.882(1)
b (Å)	11.390(2)
c (Å)	17.873(4)
α (º)	90
β (º)	95.32(3)
γ (º)	90
Z	2
V ($Å^3$)	1192.3(4)
ρ_{calc}(g cm^{-1})	2.258
μ (Mo Kα) (mm^{-1})	11.776
F(000)	764
Temperature (K)	293(2)
θ range (º)	2.12-26.39
No. reflections collected	2431
No. reflections observed I>2σ(I)	1787
No. parameters refined	137
R_1 (obs. data)	0.0428
wR_2 (obs. data)	0.1038
Goodness-of-fit, S	1.012
Residual ρ_{max}, ρ_{min} (e $Å^{-3}$)	2.495, 1.535

Table I-9: Crystallographic data for compound **I-9**.

Compound	[{Pd(Cytd$^-$-*N3*,*N4*)(tmeda)}$_3$](ClO$_4$)$_3$·6H$_2$O
Formula	$C_{45}H_{90}N_{15}O_{33}Cl_3Pd_3$
Formula weight (g mol^{-1})	1794.89
Crystal color and habit	Yellow cubes
Crystal system	trigonal
Space group	P321
a (Å)	19.300(3)
b (Å)	19.300(3)
c (Å)	12.777(3)
α (º)	90
β (º)	90
γ (º)	120
Z	2
V (Å^3)	4122(1)
ρ_{calc}(g cm^{-1})	1.431
μ (Mo Kα) (mm^{-1})	0.826
F(000)	1812
Temperature (K)	150(2)
θ range (º)	3.22-24.99
No. reflections collected	4639
No. reflections observed I>2σ(I)	3211
No. parameters refined	300
R_1 (obs. data)	0.0552
wR_2 (obs. data)	0.1272
Goodness-of-fit, S	0.966
Residual ρ_{max}, ρ_{min} (e Å^{-3})	0.504, -0.346

Table II-1: Crystallographic data for compound **II-1.**

Compound	[Pd(tmeda)(Hampy-*N1*)$_2$](NO$_3$)$_2$·2H$_2$O
Formula	$C_{16}H_{32}N_8O_8Pd$
Formula weight (g mol^{-1})	570.89
Crystal color and habit	Yellow cubes
Crystal system	Orthorhombic
Space group	Pbca
a (Å)	18.175(4)
b (Å)	12.672(3)
c (Å)	20.633(4)
α (º)	90
β (º)	90
γ (º)	90
Z	8
V (Å^3)	4752(2)
ρ_{calc}(g cm^{-1})	1.585
μ (Mo Kα) (mm^{-1})	0.838
F(000)	2320
Temperature (K)	150(2)
θ range (º)	2.19-23.79
No. reflections collected	3637
No. reflections observed I>2σ(I)	1661
No. parameters refined	295
R_1 (obs. data)	0.0387
wR_2 (obs. data)	0.0817
Goodness-of-fit, S	0.801
Residual ρ_{max}, ρ_{min} (e Å^{-3})	0.81, -0.337

Table II-5a: Crystallographic data for compound **II-5**.

Compound	[{(tmeda)Pd(*N2*-ampy$^-$-*N1*)}$_2$Ag(μ-NO_3)$_2$Ag(NO_3)$_2$]
Formula	C_{22} H_{42} Ag_2 N_{12} O_{12} Pd_2
Formula weight (g mol^{-1})	1095.22
Crystal color and habit	Orange cubes
Crystal system	Monoclinic
Space group	C2/c
a (Å)	16.948(3)
b (Å)	11.140(2)
c (Å)	18.296(4)
α (º)	90
β (º)	98.73(3)
γ (º)	90
Z	4
V (Å^3)	3414(1)
ρ_{calc}(g cm^{-1})	2.131
μ (Mo Kα) (mm^{-1})	2.243
F(000)	2160
Temperature (K)	150(2)
θ range (º)	2.2-25.06
No. reflections collected	2998
No. reflections observed I>2σ(I)	1660
No. parameters refined	226
R_1 (obs. data)	0.0855
wR_2 (obs. data)	0.2267
Goodness-of-fit, S	0.983
Residual ρ_{max}, ρ_{min} (e Å^{-3})	3.226, -1.027

Table II-5b: Crystallographic data for compound **II-5a**.

Compound	[{(tmeda)Pd(*N2*-ampy$^-$-*N1*)}$_2$Ag(ClO_4)$_2$](ClO_4)·2H_2O
Formula	C_{22} H_{46} Ag Cl_3 N_8 O_{14} Pd_2
Formula weight (g mol^{-1})	1073.71
Crystal color and habit	Orange cubes
Crystal system	Monoclinic
Space group	P2/C
a (Å)	11.502(2)
b (Å)	9.883(2)
c (Å)	18.333(6)
α (º)	90
β (º)	120.77(2)
γ (º)	90
Z	2
V (Å^3)	1790.6(8)
ρ_{calc}(g cm^{-1})	1.98
μ (Mo Kα) (mm^{-1})	1.832
F(000)	1060
Temperature (K)	150(2)
θ range (º)	2.34-25.62
No. reflections collected	2784
No. reflections observed I>2σ(I)	1571
No. parameters refined	227
R_1 (obs. data)	0.0526
wR_2 (obs. data)	0.1045
Goodness-of-fit, S	0.864
Residual ρ_{max}, ρ_{min} (e Å^{-3})	1.003, -0.744

Table II-6: Crystallographic data for compound **II-6**.

Compound	[{Pd(ampy$^-$-*N1,N2*)(bpy)}$_2$](NO$_3$)$_2$
Formula	C_{30} H_{26} N_{10} O_6 Pd_2
Formula weight (g mol^{-1})	835.41
Crystal color and habit	Red cubes
Crystal system	Monoclinic
Space group	P2(1)/n
a (Å)	14.188(3)
b (Å)	16.115(3)
c (Å)	16.583(3)
α (º)	90
β (º)	70.60(3)
γ (º)	90
Z	4
V (Å^3)	3576(1)
ρ_{calc}(g cm^{-1})	1.552
μ (Mo Kα) (mm^{-1})	1.059
F(000)	1664
Temperature (K)	293(2)
θ range (º)	2.07-23.74
No. reflections collected	5227
No. reflections observed I>2σ(I)	1834
No. parameters refined	393
R_1 (obs. data)	0.0902
wR_2 (obs. data)	0.2661
Goodness-of-fit, S	0.834
Residual ρ_{max}, ρ_{min} (e Å^{-3})	1.328, -0.607

Table III-1: Crystallographic data for compound **III-1**.

Compound	[PtCl(tmeda)(Pz)](ClO$_4$)
Formula	C_{10} H_{20} Cl_2 N_4 O_4 Pt
Formula weight (g mol^{-1})	526.29
Crystal color and habit	Yellow prisms
Crystal system	Orthorhombic
Space group	P2(1)2(1)2(1)
a (Å)	9.692(2)
b (Å)	10.438(2)
c (Å)	15.734(3)
α (º)	90
β (º)	90
γ (º)	90
Z	4
V (Å^3)	1591.7(5)
ρ_{calc}(g cm^{-1})	2.196
μ (Mo Kα) (mm^{-1})	9.17
F(000)	1008
Temperature (K)	150(2)
θ range (º)	2.34-23.99
No. reflections collected	2443
No. reflections observed I>2σ(I)	1457
No. parameters refined	181
R_1 (obs. data)	0.0578
wR_2 (obs. data)	0.1257
Goodness-of-fit, S	0.863
Residual ρ_{max}, ρ_{min} (e Å^{-3})	4.256, -0.603

Table IV-1: Crystallographic data for compound **IV-1**.

Compound	[{*cis*-Pt(NH_3)$_2$(2,2'-bpz-*N4,N4'*)}$_4$](NO_3)$_8$·4H_2O
Formula	C_{32} H_{56} N_{32} O_{28} Pt_4
Formula weight (g mol^{-1})	2117.30
Crystal color and habit	Pink Prisms
Crystal system	Triclinic
Space group	P-1
a (Å)	10.276(2)
b (Å)	13.235(3)
c (Å)	14.105(3)
α (º)	114.66(3)
β (º)	98.60(3)
γ (º)	93.16(3)
Z	1
V (Å^3)	1709.0(6)
ρ_{calc}(g cm^{-1})	2.05
μ (Mo Kα) (mm^{-1})	8.259
F(000)	1000
Temperature (K)	150(2)
θ range (º)	3.09-25.01
No. reflections collected	6000
No. reflections observed I>2σ(I)	4480
No. parameters refined	382
R_1 (obs. data)	0.0739
wR_2 (obs. data)	0.239
Goodness-of-fit, S	1.434
Residual ρ_{max}, ρ_{min} (e Å^{-3})	4.153, -2.443

List of compounds

I-1* [{Pd(1-MeC$^-$-*N3,N4*)(bpy)}$_2$](ClO$_4$)$_2$·4H$_2$O

I-2* PdCl$_2$(bipzp)

I-3* [{Pd(1-MeC$^-$-*N3,N4*)(bipzp)}$_2$](NO$_3$)$_2$·7H$_2$O

I-4* PdCl$_2$(tmeda)

I-5* [Pd(tmeda)(1-MeC-*N3*)$_2$](NO$_3$)$_2$·2H$_2$O

I-6* [{Pd(*μ*-OH)(tmeda)}$_2$](ClO$_4$)$_2$

I-7* [{Pd(1-MeC$^-$-*N3,N4*)(tmeda)}$_3$](ClO$_4$)$_3$·5.5H$_2$O

I-8a* [{Pt(*μ*-OH)(tmeda)}$_2$](ClO$_4$)$_2$

I-8b* [{Pt(*μ*-OH)(tmeda)}]$_2$(NO$_3$)$_2$

I-9* [{Pd(Cytd$^-$-*N3,N4*)(tmeda)}$_3$](ClO$_4$)$_3$·6H$_2$O

II-1 [PdCl(tmeda)(Hampy-*N1*)](NO$_3$)

II-2* [Pd(tmeda)(Hampy-*N1*)$_2$](NO$_3$)$_2$·2H$_2$O

II-3 [PtCl(tmeda)(Hampy-*N1*)](NO$_3$)

II-4 [Pt(tmeda)(Hampy-*N1*)$_2$](ClO$_4$)$_2$

II-5* [{(tmeda)Pd(*N2*-ampy$^-$-*N1*)}$_2$Ag(*μ*-NO$_3$)$_2$Ag(NO$_3$)$_2$]

II-5a* [{(tmeda)Pd(*N2*-ampy$^-$-*N1*)}$_2$Ag(ClO$_4$)$_2$](ClO$_4$)·2H$_2$O

II-6* [Pd(ampy$^-$-*N1,N2*)(bpy)]$_2$(NO$_3$)$_2$

III-1* [PtCl(tmeda)(Pz)](ClO$_4$)

III-2 [{Pt(tmeda)(Pz)}$_3$](NO$_3$)$_6$·2.5H$_2$O

III-3 *trans*-[Pt(NH$_3$)$_2$(dmpz)$_2$](NO$_3$)$_2$

III-4 *cis*-[Pt(NH$_3$)$_2$(dmpz)$_2$](NO$_3$)$_2$

IV-1* [{*cis*-Pt(NH$_3$)$_2$(2,2'-bpz-*N4,N4'*)}$_4$](NO$_3$)$_8$·4H$_2$O

IV-2 [{*cis*-Pt(NH$_3$)$_2$(2,2'-bpz-*N4,N4'*)}$_3$](NO$_3$)$_6$

IV-3 [{*cis*-(NH$_3$)$_2$Pt(*N1,N1'*-2,2'-bpz-*N4,N4'*)Pd(en)}$_3$](NO$_3$)$_{11}$(PF$_6$)(H$_2$O)$_6$

Compounds studied by X-ray crystallography are indicated by *.

List of abbreviations

2-ampy	2-aminopyridine
ampy$^-$	2-amidopyridine deprotonated at N2
AFM	Atomic Force Microscopy
bpy	2,2'-bipyridine
bipzp	bis(pyrazol-1-yl)propane
bp	base pair
2,2'-bpz	2,2'-bipyrazine
CD	Circular Dichroism
Cytd	cytidine
Cytd$^-$	cytidine anion (deprotonated at N4)
Cp*	η^5-pentamethylcyclopentadienyl
d	doublet
dd	doublet-of-doublet
ddd	doublet-of-doublet-of-doublet
dmpz	2,3-dimethylpyrazine
DMSO	dimethylsulfoxide
DNA	deoxyribonucleic acid
δ	chemical shift
en	ethylenediamine
h	hours
hh	*head-head*
ht	*head-tail*
Hampy	2-aminopyridine
HSQC	Heteronuclear Single Quantum Coherence
IR	infrared
LD	Linear Dichroism
m	multiplet

M	mol/L^{-1}
1-MeC	1-methylcytosine
1-MeC^-	1-methylcytosine anion (deprotonated at N4)
NMR	Nuclear Magnetic Resonance
NOE	Nuclear Overhauser Effect
NOESY	Nuclear Overhauser Effect Spectroscopy
Pd_3(1-MeC^-)$_3$	[{Pd(1-MeC^--*N3,N4*)(tmeda)}$_3$]$(ClO_4)_3 \cdot 5.5H_2O$
Pd_3($Cytd^-$)$_3$	[{Pd($Cytd^-$-*N3,N4*)(tmeda)}$_3$]$(ClO_4)_3 \cdot 6H_2O$
pD	negative logarithm of the deuteron concentration
pH	negative logarithm of the proton concentration
pK_a	negative logarithms of the acidity constant
ppm	parts per million
Pt_4	[{*cis*-Pt$(NH_3)_2$(2,2'-bpz-*N4,N4'*)}$_4$]$(NO_3)_8 \cdot 4H_2O$
Pt_3	[*cis*-Pt$(NH_3)_2$(2,2'-bpz-*N4,N4'*)$_3$$(NO_3)_6$
py	pyridine
pz	pyrazine
RNA	ribonucleic acid
RT	room temperature
s	singlet
S-8er	single stranded DNA oligonucleotide 5'-d(TAGGGTTA)
t	triplet
TMAB	tetramethylammonium tetrafluoroborate
tmeda	*N,N,N',N'*-tetramethylethylenediamine
TOCSY	Total Correlation Spectroscopy
TSP	sodium 3-trimethylsilyl-propanesulfonate
^3J	spin-spin coupling constant (here via three bonds)

Curriculum Vitae

Personal Information

Name: Wei-Zheng Shen
Gender: Female
Marital Status: Married
Health: Excellent
Date of Birth: May. 28th, 1978
Place of Birth: Tianjin, P. R. China

Education Background

Jan. 2004 – present	International Max Planck Research School **Max Planck Institute for Molecular Physiology** University of Dortmund, Department of Chemistry, Germany **The group of Inorganic Chemistry of Prof. Bernhard Lippert**
Sept. 2000 – Jul. 2003	M.S. candidate for Chemistry, Nankai University, China **GPA**: Overall 87.4/100 **Rank**: **Top 5%** of 90
Sept. 1996 – Jul. 2000	B.S. in Department of Chemistry, Tianjin Normal University, China **GPA**: Overall 83.2/100 **Rank**: **Top 10%** among 120 students of my academic year

Professional Experience

Jan. 2004 – present	**Dr. rer. nat. Thesis Project** Cyclic, Cationic Complexes of Pt^{II} and Pd^{II} with Heterocyclic Ligands, including Nucleobases: Synthesis, Structure, Host-guest Chemistry with Anions and Non-covalent Interactions with DNA.
Sept. 2001 – Jul. 2003	**M. S. Thesis Project** Study on Structures and Properties of Bridged Polynuclear and Multi-dimensional Coordination polymers
Sept. 2001– Jan. 2002	**Teaching Assistant** of Inorganic Chemistry teaching and research group Gave lectures to undergraduate students Gathered and graded paper sheets Helped students solve problems
Mar. 2002 – Jul. 2002	**Writing Assistant** Help Pro. Shi-Ping Yan translate and write his book
Feb. 2000 – Jul. 2000	**B. S. Thesis Project** Study on "Synthesize Super-effect Polymers of Fluorescence"
Sept. 1999 – Nov. 1999	**Educational Practice** Act as a teacher of chemistry in Nankai University Adjunctive Middle School
Sept. 1998 – Jun. 1999	**Researching Practice** Study on the synthesis technique producing efficient green fluorescent compound of 9,10-Bis(phenylethynyl)anthracene in the practical group

Publications

- Ying-Ji Sun, **Wei-Zheng Shen**, Peng Cheng*, The first example of half-sandwich cobalt(III) complex with hydrotris(pyrazolyl)borate ligand *Inorganic Chemistry Communication* 5 (2002) 512-515.
- Xiao-yan Chen, **Wei-Zheng Shen**, Peng Cheng*, Molecular and low-dimensional coordination compounds of copper(II) and 3,5-dimethylpyrazole. Synthesis, crystal structure and properties. *Z. Anorg. Allg. Chem*. 629 (2003) 697-702.
- **Wei-Zheng Shen**, Feng Kang, Ying-Ji Sun, Peng Cheng*, The synthesis and crystal structure of $[M\{H_2B(tz^*)_2\}_2(H_2O)]$ (M=Cu, Zn and tz* = 3,5-dimethyl-1,2,4-triazole) *Inorganic Chemistry Communication* 6 (2003) 408-411.
- **Wei-Zheng Shen**[a], Cheng-Zhi Xie[a], Peng Cheng*[a], Synthesis and Crystal Structure of $[Cu\{HC(pz)_3\}(SCN)_2]$ and $[Cu(tacn)(SCN)_2]$ ($HC(pz)_3$: tris(pyrazolyl)methane; tacn: 1,4,7-triazacyclononane) *Journal of Chemical Research* 5 (2003) 307-309
- **Wei-Zheng Shen**, Xiao-Yan Chen, Peng Cheng*, Dai-Zheng Liao, Shi-Ping Yan and Zong-Hui Jiang, Cobalt(II) complexes with dicyanamide - from binuclear entities to chains *Z. Anorg. Allg. Chem*. 629 (14) (2003) 2591-2595
- Ying-Ji Sun, **Wei-Zheng Shen**, Peng Cheng*, Synthesis, crystal structure, and properties of a binuclear copper(II) complex containing an oxalate bridge *Polyhedron* 23 (2004) 211-218
- **Wei-Zheng Shen**, Long Yi, Peng Cheng, Shi-Ping Yan, Dai-Zheng Liao and Zong-Hui Jiang, Synthesis of a serious of copper(II)-pyrazolyl complexes in different solvents and anions, *Inorganic Chemistry Communication* 7 (2004) 819.
- **Wei-Zheng Shen**, Xiao-Yan Chen, Peng Chen, Shi-Ping Yan, Bin Zhai, Dai-Zheng Liao, Zong-Hui Jiang, A Structural and Magnetic Investigation of Ferromagnetically Coupled Copper(II) Isophthalates, *Eur. J. Inorg. Chem.* 12 (2005) 2269.
- **Wei-Zheng Shen**, Deepali Gupta, and Bernhard Lippert, Cyclic Trimer vs. Head-Tail Dimer in Metal-Nucleobase Complexes: Importance of Relative Orientation (syn, anti) of the Metal Entities and Relevance as a Metallaazacrown Compound. *Inorg. Chem.* 44 (2005) 8249.
- Bin Ding, Long Yi, **Wei-Zheng Shen**, Peng Cheng *, Dai-Zheng Liao, Shi-Ping Yan, Zong-Hui Jiang, Synthesis, crystal structure and magnetic properties of N1,N2-bridged polynuclear Ni(II) complexes. *Journal of Molecular Structure* 784 (2006) 138.
- **Wei-Zheng Shen**, Burkhard Costisella and Bernhard Lippert, Pd_2Ag triangle supported by two μ_3-amidopyridine ligands. *Dalton Trans.* 8 (2007) 851.

Conference Attendance

Feb. 2007	**Koordinationschemie-Treffen** in Berlin, presentation with a title "Cyclic, cationic complexes of Pt^{II} and Pd^{II} with heterocyclic ligands, including nucleobases".
Oct. 2006	**AsBIC-III** Conference, Nanjing, poster with a title "Cyclic, cationic complexes of Pt^{II} and Pd^{II} with heterocyclic ligands, including nucleobases".
Oct. 2005	**1st European Conference on Chemistry for life sciences** **COST D20 Conference**, Rimini, presentation with a title "A cyclic, trinuclear metal-nucleobase complexes: a model for host-guest interaction study".
Aug. 2004	**COST D20 Conference**, Garmisch-Partenkirchen, poster **EUROBIC 7 Conference**, poster with a title "Coordination chemistry of $enPd^{II}$ with the 1-methylcytosine model nucleobase".